Generation of a *Pax6* Reporter mouse

By

David Antony Tyas

Thesis submitted for the degree of doctor of philosophy at the

University of Edinburgh

2004

Declaration

This thesis and the research described herein is solely my own work. Any collaborative work or assistance from others is explicitly acknowledged at the relevant point within the text. No part of this work has been, or is being submitted for any other degree or qualification.

David Antony Tyas

Abstract

Pax6 is a member of a highly evolutionarily conserved family of transcription factors. These genes are characterised by the presence of a 'paired-type' DNA binding domain. *Pax6* is developmentally regulated and is required for the normal embryonic development of the central nervous system, eye and pancreas. In adults it is thought to be involved in the correct function of the pancreas and cerebellum, although its precise mechanism of action is not as yet fully understood.

In order to better understand Pax6 function I generated a novel tool - a '*Pax6* reporter' transgenic mouse that expresses GFP under the control of *Pax6* regulatory elements. The transgenic mouse was generated from a modified yeast artificial chromosome (YAC) that contains the human *PAX6* gene and has been previously demonstrated to rescue loss of endogenous *Pax6* in *Pax6* $^{sey/sey}$ mice.

The key advantages of a YAC addition transgenic include that it is already known that *Pax6* regulatory elements are present over a 200Kb region and inserting a reporter gene into the endogenous *Pax6* would not be independent of the endogenous locus.

An expression cassette encoding GFP and an IRES-neoR vector were inserted into the YAC in frame with the normal *PAX6* translation start point in exon 4, preserving the rest of the *PAX6* locus. This put GFP and neomycin under the control of the *PAX6* regulatory elements. The modified YAC was then injected into fertilised mouse oocytes to generate nine lines of transgenic mice.

Once generated the expression pattern in each line was analysed at a range of developmental stages by imaging appropriate sections of agarose embedded mouse embryos. This confirmed that the expression was the same as the previously reported *Pax6* expression pattern. In addition, the copy number and extent of the YAC incorporated in each of the nine lines was investigated.

Abbreviations

5-FOA	5-fluoroorotic acid
BAC	Bacterial artificial chromosome
CAT	chloramphenicol acetyltransferase
CHEF	Alternating Contour-Clamped Homogeneous Electric Field
CNS	Central Nervous System
DNA	Deoxyribonucleic Acid
E	Embryonic Age (E0.5 is defined here as the day of discovering vaginal plug)
EDTA	Ethylenediaminetetraacetic acid
ES	Embryonic Stem Cells
EtBr	Ethidium Bromide
FACS	Fluorescence Activated Cell Sorting
GFP	Green Fluorescent Protein
hAP	human placental alkaline phosphatase
HRP	horseradish peroxidase
IRES	Internal Ribosome Entry Site
LacZ	Bacterial gene that encodes the protein β-galactosidase
LoxP	Locus of crossover of P1
mRNA	Messenger Ribonucleic Acid
neo^R	Neomycin Resistance
PAC	P1-derived artificial chromosome
PCR	Polymerase Chain Reaction
PFG	Pulse Field Gel
PFGE	Pulse Field Gel Electrophoresis
RNA	Ribonucleic Acid
RT-PCR	Reverse Transcription-Polymerase Chain Reaction
SDS	Sodium dodecyl sulphate
TAE	Tris-acetate buffer
Taq	*Thermus aquaticus* DNA polymerase
TBE	Tris-borate buffer
UMS	Upstream Mouse Sequence
UV	Ultraviolet
YAC	Yeast Artificial Chromosome

Contents Page

Development of the brain

The vertebrate brain develops from the planar sheet of proliferating neuroepithelial cells arising from the embryonic ectoderm germ layer, the neural plate. The process of neurulation converts the neural plate into the neural tube. Briefly, folds arise in the neural plate, appose and later fuse to form the neural tube. The process extends rostrally and caudally in a zipper-like fashion. Some cells break off and become neural crest cells that later contribute to the peripheral nervous system. A series of ring-like constrictions appear in the neural tube and mark the approximate boundaries between the primordia of the major brain regions: the forebrain (prosencephalon), midbrain (mesencephalon), and hindbrain (rhombencephalon). Further subdivision generates a series of segment-like swellings or neuromeres, within each of these regions. Caudal to the hindbrain the neural tube remains a uniformly narrow cylinder, the precursor of the spinal cord. Concurrent with subdivision, the neural tube undergoes pronounced bending. These flexures result in previously distant parts of the neural tube coming into close contact, see Figures 1.1 and 1.2.

The forebrain comprises two regions, the telencephalon and the diencephalon. The telencephalic vesicles appear as two dorsolateral expansions of the primary forebrain. These continue to enlarge disproportionately to the rest of the developing brain. The diencephalic structures (such as the thalamus and hypothalamus) form from an evagination of the more medial prosencephalic wall of the forebrain.

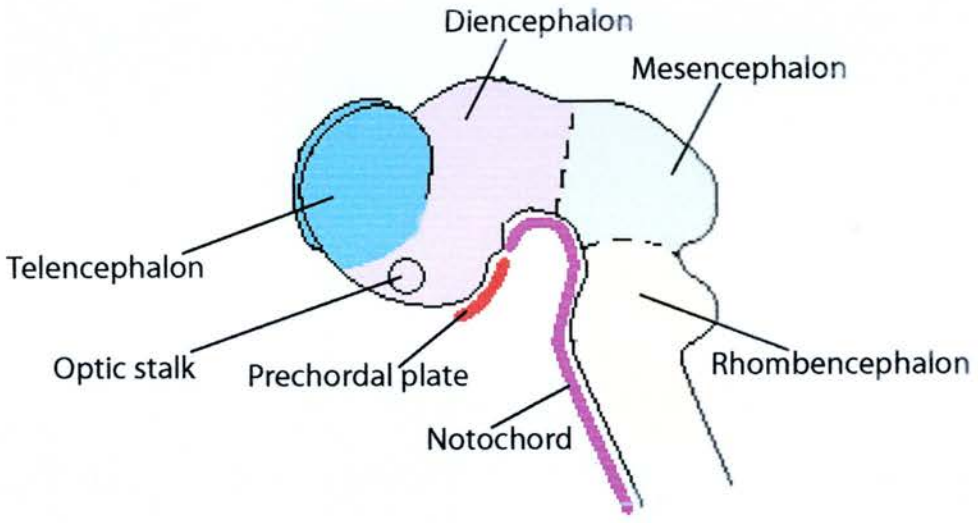

Figure 1.1. Diagram of the mouse brain viewed from the side around mid gestation (E10.5), after neural tube closure. This diagram is adapted from Zaki et al., (2003).

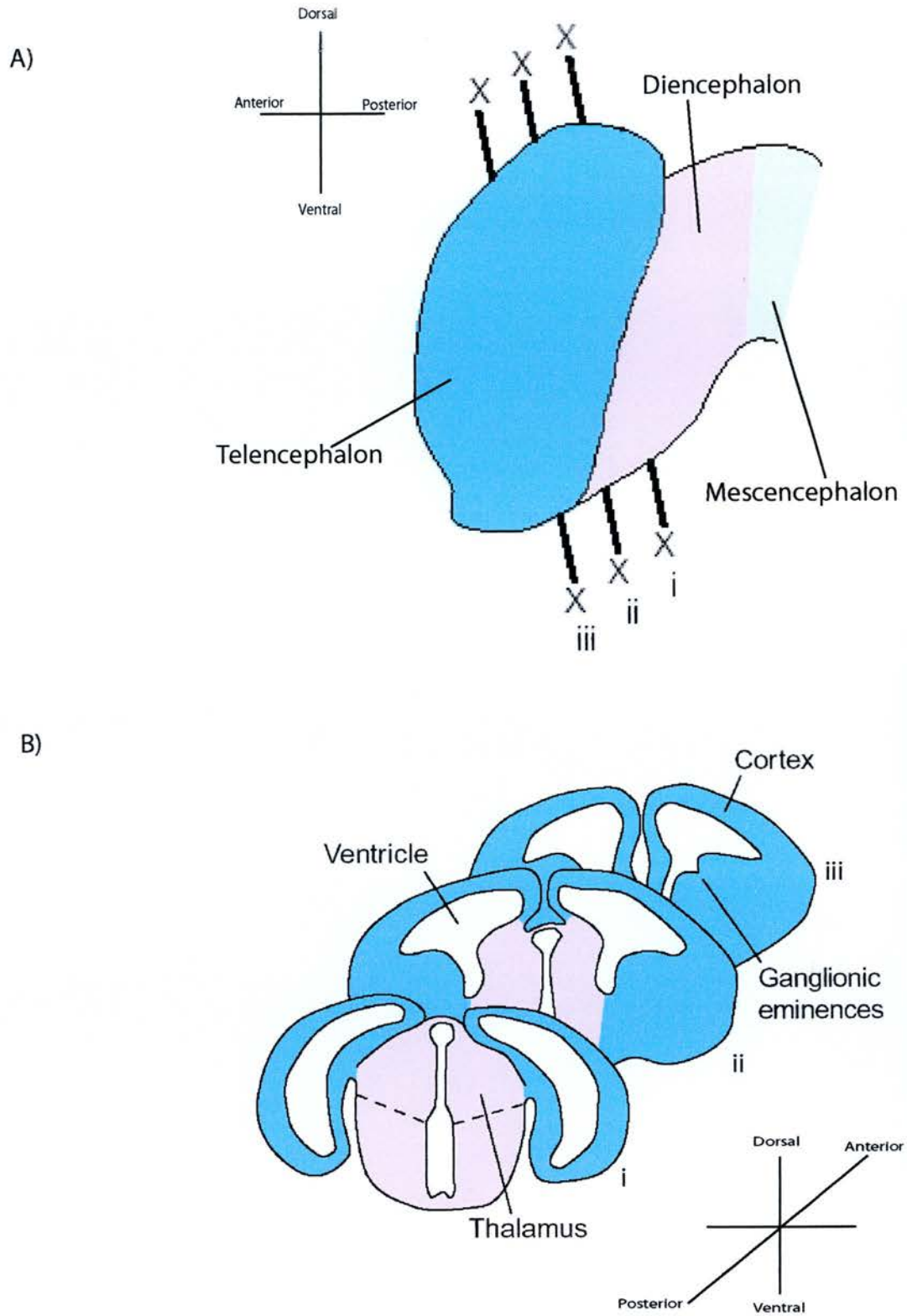

Figure 1.2 Schematic diagrams of the telencephalon during development. Both diagrams are from around birth. (A) The X shows the locations of the three sections in (B). The figures are adapted from Zaki et al., (2003).

The developing telencephalon can be divided into two areas. The dorsal telencephalon is referred to as the pallium (this gives rise to the glutamatergic cortical structures) and the ventral telencephalon as the subpallium (this gives rises to the GABAergic basal ganglia). Both of these areas can be further subdivided. The pallium can be divided into four areas. The medial pallium which gives rise to the archicortex, including the hippocampus; the dorsal pallium where the neocortex forms; the lateral pallium which generates the olfactory cortex and the ventral pallium from which the claustroamygdaloid complex is generated. The subpallium can be subdivided into two distinct domains, the lateral (LGE) and medial (MGE) ganglionic eminences. The LGE can be further subdivided into the dorsal and lateral ganglionic eminences. See Figure 1.3 for summary of these areas in an embryonic day 12.5 (E12.5) mouse.

In normal development of the mouse, cortical neurogenesis occurs from embryonic day 12 (E12) to E18 (Gillies and Price 1993; Levers *et al.* 2001). At these ages, the lateral ventricle is lined by a population of proliferating cells in a region called the ventricular zone, which gives rise to most neurones and glial cells of the mammalian cortex. These cortical progenitor cells are not a homogenous population and there is mounting evidence that different progenitor cells generate different differentiated cell types (Grove *et al.* 1993; Luskin *et al.* 1993; Reid *et al.* 1995; Tan *et al.* 1998; Heins *et al.* 2002).The mechanisms controlling the fates of these progenitor cells are not yet elucidated.

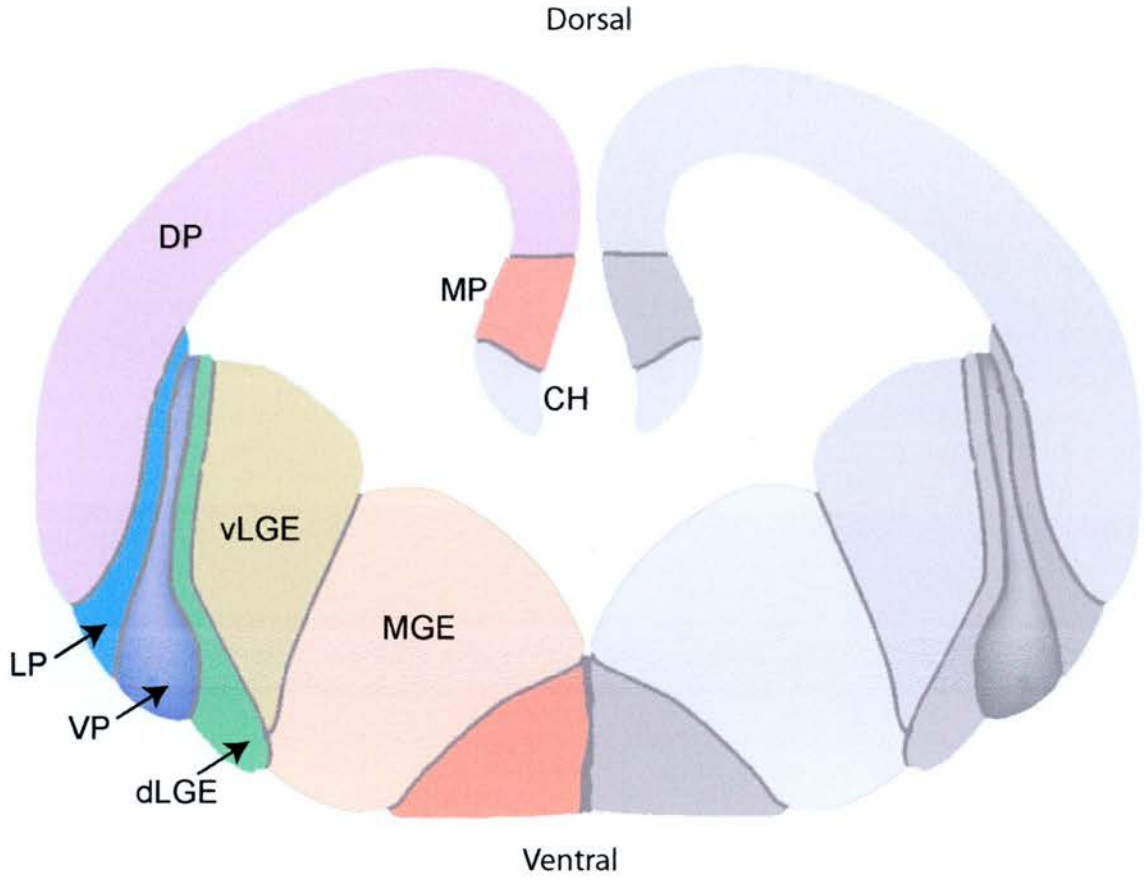

Figure 1.3 Schematic coronal section through the telencephalic vesicles at E12.5 showing dorsal and ventral subdomains. Cortical Hem (CH). Medial Pallium (MP). Dorsal Pallium(DP). Lateral Pallium (LP). Ventral Pallium (VP). Dorsal Lateral (dLGE) and ventral lateral ganglionic eminence (vLGE). Medial ganglionic eminences (MGE). The Figure is adapted from a figure in Schuurmans and Guillemot (2002).

Nuclei of ventricular progenitor cells undergo dynamic intracellular migration during the cell cycle. Nuclei move away from the apical surface during G1, occupy the outer half of the ventricular zone during S phase and return apically in G2 so that mitosis occurs at the ventricular surface (Sidman *et al.* 1959; Fujita 1964). Neurones exit the cell cycle in contact with radial glial fibres to migrate into more superficial positions. When neurones reach the top of the cortical plate they detach and associate into layers with cohorts of a similar birth date. This results in the cortex being formed in an 'inside-out' laminar fashion. After neural production has finished, astrocytes and oligondendrocytes are produced in large numbers from precursors in the subventricular zone (Gleeson and Walsh 2000; Morrison 2000).

The second group of neurons that cooperate in the formation of the mammalian cortex are the tangentially migrating neurons. These GABAergic neurons originate in the ventricular zone of the LGE and MGE; the majority originate in the MGE (recently reviewed by (Marin and Rubenstein 2001; Nadarajah and Parnavelas 2002)). These neurones then move parallel to the surface of the brain along axons of other neurons through the intermediate zone of the developing cortex to their final destination in the cortex.

Cortical regionalisation

As has been discussed above the developing telencephalon is often described as a series of subdivisions. These subdivisions were originally based on differences in morphology, connectivity and neurochemical profile. The mechanism behind this

regionalisation has been contested. It is currently believed that the specification and differentiation of neocortical areas during development are controlled by an interplay between genetic regulation intrinsic to the neocortex and extrinsic influences arising from outside the neocortex. The intrinsic influences are believed to be set up in the progenitor cell layer of the cortex by regionalised expression of genes (Rakic 1988; Dehay *et al.* 1993; Rakic 1995). The extrinsic influences are thought to be cues from axons growing into the cortex later on in development, for example thalamocortical axons (TCAs) coming from the thalamus (O'Leary 1989; Schlaggar and O'Leary 1991). These innervating axons, when they arrive, could modify and refine the early regionalisation set up by the intrinsic factors.

Evidence of the importance of extrinsic factors comes from experiments such as heterotopic transplantation experiments in rats(Stanfield and O'Leary 1985). Here, when portions of the occipital cortex from foetal rats were transplanted to more rostral cortical regions of newborn rats, it was found that the ectopic immature cortical tissue developed efferent projections and histology that were characteristic of the local cortical tissue(Stanfield and O'Leary 1985). This demonstrates that anatomical and/or functional changes in axonal inputs to the neocortex can play a role in modifying existing, and generating new, neocortical subdivision. However, in the *Gbx2* mutant mouse there are no thalamic axons innervating the cortex, but the neocortical region-specific gene expression develops normally, thus demonstrating that early neocortical regionalization does not require extrinsic information from the thalamus (Miyashita-Lin *et al.* 1999). More recently, there have been many descriptions of graded or restricted patterns of gene expression across the ventricular

zone or the cortical plate before TCAs enter the neocortex (Donoghue and Rakic 1999; Miyashita-Lin *et al.* 1999; Nakagawa *et al.* 1999).

These intrinsic mechanisms that pattern the cortex are just beginning to be elucidated. It is currently thought likely that there are several patterning centres that control regionalisation of the telencephalon (recently reviewed (Rubenstein and Beachy 1998; Rubenstein *et al.* 1998; Ragsdale and Grove 2001; Zaki *et al.* 2003)). The basic regionalisation in the developing forebrain is discussed here.

Anterior neural ridge and anterior-posterior specification

The earliest definitive step in cortical regionalisation is mediated by an organizer at the rostral most end of the developing embryo known as the anterior neural ridge (ANR). This forms after neural induction and is found at the junction between the anterior neural plate and the anterior non-neural ectoderm. Removal of the ANR from explants resulted in a failure to express the winged helix transcription factor *Foxg1* (also known as *Brain Factor 1* or *BF1*)(Tao and Lai 1992; Shimamura and Rubenstein 1997). *Foxg1* is normally expressed in the developing neural tube in the progenitor population at the rostral end (Tao and Lai 1992). In addition, *Foxg1* homozygous null mutants die at birth and have a dramatic reduction in the size of the cerebral hemispheres (Xuan *et al.* 1995).

Interestingly the ANR also expresses the gene *fibroblast growth factor 8 (FGF8)* (Crossley and Martin 1995; Shimamura and Rubenstein 1997). FGF8 is a secreted

signalling polypeptide and ectopic expression of FGF8 protein is capable of inducing *Foxg1* expression, suggesting that FGF8 may regulate the development of anterolateral neural plate derivatives. However, in the *Foxg1* mutant mice some cortical tissue remains so there must be more unknown factors involved in establishing the cortex (Xuan *et al.* 1995; Shimamura and Rubenstein 1997; Dou *et al.* 1999; Storm *et al.* 2003).

As well as inducing the anterior neural plate to become telencephalon, these signalling processes can influence later anterior-posterior organisation in the telencephalon. An anterior increase in FGF8 signalling results in a posterior shift in cortical areal boundaries, a decrease in FGF8 signalling results in an anterior shift in these boundaries, and the introduction of a posterior source of FGF8 results in partial areal duplications (Fukuchi-Shimogori and Grove 2001).

Dorsal Ventral specification

Dorsal-ventral (DV) patterning mainly occurs later than anterior-posterior patterning. The earliest event is the induction of the floor plate at the ventral midline of the neural tube. At telencephalic levels this is influenced by the prechordal plate. The prechordal plate is an axial mesendoderm derivative of the node (its role was recently reviewed (Kiecker and Niehrs 2001)). The importance of the floor plate and the notochord in dorsoventral patterning of cell differentiation along the dorsoventral axis was shown in the chick neural tube by grafting an additional notochord or floor plate into ectopic positions, or by deleting both cell groups. These resulted in

changes in the fate and position of neural cell types, defined by expression of specific antigens, suggesting that the differentiation of neural cells is controlled, in part, by their position with respect to the notochord and floor plate (Yamada *et al.* 1991). More specifically it has been shown that the vertebrate hedgehog-related gene *Sonic hedgehog (Shh)* is expressed in the notochord and the floor plate (Echelard *et al.* 1993). Ectopic expression of *Shh* in the mouse developing central nervous system led to the activation of floor plate-expressed genes suggesting that *Shh* may play a role in the normal inductive interactions that pattern the ventral central nervous system(Yamada *et al.* 1991; Echelard *et al.* 1993). In addition, once the floor plate is induced it then expresses *Shh* as well(Yamada *et al.* 1991). *Shh* mutants lack basal telencephalic structures and have defects in the establishment and maintenance of midline structures such as the notochord and floor plate (Chiang *et al.* 1996). The role of the secreted Shh glycoprotein signalling molecule as an important molecule in DV patterning in the developing forebrain has been recently reviewed (Monuki and Walsh 2001 ; Schuurmans and Guillemot 2002; Muzio and Mallamaci 2003).

Interestingly, loss of *Foxg1* leads to specific loss of *Shh* expression in the ventral telencephalon(Huh *et al.* 1999). This is consistent with dorsal-ventral specification probably following the anterior-posterior specification. However, the role of the *Shh* is not straightforward. *Nkx-2.1* homeobox gene (a transcription factor) expression is restricted to the forebrain (Price *et al.* 1992; Shimamura *et al.* 1995; Qiu *et al.* 1998). Loss of *Nkx-2.1* leads to a dorsalization of the pallidal parts of the basal ganglia (Sussel *et al.* 1999). Furthermore, *Shh* has been shown to induce *Nkx2.1* expression (Barth and Wilson 1995; Ericson *et al.* 1995; Pera and Kessel 1997; Shimamura and

Rubenstein 1997; Qiu *et al.* 1998). Interestingly, analysis of *Nkx-2.1* mutants showed that the histogenesis of the major cortical subdivisions appear normal, although the telencephalic expression of *Shh* is almost eliminated (Sussel *et al.* 1999). Thus this suggests that *Shh* expression within the forebrain is not essential for cortical regionalisation.

In the developing mouse-forebrain members of the *cubitus interruptus (ci) Gli* zinc-finger-containing gene transcription factor family have been implicated as transducers of the *Shh* signal (Matise *et al.* 1998). Loss of *Gli 1* and *2* function have no discernable telencephalon phenotype(Park *et al.* 2000). However, in *Gli3* mutants ventral telencephalic markers expand dorsally into the cortex (Grove *et al.* 1998; Theil *et al.* 1999; Park *et al.* 2000; Rallu *et al.* 2002). This is opposite to the phenotype observed in *Shh* mutants and suggests that a balance between the two may be important in the establishment of DV patterning in the telencephalon.

Dorsal midline roof plate

Dorsal structures, such as the roof plate and the adjacent nonneural ectoderm, also function to confer DV identities to early neuroectodermal cells (Lee and Jessell 1999). The roof plate expresses members of the bone morphogenetic protein (BMP) family of secreted molecules (recently reviewed (Monuki and Walsh 2001; Ragsdale and Grove 2001)). Recent *in vitro* evidence indicates that BMPs from the roof plate regulate dorsal telencephalic expression of the homeodomain transcription factor *Lhx2*(Monuki *et al.* 2001). If the roof plate is ablated genetically in mouse embryos,

Lhx2 expression extends dorsally and expression levels are greatly reduced in cortex, which is diminished in size(Monuki *et al.* 2001). The importance of BMP signalling for local patterning of the dorsal midline has also been shown *in vivo* using a CRE/loxP approach to disruption the BMP receptor type 1a in the telencephalon (Hebert *et al.* 2002). In addition, ectopic application of BMPs into the neural tube has been shown to dorsalize the chick telencephalon (Golden *et al.* 1999).

Interestingly, ectopic expression of BMPs in tissue explants has been shown to repress *Foxg1* expression(Furuta *et al.* 1997). Furthermore, in *Foxg1* mutants BMPs are ectopically expressed in the telencephalon (Dou *et al.* 1999). This suggests there is interplay between *BMP* and *Foxg1* in the regionalisation of the telencephalon.

Cortical hem

Another important dorsal signalling centre is the cortical hem. This lies along the medial edge of the cortex between the hippocampus and choroid plexus (Figure 1.3). The cortical hem has been shown to expresses several *Bmp* and *Wnt* genes (recently reviewed (Ragsdale and Grove 2001)). *Wnt* genes like *BMP* genes code for secreted molecules that have been implicated in cell signalling in other areas of embryonic development. For example, *Wnt3a* is normally expressed at the cortical hem and mutations in this gene result in near complete deletion of the hippocampus (archicortex) (Lee *et al.* 2000).

The exact mechanism by which molecules from signalling centres surrounding and within the developing telencephalon initiate the anterior-posterior and dorsal-ventral patterning effects and exert their subsequent actions on cell morphogenesis is still unknown. Many transcription factors are expressed in telencephalic sub regions (some have been described above) and experiments on mutant mice have contributed to an understanding of the functional importance of these factors (recently reviewed (Monuki and Walsh 2001; Ragsdale and Grove 2001; Rallu *et al.* 2002; Schuurmans and Guillemot 2002)). Therefore, it seems likely that the regional activation of transcription factors in the telencephalon is an important intermediate step. One such transcription factor is the homeobox containing transcription factor, *Pax6*. Pax6 has not only been shown to have a role in forebrain regionalisation but also in development of many structures of the developing embryo including the eye and pancreas. It is the study of this transcription factor and its downstream targets that forms the topic for this thesis.

The transcription factor PAX6

Pax6 is a member of a family of transcription factors characterised by the presence of an N-terminal 128 amino acid DNA binding domain, the paired box. This domain is divided into two helical sub-domains called PAI and RED that can each bind DNA independently (Jun and Desplan 1996). Nine murine and human paired box genes have been identified to date (Callaerts *et al.* 1997). Separated from the paired box by a 78 amino acid glycine-rich linker sequence is a second 60 amino acid DNA binding domain, the homeobox. These two domains can interact independently and cooperatively with DNA. At the C-terminal of Pax6 is a 153 amino acid proline-

serine-threonine (PST) rich domain that is thought to be the transcriptional regulatory domain (Figure 1.4).

Pax6 is expressed in the retina, lens and cornea of the developing vertebrate eye (Walther and Gruss 1991; Grindley *et al.* 1995). It is also expressed at a range of developmental stages in regions of the forebrain, hindbrain, cerebellum, the ventral neural tube and the pancreatic islet cells (Walther and Gruss 1991; Stoykova and Gruss 1994; Grindley *et al.* 1995; St-Onge *et al.* 1997; Warren and Price 1997; Kioussi *et al.* 1999). The expression pattern of *Pax6* in the embryonic central nervous system is summarised in Figures 1.5 and 1.6.

Humans heterozygous for mutations in *PAX6* suffer from aniridia (iris hypoplasia), which is associated with cataracts, lens dislocation, foveal dysplasia, optic nerve hypoplasia and nystagmus (Jordan *et al.* 1992; Glaser *et al.* 1994). The vast majority (92%) of known *PAX6* mutations in humans are nonsense mutations (Hanson *et al.* 1999). A rare case of an infant with a compound heterozygous mutation in *PAX6* suffered severe craniofacial and central nervous system defects, had no eyes, no adrenal glands, and died neonatally, a phenotype similar to the homozygous null mutation in mice (Glaser *et al.* 1994).

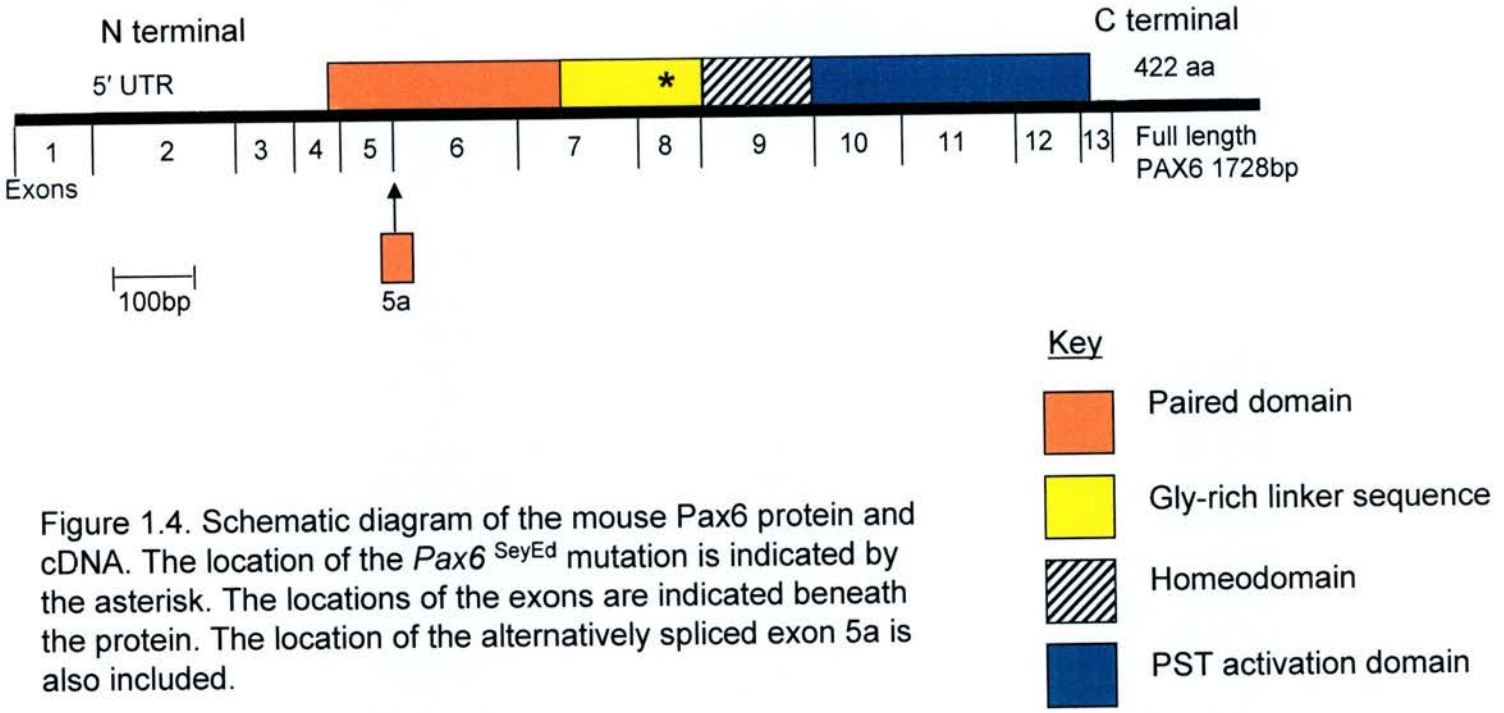

Figure 1.4. Schematic diagram of the mouse Pax6 protein and cDNA. The location of the *Pax6* ^{SeyEd} mutation is indicated by the asterisk. The locations of the exons are indicated beneath the protein. The location of the alternatively spliced exon 5a is also included.

Figure 1.5. A summary of the main sites of expression of Pax6 (shaded) during murine central nervous system development. (A) Shows expression of *Pax6* at E8-8.5 in regions of the anterior neural plate that will become telencephalon (t), eyes (e) and diencephalon (d). The domain of *Pax6* expression has a sharp posterior boundary at the border between diencephalon and mesencephalon (m). The neural plate folds in the directions shown by the curved arrows to form the forebrain vesicles. (B) Shows a coronal section cut through the left telencephalic vesicle at E11.5-E12.5; the section is at the level indicated by an arrow in (A), with dorsal at the top. Within the telencephalon, expression of *Pax6* is found in the ventricular zone of the dorsal telencephalon, in the neuroepithelium of the intermediate territory (separating the dorsal and ventral telencephalon), and in a stripe of cells linking this territory with *Pax6*-expressing cells in the basal part of the ventral telencephalon (in the region of the amygdala). The dorsal telencephalon contains the presumptive neocortex and the ventral telencephalon contains the ganglionic eminences, or striatum. (C) + (D) Show parasagittal sections through the forebrain at E12.5-E14.5, at approximately the level shown by an arrow in (A); anterior is at the top, ventral is to the left, dorsal is to the right and abbreviations are as in (A). It is as if the diagram in (A) were to be folded and then viewed from its left-hand side. As the embryo develops, diencephalic expression becomes more restricted. These summary diagrams are taken from a recent review on Pax6 Simpson *et al.*, (2002).

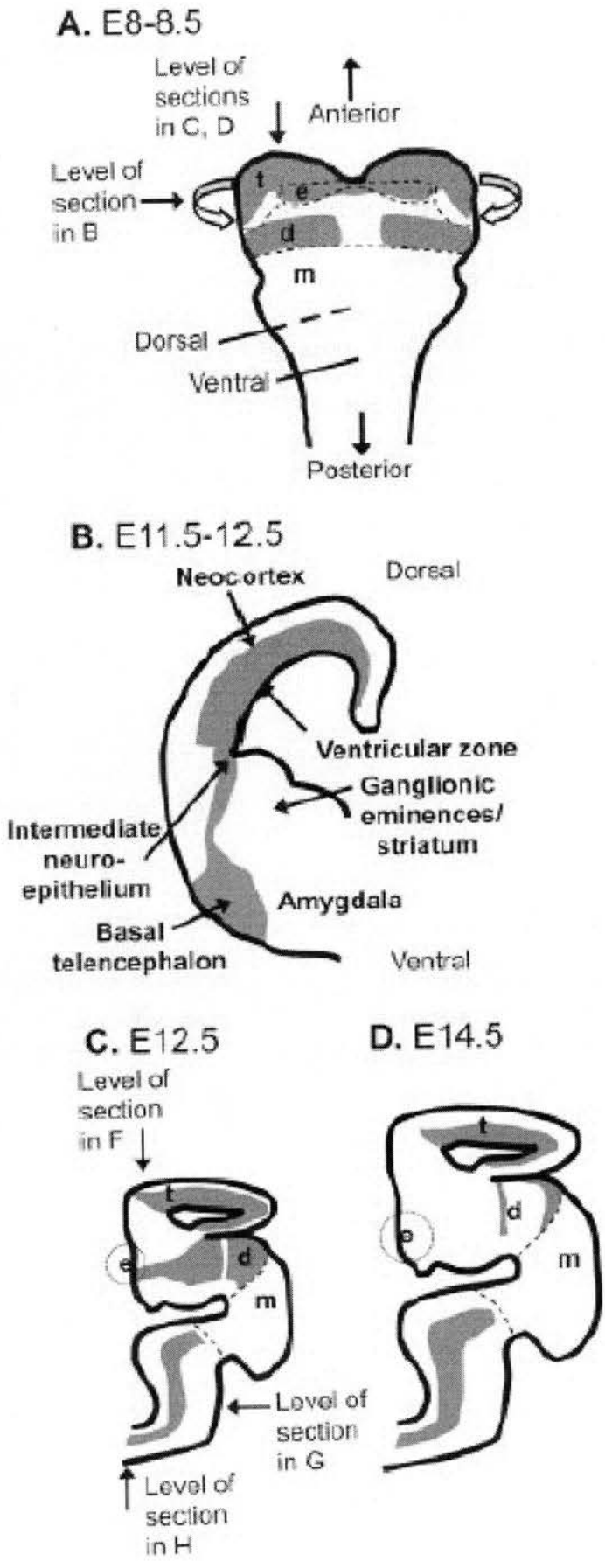
A. E8-8.5
Level of sections in C, D
Anterior
Level of section in B
t
e
d
m
Dorsal
Ventral
Posterior
B. E11.5-12.5
Neocortex
Dorsal
Ventricular zone
Ganglionic eminences/ striatum
Intermediate neuro-epithelium
Amygdala
Basal telencephalon
Ventral
C. E12.5
Level of section in F
t
e
d
m
Level of section in G
Level of section in H
D. E14.5
t
d
e
m

Figure 1.6. (E): A section at a similar level and plane to that in B, but at E15.5 and showing not just telencephalon but also diencephalon. Thalamocortical axons grow from the dorsal thalamus, penetrate the ventral thalamus, avoid the hypothalamus, travel dorsal to the amygdaloid region and enter the cortex. Although Pax6 is expressed throughout the neuroepithelium of the thalamus at ages up to E12.5, subsequently it becomes restricted to the ventral thalamus. F,G,H: Sections cut at E12.5 in the planes indicated in C, showing expression of Pax6 in (F) the olfactory epithelium and eye, G: the hindbrain or rhombencephalon (sm, somatic motor neurons), and (H) the spinal cord. These summary diagrams are taken from a recent review on *Pax6* (Simpson,*et al* 2002).

E. E15.5

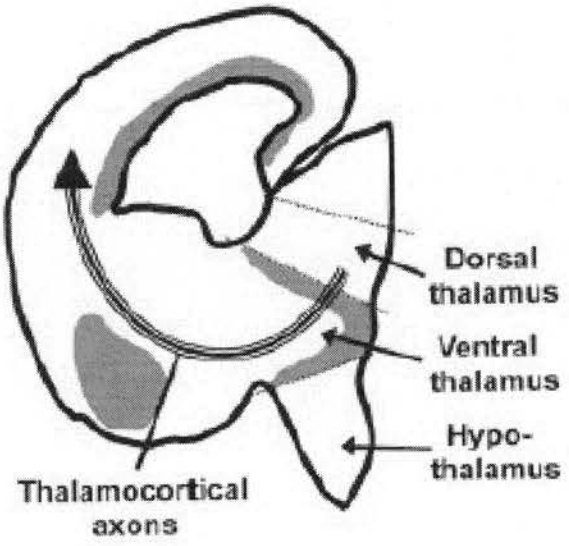

F. E12.5

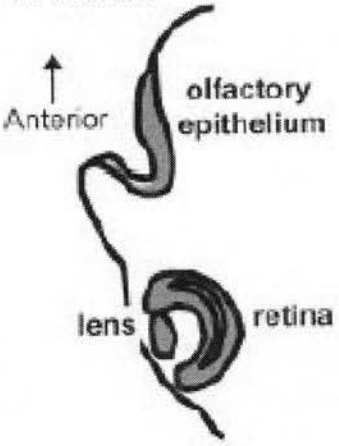

G. E12.5

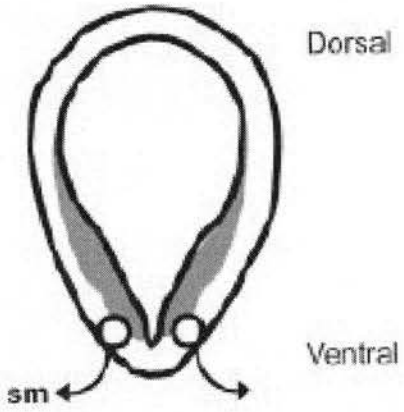

H. E12.5

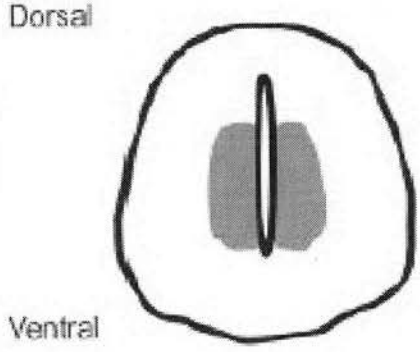

Pax6 mutation in the mouse results in the *Small eye* (*Sey*) phenotype. At least eight alleles of *Pax6* have been identified in the mouse so far (Glaser *et al.* 1990; Hill *et al.* 1991; St-Onge *et al.* 1997; Lyon *et al.* 2000). A premature stop codon (marked on Figure 1.4) in the linker domain generates the $Pax6^{SeyEd}$ allele (Hill *et al.* 1991). Heterozygous mice have a reduced eye size, iris hypoplasia, corneal opacification, and cataracts. Homozygotes die immediately after birth with no eyes, no nasal structures and severe brain abnormalities, including malformed cerebral cortex (Hogan *et al.* 1986; Hill *et al.* 1991; Schmahl *et al.* 1993; Caric *et al.* 1997). The diencephalon is reduced in size, is not differentiated to a normal extent (Stoykova *et al.* 1996; Warren and Price 1997), and fails to innervate the cortex (Pratt *et al.* 2000).

Vertebrates primarily express two alternatively spliced isoforms of *Pax6* that differ by the presence or absence of exon 5a that encodes an additional 14 amino acid residues within the paired domain (Figure 1.4). This insertion changes the DNA-binding specificity of the paired domain and has been proposed as a means of modifying the downstream target genes of the transcription factor(Epstein *et al.* 1994; Kozmik *et al.* 1997). The isoform containing the extra exon is denoted here as *Pax6+5a*. The ratio of canonical *Pax6* mRNA to *Pax6+5a* mRNA seems to vary in different tissues; this has been observed in bovine (Jaworski *et al.* 1997) and in mice (Richardson *et al.* 1995). Unlike *Pax6*-null mice that exhibit anopthalmia with central nervous system defects and lethality, 5a isoform-null mice had iris hypoplasia and defects in the cornea, lens, and retina (Singh *et al.* 2002). Interestingly two human cases with eye defects have been described that have a missense mutation in

the 5a isoform (Nanjo *et al.* 2004). This requirement of the 5a isoform is believed to be evidence that the evolution of this isoform contributed to advanced features of the vertebrate eye (Singh *et al.* 2002). However, recent evidence has emerged that the Notch signal promotion of growth of the eyes in the invertebrate *Drosophila* is through the *Pax6*-like gene *eyegone* (*Eyg*), which has a truncated paired domain (Dominguez *et al.* 2004). Like the vertebrate *Pax6+5a* isoform, *eyegone* recognises DNA exclusively through the C-terminal sub region of the paired domain (Dominguez *et al.* 2004). The two other *Drosophila Pax6* genes are *eyeless* (*ey*) and *twin of eyeless* (*toy*).

A role for Pax6 in forebrain development

In *Pax6*$^{-/-}$ mice both the cortical ventricular zone and the subventricular zone are enlarged (Schmahl *et al.* 1993; Stoykova *et al.* 1996; Caric *et al.* 1997). In addition, the cortical plate is thinner and within the intermediate zone (i.e. between the subventricular zone and cortical plate) there are large collections of cells characteristic of those in the subventricular zone. Cumulative labelling with bromodeoxyuridine (BrdU) has revealed that proliferative rates in the early *Pax6*$^{-/-}$ embryonic cortex increase (Estivill-Torrus *et al.* 2002). In addition, proliferating cells in S phase are found scattered throughout the ventricular zone, suggesting either a failure in interkinetic nuclear migration or asynchronous cycling of precursor cells in the mutant cortex (Gotz *et al.* 1998; Estivill-Torrus *et al.* 2002). Birth dating studies with BrdU *in vivo* show that many later-born neurones fail to migrate to the cortical plate and accumulate in the subventricular zone (Caric *et al.* 1997).

Immunohistochemical analysis of neurone-specific class III β-tubulin isotype (TuJ1), an early marker for postmitotic neurones (Lee *et al.* 1990), has shown that cells in *Pax6*$^{-/-}$ mutant cortices that fail to migrate do begin neuronal differentiation (Caric *et al.* 1997). There is a similar defect in Small eye rats (*rSey*): the E20 cortices have an abnormal clustering of cells in the ventricular and intermediate zones of the cortex (Fukuda *et al.* 2000).

Not all cells in the ventricular zone express *Pax6*; rather, expression appears to be localised to a subset of radial glial cells (Gotz *et al.* 1998). In *Pax6*$^{-/-}$ embryos, the morphology of radial glial cells is altered. At E15.5, wild-type radial glia have straight processes running towards the pial surface whereas mutant radial glial processes appear wavy and have frequent small extrusions and branches (Gotz *et al.* 1998). Co-culture experiments mixing E13.5 *Pax6*$^{-/-}$ cortical cells and wild-type cells failed to rescue the phenotype of mutant radial glial cells suggesting that the defect may be cell-autonomous (Gotz *et al.* 1998). Work over the past few years has shown that radial glial cells are able to generate not only glial cells but also neurons (Campbell and Gotz 2002). In cultures of *Pax6*$^{-/-}$ radial glial cells, less neural clones and more non-neural clones were produced than in cultures of wild-type radial glial cells (Heins *et al.* 2002). Furthermore, *in vivo* quantification showed a 50% reduction of radial glial-derived neurones in the *Pax6*$^{-/-}$ cortex at E14 and E16 (Heins *et al.* 2002). Infecting cells from E14 *Pax6*$^{-/-}$ cortex with a retroviral vector containing full length *Pax6* cDNA increased the number of differentiated neurones and appeared to reduce proliferation (Heins *et al.* 2002). These findings suggest that Pax6 may play a cell-autonomous role driving radial glial cells to produce cells of a neuronal fate.

Some defects in the developing central nervous system of *Pax6*$^{-/-}$ embryos are not due to a direct cell-autonomous requirement for Pax6 in the affected process. Transplantation of *Pax6*$^{-/-}$ cortical precursors into a wild-type cortical environment can rescue their migrational defect, suggesting that it may be secondary to defects of other cells such as radial glia which normally guide migration (Caric *et al.* 1997). Abnormally high levels of cell death among late-embryonic *Pax6*$^{-/-}$ dorsal thalamic cells are most likely secondary to the inability of these cells to obtain trophic support from the cerebral cortex, to which they do not connect (Lotto *et al.* 2001).

A role for Pax6 in cortical regionalisation

The basic principle of cortical regionalisation was introduced above. Moving along the developing telencephalic wall in a dorsal to ventral direction the telencephalon is divided into two distinct parts; the pallium and the subpallium. The area of the pallium that meets the subpallium is the ventral pallium. The part of the subpallium that meets the pallium is called the dorsal lateral ganglionic eminence (dLGE) (see Figure 1.3). In the absence of Pax6, cell migration from the subpallium into the cortex is strongly enhanced, whereas migration from the pallium into the subpallium is affected much less(Chapouton *et al.* 1999). This change in cell migration must be due to changes in the expression of downstream targets from *Pax6*. Furthermore, this demonstrates *Pax6* has a role to play in cortical regionalisation. In wild type mice *Dlx1* and *Vax1* are usually expressed in the subpallium and not in the pallium(Valerius *et al.* 1995). In *Pax6* mutant mice *Dlx1* and *Vax1* expression is

found in the pallium (Stoykova *et al.* 1996; Hallonet *et al.* 1998; Yun *et al.* 2001). In addition, in the wild type the expression domains of the basic helix-loop-helix transcription factors, *Mash1*(*Ascl1*) and *Neurogenin 1* (*Ngn1*; also known as *Neurod3*), *Ngn2* (also known as *Atoh4*; *Atonal homolog 4*) are expressed in a defined dorsoventral pattern, with *Mash1* expressed at high levels in the developing ganglionic eminence and *Ngn1/2* restricted to the developing cortex (Gradwohl et al., 1996; Ma et al., 1997). In *Pax6* mutants the expression of *ngn1*, *ngn2*, and *Mash1* are completely changed; *ngn1* and *ngn2* expression is reduced dorsally and *Mash1* is no longer confined to the subpallial area and is expressed in the neuroepithelium of the ventral and lateral pallium (Stoykova *et al.* 2000; Toresson *et al.* 2000).

This progressive dorsal spread of gene expression from the subpallium structures of the dLGE into the pallium is consistent with *Pax6* being involved in the correct dorsoventral regional specification of the developing telencephalon(Toresson *et al.* 2000; Yun *et al.* 2001; Muzio and Mallamaci 2003). In turn this specific expression of Pax6 affects region-specific phenotypes, such as the migratory behaviour of neurons(Casarosa *et al.* 1999; Fode *et al.* 2000).

Gsh2 is a homeobox containing transcription factor and is expressed in subpallial progenitor cells (Valerius *et al.* 1995). In *Pax6* mutants *Gsh2* expression is found to have expanded from the subpallium into the pallium (Valerius *et al.* 1995). Interestingly, in *Gsh2* mutants there is a reduction in the size of the LGE and a loss of *Dlx2* expression in the LGE but not a loss in the MGE (Szucsik *et al.* 1997; Yun *et al.* 2001). Also *Ngn2* expression is expanded ventrally into the dLGE (Yun *et al.*

2001). In the absence of *Ngn2*, *Mash1* is ectopically expressed in the dorsal telencephalon while most other ventral transcription factors do not expand dorsally(Fode *et al.* 2000). This demonstrates that many genes are also necessary for the maintenance of gene expression in telencephalic progenitors.

Pax6 is expressed in a gradient in the developing cortex. It is low-caudal-to-high-rostral and low-medial-to-high-lateral (Walther and Gruss 1991; Bishop *et al.* 2000; Bishop *et al.* 2002). Conversely, *Emx2* a vertebrate homologue of the *Drosophila* head gap transcription factor *ems,* is expressed in a gradient that is high-caudal-to-low-rostral and high-medial-to-low-lateral(Gulisano *et al.* 1996). These opposing expression patterns suggest there may be an interplay to confer regionalisation to the developing neurones of the cortex. In the *Emx2* mutants rostral areas are expanded and caudal areas are contracted, which is the opposite effect seen in *Pax6* mutants (Bishop *et al.* 2000). Analysis of *Emx2* mutant mice demonstrate that, like *Pax6* mutants, there are specific changes in gene expression patterns and area-specific connections between the cortex and thalamus(Bishop *et al.* 2000; Bishop *et al.* 2002). In addition, analysis of double *Pax6* and *Emx2* mutants shows a similar affect on these regionalised genes(Muzio and Mallamaci 2003). In the double mutant the cortex is largely absent but there were residual signs of a cortex. Pallium specific gene *Ngn1* and *Ngn2* were absent, but there was expression of the subpallium genes *Vax1*, *Dlx1*, *Gsh2* and *Mash1* (Muzio and Mallamaci 2003). This indicates a dorsal to ventral transformation in the telencephalic specificity (Muzio and Mallamaci 2003).

A role for Pax6 in diencephalon patterning

From E10.5 onwards *Pax6* expression is seen extending from the telencephalon into the diencephalon up to a sharp caudal boundary thought to be where the future morphological boundary between the prosencephalon and mesencephalon forms(Walther and Gruss 1991). *Pax6* mutants lack this morphological boundary and some gene expression in the caudal prosencephalon (such as *Lhx1* and *Gsh1*) is lost and *Dbx* expression which is typical of the mesencephalon is expanded rostrally into the prosencephalon(Mastick *et al.* 1997). This could indicate that the caudal prosencephalon is possibly partially transformed into mesencephalic fate and so demonstrates that *Pax6* may play a role in establishing this boundary.

In *Pax6* homozygous mutants the anterior posterior pattern of gene expression in the diencephalon is relatively normal (Stoykova *et al.* 1996; Warren and Price 1997). *Vmaz2*, *HbnF*, are normally expressed in the dorsal thalamus (Lebrand *et al.* 1998; Pratt *et al.* 2000). In wild types *Lhx1* (also known as *Lim1*) and *Nkx2.2* are expressed in the diencephalon but not in the dorsal thalamus. In the *Pax6* homozygous mutant they are now expressed in the dorsal thalamus (Pratt *et al.* 2000). This indicates that *Pax6* may have a role in conferring a dorsal identity in the developing thalamus.

A role for *Pax6* in eye development

An important role of *Pax6* in eye development was indicated by its early expression in all structures of the developing eye from E8.5 (Walther and Gruss 1991).

Moreover, there is compelling evidence that Pax6 is necessary for eye formation in vertebrates.

In mice the *Pax6* homozygous *Small eye* (*Sey*) mutant completely lacks eyes (Hill *et al.* 1991). Similarly, in humans, compound *PAX6* heterozygotes have no eyes (Glaser *et al.* 1994). This important role for *Pax6* in eye development has been recently reviewed (Ashery-Padan and Gruss 2001; Pichaud and Desplan 2002). Expressing too much Pax6 protein also generates a similar phenotype to that of heterozygous mutants (Schedl *et al.* 1996).

The refractive properties of the lens are dependent on the accumulation of high concentrations of water-soluble proteins known collectively as crystallins (Bloemendal and de Jong 1991). *Pax6* has been shown to contribute to the transcriptional activation of several crystallin genes: in the lens placode chicken δ1-crystallin (Cvekl *et al.* 1995) and mouse αB-crystallin (Gopal-Srivastava *et al.* 1996); and in the lens, guinea pig ζ-crystallin (Richardson *et al.* 1995) and mouse αA-crystallin (Cvekl *et al.* 1995).

Using the cre/loxP approach to inactivate *Pax6* in the eye surface ectoderm, it was shown that *Pax6* activity was essential for correct lens placode formation (Ashery-Padan *et al.* 2000). Initially expression of *Pax6* was detected in the surface ectoderm at E9 but was no longer detectable by E9.5. Initial lens induction occurred in the mutant but further development of the lens was arrested.

Work in the last ten years has suggested that *Pax6* function in eye development seems to have been at least partially conserved between invertebrates and vertebrates. This was first suggested when it was identified that *eyeless (ey)* of *Drosophila*, *Small eye* of the mouse, and human aniridia are encoded by homologous genes (Quiring *et al.* 1994). Later it was shown that expression of mouse *Pax6* or *Drosophila ey* in *Drosophila* imaginal discs resulted in the formation of ectopic eyes (Halder *et al.* 1995). Ectopic expression of *Pax6* in *Xenopus* animal caps was also shown to be sufficient for lens induction (Altmann *et al.* 1997). Further, misexpression of *Pax6* in *Xenopus laevis* can induce a small but fully differentiated ectopic eye (Chow *et al.* 1999). More recently, expression of the human *PAX6+5a* isoform induced strong eye overgrowth when expressed in *Drosophila*, whereas expression of canonical *PAX6* acted primarily on the specification and differentiation of eye cells *in vivo* (Dominguez *et al.* 2004).

Pax6 has also be shown to be required later in uncommitted retinal cells, retinal progenitor cells (RPCs), to retain their pluripotencey, thereby mediating the full retinogenic potential of RPCs to generate the different cell types that compose the retina (Marquardt *et al.* 2001). Examples of the retina cells generated from RPCs are retinal ganglion cells, cones, and rods.

A role for Pax6 in hindbrain/spinal cord patterning

Pax6 expression is first detected in the presumptive hindbrain at E8.5 (Walther and Gruss 1991). However, Pax6 expression in the metencephalon is not seen until E15,

when it is seen in the external granular layer and in cells distributed in the dorsal cerebellum (Walther and Gruss 1991).

In the spinal cord onset of *Pax6* expression is coincident with neural tube closure at E8.5 (Walther and Gruss 1991). Expression extends along the entire anteroposterior axis up to the rhombencephalic isthmus and is mainly restricted to mitotically active cells in the ventral ventricular zone (Walther and Gruss 1991). At this stage neural differentiation in the spinal cord has not yet occurred and so *Pax6* expression could affect neural differentiation here (Walther and Gruss 1991). Interestingly in the spinal cord there is a characteristic DV pattern, with specific classes of neurons differentiating according to their DV position. Not only are different cell types produced according to their DV position but also they emerge at different times. As well as having a role in regionalisation of the forebrain *Shh* was first shown to be very important for determining the DV pattern of the spinal cord and hindbrain. For example *Shh* induces hindbrain progenitors to produce motor neurones (Ericson *et al.* 1995). More recent work has identified that *Pax6* is a key intermediary in the *Shh* dependent control of neuronal subtype identity in the ventral spinal cord and hindbrain (Ericson *et al.* 1997). Elimination of *Pax6* resulted in a dorsal to ventral transformation in the identity of ventrally located progenitor cells and a consequent change in motor neuron fate (Burrill *et al.* 1997; Ericson *et al.* 1997). This has also been seen in the hindbrains of *Pax6* homozygous mutant rats where the somatic motor (SM) neurones were found to be missing (Osumi *et al.* 1997).

In the myelencephalon of the hind brain *Pax6* expression is very similar to expression in the spinal cord (Walther and Gruss 1991). Essentially, *Pax6* is expressed most abundantly in the ventricular zone (Walther and Gruss 1991). As with the spinal cord it has been suggested that *Pax6* may be involved in regulating the specification of the ventral neurones by establishing the correct progenitor domains (Takahashi and Osumi 2002).

Regulation of *Pax6* transcription

The *PAX6* gene is spread over 22kb of chromosome 11 in humans. Figure 1.7 shows a schematic of the gene locus. The next 5′ gene to *PAX6* is *reticulocalbin 1 precursor* (*RCN1*), which is 340kb upstream. The next 3′ gene to *PAX6* is *elongation protein 4 homolog* (*ELP4*) previously called *Pax6 neighbour gene* (*PAX6NEB*). This gene runs antisense to *PAX6* and the final exon (exon 12) is 6kb 3′ to the last exon *PAX6*. The canonical translation start point for *PAX6* is in exon 4 (Glaser *et al.* 1992).

Figure 1.7. The genomic organisation of the *PAX6* locus. Red boxes are the *PAX6* exons. The yellow box is exon 5a. Blue boxes are the 3' exons of the antisense neighbour gene *ELP4*. The extent of the *PAX6* locus included in the two YACs (Y589 and Y593) is indicated. P/EE is the pancreas/ectoderm enhancer. P0 and P1 are promoters 1 and 2. a is the alpha element. NRE is the neuroretina enhancer. CE1, CE2, and CE3 are the intron 7 regulatory elements. E100+ (Box 123) and HS234 are long range highly evolutionary conserved elements. SIMO is the most distant human patient breakpoint. The extent of these regions is indicated by the horizontal black bars. T0, T1, Ta, and arrow heads are three of the transcription start sites.

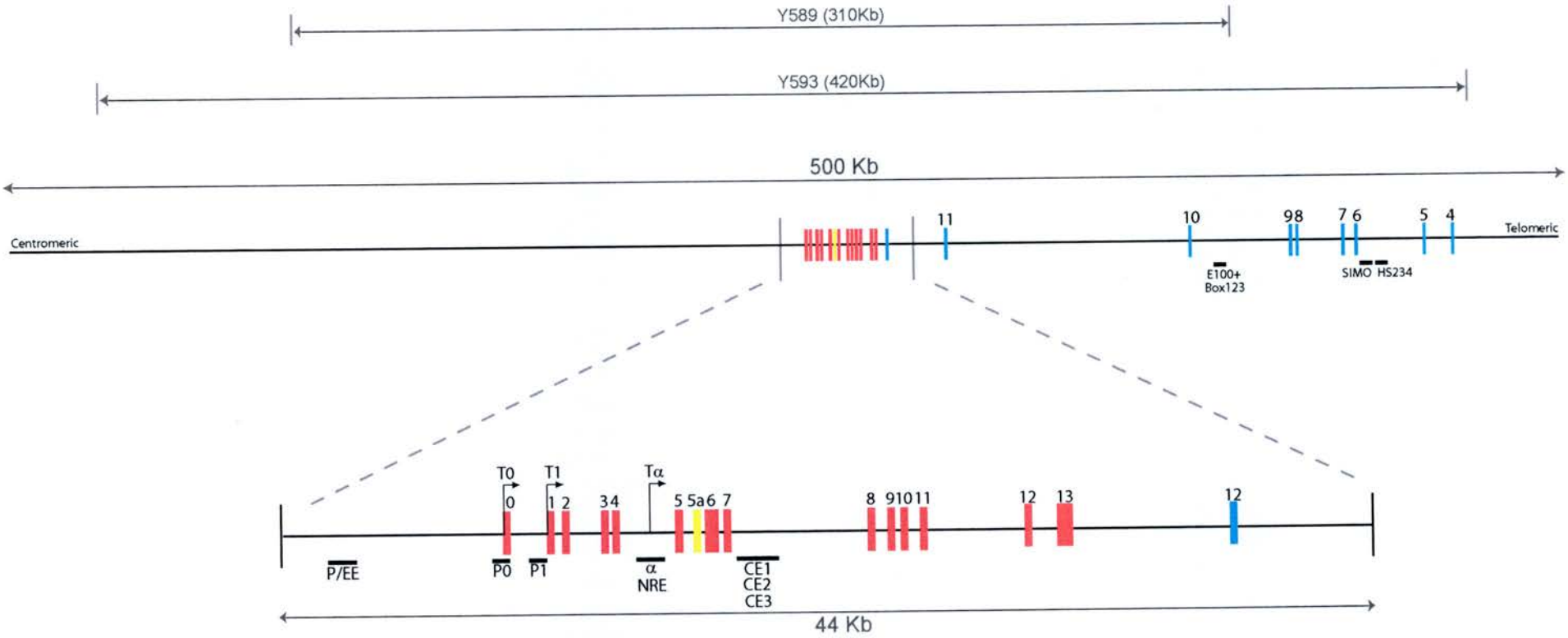
Y589 (310Kb)
Y593 (420Kb)
500 Kb
Centromeric
Telomeric
11
10
98
7 6
5 4
E100+
Box123
SIMO HS234
T0
T1
Tα
0
1 2
3 4
5 5a 6 7
8 9 10 11
12 13
12
P/EE
P0
P1
α
NRE
CE1
CE2
CE3
44 Kb

Transcription start site T1 and promoter P1

In 1992 a *PAX6* cDNA sequence that contained 14 exons (exon 1 to 5, 5a, and 6 to 13) was identified (Glaser *et al.* 1992). A few years later in 1997, using a combination of primer extension and RNase protection, a transcripton initiation site was identified 108bp upstream of this cDNA sequence (Xu and Saunders 1997). In this region several candidate promoter sites were identified and their activity tested using promoter and enhancerless β-galactosidase vectors. One 92bp region was found to be required for basal level *PAX6* promoter activity. This promoter site is indicated on Figure 1.7 as P1 and the transcription start site indicated by T1 and the arrowhead.

Transcription start site T0, exon 0, and promoter 0

In 1999 several *Pax6* cDNAs were identified (Xu *et al.* 1999). Some contained either exon 1 or exon 0 at their 5′ end. Studies using *in situ* hybridisation identified that the two set of transcripts are differentially expressed during brain and eye development (Xu *et al.* 1999). Further studies using transgenic mice generated using the promoters and β-galactosidase demonstrated the elements direct gene expression in distinct regions (Kammandel *et al.* 1999; Xu *et al.* 1999). The additional transcriptional start site is marked as T0 and by the arrowhead on Figure 1.7. Earlier studies in quail identified two promoters in quail *Pax6* (designated P0 and P1) that generated two transcripts with different 5′UTRs (Dozier *et al.* 1993; Plaza *et al.* 1995).

NRE and Pα

Comparison of nucleotide sequence identity between human, quail and mouse identified a highly conserved 216bp element in *Pax6* intron 4 (Plaza *et al.* 1995). Further *in vitro* cell culture work identified that this functions as an enhancer in quail neuroretina cells (Plaza *et al.* 1995). This element is identified on Figure 1.7 as NRE.

β-galactosidase transgenic mice generated with the 216bp element in either orientation and either promoter P0 or P1 showed identical expression patterns in the eye distinct from those conferred by the P0 or P1 alone (Kammandel *et al.* 1999; Xu *et al.* 1999). Mice generated with just the 216bp element failed to produce any β-galactosidase suggesting that the element had no promoter activity itself (Kammandel *et al.* 1999).

Similar transgenic mice experiments with a human PAX6 promoter and the human 216bp conserved sequence (designated by this group as ele4H) showed that it functioned as a spinal cord-specific enhancer (Xu and Saunders 1998). The β-galactosidase was expressed at the thoracic and lumbar levels of the spinal cord when it was linked to a functional PAX6 promoter; again the element had no promoter activity on its own (Xu and Saunders 1998).

Using a combination of primer extension, RT-PCR, and genomic sequencing a transcription start site was identified in intron 4 (Kammandel *et al.* 1999). This is marked on Figure 1.7 with Tα and an arrowhead. The exact function of the 216bp element is still controversial. Kammandel *et al,* (1999) describe the element as exon α. Xu *et al.* (1999) described it as an enhancer. The same element has also been

described as neuroretina enhancer (NRE) (Van Heyningen and Williamson 2002). However, Kleinjan *et al.* (2004) referred to it as a promoter and Anderson *et al.* (2002) as an exon, exon/enhancer and putative promoter.

P/EE

Construction of transgenic mice with a 341bp piece of *Pax6* located approximately 3.5 kb upstream of the most proximal promoter (PO) of the *Pax6* gene faithfully reproduced the expression of Pax6 in the pancreas, surface ectoderm, lens, cornea, conjunctiva, and lachrymal gland (Williams *et al.* 1998). This regulatory element is designated pancreas/ectoderm enhancer (marked as P/EE on Figure 1.7). Similar work confirmed that only 340bp of the fragment was necessary to reproduce the expression (Kammandel *et al.* 1999). Further generation of mice with truncated versions of this fragment found that a 107 bp fragment can reproduce the cornea and lens expression (Kammandel *et al.* 1999). However, some ectopic expression was also observed. This suggested that the 341 bp fragment might contain a regulatory repression sequence.

Sequence alignment between the human and mouse *Pax6* genes identified the region is 93% identical; this is further evidence of conservation of *Pax6* transcriptional regulatory elements (Williams *et al.* 1998).

CE1, CE2, and CE3

Control elements 10kb downstream from P0 and P1 have been identified. Genomic sequence comparisons between human, mouse, pufferfish, and zebrafish have

identified three conserved *cis*-regulatory elements in intron 7: CE1; CE2; and CE3 (Kleinjan *et al.* 2004). These elements are shown on Figure 1.7. Transgenic mice made with these elements and β-galactosidase have demonstrated that they regulate gene expression within distinct tissues (Kleinjan *et al.* 2004). EMSA on nuclear extracts from the *Pax6* expressing cell line ARPE showed that Pax6 can bind to a site in CE2 (Kleinjan *et al.* 2004). As well as demonstrating the longer range of Pax6 control elements it is evidence that Pax6 can directly regulate its own expression.

Alternative translation start sites

Pax6 expression has been more recently complicated by the finding of more possible translational start sites. Examination of the *Pax6* open reading frame revealed four additional possible ATG translation start sites in exons 7 and 8 downstream from the ATG in exon 4. Truncation of quail *Pax6* to remove the first ATG in exon 4 and then *in vitro* transcription experiments produced 32 and 33KDa proteins that are consistent with proteins made from some of these internal ATG sites (Carriere *et al.* 1995). More recently, a potential antisense transcript has been identified (Anderson *et al.* 2002). The transcript is believed to begin at the α element but to run antisense to the previously identified transcript. A protein product has not been identified.

Other control elements

Other, less well described elements have also been identified in the Pax6 locus. A potential silencer element was identified in the region surrounding P1, approximately 1.5kb to 2.5kb upstream of *PAX6*. No single element was identified and it was suggested that a combination of elements controlled the expression of

PAX6. Later analysis of human *PAX6* sequence with transient transfection assays in glioblastoma cells and leukemia cells confirmed the presence of a human *PAX6* transcriptional silencer (Xu and Saunders 1997). This silencer seemed to have different activities in different cell types (Xu and Saunders 1997). In addition, a 5kb fragment between promoters P0 and P1 seemed to control expression in the telencephalon, hindbrain, and spinal cord (Kammandel *et al.* 1999).

Experiments using electrophoretic mobility shift assays (EMSA) and co-immunoprecipitation of nuclear extracts have identified protein-DNA interactions between other upstream transcription factors and *PAX6* (Zheng *et al.* 2001). These led to the identification of a 57bp *cis*-regulatory element in exon 1 of the human *PAX6* gene, designated exon 1 enhancer (EIE) (Zheng *et al.* 2001). Protein-DNA interactions have also been investigated in quail. DNA foot printing experiments identified a binding site for the quail Pax6 (Pax-QNR) protein within the promoter region (Plaza *et al.* 1993). Thus Pax-QNR can potentially *trans*-activate its own promoter (Plaza *et al.* 1993).

Long range control elements

Genomic sequence comparisons have also identified long-range control elements in humans, mice and *Fugu* (Griffin *et al.* 2002). The sequence comparison between humans, mice and *Fugu* identified a 3′ cis-regulatory region, Box123, as an enhancer 100kb from the 3′ end of *Pax6* (Griffin *et al.* 2002). This was confirmed by expression studies in mice (Griffin *et al.* 2002). The location of Box123 in human *PAX6* is shown in Figure 1.7 as E100+.

Interestingly there are also a few cases of PAX6 mutations in humans where the mutation in *PAX6* has been found several hundred kilobases away from the *PAX6* transcriptional start site. Firstly, in 1995 two aniridia patients were identified in which the *PAX6* gene is not disrupted but in both cases a chromosomal breakpoint was found at least 85 kb distal of the 3' end of *PAX6* (Fantes *et al.* 1995). In 1996 another aniridia case was identified where the breakpoint lay between the *PAX6* locus and a region approximately 100 kb distal to *PAX6* (Crolla *et al.* 1996). Again no detectable deletion was found within *PAX6*, suggesting again that the aniridia may have resulted from the distal chromatin domain containing either enhancers or regulators (Crolla *et al.* 1996). Later, two more human aniridia patients were found to have deletions 11kb away from the 3′ end of *PAX6* (Lauderdale *et al.* 2000). 3′ RACE data strongly suggested it was *PAX6* transcription rather than mRNA stability that was causing the disease (Lauderdale *et al.* 2000).

Transgenic mice made using a 310kb YAC (YAC Y589) that contains human *PAX6* and flanking regions in which the 3′ end of the YAC ends approximately 100kb 3′ to *PAX6* , failed to rescue *Pax6 Small eye* phenotype in mice (Figure 1.7) (Kleinjan *et al.* 2001). Further evolutionary sequence comparison and DNaseI hypersensitivity analysis identified a region more than 150 kb distal to the major *PAX6* promoter P1 containing regulatory elements (Kleinjan *et al.* 2001). This is indicated in Figure 1.7 as HS234. Previously a 420kb YAC Y593 containing human *PAX6* and flanking regions was shown to rescue mouse homozygous *Small eye* lethality (a schematic of the extent of the YAC is shown in Figure 1.7) (Schedl *et al.* 1996). YAC Y593

extends well beyond the most distant human patient breakpoint, SIMO, identified so far (Figure 1.7).

In summary, regulation of *Pax6* transcription is extremely complex and not fully understood. Regulatory elements are spread over a very considerable distance. Importantly YAC Y593 has been functionally proven to include all of the necessary elements for the correct expression of *PAX6* (Schedl *et al.* 1996).

Regulation of transcription by *Pax6*

As described above *Pax6* has been shown to affect cell proliferation, migration, differentiation, adhesion, and signalling(Caric *et al.* 1997; Gotz *et al.* 1998; Campbell and Gotz 2002; Estivill-Torrus *et al.* 2002; Heins *et al.* 2002). These effects are brought about through the changes in expression in downstream genes, either direct targets of Pax6 or indirectly. Some target genes have a distinct function in cellular behaviour; others, such as transcription factors, have a broader effect on cellular behaviour. Many potential target genes have been identified by virtue of changes in their expression level in animals lacking functional *Pax6*. In addition, studies using micro arrays of eye mRNA from various *Pax6* over-expressing and null mutant cells have shown changes in the expression of around 400 genes(Chauhan *et al.* 2002; Chauhan *et al.* 2002). There are some examples of direct binding of Pax6 to down stream targets. Accordingly, the following discussion on some of the known targets of Pax6 is grouped by two mechanisms by which Pax6 has been shown to function. The first way is by the Pax6 protein binding to regulatory elements in the DNA of a downstream gene and either activating or repressing transcription. The

transactivating function associated with the C-terminal region of *Pax6* has been demonstrated by the fusion of the proline-, serine-,and threonine-rich C-terminal domain of sea urchin and mouse *Pax6* to the DNA-binding domain of the yeast GAL4 transcription factor and subsequent activation of GAL4-responsive(Czerny and Busslinger 1995). Similar results were obtained with GAL4-human *Pax6* fusion proteins (Glaser *et al.* 1994). Transcriptional repression by Pax6 has been most closely described in the crystallin genes(Chauhan *et al.* 2002).

The second method by which *Pax6* has been shown to regulate the transcription of other genes is by the Pax6 protein binding to another protein, a binding partner, and then modulating transcription of a downstream target. To further complicate the mechanism by which Pax6 regulates transcription some evidence has emerged of Pax6 protein binding to both regulatory DNA elements in a gene and other proteins involved in the transcription of the downstream gene. Both of these methods of function are discussed in turn here.

Pax6 Binding targets

As has been discussed above, Pax6 contains two distinct DNA binding motifs, the paired domain and the homeodomain. These DNA binding domains can bind the target DNA either independently or cooperatively. Figure 1.8 is a diagram showing the consensus binding sites. The original sites were suggested based on comparing *Pax6* sequence homology between different species and comparing the *Pax6*

A) The paired domain(without exon 5a)

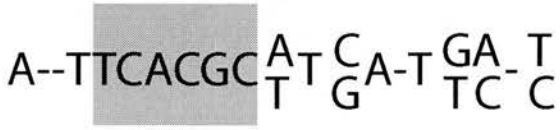

B) The paired domain(including exon 5a)

ATGCTCAGTGAATGTTCATTGA

C) The homeodomain

FIGURE 1.8. Pax6 DNA binding consensus sites. A) Paired domain without exon5a (Epstein et al., 1994. The grey box is the core motif. B) Paired domain including the extra 14 amino acids coded by exon5a (Epstein et al., 1994). C) Homeodomain DNA binding sequence (Wilson et al., 1995).

sequence with other genes containing DNA binding domain. More recently, the DNA-binding sites have been demonstrated to function *in vitro* (Epstein *et al.* 1994; Wilson *et al.* 1996). In addition, the paired domain binding has been confirmed by X-ray crystallography (Xu *et al.* 1999).

A) Crystallins

The *Pax6* regulation of crystallin genes has been mentioned already above in the section about eye development. Crystallins, which make up 80–90% of the soluble protein of the lens, are the most numerous set of genes known to be targets of Pax6(Simpson and Price 2002). Many have dual functions, both as components of the refractive properties of the lens and also as either metabolic enzymes or heat shock proteins(Piatigorsky 1998). Evidence of a direct interaction between Pax6 protein and crystallin genes has been demonstrated in the promoter of αA-crystallin by electrophoretic mobility shift assays (EMSA) studies(Cvekl *et al.* 1995). Subsequent co-transfection experiments demonstrated that Pax6 highly activates the promoter of αA-crystallin (Cvekl *et al.* 1995)

β-crystallin gene is an example of a target that appears to be repressed by *Pax6*. Co-transfection of *Pax6* expression constructs into chick retinal epithelial cells led to >90% reduction in reporter gene expression driven from the β-crystallin promoter(Duncan *et al.* 1998). In this experimental system, deletion of the C-terminal transactivation domain of Pax6 in the expression construct did not ablate repression, suggesting a critical role for the paired and/or homeodomains. *Pax6* also appears to repress γF- and γE-crystallin promoters when studied in transient

transfections(Kralova *et al.* 2002). Interestingly, *in vivo* studies have demonstrated that Pax6 interacts with the chicken δ1-crystallin enhancer at two sites, one acting as a positive element while the other represses expression (Muta *et al.* 2002).

Regulation of the crystallin genes by *Pax6* also provides an illustration of a second complexity of Pax6 biochemical control. The eye predominantly expresses the isoform of Pax6 lacking exon 5a (Jaworski *et al.* 1997). This isoform binds preferentially to a promoter element of the ζ-crystallin gene at a site that is highly similar to the consensus paired domain binding sequence (Epstein *et al.* 1994; Richardson *et al.* 1995; Jaworski *et al.* 1997). This preference for binding the *Pax6* isoform lacking exon 5a allows high levels of ζ-crystallin to be expressed specifically in the eye rather than in other regions where the *Pax6* exon5a splice forms are more equally represented.

B) Regulation of cell adhesion molecules by Pax6

The expression patterns of some adhesion molecules are altered in *Pax6* mutants. Expression of the extracellular matrix molecule tenascin-C (TN-C) at the cortico-striatal boundary is abolished and the expression of some cadherins (calcium dependent adhesion molecules) is altered in the cortex (Stoykova *et al.* 1997; Bishop *et al.* 2000). The expression domain of the homophilic adhesion molecule R-cadherin and that of Pax6 have some overlap (Ganzler and Redies 1995; Matsunami and Takeichi 1995) and, in the absence of functional Pax6, expression of R-cadherin mRNA is reduced considerably in areas that normally

show co-expression (Stoykova *et al.* 1997). Expression of P120 catenin ($p120^{ctn}$), a member of the armadillo family of proteins implicated in cell-cell adhesion and signal transduction, and Paxillin, a focal adhesion adapter protein implicated in integrin mediated signalling pathways, are highly elevated. Expression of N cadherin and α catenin are both slightly elevated, α5 integrin and β1-integrin accumulate in lens although E cadherin and α6 integrin expression appears normal (Duncan *et al.* 2000).

There is evidence to suggest that Pax6 protein may directly interact with the regulatory elements of genes encoding adhesion molecules. The gene for neural cell adhesion molecule (N-CAM) has a Pax6 paired-domain binding region within its promoter(Holst *et al.* 1997). In addition, Pax6 activates the expression of L1-luciferase reporter constructs in neuroblastoma cells(Meech *et al.* 1999). Although this and other studies suggests an interaction between Pax6 and the cell adhesion molecule L1, which regulates axonal guidance and fasciculation during development (Chalepakis *et al.* 1994; Meech *et al.* 1999; Honig *et al.* 2002), the interaction is likely to be complex. For example, the expression domains of Pax6 and L1 only partially overlap and it has been shown that there is no change in L1 expression in the intermediate, ventricular and subventricular zones of E19 *Pax6*$^{-/-}$ mice(Caric *et al.* 1997).

In summary, a large body of evidence indicates that Pax6 regulates the expression of cell surface molecules mediating cell-cell adhesion and signalling. Many of the developmental processes in cortical and eye development require

correct cell adhesion and signalling. For example, when wild-type and homozygous *Pax6*^{Sey} cells are mixed in either *in vitro* aggregation assays or in chimaeric animals, they segregate from each other. This has been observed in tissues including the eye and forebrain and indicates that *Pax6* exerts a strong influence on the molecular composition of the cell membrane(Quinn *et al.* 1996; Stoykova *et al.* 1997; Warren *et al.* 1999). Defects in cell adhesion and signalling may explain some of the abnormalities, including the restriction of cells within discrete territories, defective cell migration and axon growth, seen in the cortex of animals lacking *Pax6*.

c) Keratins

Cellular morphology and adhesion are also affected by *Pax6* mediated effects on the expression of a number of structural eye genes. Keratins contribute to intermediate filaments and are expressed by many different types of epithelial cells throughout development. In most epithelial cells a basic keratin is coexpressed and paired with an acidic keratin. The expression of keratins is characteristic of the epithelial tissue. For example, expression of *keratin complex 1, acidic gene 12* (*Krt1-12*) is restricted to the corneal epithelium(Liu *et al.* 1999). In cotransfection experiments using human corneal epithelial cells *Pax6* has been shown to up regulate the *Krt1-12* promoter(Liu *et al.* 1999).

d) Transcription factors

As described earlier many transcription factors have altered expression patterns in *Pax6* mutants. Regulating the expression of other transcription factors allows for complex changes in individual cell behaviour and characteristics. There is

evidence that Pax6 can directly affect expression of several transcription factor genes. The basic helix-loop-helix family members *Mash1*, *Math5* and *Ngn2* are known to play important roles in cell lineage determination and differentiation during embryonic development(Guillemot 1999). As mentioned above, in *Pax6* mutants the expression of these transcription factors is altered. Pax6 has been shown to bind directly to sequences in the enhancers and promoters of *Mash1*, *Math5* and *Ngn2* (Marquardt *et al.* 2001; Scardigli *et al.* 2001).

e) Finally, the *Pax6* gene itself contains putative Pax6 binding sites within some of its regulatory elements. This may mean Pax6 is able to regulate its own expression (Plaza *et al.* 1993). Indeed, Plaza et al (1993) showed that quail Pax6 can bind to and transactivate its own promoter in a cell culture assay.

Protein-Binding targets

The chick δ-crystallin gene contains an enhancer site designated DC5 (Kamachi and Kondoh 1993). This has been shown to have lens specific activity that is dependent on the binding of SOX2 protein in the presence of a previously unknown protein(Kamachi *et al.* 1995). This protein has been recently demonstrated to be Pax6 (Kamachi *et al.* 2001). Not only are both transcription factors required to be bound for the activation of chick δ-crystallin gene but Pax6 protein and SOX2 protein were shown *in vivo* and *in vitro* to be able to bind each other (Kamachi *et al.* 2001). Furthermore the DNA binding site in DC5 is distinct to the Pax6 consensus

binding site and in the absence of SOX2 Pax6 binds to it 25-fold less efficiently to the Pax6 consensus binding sequence (Kamachi *et al.* 2001).

gelB is a member of the matrix metalloprotease (MMP) family of zinc proteases and is important in eye development (Sivak *et al.* 2004). gelB has been demonstrated by EMSA to contain two Pax6 binding sites(Sivak *et al.* 2004). Pax6 via its paired domain has been shown to bind to one (Sivak *et al.* 2004). The other site has been shown by gel shift assays and immunoprecipitation to bind the protein complex of Pax6 bound to the transcription factor AP-2α(Sivak *et al.* 2004). The binding of Pax6 to AP-2α was demonstrated by deletion series to be via the Pax6 C-terminal activation domain(Sivak *et al.* 2004).

Immunoprecipitation experiments have demonstrated that Pax6 binds to retinoblastoma protein via the Pax6 homeodomain. (Cvekl *et al.* 1999). Retinoblastoma protein/Pax6 complexes were found in lens nuclear extracts and it has been suggested that Pax6 and retinoblastoma protein may have a role in controlling epithelial cell division, fiber cell elongation, and crystallin gene expression during lens development. (Cvekl *et al.* 1999).

The *glucagon* gene is expressed in the pancreatic endocrine α-cells of the pancreatic islets. Caudal-related factor 2 (cdx2) and Pax6 can bind the G1 element of the *glucagon* promoter and transactivate expression (Hussain and Habener 1999). Interestingly, isolated nuclear extracts have been found to contain several protein complexes, one of which contained Pax6 protein in a heterodimer with the cdx2

protein(Ritz-Laser *et al.* 1999). It has also been demonstrated that Pax6 protein can bind to cdx-2/3 protein in the absence of DNA (Ritz-Laser *et al.* 1999). Furthermore, cdx2 and Pax6 have also been shown to bind with p300 in a transcription complex (Hussain and Habener 1999).

The transcription of *glucagon* is further complicated by the emerging evidence that *Maf,* a member of a family of transcription factors containing a basic region leucine zipper DNA-binding domain, may be involved. It has also been found that Pax6 binding to the glucagon transcription element G1 is enhanced by the presence of Maf (Planque *et al.* 2001). A binding site has been identified in the G1 promoter and demonstrated to be bound to and activated by Maf family members(Planque *et al.* 2001). However, binding of Maf protein to G1 is not required for G1 activation (Planque *et al.* 2001). It is possible that Maf has a role in interacting with the Pax6 protein. Furthermore Maf transcription has itself been shown to be regulated by Pax6 during vertebrate eye development in *in vitro* studies (Sakai *et al.* 2001). Analysis with EMSA and DNase 1 footprinting has shown that there are at least three Pax6-binding sites located in the 5′-flanking and 5′-non-coding regions of the *Maf* gene(Sakai *et al.* 2001). *Maf* has also been shown to play an important role in the cellular differentiation of several other tissues (Blank and Andrews 1997). In addition, it is possible that the interactions of Maf and Pax6 vary depending on which tissue they are expressed in.

Identifying characteristics of cells capable of expressing *Pax6*

Clearly Pax6 affects many cellular processes via interactions of downstream targets through a number of different mechanisms. One way of understanding these processes is to investigate the role of Pax6 using tissue culture experiments. Currently if cells are collected for cell culture experiments, cells are dissected from tissues, invariably resulting in heterogeneous cell populations. A transgenic mouse with green fluorescent protein (GFP) as a reporter for the gene *Sox1* has recently been made and fluorescence activated cell sorting (FACS) used to separate *Sox1* positive cells from *Sox1* negative (Aubert *et al.* 2003). A similar approach could be used to isolate highly purified populations of *Pax6* expressing cells.

By designing a transgenic mouse that expresses a marker (such as GFP) in all cells that express Pax6, bins of cells expressing *Pax6* can be identified by FACS using the GFP signal. Alternatively, resistance to antibiotics, for example neomycin resistance, could be used to isolate a purified cell population. Creating discrete homogenous *Pax6* expressing cell populations will allow investigation of cell proliferation, differentiation, cell signalling, and factors that affect *Pax6* expression and function both up-stream and down-stream without the extraneous non *Pax6* expressing cells interfering with the analysis. Crossing such a '*Pax6* reporter' mouse with mice with a different status of *Pax6* (e.g. $Pax6^{+/+}$, $Pax6^{+/-}$, $Pax6^{-/-}$, conditional *Pax6*, etc) will enable bins of cells with different levels of Pax6 protein to be analysed.

Influence of Pax6 levels on target gene expression

A mass of experimental evidence has been presented above, showing that Pax6 alters the expression of many downstream targets. One approach to rapidly identifying candidate downstream targets is the use of micro arrays to examine gene expression changes in isolated mRNA from wild type and *Pax6* mutants. One study using a micro array has been conducted on different tissues from wild type and *Pax6* mutants and identified 400 possible targets in the developing eye(Chauhan *et al.* 2002; Chauhan *et al.* 2002).

In order for the changes in expression to be meaningful the tissue that the mRNA comes from must be exactly the same tissue in both the wild type and the mutant. However, in homozygous null mice this creates an obvious problem for the analysis of the roles of Pax6 in tissues such as the corneal epithelium and retina that never form in the mutants. This means analysis of later roles during the differentiation of the lens and olfactory epithelium is not possible.

One way to purify large numbers of *Pax6* expressing cells is to use cells collected from the *Pax6* reporter mouse and sort them by FACS. The two populations of cells will be purified populations of *Pax6* expressing cells and non-*Pax6* expressing cells.

For instance if the reporter mouse is bred onto a *Pax6* mutant background to derive the genotype $Pax6^{+/-}$:Pax6 Reporter and this is in turn bred with $Pax6^{+/-}$ and the embryos collected then a full range of Pax6 status can be investigated (see Table 1.1 for details of the genotypes of the embryos and the six bins that could potentially be

Embryo	Genotype of embryo	Endogenous *Pax6* status	Description of bins of cells generated from each embryo by FACS sort by GFP signal			Bin number
			GFP +ve or - ve cells	Cells able to express Pax6?	Cells actually producing Pax6 protein?	
1	$Pax6^{+/+}$:Pax6 Reporter	$Pax6^{+/+}$	+ve	Yes	Yes	1a
			-ve	No	No	1b
2	$Pax6^{+/-}$:Pax6 Reporter	$Pax6^{+/-}$	+ve	Yes but heterozygous mutants	Yes but from heterozygous cells	2a
			-ve	No	No	2b
3	$Pax6^{-/-}$:Pax6 Reporter	$Pax6^{-/-}$	+ve	Yes but homozygous mutants	No*	3a
			-ve	No	No*	3b

Table 1.1 Table of bins of cells of interest from the cross of $Pax6^{+/-}$:Pax6 Reporter mice and $Pax6^{+/-}$ mice. (* Analysis possible until near birth).

isolated from the FACS). Bins 1a, 2a, and 3b all have the same upstream signals activating *Pax6* but they each have a different *Pax6* status and hence a different Pax6 protein status. This means bin 1a cells are wild-type *Pax6* expressing cells. Bin 2a contains cells capable of *Pax6* expression but the cells are *Pax6* heterozygotes and hence may have a difference in amount of Pax6 protein produce compared to the wild-type. Bin 3a contains cells capable of *Pax6* expression but the cells are *Pax6* homozygotes and hence no Pax6 protein is produced. Collecting mRNA from these bins of cells and comparing gene expression with micro arrays will reveal what difference the amount of Pax6 protein is making to the cells and hence will help understand the role of Pax6. The original tissue that was used as the source of cells could be as crude as whole brain or whole eye, or come from a dissection such as the telencephalon. The benefits of this system are:

1. The cells are homozygous populations since the FACS sorts each cell one by one.
2. This experimental system separates the up stream signals that are regulating *Pax6* expression from the downstream targets of Pax6.

These are powerful gains over other techniques in identifying candidate targets of *Pax6* and will greatly aid in contributing to the emerging understanding of the role of *Pax6* in transcription regulation. Once these candidate genes have been identified then other techniques should be used to understand the mechanism further. For example EMSA could be used to demonstrate whether Pax6 is directly regulating the candidate gene transcription or not.

More complex analysis of the role of Pax6 in gene regulation is possible by breeding the Pax6 reporter with other mutants, for instance, either a *Gsh2* or *Emx2* mutant, and then using the Pax6 reporter to identify cells capable of expressing Pax6 in the telencephalon. This will be of immense interest in understanding the interacting roles of these three genes in regionalising the telencephalon; particularly when the reporter is bred onto a double knock-out of *Gsh2* and *Pax6* or *Emx2* and *Pax6*. Dissection of the telencephalon from the double knock outs on a Pax6 reporter background and purifying the Pax6 capable cells by FACS will allow identification of changes in gene targets. A previous study using double knock-outs of *Gsh2* and *Pax6* or *Emx2* and *Pax6* was complicated by the absence of a cerebral cortex (Muzio and Mallamaci 2003). Extreme anatomical changes as a result of mutations make it difficult to be accurate with dissection and so complicates the isolation of cells. This makes analysis of mRNA changes to identify changes in gene expression difficult. However, if the Pax6 reporter is used then the actual Pax6 capable cells in the mutants can be identified rapidly and accurately by FACS rather than having to estimate where the cortex and the striatum would have formed, as was necessary in Muzio *et al.*, 2001 study, and then isolate this "cortex"-like and "striatum"-like tissue by assumed anatomical features which will result in heterogeneous cell populations. In the Muzio *et al.*, 2001 study the tissue could have been prepared for *Pax6* mRNA *in situ* using a label that is stable for single cell dissociation and FACS analysis and then the Pax6 positive cells identified and mRNA isolated for identifying down stream targets. However, once generated the Pax6 reporter can be bred onto any viable mutant background and Pax6 capable cells rapidly identified.

Examining autoregulation of Pax6

One of the downstream targets of Pax6 is potentially *Pax6* itself. As described above, the transcription regulatory elements for Pax6 are extremely complex and there is emerging evidence that expression of *Pax6* may be, in part, regulated by Pax6 itself. Direct binding of Pax6 protein to Pax6 control elements was first demonstrated with quail Pax6 protein(Plaza *et al.* 1993). Autoregulation of Pax6 has been mostly investigated in the developing eye. It has been shown that Pax6 regulates its own expression in the presumptive lens ectoderm (Grindley *et al.* 1995). Pax6 is initially detected in a broad area of the head surface ectoderm before the lens placode has appeared. Later expression is more concentrated in the lens placode and lens vesicle. It has been shown *in vivo* that *Pax6* in the prospective lens ectoderm is itself required in the ectoderm for sustained *Pax6* gene transcription. Detailed analysis of chimeric mouse embryos consisting of $Pax6^{-/-}$ and wild type cells indicates that *Pax6* auto regulates during lens development in a cell autonomous fashion(Quinn *et al.* 1996; Collinson *et al.* 2000). It has been demonstrated using reporter assays that the *Pax6* enhancer is activated by Pax6 (Aota *et al.* 2003). This interaction may be complicated by a role of Sox2/3 co-binding to the *Pax6* enhancer (Aota *et al.* 2003).

In transgenic mice that express a reporter gene, such as GFP, under the control of the *Pax6* regulatory elements the level of GFP intensity and hence *Pax6* expression in individual cells could be established using FACS. In addition, by breeding the reporter mouse to other animals with a different status of Pax6 this would allow rapid

quantification of *Pax6* expression levels across different Pax6 protein status. More specifically, you could tell:

a) If the absolute number of cells expressing *Pax6* changes with Pax6 status.

b) If the same number of cells are expressing *Pax6* but at a different expression level.

Autoregulation of *Pax6* has only been described in the developing eye to date. However, it is possible that autoregulation occurs in other tissues, including forebrain, but has not yet been documented.

Making a 'Pax6 reporter' transgenic mouse

Transgenic reporter strains

Many reporter transgenic mice have been developed for many genes using a variety of strategies, each with its own advantages and limitations. For a recent review of reporter transgenic mice see (Kisseberth *et al.* 1999; Naylor 1999). Several reporter genes are available. A very commonly used reporter gene used is *lacZ.* This is a bacterial gene that encodes the protein β-galactosidase. The expression pattern is visualised by fixing and then staining tissue from the transgenic animal. The most commonly used chemical substrate for visualising β-galactosidase activity is X-gal. Other reporter genes commonly used that require chemical substrates are chloramphenicol acetyltransferase (CAT), horseradish peroxidase (HRP), *Luciferase,* and human placental alkaline phosphatase (hPLAP). An alternative to using reporter genes that require a chemical substrate for visualisation is GFP. Since the tissue and cells require no prior fixing or the addition of a substrate, the expression pattern in living cells can be identified. Also since no intermediary substrate is needed, and

hence no signal amplification used, the level of gene expression can be examined by measuring the GFP fluorescence.

Whichever reporter gene is used, transgenic mice are particularly useful because they provide both temporal and spatial information about a particular gene product, even at a single cell level (discussed more below). Other typical uses of reporter transgenic include analysing the activity of *cis*-acting genetic elements such as enhancer and promoters as described above for *Pax6*. This is not the only way to examine the activity of these elements but it is a commonly used technique. They have also been used to characterise receptors and their ligands; for example, the use of the Ca^{2+} -sensitive photoprotein aequorin as a reporter (Stables *et al.* 1997). Changes in intracellular Ca^{2+} as a result of ligand binding are visualised as flash response (Stables *et al.* 1997). They are also a convenient way to identify cells that have come from a particular animal in chimeras.

There are basically two types of reporter transgenic mouse. The first is generated using homologous recombination in ES cells to introduce reporters such as β-galactosidase or GFP into the gene of interest; commonly known as "knock-in" transgenic animals. The reporter gene is placed into the open reading frame of the gene of interest. This has been done previously with *Pax6*: a "knock-in" mouse $Pax6^{tm1pgr}$ was made with β-galactosidase placed into the translational start site in exon 4. This placed β-galactosidase under the control of the endogenous promoter and enhancers (St-Onge *et al.* 1997). It was found that the β-galactosidase activity in heterozygous embryos was identical to the expected *Pax6* expression. However, this

has a clear disadvantage that because the *Small eye* mutation is caused by *Pax6* haploinsufficiency, and the β-galactosidase reporter sequence disrupts one of the copies of *Pax6,* the animal is now *Pax6* heterozygous and therefore a *Small eye* mutant. In such mice it is not possible to study the expression pattern in wild-types.

A way round the problem of creating a heterozygous mutant with this type of transgenic is to use an internal ribosome entry site (IRES). An IRES is believed to allow the translation of two cis genes from a single transcript by a cap-independent recruitment of the 40S ribosomal subunit to the mRNA (recently reviewed (Vagner *et al.* 2001)). The strategy is to place the IRES into the 3′ untranslated region (3′ UTR) of the gene of interest. Downstream to the IRES a reporter gene is placed and the reporter gene should be expressed in the same cells that are expressing the gene of interest. Since the IRES reporter is not placed into the open reading frame of the gene of interest this strategy is less likely to create a heterozygous mutant. This approach has been successfully used to make a reporter transgenic for the gene *Oct-4* (Mountford *et al.* 1994). In this transgenic the IRES and the reporter gene β-galactosidase were introduced into the 3′ UTR of *Oct-4*. The disadvantage of using this technique with a gene with many control elements dispersed over a large area, such as with *Pax6,* is that it may be difficult to find a position where the insertion of the IRES reporter will have no effect on the expression of *Pax6.* A second disadvantage is that some reports have indicated that there can be problems with reduced expression of the 3′ cistron (recently reviewed (Kozak 2003)). Thus the IRES driven expression of the reporter gene may be at a level either too low to be detectable or useful.

The second type of transgenic animal is the addition transgenic. These are commonly made by pronuclear microinjection of a DNA construct into fertilised mouse eggs. The construct contains promoter and enhancer elements of the gene of interest, and a suitable reporter gene such as β-galactosidase or GFP. Thus, in theory the reporter gene will be expressed at the same time and in the same place as the endogenous protein. However, genes often have more than one set of promoters and enhancers. Many of these are tissue or temporally specific and so control a subset of the overall expression pattern. This approach has been successfully used with *Pax6* by making reporter transgenic lines with some of the *cis* elements from *Pax6* and β-galactosidase (Kammandel *et al.* 1999; Xu *et al.* 1999; Kleinjan *et al.* 2004). As described above it is now known that *Pax6* has several long range control elements, some as much as 200kb away from the *Pax6* locus.

Many possible vectors are available: plasmid; bacteriophage; cosmid; PAC (P1-derived artificial chromosome); BAC (Bacterial artificial chromosome); YAC. Each one has a size limitation which limits the length of genomic sequence that can be included with the reporter gene. Plasmids, bacteriophage and cosmids can hold 40-50kb of DNA (Peterson *et al.* 1997). PACs and BACs have been reported to contain as much as 300kb (Huxley 1998). YACs can contain up to about 2MB of DNA (Peterson *et al.* 1997).

There is already a YAC (YAC Y593) containing the human *PAX6* gene that has been demonstrated to contain enough of the surrounding genomic sequence to rescue *Pax6*

mutant mice (Schedl *et al.* 1996). Therefore, I decided to modify the YAC Y593 by the introduction of a reporter gene, and then generate an addition transgenic mouse with the modified YAC, generating a '*Pax6* reporter' mouse. The detailed design of the '*Pax6* reporter' YAC transgenic is discussed in detail in Chapter 2 and 3. Briefly, a GFP and neomycin resistance cassette was placed under the control of *PAX6* regulatory elements. Importantly the *PAX6* gene in the YAC is disrupted so that it is no longer able to produce PAX6 protein from the main canonical translational start site in exon 4.

When this modified YAC integrated into the mouse genome it integrated at a distant position away from the endogenous *Pax6* gene; an addition transgenic. This meant it would not affect endogenous *Pax6* expression, unlike alternative strategies that use either a reporter gene inserted into the endogenous gene (commonly known as a "knock-in") or an IRES reporter inserted into the 3′UTR. This should mean that every cell capable of expressing *Pax6* will also express GFP and be neomycin resistant. More specifically in *Pax6* $^{-/-}$ mice even though no functional Pax6 protein is thought to be expressed, the cells that have upstream signals activating the mutated endogenous *Pax6* gene will also activate the reporter gene so the cell will be labelled with GFP regardless of the fact no functional Pax6 protein is actually being produced. Therefore, this novel tool should allow the identification and isolation of *Pax6* expressing cells, independent of any mutation at the endogenous *Pax6* locus, thereby helping to understand the normal function of Pax6. This means the '*Pax6* reporter' mouse could be mated with mice with any *Pax6* status to identify those cells that are capable of expressing *Pax6*. Further, by incorporating a neo selectable

marker under the control of *Pax6*, the reporter mouse will allow isolation and purification of *Pax6* expressing cells in vitro.

Making YAC transgenics

There are several different ways to transfer the YAC into the mouse embryo and these techniques can be divided into two groups. The first group requires the isolation of the YAC DNA from the rest of the yeast endogenous chromosomes and then the transfer of the DNA into the cell, usually by lipofection or microinjection. The second way is to do yeast spheroplast-cell fusion. This obviates the need to isolated YAC DNA and has been done several times (Davies *et al.* 1993; Jakobovits *et al.* 1993; Green *et al.* 1994; Mendez *et al.* 1995; Mendez *et al.* 1997). However, the YAC is not separated from the yeast endogenous chromosomes and some of the endogenous chromosomes are also inserted into the mouse genome along with the YAC. The exact implications of the yeast genome DNA on mammalian cells is still unclear (Peterson *et al.* 1997).

I decided that since the implications of including pieces of the yeast genome in transgenic are not understood the best method was to generate the transgenic mouse using isolated modified-YAC DNA, discussed in Chapter 3, and microinject it into one cell embryos, discussed in Chapter 4. This was a very technical and time consuming procedure and is discussed in detail in the relevant chapters. The procedure was successful and nine transgenic lines were generated and the analysis is discussed in Chapter 5.

Specific aims of the project

The primary aims of this study were to investigate the downstream targets of *Pax6*. Previous studies have demonstrated changes in expression of Pax6 downstream targets in *Pax6* mutant mice. The first step at looking at these targets is the generation of a *Pax6* reporter transgenic mouse that expresses reporter genes in cells that are capable of expressing *Pax6.* Once this mouse is generated it is clear that it can be used for a wide range of analysis. For the purpose of this thesis I specifically wished to examine the following areas:

1. Demonstrate that using a 420kb YAC containing the human *PAX6* contains enough of the regulatory Pax6 elements to drive GFP expression to recapitulate the *Pax6* expression pattern in developing mouse embryos.
2. Examine changes in target gene expression using micro arrays in discrete FACS sorted populations of *Pax6* expressing cells depending on changes to *Pax6* status
3. Demonstrate autoregulation in discrete isolated cells that are expressing *Pax6* using FACS to identify and sort the cells capable of *Pax6* expression and to quantify the number and amount of fluorescence.

Unfortunately due to an underestimation of the complexity of generating the Pax6 reporter mouse only the first aim was achievable in the time available.

Summary of remaining chapters

The description of the production and subsequent analysis of the reporter mouse is broken down into four parts. Chapter 2 describes the modification of the original Y593 YAC with a bacterial construct, pDT1. Chapter 3 describes how this new modified YAC was isolated and the DNA purified ready for microinjection. Chapter 4 describes the microinjection of the modified YAC into mouse one cell embryos. Chapter 5 describes analysis of the expression pattern of the nine generated lines of transgenic mice.

Chapter 2. Generation of *Pax6* reporter construct.

Introduction

My aim was to generate a transgenic mouse that will express GFP and neomycin resistance under the control of *PAX6* regulatory elements - a '*Pax6* reporter' mouse. As discussed in Chapter 1 this novel tool will allow the identification and isolation of Pax6 expressing cells, independent of any mutation at the endogenous *Pax6* locus, thereby helping to understand the normal function of Pax6. The only practical way to produce this transgenic line was to modify the yeast artificial chromosome (YAC) that contains the human *PAX6* gene, YAC Y593. This YAC also includes approximately 200kb of flanking sequence and has been previously demonstrated to rescue loss of endogenous *Pax6* in $Pax6^{sey/sey}$ mice (Schedl *et al.* 1996).

The description of the production of the reporter mouse is broken down into four parts. This Chapter describes the modification of the original Y593 YAC. Chapter 3 describes how this new modified YAC was isolated. Chapter 4 describes the microinjection of the modified YAC into mouse one cell embryos. Chapter 5 analyses the expression pattern of the generated lines of transgenic mice.

PART I. Generation of YAC targeting construct pDT1

The starting point for the *Pax6* reporter mouse was the YAC Y593 isolated by Schedl et al in 1996. An expression cassette containing a GFP reporter and a neomycin resistance cassette was inserted immediately in frame into the translation start site AUG (in exon 4) by homologous recombination using a yeast URA3 selectable marker. It was critical for the construct to be in frame with the start site or the GFP would not be expressed. It was also highly desirable that the first codon of the GFP immediately follow the AUG otherwise extra amino acid(s) could be introduced. The introduction of an extra amino acid at the beginning of the tau protein could lead to protein misfolding and the tau failing to work properly.

The YAC targeting construct pDT1 contains the following features (see figure 2.1).

a) Approximately 1kb *PAX6* homology arms. tauGFP was to be precisely inserted at the normal ATG of *PAX6* located in exon4. This meant that a bacterial construct needed to be positioned in exactly the correct part of *PAX6* in Y593. In order to do this I flanked both ends of the bacterial construct with about 1kb of human *PAX6* from either side of the *PAX6* ATG (*PAX6* 5′arm and *PAX6* 3′arm in Figure 2.1). The homology arms were made using PCR and the arms cloned into the final targeting construct. The exact mechanism how pDT1 was inserted into Y593 is described in Chapter 2 Part II. One of the requirements was that one of the homology arms must have a unique restriction site that could be used to linearise the plasmid. This site

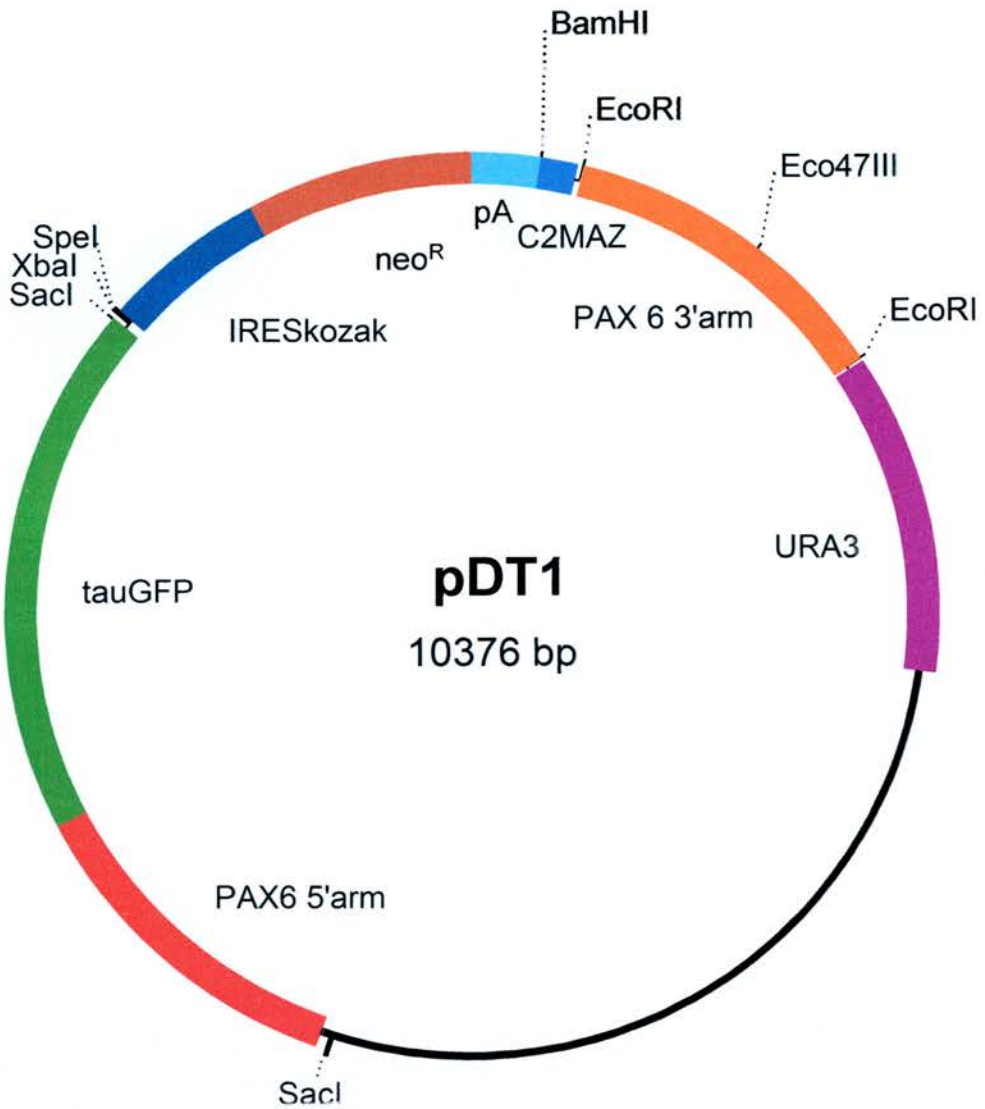

Figure 2.1. Map of the final YAC targeting construct pDT1. The map also includes the location of the restriction site Eco47III that is used to linearise the plasmid in order for it integrate into the YAC Y593.

should be approximately in the centre of the arm and must not appear elsewhere in the targeting construct; in this case I identified Eco47III as a suitable site.

b) Coding sequence for tauGFP fusion protein. GFP can easily be visualised in living cells under appropriate illumination. This would visually identify the cells expressing *Pax6*. tau is a microtubule binding protein. tauGFP is a fusion protein between tau and GFP. The coding sequence for TauGFP is a gift from Tom Pratt, Edinburgh University. As shown by Pratt et al (2000a, 2000b) the tau domain of the fusion protein causes localisation of the GFP signal to the cytoskeleton. This produces a sharper, more distinct expression pattern rather then the more diffuse pattern that we would get with soluble GFP. tauGFP is also particularly useful at identifying axonal projections(Pratt *et al.* 2000).

c) Internal Ribosome Entry Site (IRES) that is followed by an optimised Kozak translation consensus start site (IRESKozak). I wanted the tauGFP and neomycin resistance to be expressed only where there is Pax6, therefore I used the *PAX6* promoters and control elements. IRESKozaks are believed to allow the translation of two cis genes from a single transcript by a cap-independent recruitment of the 40S ribosomal subunit to the mRNA, recently reviewed by Vagner (2001). In this instance the IRESKozak was positioned between the 5′ tauGFP gene and the 3′ neomycin resistance gene, discussed below. Some reports have suggested that there can be problems with reduced expression of the 3′ cistron, recently reviewed by Kozak (2003). So I decided that since the tauGFP reporting is more critical to the project, the tauGFP would be positioned 5′ to the IRESkozak.

d) neomycin resistance (neo^R) gene. This allows the use of G418 antibiotic resistance to select cells that are expressing *Pax6*. This would be particularly useful for tissue culture experiments where antibiotic resistance could be used to select for cells that are expressing *Pax6*.

e) Polyadenylation (pA) site is to enable polyadenylation of the tauGFP-IRES-neo^R mRNA, producing fully functional tauGFP-IRES-neo^R mRNA in eukaryotic cells.

f) C2MAZ. C2MAZ is a MAZ site that is found in between the complement gene C2 and Factor B. It is thought these sites slow down RNA polymerase II, pausing transcription and preventing misexpression of complement genes[Ashfield, 1991 #29; Ashfield, 1994 #30; Yonaha, 2000 #31]. I used it in this instance as a strong stop site in an attempt to promote transcription termination in intron4, thereby significantly reducing the likelihood of the entire locus being transcribed. The aim was to exclude the possibility of exon3 splicing to downstream exons and removing the construct from the transcript. If this were to happen then an isoform of human *PAX6* gene could be expressed from one of the putative ATG sites downstream from exon4. This could lead to the production of a PAX6 protein. It has already been demonstrated by Schedl et al (1996) that full human *PAX6* can rescue the small eye phenotype. Therefore, if splicing from exon 3 to downstream exons occurred it would prevent the analysis of *Pax6* mutant mice since their phenotype would be affected by the isoform of the human *PAX6* gene and the cells would not be labelled with GFP or neomycin resistance. The complete splicing out of transgenes has been

reported previously with the β-Amyloid Precursor Protein Gene (βAPP) transgenic mouse (Muller *et al.* 1994). The authors undertook to completely abolish the βAPP gene by inserting into exon 2 a cassette containing the neomycin resistance gene in the antisense orientation and a 1kb putative transcription termination sequence UMS (upstream mouse sequence). Unfortunately it seems that exon 2 was spliced out during mRNA splicing so that a read through transcript joining exon1 to exon3, and then exon 3 to the rest of the downstream exons was produced. The presence of the mRNA transcript was demonstrated by northern blot analysis and RT-PCR and the presence of the protein was confirmed by western blot analysis(Muller *et al.* 1994; Muller *et al.* 1996). Previously it had been shown in tissue culture experiments that the UMS acts as a potent transcription terminator in certain cell types(Heard *et al.* 1987). This therefore indicated that there was risk of the *Pax6* reporter cassette being spliced out and it ruled out using the UMS as a transcription terminator.

g) URA3 is a yeast gene coding for the pyrimidine biosynthetic enzyme OMP decarboxylase (orotidine-5′-phospahate carboxy-lyase). The strategy used here to produce the reporter construct was to modify the human *PAX6* YAC 593 with a bacterial construct. URA3 would be used initially to select for yeast colonies transformed with pDT1. It would then be used to counter select transformed yeast cells during a second round of recombination. This was possible because 5-fluoroorotic acid prevents the growth of $URA3^{+}$ yeast cell Boeke (1987). The exact mechanism of how this selection occurs and why it was used is discussed later.

Fortunately all of the sequences for the components of the construct were known. This meant a comprehensive plan could be put into place designing a thorough cloning strategy to produce the construct that could be "tested" *in silico*. Once this was achieved I was able to undertake the task of actually cloning the various pieces together. All of the techniques used are standard molecular biology protocols and are described in the Appendix.

Cloning steps to make pDT1

STEP1 (See figure 2.2)

The source of the C2MAZ element was pPHCAG-C2-egfp which was a kind gift from Ian Chambers, ISCR, University of Edinburgh; a complete map of the clone is in the Appendix. The 132bp C2MAZ fragment was then isolated using PCR.

Forward primer: actg TCTAGA GGATCC cttgggggagggga

Reverse primer: acGAGCTC ACTAGT cagctcactcccctgttga

The 5′ ends of the primers had restriction sites included in the primer sequence, indicated by the uppercase characters in the primer sequence. This would result in the 5′ end of the PCR product having an XbaI site 2bp in. The primer also included a BamHI site that would be used in a later cloning event. The 3′ PCR product included a SacI and a SpeI site that would result in a SacI and a SpeI site close to the 3′end. The SpeI site would be used later in STEP 7. The most immediate 5' end of the

Figure 2.2 Flow diagram of cloning steps 1,2 and 3. **STEP 1**. The 132bp fragment containing the C2MAZ element was amplified from pPHCAG-C2-egfp by PCR. **STEP 2**. A 252bp BamHI and XbaI fragment containing the pA site was cloned from pBS-βKnpA into the BamHI and XbaI sites of vector pBS IIKS to make pBSpA. **STEP 3**. The BamHI XbaI pA fragment from pBSpA was then inserted into vector pZeroC2MAZ that had been cut with XbaI/BamHI. This cloning product was called pZeropAC2MAZ.

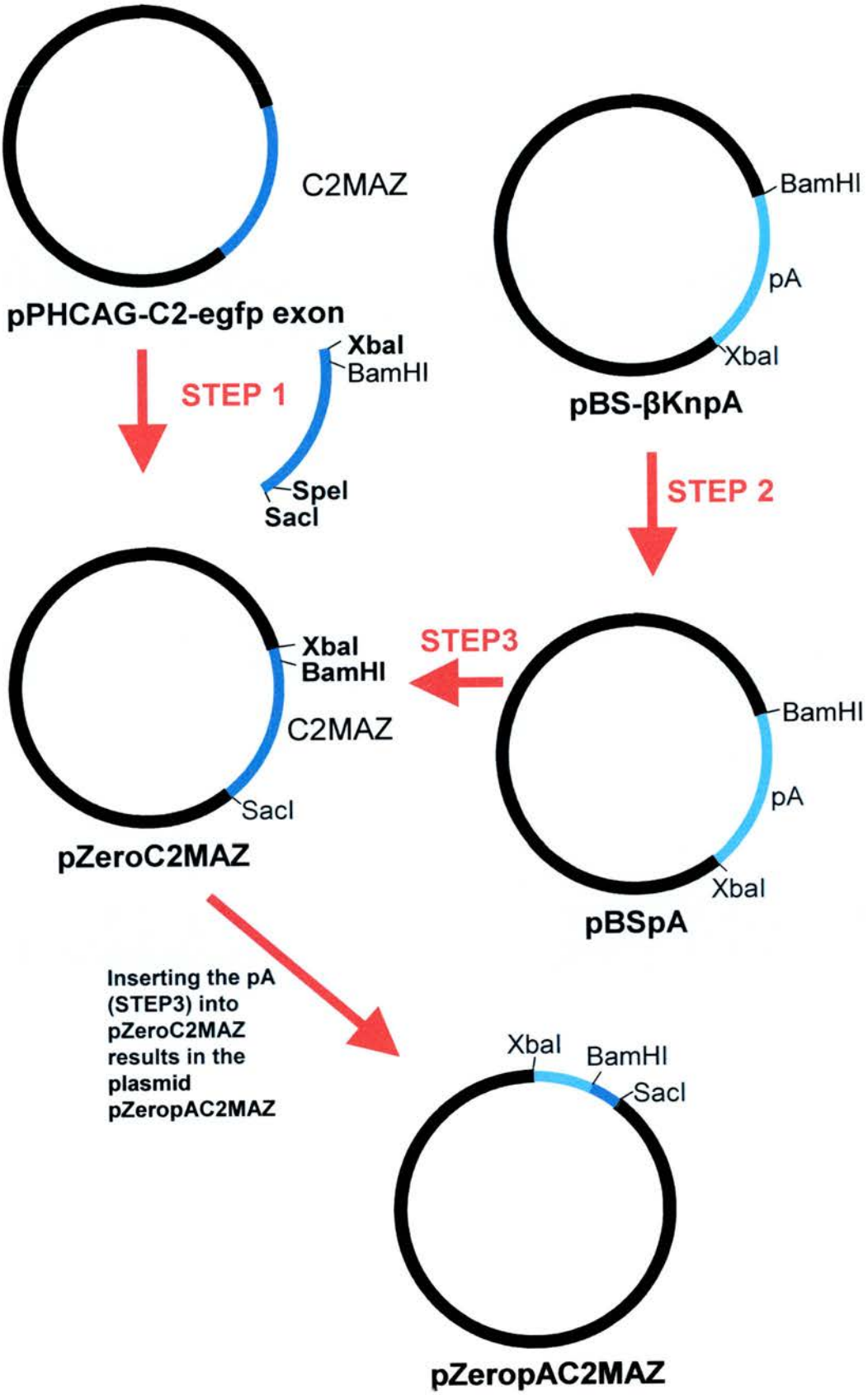
C2MAZ
pPHCAG-C2-egfp exon
XbaI
BamHI
STEP 1
SpeI
SacI
BamHI
pA
XbaI
pBS-βKnpA
STEP 2
STEP3
XbaI
BamHI
C2MAZ
SacI
pZeroC2MAZ
BamHI
pA
XbaI
pBSpA
Inserting the pA (STEP3) into pZeroC2MAZ results in the plasmid pZeropAC2MAZ
XbaI
BamHI
SacI
pZeropAC2MAZ

primer (in the case of the Forward primer "actg" is random sequence added to improve the efficiency of the restriction sites.

The purified PCR product was digested with XbaI and SacI and cloned into vector pZero2 (Invitrogen, Carlsbad, CA, USA) that had been cut with XbaI and SacI. This cloning product was called pZeroC2MAZ.

STEP2 (see Figure 2.2)

The pA site is originally from pBS-βKnpA a plasmid generated previously in the laboratory for another research project. A complete map of the clone is in the Appendix.

A 252bp BamHI and XbaI fragment containing the pA site was cloned into the BamHI and XbaI sites of vector pBS IIKS- (Stratagene, La Jolla, CA, USA) to make pBSpA. The only reason for moving the pA from its original plasmid pBS-βKnpA which has a pBS backbone into pBS IIKS- was in order to facilitate sequencing of the pA site in both directions. Previously the sequence of the pA site was known but I thought it prudent to sequence all of the components before beginning the cloning protocol.

STEP3 (see Figure 2.2)

The BamHI XbaI pA fragment from pBSpA was then inserted into vector pZeroC2MAZ that had been cut with XbaI/BamHI. This cloning product was called pZeropAC2MAZ.

STEP4 (see Figure 2.3)

The neo^R cassette came from pMMneoflox8 (a kind gift from Werner Müller, Institute for Genetics, Cologne, Germany). A complete map of the clone is in the Appendix.

An 802bp fragment encompassing neo^R was amplified using the PCR primers:

Forward primer: cacctcgagatgggatcggccattg

Reverse primer: atcACTAGTtcagaagaactcgtcaagaagg

The reverse primer includes a SpeI site in the sequence, indicated by the uppercase characters in the primer sequence. This will result in a SpeI site being near the 3′ end of the PCR product.

The purified product was cloned into pTOPO-TA (Invitrogen) following the manufacturer's instruction to form pTopoNeo. Briefly, the PCR product was generated with Taq polymerase, which often puts an extra adenosine base overhang onto the 3′ end of each PCR product strand. In the centre of the Topo vector multiple

cloning site is a thymine overhang on the 5′ end of each strand. This means the PCR fragment can be cloned into this site in the centre of the multiple cloning site.

Figure 2.3 Flow diagram of cloning steps 4 and 5. **STEP 4**. An 802bp fragment encompassing neo^R cassette was amplified from pMMneoflox8 by PCR. The reverse primer included a SpeI site in the sequence. This resulted in a SpeI site being near the 3′ end of the PCR product. **STEP 5**. An ApaI/SpeI 850bp fragment was cut from pTopoNeo containing the neo^R sequence and a small piece of the Topo vector and cloned into ApaI/XbaI cut pZeropAC2MAZ. The cloning product formed was called pZeroNeoPaC2MAZ.

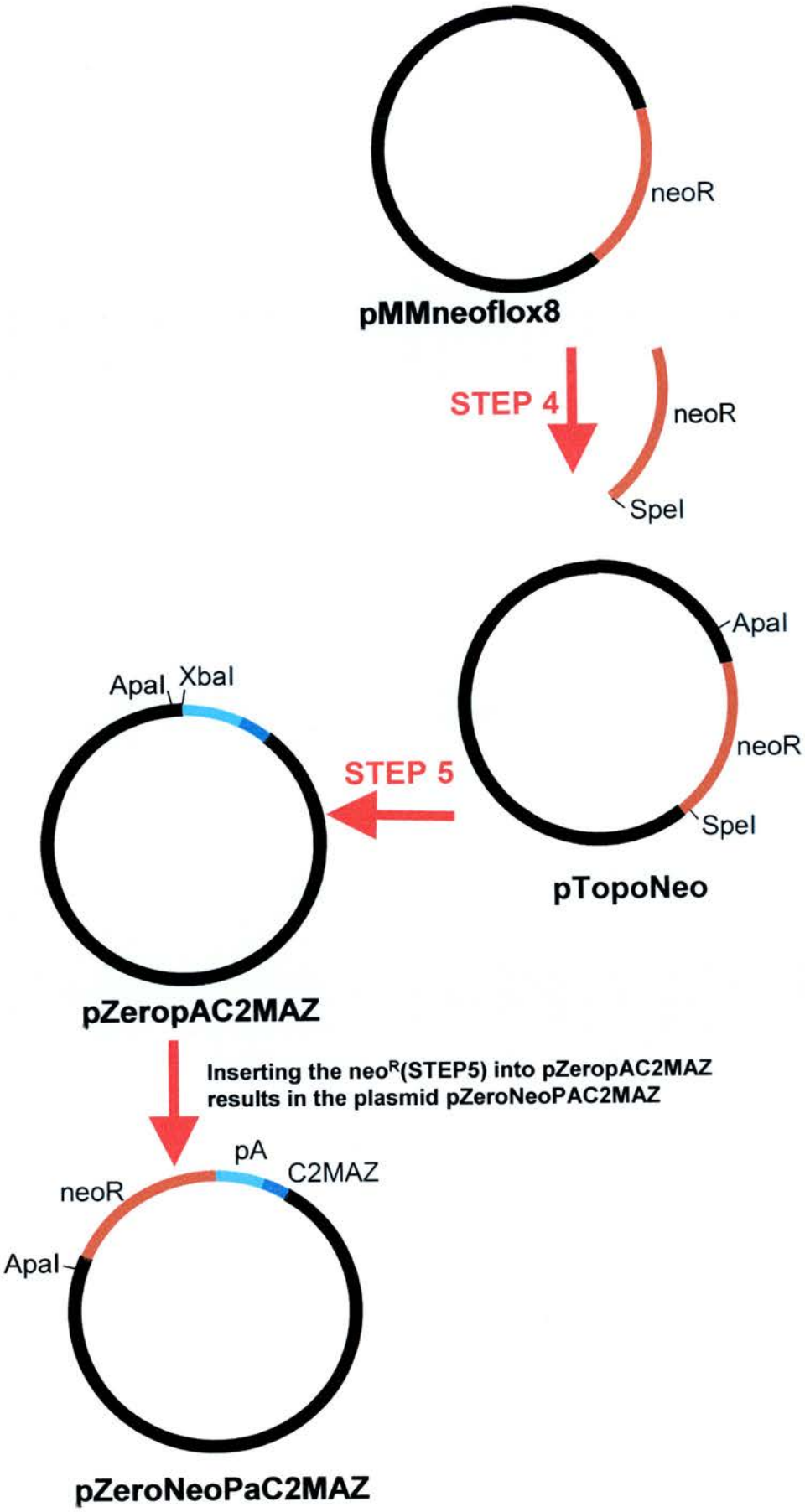
neoR
pMMneoflox8
STEP 4
neoR
SpeI
ApaI
neoR
SpeI
pTopoNeo
ApaI
XbaI
STEP 5
pZeropAC2MAZ
Inserting the neo^R(STEP5) into pZeropAC2MAZ
results in the plasmid pZeroNeoPAC2MAZ
pA
C2MAZ
neoR
ApaI
pZeroNeoPaC2MAZ

STEP5 (see Figure 2.3)

An ApaI/SpeI 850bp fragment cut from pTopoNeo containing the neo^R sequence and a small piece of the Topo vector was cut out and cloned into ApaI/XbaI cut pZeropAC2MAZ. SpeI and XbaI can ligate together because they have compatible cohesive overhangs; this results in both the SpeI and XbaI site being destroyed. The cloning product formed was called pZeroNeoPaC2MAZ.

STEP6 (see Figure 2.4)

The IRESkozak is from pIRES-EGFP (Clonetech, Palo Alto, CA). A complete map of the clone is in the Appendix.

The IRESkozak was amplified by PCR using the primers.

Forward primer: actgTCTAGA ACTAGT gggatccgcccctctc

Reverse primer: agat CTCGAG catggttgtggccatattatca

Both primers include restriction sites in their sequences so sites are engineered onto each end of the PCR product. The 5′ end of the PCR product has a XbaI site and SpeI site. The 3′ end has a XhoI site.

The 626bp PCR product containing the IRESkozak sequence was cut with XbaI/XhoI. The pZeroNeoPaC2MAZ was cut with XbaI/XhoI and the two ligated together to form pZeroIRESkNeoPaC2MAZ.

Figure 2.4 Flow diagram of cloning steps 6 and 7. **STEP 6**. The IRESkozak was amplified from pIRES- by PCR. Both primers include restriction sites in their sequences so sites are engineered onto each end of the PCR product. The 5′ end of the PCR product has a XbaI site and SpeI site. The 3′ end has a XhoI site. This 626bp PCR product containing the IRESkozak sequence was then cut with XbaI/XhoI. The pZeroNeoPaC2MAZ (from STEP5) was cut with XbaI/XhoI and the two ligated together to form pZeroIRESkNeoPaC2MAZ. **STEP 7**. A 1.8kb SpeI fragment contain the IRESkozak Neo pA C2MAZ was cut from pZeroIRESkozakNeoPaC2MAZ (generated in STEP 6) and cloned into the SpeI site of pBSURA3. This formed the cloning product pBSIRESkozakNeoPaC2MAZura3.

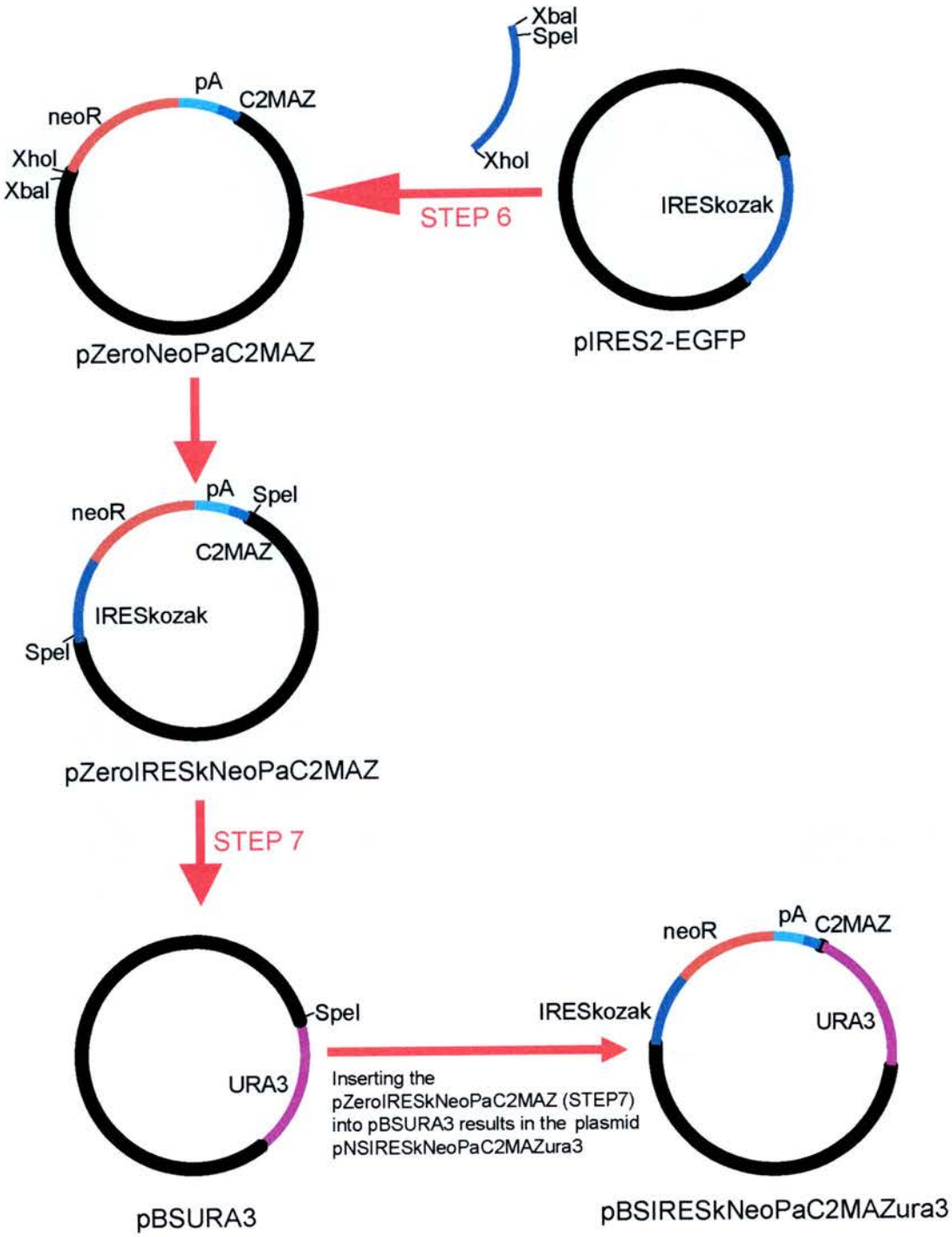
XbaI
SpeI
XhoI
pA
C2MAZ
neoR
XhoI
XbaI
STEP 6
IREScozak
pZeroNeoPaC2MAZ
pIRES2-EGFP
pA
SpeI
neoR
C2MAZ
IREScozak
SpeI
pZeroIREScNeoPaC2MAZ
STEP 7
SpeI
IREScozak
neoR
pA
C2MAZ
URA3
URA3
Inserting the
pZeroIREScNeoPaC2MAZ (STEP7)
into pBSURA3 results in the plasmid
pNSIREScNeoPaC2MAZura3
pBSURA3
pBSIREScNeoPaC2MAZura3

STEP7 (see Figure 2.4)

pBS URA3 is a kind gift from D.A. Kleinjan, HGU, Edinburgh, UK. A map of the clone is in the Appendix.

A 1.8kb SpeI fragment contain the IRESkozak Neo pA C2MAZ was cut from pZeroIRESkozakNeoPaC2MAZ and cloned into the SpeI site of pBSURA3. One SpeI site had been previously engineered onto the 5′ end of the IRESkozak by PCR (part of STEP 6) the second SpeI site had been engineered onto the 3′ end of C2MAZ by PCR (part of STEP 1). This formed the cloning product pBSIRESkozakNeoPaC2MAZura3.

STEP8 (see Figure 2.5)

The two *PAX6* homology arms were made from cFAT5, the cosmid of human *PAX6,* a gift from D.A. Kleinjan. A map of the clone is in the Appendix.

The 1.2kb homology arm immediately 5′ to the ATG site, including the ATG, was created by using the primers.

Forward primer: aaagcagtgaggcgagg

Reverse primer: catgctggctctggctgg

The purified PCR product DNA was cloned into the pTOPO cloning system following the manufacturer's instruction. The cloning product was called

Figure 2.5 Flow diagram of cloning steps 8,9,10, and 11. **STEP 8**. The 1.2kb homology arm immediately 5′ to the ATG site, including the ATG, was amplified by PCR. The purified PCR product DNA was cloned into the pTOPO cloning system, the product was called pTOPO5′arm. **STEP 9**. The 1.2kb homology arm 3′ from the ATG site, beginning immediately after the ATG was created using PCR. Both the 5′ and 3′ primers included EcoRI sites, which resulted in the *PAX6* 3′ homology arm PCR product being flanked with EcoRI sites. The purified PCR product DNA was cloned using the TOPO cloning system, creating the cloning product pTOPO3′arm. **STEP 10**. The 1.2kb SacI/XhoI fragment containing the 5′homology arm was cut from pTOPO5′arm and cloned into SacI/XhoI cut pBS II KS-. The resulting plasmid was called pBS5′arm. **STEP 11**. The *PAX6* 5′homology arm in pBS5′arm was partially digesting with EcoRI. This resulted in a solution containing two digestion products of 4.2kb. Treating both restriction digest products with Pfu and then re-ligating then resulted in a solution containing two pBS plasmids with the 5′arm insert, one plasmid with the EcoRI site ablated at the SacI 5′ end and the other plasmid with the EcoRI ablated at the XhoI 3′end. The plasmid with the EcoRI site ablated at the SacI site was the version needed and was identified by restriction mapping. Once identified this clone was renamed pBSabEcori5′arm.

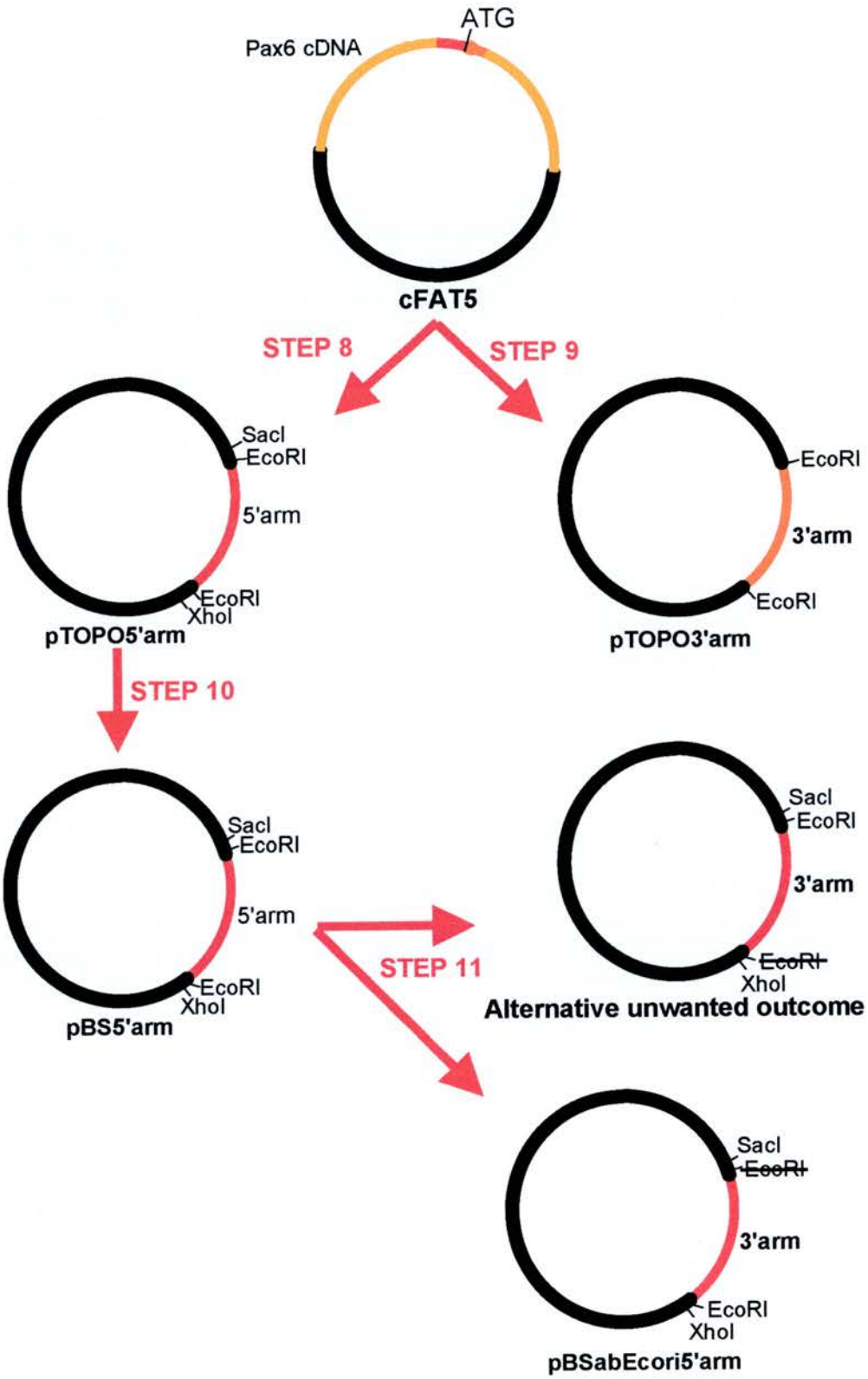
ATG
Pax6 cDNA
cFAT5
STEP 8
STEP 9
SacI
EcoRI
5'arm
EcoRI
XhoI
pTOPO5'arm
EcoRI
3'arm
EcoRI
pTOPO3'arm
STEP 10
SacI
EcoRI
5'arm
EcoRI
XhoI
pBS5'arm
STEP 11
SacI
EcoRI
3'arm
EcoRI
XhoI
Alternative unwanted outcome
SacI
EcoRI
3'arm
EcoRI
XhoI
pBSabEcori5'arm

pTOPO5′arm. The PCR product includes the ATG for *PAX6*, but this would be removed during subsequent cloning and be replaced with the ATG from tauGFP.

STEP9 (see Figure 2.5)

The 1.2kb homology arm 3′ from the ATG site, beginning immediately after the ATG was created using the following primers.

Forward primer: GAATTC agaacagtaagtgcctctggtctttc

Reverse primer: GAATTC cagcgacaaacgctcagg

Both the 5′ and 3′ primers included EcoRI sites, which resulted in the *PAX6* 3′ homology arm PCR product being flanked with EcoRI sites.

The purified PCR product DNA was cloned using the TOPO cloning system following the manufacturer's instruction, creating the cloning product pTOPO3′arm.

STEP10 (see Figure 2.5)

The 1.2kb SacI/XhoI fragment containing the 5′homology arm was cut from pTOPO-5arm and cloned into SacI/XhoI cut pBS II KS-. The resulting plasmid was called pBS5′arm.

STEP11 (see Figure 2.5)

The *PAX6* 5′homology arm in pBS5′arm was flanked at each end by EcoRI sites. Both of these needed to be removed in order for subsequent cloning reactions to work. The EcoRI site at the 3′ most end of the homology arm was removed later, but the one at the 5′ end needed to be ablated.

This was achieved by partially digesting pBS5′arm with EcoRI. If a complete EcoRI digestion was done then a 1.3kb and a 2.9kb product were produced. Conditions were set up to optimise the chances that only one EcoRI site would be cut, leaving the other one uncut. This resulted in a solution containing two digestion products of 4.2kb. EcoRI digests leave a 3′overhang, which can be removed using Pfu DNA polymerase (Stratagene). Treating both restriction digest products with Pfu and then re-ligating then resulted in a solution containing two pBS plasmids with the 5′arm insert, one plasmid with the EcoRI site ablated at the SacI 5′ end and the other plasmid with the EcoRI ablated at the XhoI 3′end. The plasmid with the EcoRI site ablated at the SacI site was the version needed and was identified by restriction mapping. Once identified this clone was renamed pBSabEcori5′arm.

STEP12 (see Figure 2.6)

The tauGFP used was from pTP6 a kind gift from T. Pratt, Edinburgh University. A complete map of the clone is in the Appendix.

A 2kb PCR product of tauGFP fusion gene was generated using the primers

Forward primer: catggctgag ccc cgcc

Reverse primer: tg CTCGAG GAGCTC ttatttgtatagttcatccatgccatgt

This was a long PCR product and needed to have no polymerase transcription errors so high fidelity proofreading Pfu polymerase (Stratagene) was used to reduce the risk of errors. This also resulted in a PCR product that was blunt ended, which was important for the next cloning step.

The reverse primer had both XhoI and a SacI sites included to engineer these at the 3′ end of the PCR product.

The plasmid pBSabEcori5arm was cut with SphI and the 3′ overhangs polished with T4 DNA polymerase to leave blunt ends; with the optimised dNTP concentration T4 DNA polymerase has 3′ to 5′ exonuclease activity. Part of the 3′ overhang included the ATG from *PAX6* but this was to be replaced with the ATG from tauGFP, thus putting the tauGFP fusion protein in frame with *PAX6*.

Next the vector was cut with XhoI to create a XhoI sticky overhang at one end.

The tauGFP PCR product was cut with XhoI. Thus the 3′ end had a XhoI cohesive end and the 5′end was still blunt. Ligating this with the SphI/XhoI cut pBSabEcori5′arm generated the plasmid pBS5′armtauGFP

Figure 2.6 Flow diagram of cloning steps 12 and 13. **STEP 12**. A 2kb PCR product of tauGFP fusion gene was generated from pTP6. The reverse primer had both XhoI and a SacI sites included to engineer these at the 3′ end of the PCR product.The plasmid pBSabEcori5arm (generated in STEP 11) was cut with SphI and the 3′ overhangs polished with T4 DNA polymerase to leave blunt ends. Next the vector was cut with XhoI to create a XhoI sticky overhang at one end. The tauGFP PCR product was cut with XhoI. Thus the 3′ end had a XhoI cohesive end and the 5′end was still blunt. Ligating this with the SphI/XhoI cut pBSabEcori5′arm generated the plasmid pBS5′armtauGFP. **STEP 13**. A 3.3Kb SacI fragment containing the 5′homology arm and tauGFP was cut from pBS5′armtauGFP and cloned into the SacI site of pBSIRESkNeoPaC2MAZura3 (generated in STEP 7) to create the cloning vector pBS5′armin.

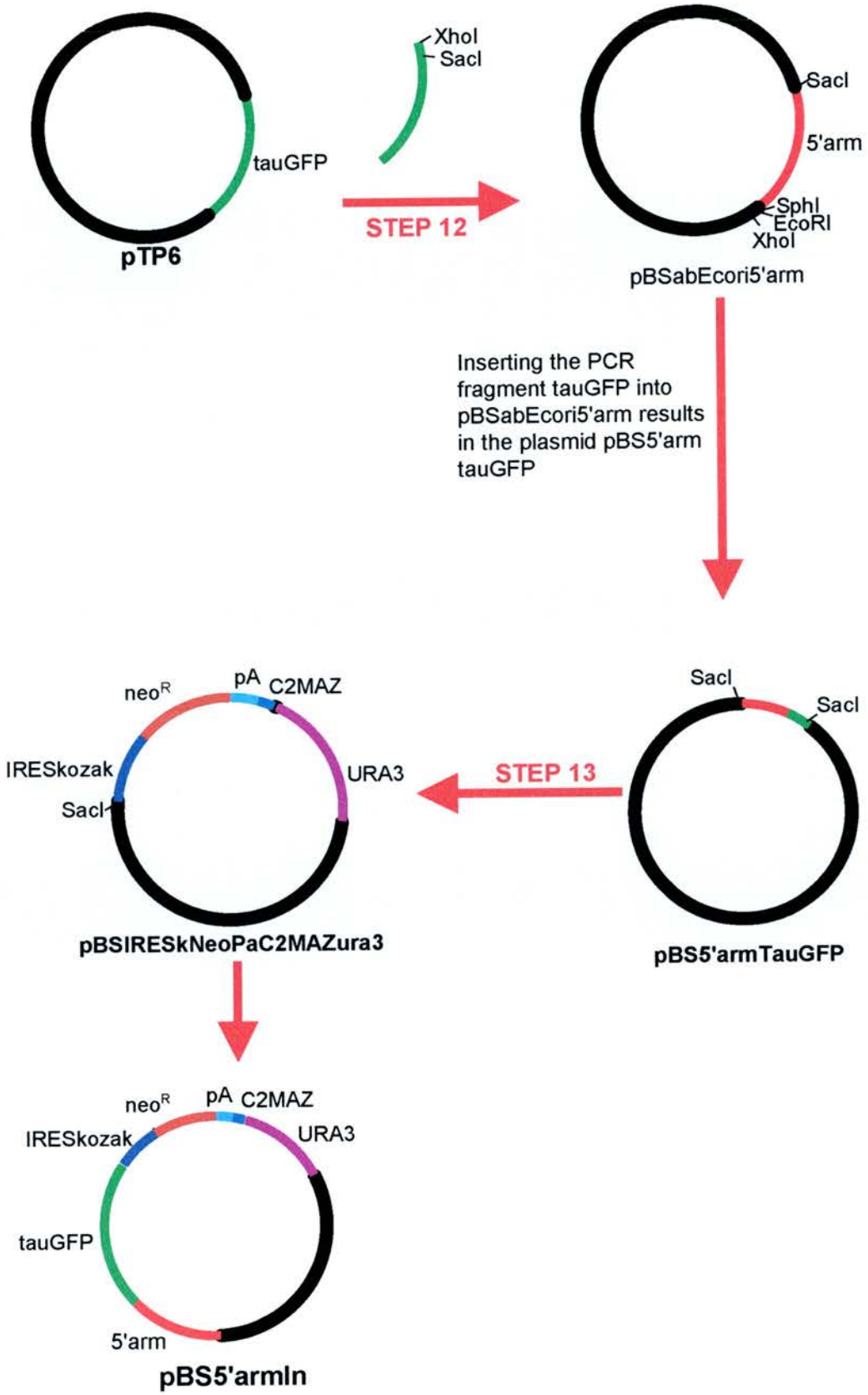
XhoI
SacI
tauGFP
pTP6
STEP 12
SacI
5'arm
SphI
EcoRI
XhoI
pBSabEcori5'arm
Inserting the PCR fragment tauGFP into pBSabEcori5'arm results in the plasmid pBS5'arm tauGFP
SacI
SacI
pBS5'armTauGFP
STEP 13
neoR
pA
C2MAZ
URA3
IRESkozak
SacI
pBSIRESkNeoPaC2MAZura3
neoR
pA
C2MAZ
URA3
IRESkozak
tauGFP
5'arm
pBS5'armIn

STEP13 (see Figure 2.6)

A 3.3Kb SacI fragment containing the 5′homology arm and tauGFP was cut from pBS5′armtauGFP and cloned into the SacI site of pBSIRESkNeoPaC2MAZura3 to generate the cloning vector pBS5′armin.

STEP14 (see Figure 2.7)

An EcoRI fragment from pTOPO3′arm containing the 3′homology arm was cloned into the EcoRI site of pBS5′armin. This completed the cloning strategy. The final 10.4kb clone was called pDT1, see Figure 2.1 and 2.8 for a complete map of the clone.

Once produced the plasmid pDT1 was extensively checked with diagnostic restriction digests and sequencing. Figure 2.8 summarises the restriction digests. The entire pDT1 was then sequenced in both directions and the primers used appear in the Appendix A.

Figure 2.7 Flow diagram of the final cloning step 14. **STEP 14**. An EcoRI fragment from pTOPO3′arm containing the 3′homology arm was cloned into the EcoRI site of pBS5′armin (generated in STEP 13). This completed the cloning strategy. The final 10.4kb clone was called pDT1.

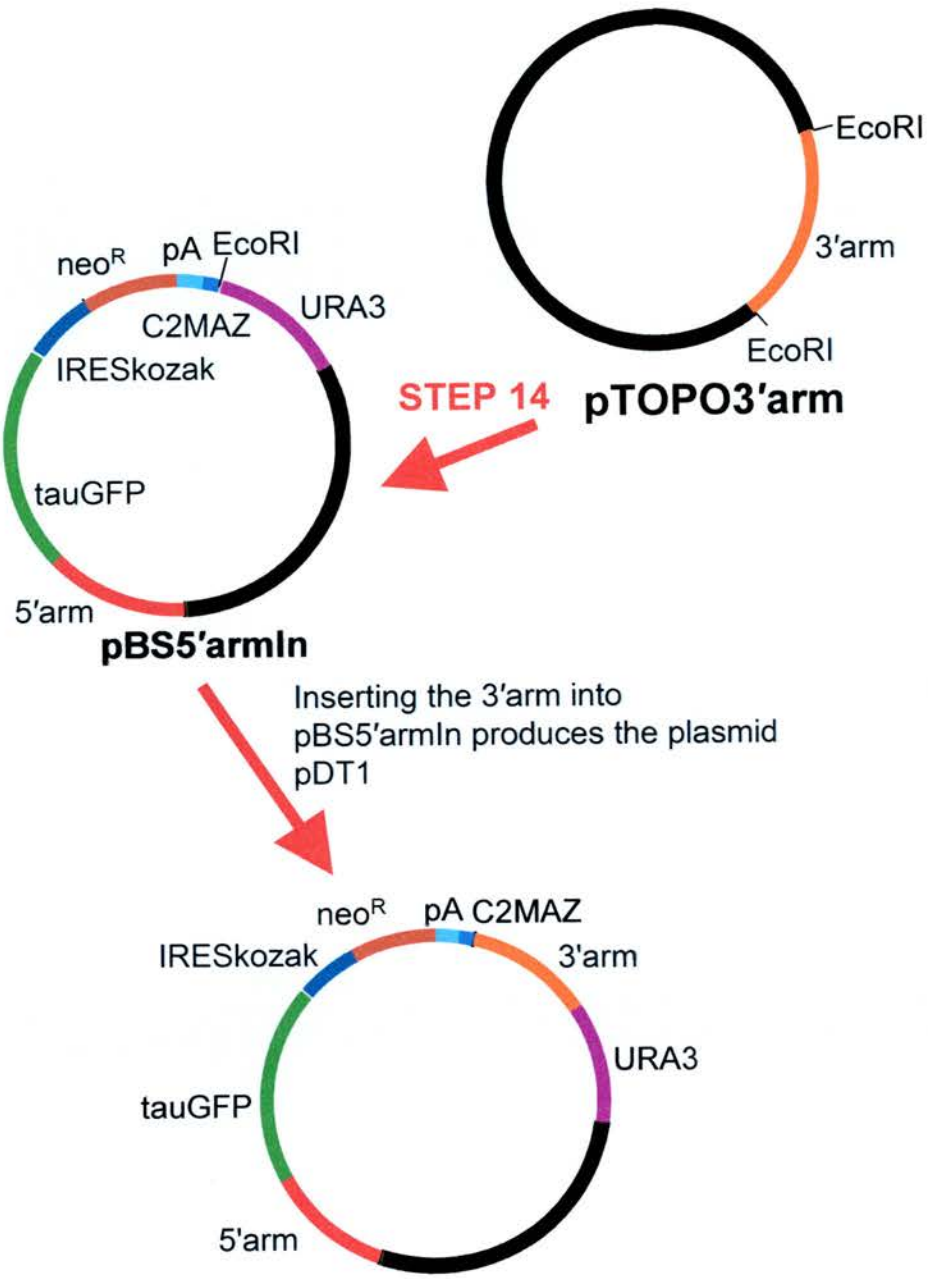
EcoRI
3′arm
EcoRI
pTOPO3′arm
STEP 14
neoR
pA
EcoRI
URA3
C2MAZ
IRESkozak
tauGFP
5′arm
pBS5′armIn
Inserting the 3′arm into
pBS5′armIn produces the plasmid
pDT1
neoR
pA
C2MAZ
IRESkozak
3'arm
URA3
tauGFP
5'arm

pDT1

Figure 2.8. Summary of restriction digests of four midi preps of clones from final cloning step. A) EcoRI digests of four midi preps, all contain the insert. B) ApaI restriction digest of two of the midi preps, both are correct. C) ApaI digest of two midi preps, both are incorrect. D) XbaI digest of four of the midi preps. 1 and 2 are correct. E) SacI digest of midis 1 and 2, both are correct. F) SacI digest of midis 3 and 4, both are incorrect. G) Restriction map of pDT1.

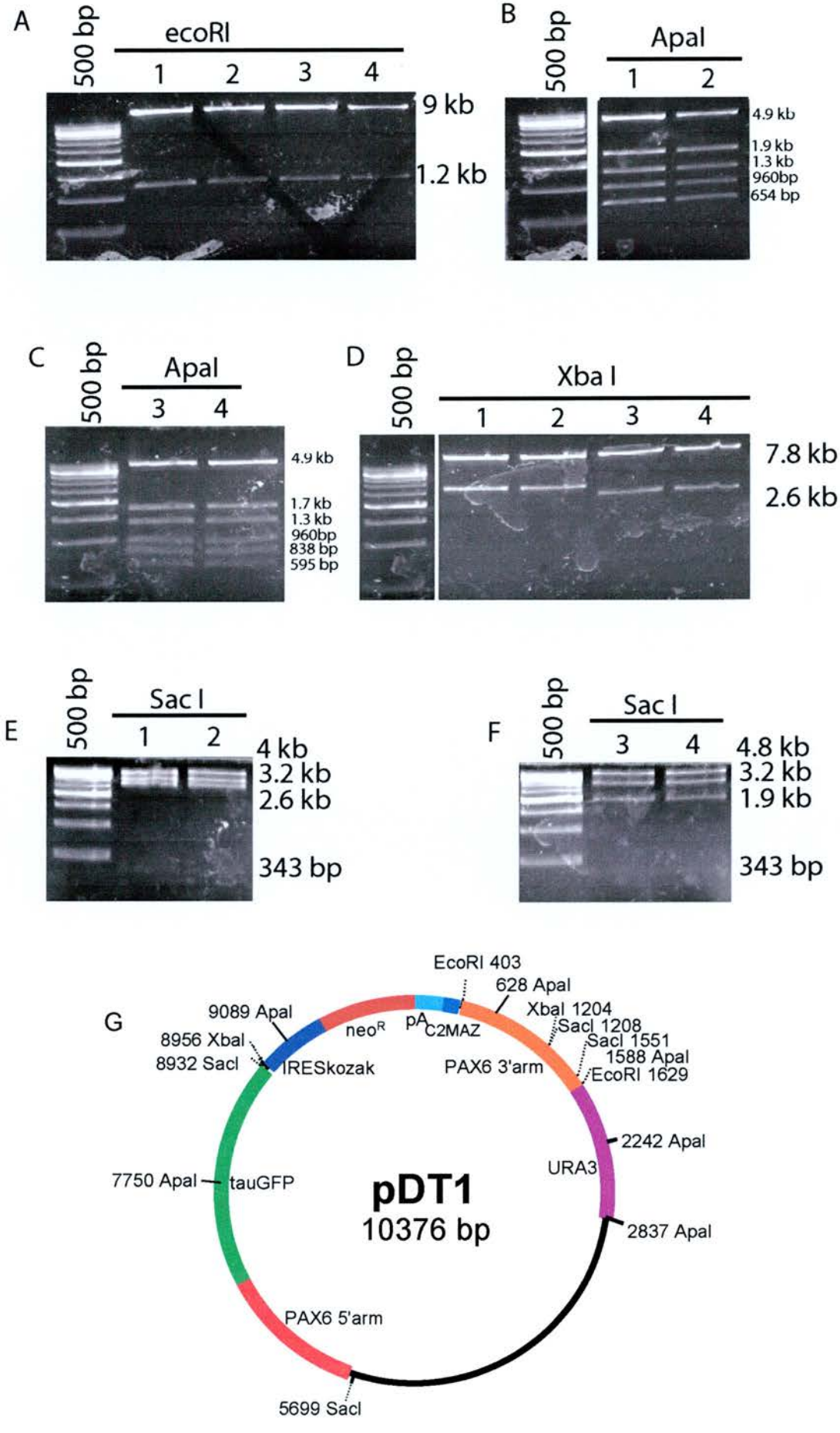
A
500 bp
ecoRI
1 2 3 4
9 kb
1.2 kb
B
500 bp
ApaI
1 2
4.9 kb
1.9 kb
1.3 kb
960bp
654 bp
C
500 bp
ApaI
3 4
4.9 kb
1.7 kb
1.3 kb
960bp
838 bp
595 bp
D
500 bp
Xba I
1 2 3 4
7.8 kb
2.6 kb
E
500 bp
Sac I
1 2
4 kb
3.2 kb
2.6 kb
343 bp
F
500 bp
Sac I
3 4
4.8 kb
3.2 kb
1.9 kb
343 bp
G
EcoRI 403
628 ApaI
XbaI 1204
SacI 1208
SacI 1551
1588 ApaI
EcoRI 1629
2242 ApaI
2837 ApaI
5699 SacI
PAX6 5'arm
7750 ApaI
tauGFP
8932 SacI
8956 XbaI
9089 ApaI
IREStkozak
neoR
pA
C2MAZ
PAX6 3'arm
URA3
pDT1
10376 bp

PART IIA. Integration of YAC Y593 into yeast window strain W3

Before modifying the parental YAC Y593 with the Pax6 reporter construct, it was introduced into a window yeast strain. This was necessary because the YAC Y593 when run on a pulse field gel (PFG) co-migrates with similar sized endogenous yeast chromosomes, therefore making it difficult to distinguish the YAC from the endogenous chromosomes. It was necessary to distinguish the YAC from the endogenous chromosomes because in order to isolate the modified YAC DNA for microinjection, it was first necessary to separate the YAC chromosome from the other yeast chromosomes. The most straight forward way to do this was using alternating contour-clamped homogeneous electric field (CHEF) pulse field gel electrophoresis (PFGE) (Chu *et al.* 1986). This technique separates the chromosomes by size. So the solution was to use yeast "window strains" (Hamer *et al.* 1995) in which appropriate yeast endogenous chromosomes were cut by using recombination-mediated chromosome fragmentation (Vollrath *et al.* 1988). The technique involves splitting a chromosome at a specific site by transformation with short linear molecules containing a target sequence from the chromosome that is being split at one end and telomeric sequences at the other. Recombination between the end of the linear molecules and homologous chromosomal sequences gives rise to chromosome fragments. A set of *Saccharomyces cerevisiae* host strains have been systematically constructed. Each strain contains defined alterations in its karyotype, which provide a large-size interval devoid of endogenous chromosomes, i.e., a "window". Window strain W3 which was produced by (Dr L. Hammer, Department of Biological Sciences, West Lafayette, IN, US) was mated with Y593 using the *kar*-cross method

(Hugerat *et al.* 1994; Spencer *et al.* 1994). Briefly, this is a technique that takes advantage of the properties of *kar1* mutants altered in a gene required for normal karyogamy (nuclear fusion) during mating. The progeny of the cross were grown in –AT yeast growth medium. –AT is a double "drop out" selective medium for this particular YAC. Typical *S. cerevisiae* growth medium YPD contains glucose, yeast nitrogen base, and all essential nutrients needed for *S. cerevisiae* to grow. The exact requirements of nutrients depend on the genotype of the *S. cerevisiae* clone being grown. Different genotypes have different auxotrophic genes from the biosynthetic pathway. YAC Y593, in addition to the Human *PAX6* gene locus, also contains the biosynthetic genes ADE2 and Trp for yeast cells to produce adenine (A) and tryptophan (T). By removing adenine hemisulfate salt and tryptophan from the list of ingredients in the growth medium it is possible to select for only yeast colonies that express these genes. Therefore, all of the colonies that grow should contain YAC Y593. Figure 2.9 shows two gels of the parental window strain W3 and the progeny of the cross between W3 and Y593. The additional YAC is clearly visible in both gels.

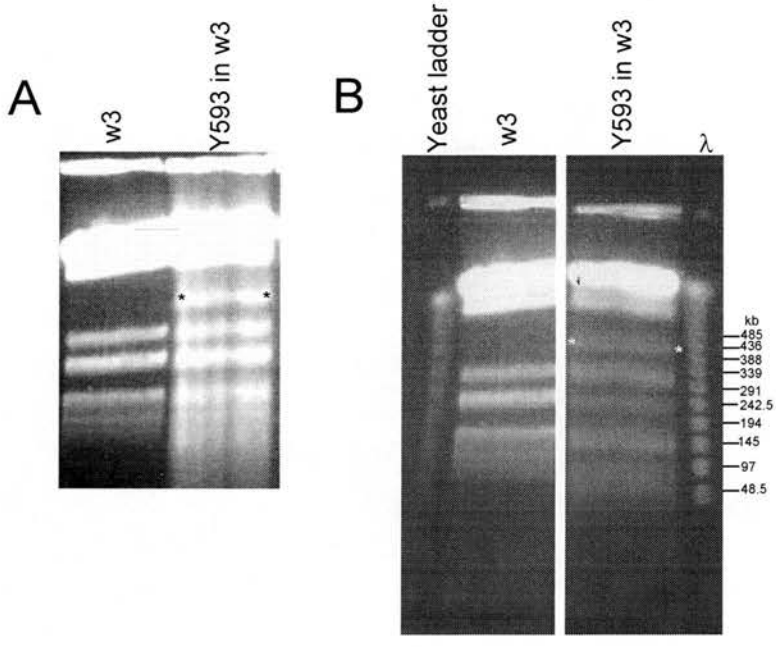

Figure 2.9. Images of the two yeast strains. (A) Lane 1 is the original parental strain. Lane 2 is the parental strain w3 crossed with Y593. (B) Lane 1 is the Yeast Chromosome PFG Marker (New England BioLabs) . Lane 2 is the original parental strain. Lane 3 is the parental strain w3 crossed with Y593. Lane 4 is the Lambda Ladder PFG Marker (New England BioLabs). The location of the YAC is indicated in both gels with an asterisk.

Part IIB. Integration of reporter cassette into Y593 by homologous recombination.

Once the Y593 had been moved into the window strain it was transformed with the bacterial construct pDT1 using modified lithium acetate yeast transformation (details of the protocol are included in the Appendix). The final step of the protocol was to plate onto –AT yeast growth medium, which selected for yeast colonies that contain Y593. Therefore, all of the colonies that grew should have contained Y593 but only a proportion of the yeast cells in the transformation event would have integrated the reporter construct pDT1. However, the window strain has a defective URA3 gene and so is unable to respond to pyrimidine starvation. Up until this point uracil has been included among the essential nutrients in order for the yeast to grow (Botstein *et al.* 1979). The bacterial plasmid contained the yeast gene URA3, which meant that any cell harbouring Y593 into which pDT1 had recombined would now have been able to survive pyrimidine starvation. Therefore, uracil was now left out of the –AT growth medium as well and only yeast colonies that contained the YAC Y593 and that had been successfully transformed were able to grow. A schematic of the integration of pDT1 into Y593 is shown in Figure 2.10.

Several colonies were picked and screened for the presence of the complete pDT1 using PCR for parts of pDT1 distant from the URA3 gene, in this case neo^R. The human *PAX6* homology arms that flanked either end of pDT1 were included to ensure that the reporter cassette pDT1 was positioned exactly in the correct part of the *PAX6* gene by homologous recombination. That is, so that the *PAX6* ATG in

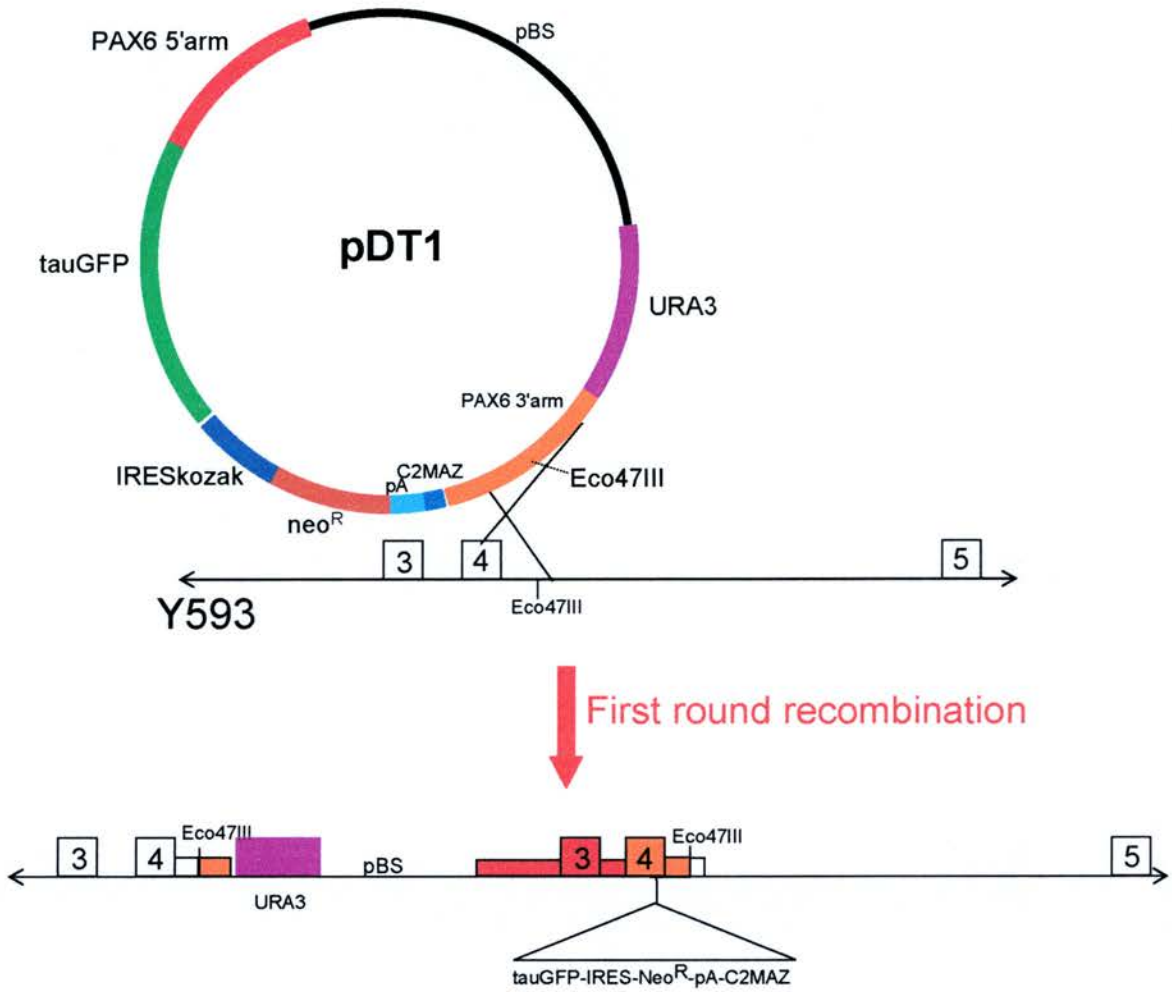

Figure 2.10. Schematic diagram of the first round of integration of pDT1 into Y593. The exons of *PAX6* are indicated by the boxes with the exon number in it.

exon 4 was immediately followed by tauGFP. The correct location of pDT1 was confirmed by Southern blot analysis; see Figure 2.11. There was still a second round of recombination, discussed below, to be done to remove the repeated *PAX6* sequence. Therefore, sequencing of the junction from *PAX6* into tauGFP to check that everything was in frame with no additional amino acids was conducted later after all recombination events had been finished.

YAC colonies harbouring the correct first round recombination event were plated on 5-fluoroorotic acid (5-FOA) plates. The presence of the URA3 gene meant that the yeast cells were unable to grow in the presence of 5-FOA (Soderholm 2001; Boeke JD 1987). Therefore, the colonies were grown for several days on 5-FOA. The 5-FOA selection would then resulted in two outcomes; either the entire pDT1 would be lost by internal homologous recombination resulting in the recreation of the original YAC Y593 or the repeated *PAX6* exons would be removed, giving the correct modification of Y593 with pDT1, see Figure 2.10. In order for the 5-FOA selection to work the growth medium had to be supplemented with uracil again otherwise all of the yeast colonies would have been unable to grow. This process of using URA3 to select for and then subsequently counter select is more commonly know as "pop-in/put-out" selection and is widely used in yeast molecular genetics(Boeke *et al.* 1987; Soderholm *et al.* 2001). See Figure 2.12 for a diagram showing the two outcomes of 5-FOA selection.

Figure 2.11. A) Southern blot screen of first round clones. Clones 1-10, 1-11, 1-13, are all incorrect. Clone 1-12 is correct. B) Schematic diagram of the first round of integration of pDT1 into Y593. The red boxes are exons of *PAX6*. The yellow is exon 5a. The purple box is the URA3 yeast gene. The green box is the reporter cassette (GFP-IRESkozak-Neo^{R}-pA-C2MAZ). The restriction sites used to digest the yeast clone DNA are shown. The location of the 374 bp southern blot probe is indicated by the asterisks.

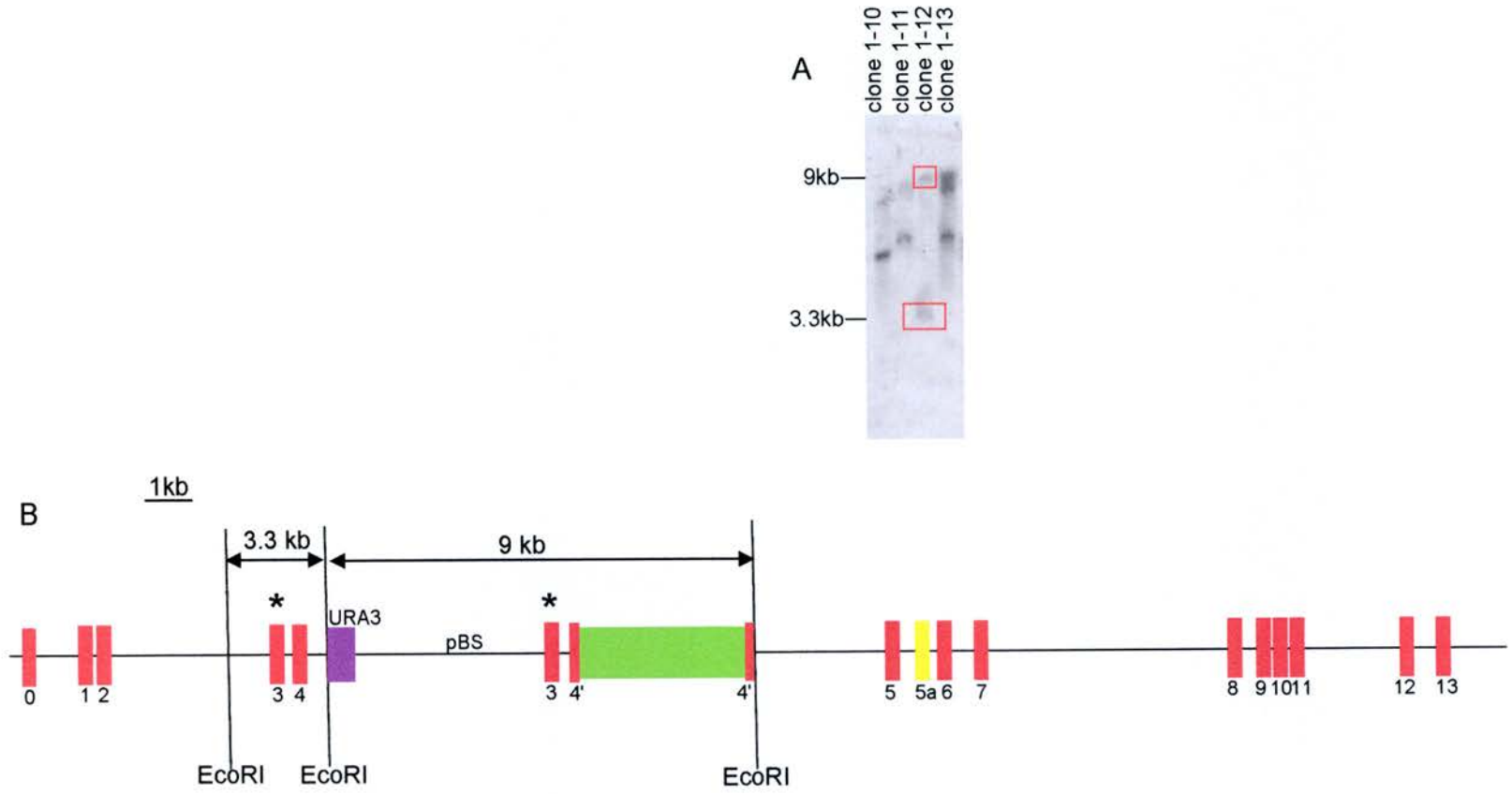
A
clone 1-10
clone 1-11
clone 1-12
clone 1-13
9kb
3.3kb
B
1kb
3.3 kb
9 kb
URA3
pBS
0
1 2
3 4
3 4'
4'
5
5a 6
7
8
9 10 11
12
13
EcoRI
EcoRI
EcoRI

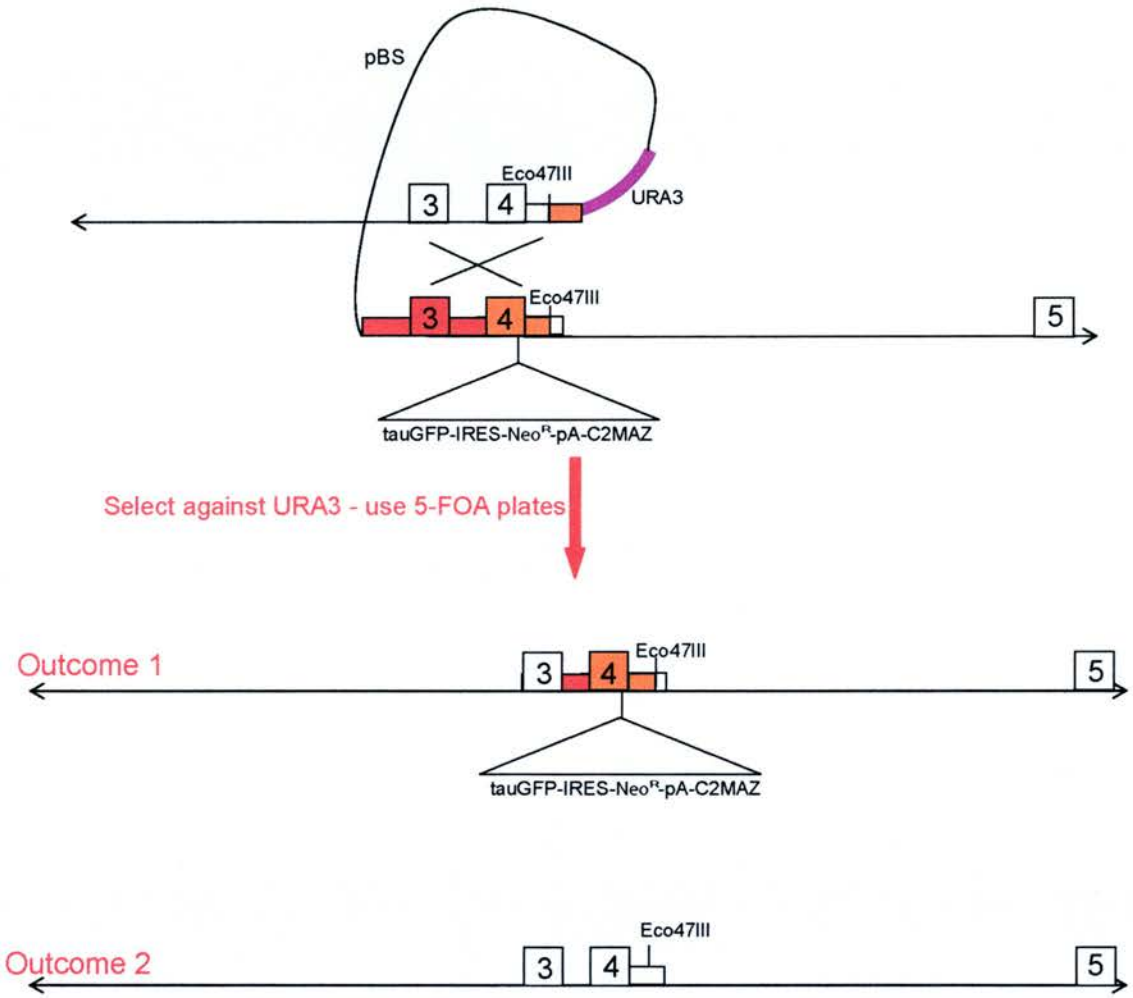

Figure 2.12. Schematic diagram of the second round of integration of pDT1 into Y593. The exons of *PAX6* are indicated by the boxes with the exon number in it. Both of the two potential outcomes are shown.

Finally, the colonies were screened by PCR for the presence of neo^R and checked for rearrangement with southern blots. 18 clones were picked and screened for correct first round rearrangement. I was happy with clone 12, giving a success rate of 1:18 or 5.6%. This clone was used in the second round 5-FOA selection. Nine clones were picked from the 5-FOA plate, designated 1121 to 1129. Southern blots were done to identify correct clones, see Figure 2.14 and 2.15. Clone 1123 was identified as correct, giving a success rate in the second round of about 11%. PCR was then conducted to confirm the individual parts of the reporter cassette were present in the clone, see Figure 2.13. The areas around where the reporter cassette integrated was also examined by PCR, see Figure 2.16. Restriction digests were done on some of the PCR products to examine them more closely, Figure 2.17. The junction from *PAX6* into tauGFP was also checked by sequencing across the junction in both directions, the primers used are in the Appendix A. Figure 2.18 shows a PFG sizing the successful clone 1123. The original YAC Y593 is 420kb. Targeting with pDT1 would have added 3.6 kb, therefore the total expected size of the targeted YAC 1123 was 424kb. This was consistent with the size of the band on the PFG panel A. Panel B is a southern blot of the PFG probed with a 375bp StuI fragment from *PAX6* exon 3. The YAC 1123 is easily distinguished from the other endogenous chromosomes.

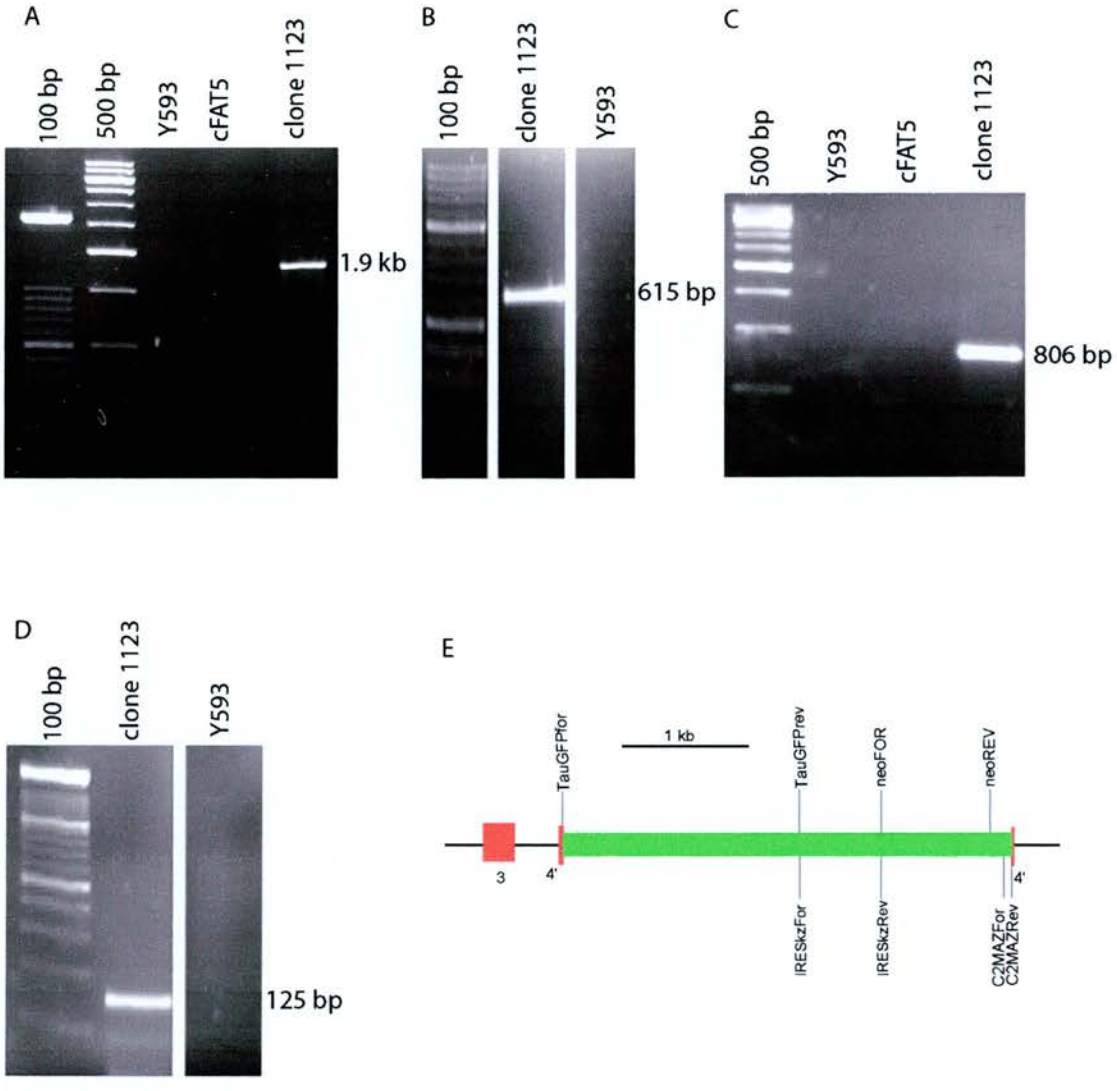

Figure 2.13. PCR reactions to confirm parts of pDT1 have integrated into the YAC. Y593 is the original targeted YAC. cFAT5 is a cosmid of the *PAX6* cDNA. (A) Primers TauGFPfor and TauGFPrev that flank tauGFP, this has an expected size of 1.9 kb. (B) Primers IRESkzFor and IRESkzRev that flank the IRESkozak., expexted size 615 bp. (C) neoFOR and neoREV flank Neo^R, expected size 806bp. (D) Primers C2MAZFor and C2MAZRev, expected size 125 bp. (E) Schematic of *PAX6* showing the locations of the primers. The red boxes are *PAX6* exons. The green box is the inserted reporter cassette (tauGFP-IRESkozak-Neo^R-pA-C2MAZ). Primer sequences are in Appendix A.

Figure 2.14. Southern blot of ApaI/EcoRI restriction digested Y1-12-3 and Y593. The red boxes are *PAX6* exons. The yellow box is exon 5a. The green box is the reporter cassette (tauGFP-IRESkozak-Neo^{R}-pA-C2MAZ). The location of the southern probe is indicated by the asterisks.

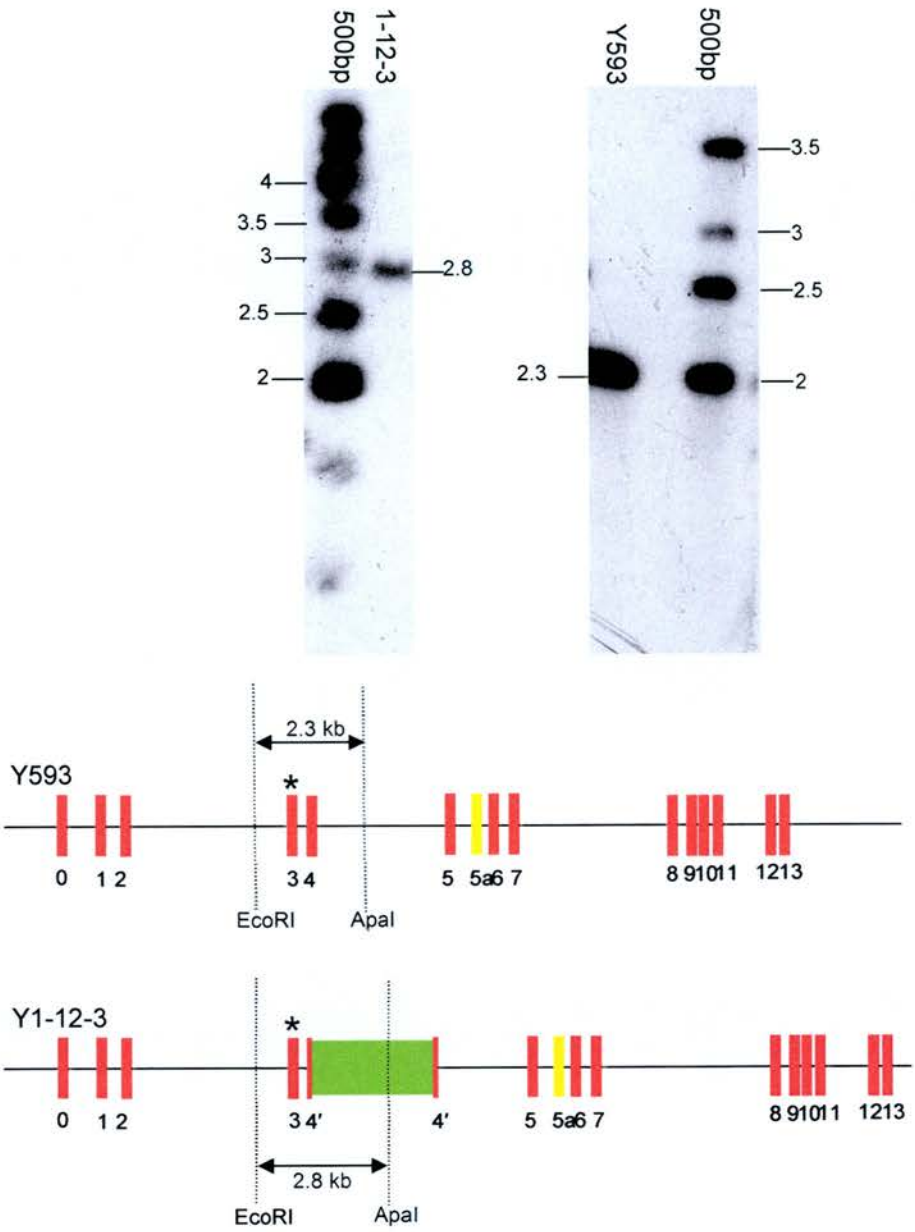
500bp
1-12-3
4
3.5
3
2.5
2
2.8
Y593
500bp
3.5
3
2.5
2
2.3
2.3 kb
Y593
*
0 1 2
3 4
5 5a6 7
8 9 10 11
12 13
EcoRI
ApaI
Y1-12-3
*
0 1 2
3 4'
4'
5 5a6 7
8 9 10 11
12 13
2.8 kb
EcoRI
ApaI

Figure 2.15. Southern blot of diagnostic restriction digests to confirm the clone 1-12-3 is correct. The locations of the restriction sites are indicated on the diagram of the genomic organization of 1-12-3. The red boxes are *PAX6* exons. The yellow is exon 5a. The green is the reporter cassette (tauGFP-IRESkozak-Neo^{R}-pA-C2MAZ). The location of the southern probe is indicated by the asterisk.

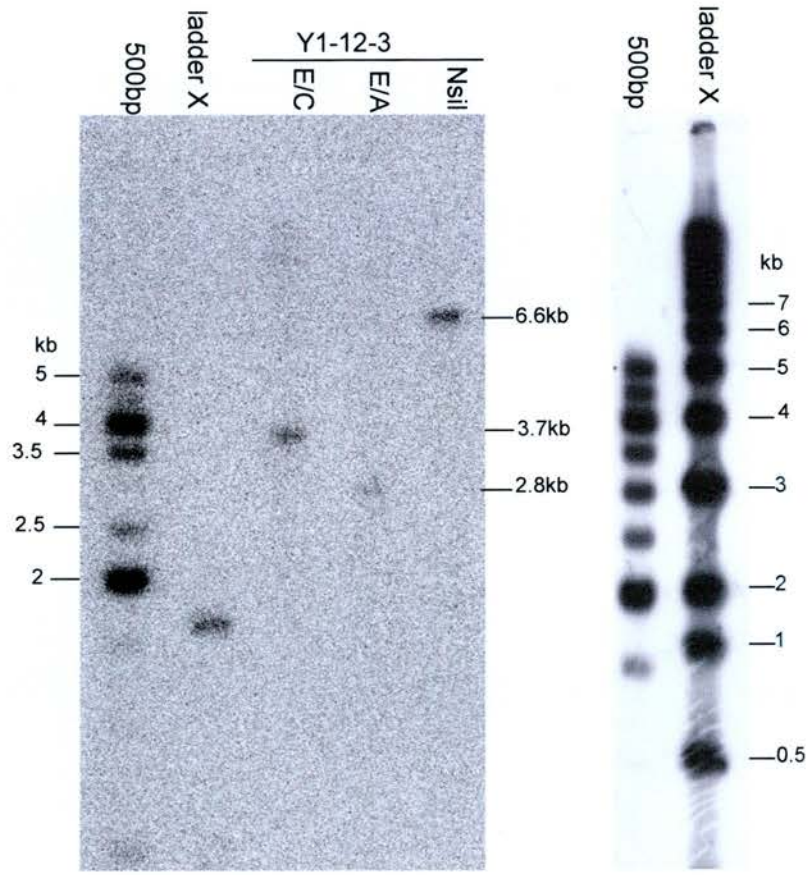
500bp
ladder X
Y1-12-3
E/C
E/A
NsiI
kb
5
4
3.5
2.5
2
6.6kb
3.7kb
2.8kb
500bp
ladder X
kb
7
6
5
4
3
2
1
0.5

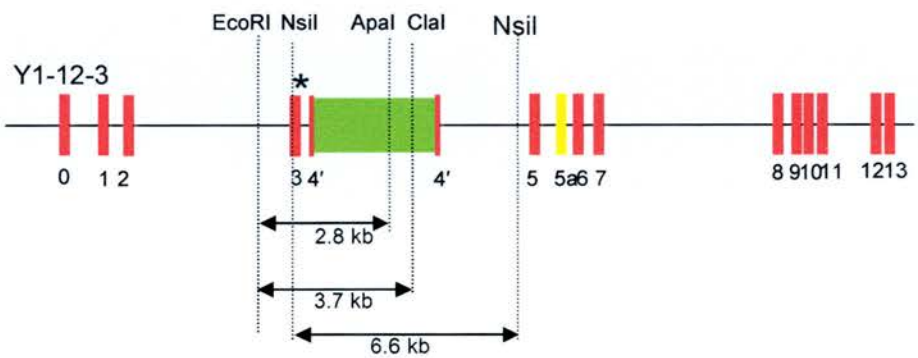
EcoRI
NsiI
ApaI
ClaI
NsiI
Y1-12-3
*
0 1 2
3 4'
4'
5 5a6 7
8 9101 1 1213
2.8 kb
3.7 kb
6.6 kb

Figure 2.16. PCR reactions to confirm the areas around where the reporter cassette integrated are present. Y593 is the original targeted YAC. cFAT5 is a cosmid of the *PAX6* cDNA. A) Primer pair Targ3.1 and Targ 4.1, that have an expected size of 1.4 kb. B) Primers Targ1.1 and Targ 2.1, expected size 1.3kb. C) Primers Targ1.1 and DTE, expected size is 4.4kb. D) Primers PAX6_5F and PAX6_5R, expected size 1.2kb. E) Primers PAX6_3F and PAX6_3F, expected size 1.2kb. F) Schematic of PAX6 showing the locations of the primers. The red boxes are *PAX6* exons. The yellow box is exon 5a. The green box is the inserted reporter cassette (tauGFP-IRESkozak-Neo^{R}-pA-C2MAZ). Primer sequences are in Appendix A.

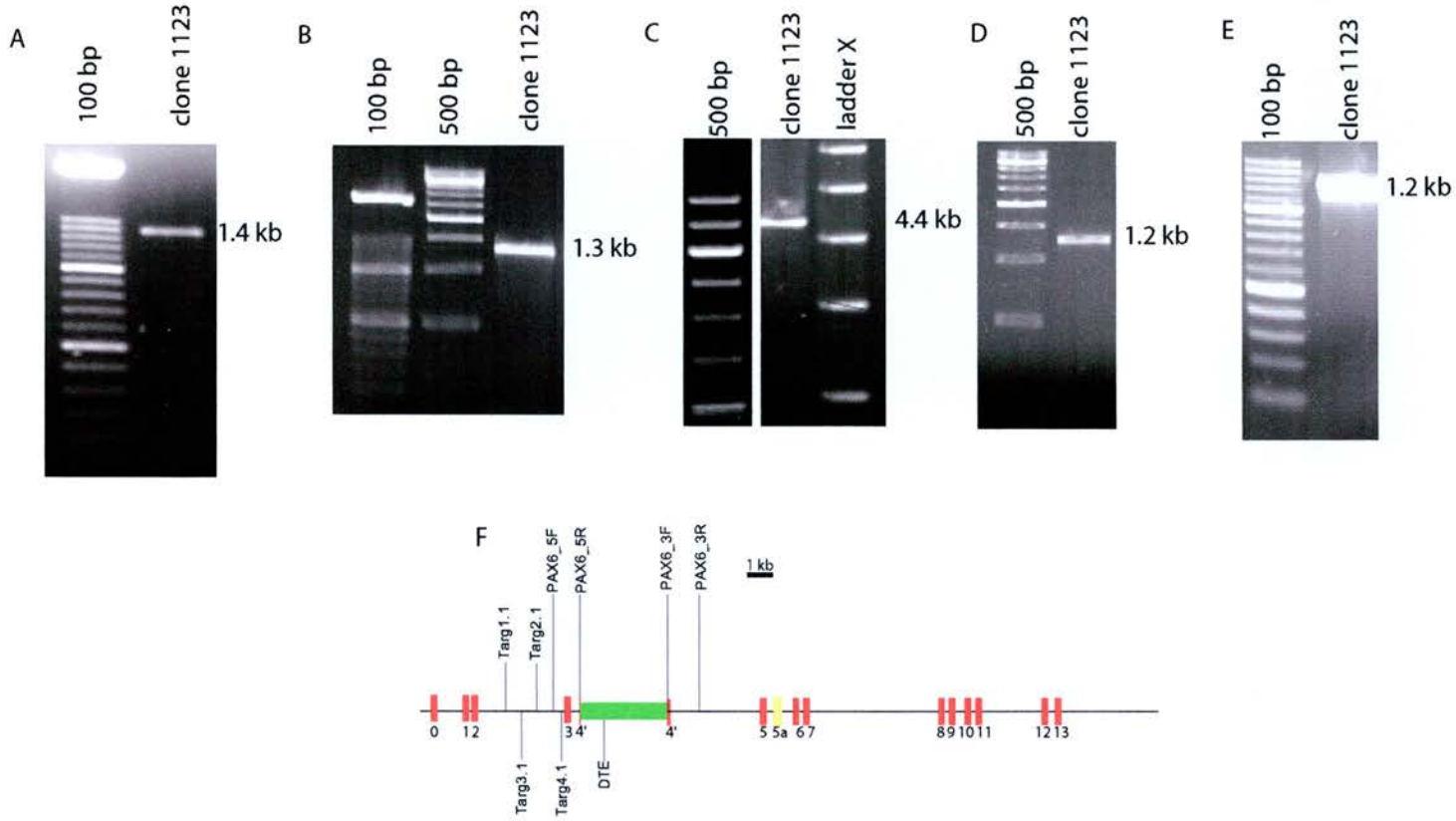
A
100 bp
clone 1123
1.4 kb
B
100 bp
500 bp
clone 1123
1.3 kb
C
500 bp
clone 1123
ladder X
4.4 kb
D
500 bp
clone 1123
1.2 kb
E
100 bp
clone 1123
1.2 kb
F
PAX6_5F
PAX6_5R
PAX6_3F
PAX6_3R
1 kb
Targ1.1
Targ2.1
Targ3.1
Targ4.1
DTE
0 1 2
3 4'
4'
5 5a 6 7
8 9 10 11
12 13

Figure 2.17. Restriction digests of PCR products. A) ApaI digest of PCR product from TauGFPfor and TauGFPrev. B) StuI digest of the PCR product PAX6_5F and PAX6_5R. C) EcoRI digest of PCR product Targ3.1 and Targ4.1. D) Schematic of area around where the reporter cassette inserted into YAC Y593. The red boxes are *PAX6* exons. The green box is the reporter cassette (tauGFP-IRESkozak-Neo^{R}-pA-C2MAZ). The locations of primers and restriction sites are shown. The sequences of the primers are given in Appendix A.

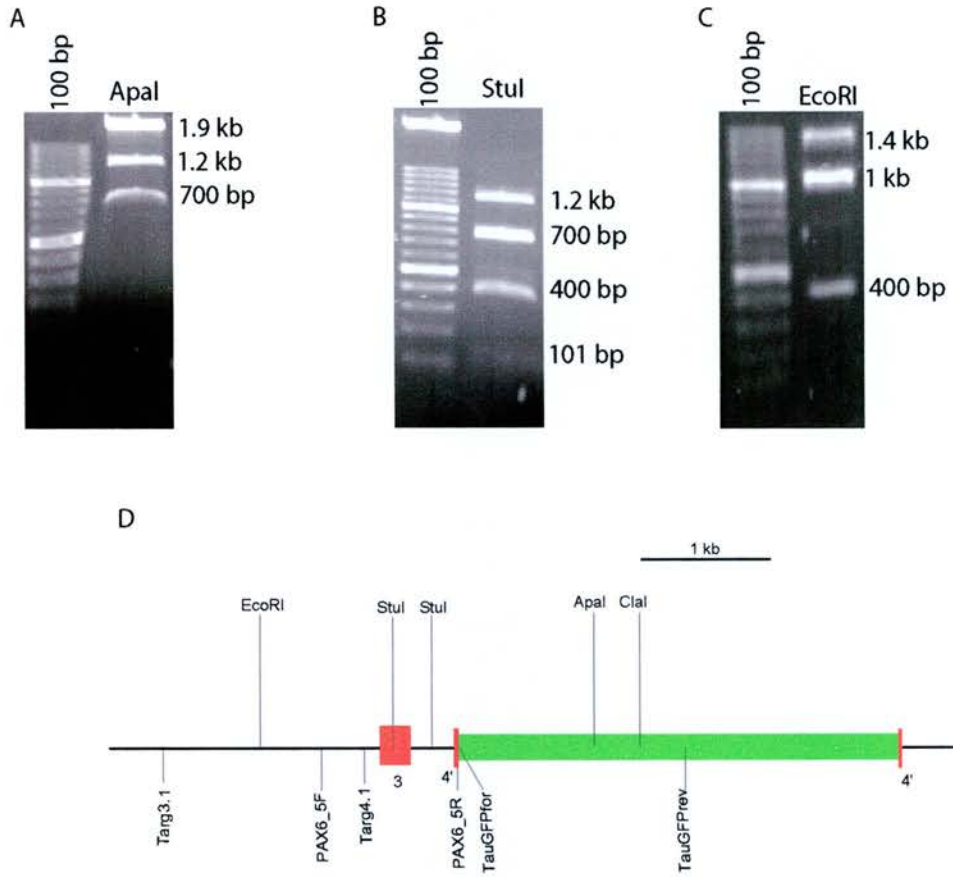
A
100 bp
ApaI
1.9 kb
1.2 kb
700 bp
B
100 bp
StuI
1.2 kb
700 bp
400 bp
101 bp
C
100 bp
EcoRI
1.4 kb
1 kb
400 bp
D
1 kb
EcoRI
StuI
StuI
ApaI
ClaI
3
4'
4'
Targ3.1
PAX6_5F
Targ4.1
PAX6_5R
TauGFPfor
TauGFPrev

Figure 2.18. Sizing of 1-12-3. A) Lane 1 is the Yeast Chromosome PFG Marker (New England BioLabs) . Lane 2 is YAC colony 1-12-3. Lane 3 is the Lambda Ladder PFG Marker (New England BioLabs). The location of the 424kb YAC is indicated with an *. B) Southern blot of the same PFG, probed with a 375bp StuI fragment from *PAX6* exon3.

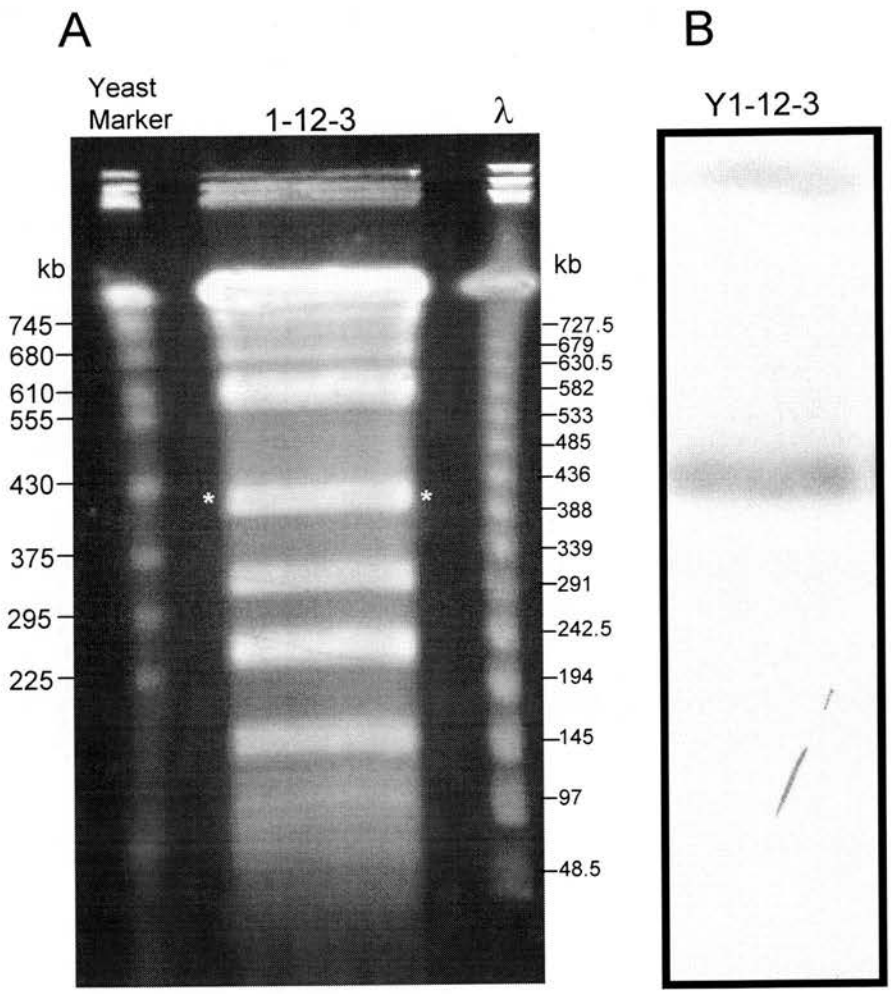
A
Yeast Marker
1-12-3
λ
kb
745
680
610
555
430
375
295
225
kb
727.5
679
630.5
582
533
485
436
388
339
291
242.5
194
145
97
48.5
B
Y1-12-3

In addition to making Y1123 a second YAC was constructed. This work was done as part of a collaboration with Dr Dirk A Kleinjan and Prof. Veronica van Heyningen at the MRC Human Genetics Unit (Edinburgh). The same YAC targeting construct pDT1 was used. However, YAC Y593 was modified before the targeting with pDT1. Dr Dirk A Kleinjan used a bacterial targeting construct to place LoxP sites around a regulatory element in intron 7 of *PAX6* in YAC Y593. This modified YAC was then targeted with pDT1 in the same manner as described for generating YAC Y1123. Eight clones were picked and screened for correct first round rearrangement. I was happy with clone seven, giving a success rate of 1:8 or 12.5%. This clone was used in the second round 5-FOA selection. 12 clones were picked from the 5-FOA plate, designated 371 to 3712. In the same manner for identifying clone 1123 PCR, restriction digests, and southern blots were used to identify clone 374 as correct. This gave a success rate in the second round of about 8%. The junction from *PAX6* into tauGFP was also checked by sequencing across the junction in both directions, the primers used are in the Appendix A. The addition of the LoxP sites added 64bp to intron 7 of YAC Y593. It is believed that this will make no difference to the *Pax6* expression pattern. The LoxP sites have no bearing on this project and are going to be used by Dr Dirk A Kleinjan and Prof. Veronica van Heyningen in their ongoing research. Therefore, the difference in the two YACs is ignored for the remainder of the work in this thesis.

As a precaution a frozen stock was made from the two correct second round recombination clones Y1123 and Y374 before proceeding to isolating and purifying the modified YAC prior to microinjections.

Chapter 3. Isolation and purification of YAC.

Background

The description of the production of the reporter mouse has been broken down into four parts. The previous Chapter described the modification of the original Y593 YAC with a bacterial targeting construct pDT1. Once these new modified YACs (Y1123 and Y375) were constructed they were isolated from the yeast endogenous chromosomes and the YAC DNA microinjected into one cell mouse embryos.

There is no generally accepted protocol to isolate and purify YAC DNA. Every laboratory empirically determines an optimum protocol for their circumstances. This Chapter describes the optimisation of an appropriate protocol. Chapter 4 then goes on to describe the microinjection of the isolated YAC DNA into mouse one cell embryos, and Chapter 5 analyses the expression pattern of the generated lines of transgenic mice.

High molecular weight DNA, such as isolated YAC DNA, is at risk from degradation because its long length means that it is susceptible to shearing forces. Therefore the following precautions were taken throughout.

1. Cut-off or wide bore pipette tips were used at all times when handling the DNA. Although shearing of the DNA by the microinjection needle will take place, this was unavoidable.
2. The YAC is separated from the yeast endogenous chromosomes by gel electrophoresis. Any gel containing YAC DNA that was stained with ethidium bromide (EtBr) and exposed to high intensity UV (ultraviolet) light for visualising was not used in the preparation of the final DNA for injection.

This was because the high molecular weight DNA was very vulnerable to degradation when it was visualised this way. This degradation was verified empirically by visualising the YAC DNA with EtBr staining and UV light. When this DNA was analysed there was strong evidence of degradation. In addition, any carry over of EtBr could be a potential mutagen to the embryos when the DNA solution was used for microinjection. This meant that at any point when the location of YAC DNA needed to be identified the gel was divided longitudinally into three sections in the direction the gel had been run (see Figure 3.1). The middle section (approximately 90% of the gel width) was left unstained, and the two flanking slices (each approximately 5% of the gel width) were stained and used for visualising the location of the DNA. The location of the DNA in the thin slices was marked by cutting the slices with a blade. The whole gel could then be reassembled and the location of the DNA in the rest of the gel could be determined from these marks. The slices that had been stained with EtBr would no longer be used for the preparation of the final DNA.

3. It is standard procedure when cutting out high molecular weight DNA from a preparative agarose gel not to use metal blades, since the metal ions may bind to the DNA and contribute to degradation (Smith *et al.* 1988). Instead it was recommended using a glass cover slip to cut the agarose. Prior to use the glass cover slip was cleaned with ethanol and rinsed with deionised water.
4. Lowering the concentration of the DNA in solution was a straightforward dilution; increasing it was difficult. Standard molecular biology techniques

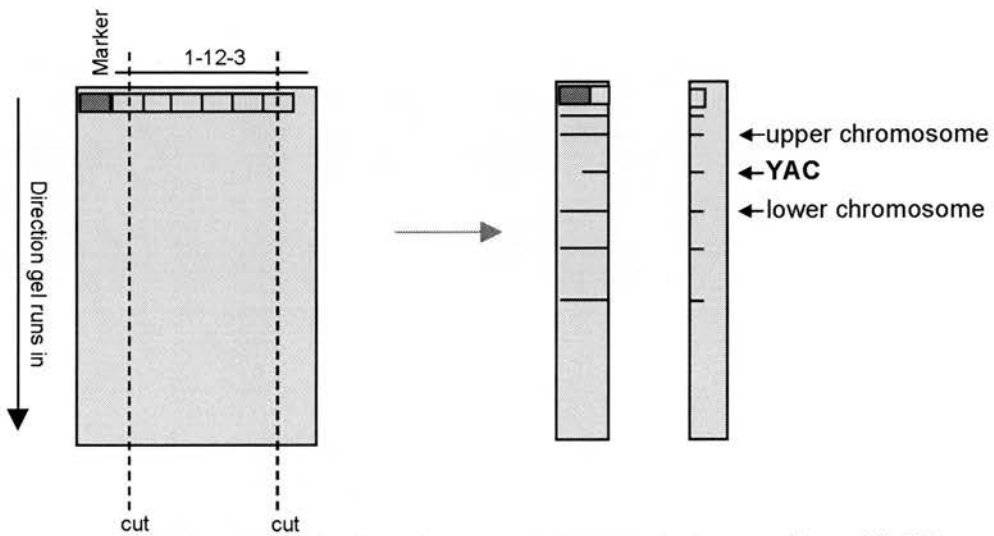

STEP1. After running gel cut two thin slices from each flank with a glass cover slip and remove slices for staining.

STEP2. Stain the two slices with EtBr and visualise with UV light.

STEP3. Whilst visualising with EtBr mark the location of the three chromosomes with a nick made with a glass cover slip

STEP4. Reassemble gel pieces on a clean EtBr-free surface. Location of three chromosomes can now be determined by location of marks. Excise the three slices containing the YAC, and two markers.

Figure 3.1. Staining the gels without contaminating the whole gel with EtBR or exposing the DNA to UV light.

such as ethanol and salt precipitation, or evaporating the solution away were not suitable. These techniques require incubation and or centrifugation. Neither of these is desirable in isolating high molecular weight DNA because these would expose the DNA to shearing forces.

Initial protocol

There are several different schemes used by different researchers to isolate YAC DNA. The original protocol that was used for the isolation of the YAC DNA was suggested by Dr Andreas Schedl (Institute of Human Genetics, University of Newcastle upon Tyne), and was used in the production of the transgenic mouse PAX77 using YAC Y593 (Schedl *et al.* 1996). The scheme is outlined below. A complete description of the scheme is described in the Appendix, Protocol 1: Preparation of High Density Plugs Protocol A, followed by Protocol 2: Preparation of YAC DNA for Pronuclear Injection Protocol. The basic scheme is broken down into five sections, see figure 3.2 for a flow diagram.

1. High concentration plugs

From frozen storage stocks the yeast colony was grown for 144hours at 30°C with shaking. The final saturated culture should contain between 1 x 10^8 and 4 x 10^8 cells. The colonies were spun down and the weight of the pellet determined. An equal volume of 1% low melting point agarose solution containing Zymolyase (ICN) and 14mM β- mercaptoethanol was added and mixed and the resulting solution poured into a plug mould that had been chilled on ice. Zymolyase , which is

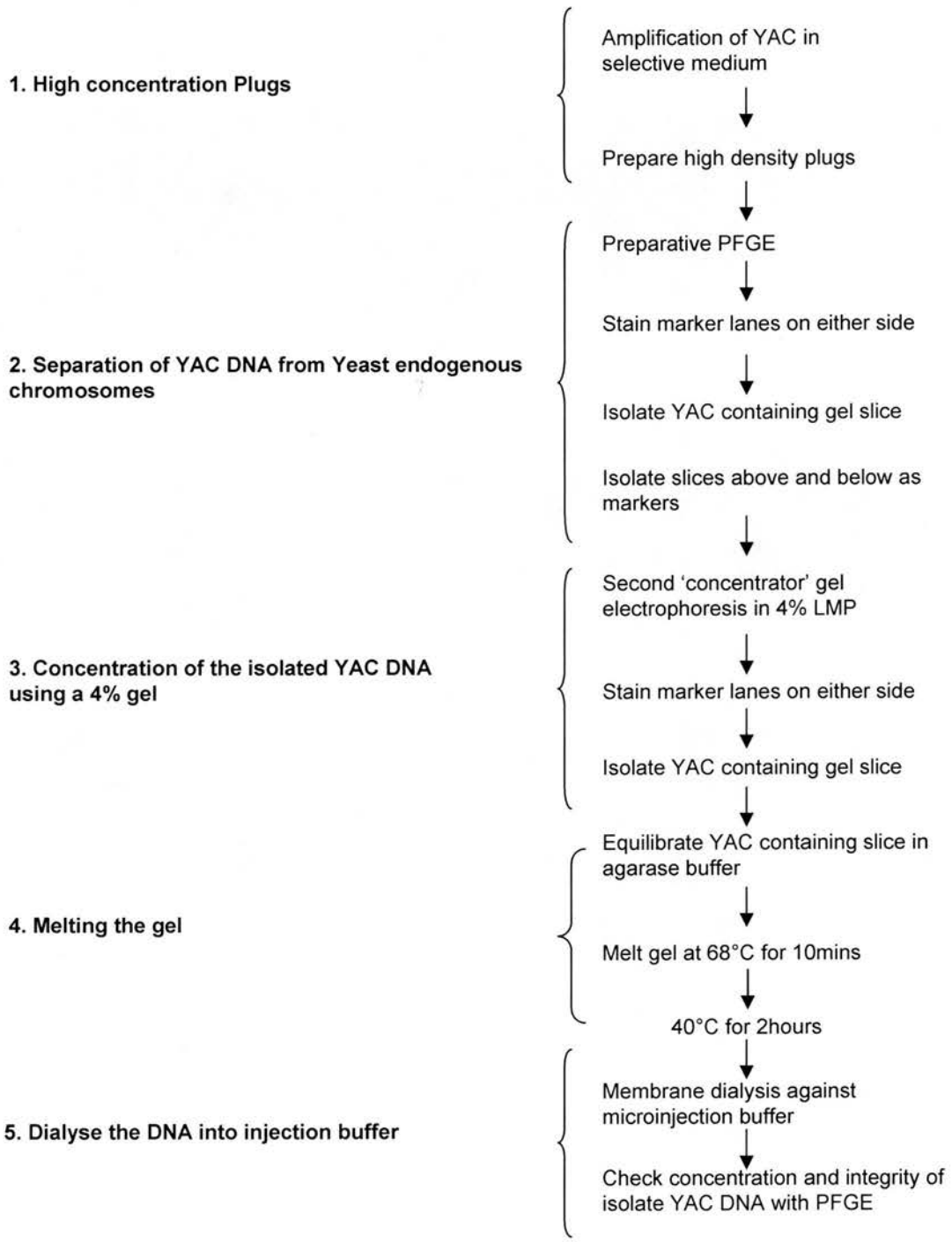

Figure 3.2. Schematic diagram of original YAC isolation protocol.

available commercially in a purified form, is prepared from *Arthrobacter luteus*. The primary yeast lytic activity of Zymolyase is β-1, 3-glucan laminaripentaohydrolase. This hydrolyzes glucose polymers at the β-1,3-glucan linkages in yeast cell walls releasing laminaripentaose as the principal product and so breaks down the thick cell wall of yeast cells (Kitamura *et al.* 1971). Once the plugs had set they were washed in a solution containing more Zymolyase for several hours at 37°C and then overnight in an SDS wash solution containing β-mercaptoethanol and proteinase K. Finally, the plugs were washed in TE and then stored in 0.5M EDTA at 4°C until needed.

2. Separation of YAC DNA from yeast endogenous chromosomes.

A 0.5% TAE agarose gel was cast with a continuous slot for a well to load the plugs into. This gel has to be made with TAE because the boric acid in TBE has been observed to inhibit subsequent agarase reactions (New England BioLabs, β-Agarase, product information). The plugs were loaded into the slot and the gel run. The individual setting for the PFGE depend on the size of the YAC. By trial and error the optimal settings were found to separate the YAC from the endogenous chromosomes.

Once separated the gel was divided longitudinally, perpendicular to the well, as described above. Roughly 3cm edge strips were used for the EtBr staining and the centre portion of the gel kept. Once the 3cm edge strips were stained the DNA was visualised under UV light. The gel strips were nicked with a blade to mark the position of the YAC, and the upper and lower chromosomes flanking the YAC. The

gel was then reassembled on a glass sheet and thin slices cut that contained the YAC, and the lower and upper chromosomes. The lower and upper chromosomes were subsequently used as markers to calculate the migration of the YAC DNA (Figure 3.1).

3. Concentration of the isolated YAC DNA using a 4% gel.

The isolated gel slices containing the YAC and the upper and lower chromosomes were turned through 90° and a 4% TAE low melting point agarose gel cast around them. This concentrating gel was run overnight at 4°C with the buffer re-circulated. The gel was then cut into three longitudinal sections and the upper and lower chromosomes stained with EtBr. Visualisation with UV light showed the location of the compacted bands of the upper and lower chromosomes. With ordinary electrophoresis gels as opposed to PFGE, DNA longer than 45kb migrates at a rate independent of the size of the DNA. This means the upper and lower chromosomes will have migrated the same distance as the YAC. Therefore, the location of the concentrated YAC DNA can be identified and removed.

4. Melting the gel.

The YAC gel slice was then melted at 68°C for 5 minutes and then incubated at 40°C for 2 hours with 1U agarase per 100mg of gel slice. The YAC DNA solution was then placed at 4°C. This verified that all of the agarose had been digested, any undigested agarose would solidify. If digestion was not complete then the protocol suggested repeating the melting process.

5. Dialyse the DNA into injection buffer.

The YAC DNA was dialysed using floating boat dialysis against injection buffer. The solution was dialysed overnight and then the DNA was carefully taken up and 40-50 µl was loaded onto a 1% agarose PFG to confirm the DNA was intact. A YAC plug was loaded next to it to act as a molecular weight marker.

Even after repeating the above scheme several times to eliminate technical inexperience there was very little DNA isolated. The DNA was never visualised on a gel even if the entire 150µl solution of isolated DNA was loaded on to a PFG. Figure 3.3 is a typical outcome of the isolation procedure. In the two attempts shown (Figure 3.3) there is clearly no isolated DNA of the correct size. There is lower molecular weight DNA in both of the attempts shown that was interpreted as DNA degradation. Generally speaking you would expect to see greater than 50ng of DNA stained with ethidium bromide (Sharp *et al.* 1973): so 150µl of solution at a concentration greater than 0.3ng/µl would be visible. This indicates that if there was any high molecular weight DNA in the final product it would have to be at a concentration lower than 0.3ng/µl otherwise it would be visible. The concentration of DNA needed for microinjection is 0.3 to 5 ng/µl. So even if there was intact high molecular weight DNA in the final solution at a concentration too low for detection by ethidium bromide it was also at a concentration too low for microinjection. In addition, from the PFG it was clear that the vast majority of the isolated DNA was degraded low molecular weight DNA, so the vast majority of any transgenic mice made would only have short transgenes made from these fragments. Given the time and effort involved in microinjection and then the subsequent screening of the few

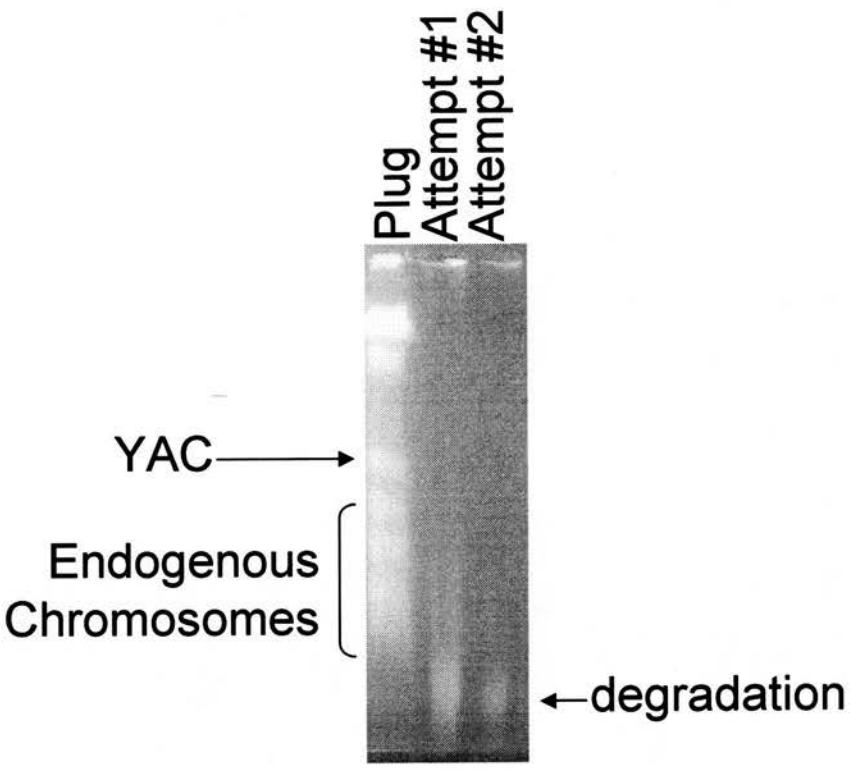

Figure 3.3. Results of Isolating Intact YAC DNA.

offspring that are produced it seemed it was not an option to use the DNA in this state to produce mice carrying the entire 424kb YAC.

Trouble shooting the isolation of the high molecular weight DNA

At this stage, it was unclear if the bulk of the DNA was either simply being lost due to procedural error during the protocol or if the DNA was all being lost due to degradation or a combination of the two.

Identifying at which specific step the intact DNA was being lost

The scheme to isolate the YAC DNA is a long protocol with a number of steps. In theory the DNA could be lost or degraded at any one of the steps. To address this problem the original protocol was followed but samples of DNA were removed at all points and analysed on a diagnostic PFG to see what condition the DNA was in at each point. It was expected that this would identify either the stage where the DNA was being lost or if there was further evidence of major DNA degradation.

From the first PFG (step 2 in Figure 3.2) it was clear that YAC DNA was intact at this point, that is YAC DNA was initially being separated from the endogenous yeast chromosomes. So samples were removed after the 4% concentrator gel (step 3), after heating to 68°C (step 4), after 2 hours at 40°C (step 4), and after dialysis (step 5). Looking at the gels the DNA was intact after steps 1,2 and 3. The DNA was still mostly intact immediately after melting at 68°C, although there were some signs of smearing (midway through step 4). However, at the end of the 40°C incubation (end

of step 4) the DNA was no longer visible on a PFG. Therefore, it seemed that the problem was due to one or more of the following.

a) DNA escaping from the micro-centrifuge tube that it was in during the melting and heating.
b) The 40°C incubation process was somehow degrading the entire DNA; possibly some factor in the DNA solution was causing this (e.g. nucleases).
c) Something prior to the 40°C incubation was priming the DNA so that during the 40°C step the process of complete degradation was being finished.

It seemed very unlikely that the DNA was escaping from the micro-centrifuge tube. So the protocol was repeated removing samples as described before. However, at step 4 several options were taken. Some of the DNA was melted at 68°C and kept. Some was melted in the same manner and incubated at 40°C. Some was only incubated at 40°C and some was neither melted nor incubated at 40°C. It was found that DNA was not lost if it was untreated or only incubated at 40°C. DNA that was melted at 68°C and then kept had signs of smearing that were taken to be degradation and the DNA melted at 68°C and incubated at 40°C was completely lost. Therefore, it was concluded that the heating of the DNA to 68°C was definitely contributing to the loss of DNA, possibly by mechanical degradation, and the 40°C step was finishing the process off, possibly through the action of enzymes.

Removing the melting stage was not an option in this scheme, and neither was reducing the temperature, since 68°C is the minimum temperature required to melt the low melting point agarose. But eliminating repeating the heating stage when part of the agarose was not melted was done and became standard.

This scheme had been shown to work by several people in different laboratories. This suggested that there was something wrong with the way the protocol was being followed, or a subtle and undocumented but essential part of the protocol was missing, or this particular YAC is very sensitive to degradation.

Identifying the unknown factor that resulted in DNA being degraded during the melting of the agarose.

There are several potential factors that could lead to the loss of the DNA and each once is discussed in turn below.

a) Nucleases in the solutions, for example in the TAE. Initially the solutions had been made using general laboratory stocks of reagents and deionised water produced in the laboratory. Therefore, all solutions were remade taking great care that the reagents supplied were certified DNAse and RNAse free and that any lab ware, e.g. to measure out the reagents, was also DNAase and RNAase free. It was also ensured that any water used was the highest quality polished deionised water. In addition, using the autoclave to sterilise solutions was avoided since the metal ions from the autoclave itself could be contaminating the solutions. Very small amounts of metal ions from using steel blades to cut the agarose containing high molecular weight DNA have been suggested previously to cause degradation. It therefore, seemed possible that very small amounts of metal ions from the autoclave itself could contaminate the solutions. After making these minor changes there was still no DNA

isolated. However, these high standards for reagents seemed prudent and so were maintained subsequently.

b) The growth of the yeast was examined closely by looking at and counting the growing colonies at regular time points for signs of anything unusual. There were no obvious problems with the growth. In addition, the plug forming protocol used proteinase K and EDTA in the solutions. Both of these should have prevented the action of any nucleases from the yeast culture that were carried over into later steps.

An additional reason for analysing the growth is that previously it has been found that the use of yeast concentrations greater than $6x10^{9}$ per ml in agarose plugs leads to a significant loss of resolution of the YAC DNA on PFGs (Bauchwitz and Costantini 1998). It was feasible that the smearing which was evident on the PFGs was due to this; however, routinely counting the growth of the yeast colonies with a haemocytometer proved the final yeast concentration was always $<6x10^{9}$ per ml.

c) Examination of the protocol for forming the plugs. The PFG gels that were used to separate the YAC from the endogenous yeast chromosomes had some background smearing that originally had been understood to be normal but, after discussions with other groups, was thought more likely to indicate degradation. Therefore, alternative protocols for the way the plugs were made were investigated. There are a few groups that work with high molecular weight DNA. Initially it seemed best to make minor modifications to the protocol before embarking on changing the entire protocol. It was still unknown if technical inexperience was a factor and continually changing

the protocol and making new errors due to inexperience rather than learning how to carry out one of the protocols correctly seemed a possibility.

Originally the plugs were made by preparing a 50:50 mix of pelleted yeast culture and 1% low melting point agarose in SE buffer. This buffer was 1M sorbitol, 20mM EDTA, pH8.0, Zymolyase , and 14 mM β-mercaptoethanol. The function of Zymolyase has already been discussed (it is a typical reagent used to break down yeast cell walls). The addition of β-mercaptoethanol is believed to predispose the yeast cells to action of the lytic enzyme Zymolyase (Campbel and Duffus).This works by breaking disulphide bonds in yeast cell proteins, therefore giving Zymolyase easier access to its target the cell wall protein β-glucan. EDTA stops phosphomannose (part of the wall polymer) from inhibiting the digestive activity of Zymolyase (Rayner and Munro 1998). The sorbitol stabilises the yeast cells osmotically. Once the plugs were set they were washed overnight in 1% SDS, 0.1M Tris pH 8.0, 200mM EDTA pH 8.0, 0.5M NaCl, 0.5 M β-mercaptoethanol, 1mg/ml proteinase K.

A subtly different plug preparation protocol was suggested by Dr Simon Fisher (Oxford University). The protocol leaves out the proteinase K, exchanges the detergent 1% SDS for 1% lithium dodecyl sulphate, and adjusts some of the concentrations of EDTA and Tris in some of the solutions; complete protocol is in the Appendix, Protocol 3: Preparation of High Density Plugs Protocol B. The protocol was tried a few times. It reduced the amount of background smear, which probably indicates less degradation was taking place. Figure 3.4 is a comparison of the original plug making protocol (Protocol 1: Preparation of High Density Plugs Protocol A) and this protocol (Protocol 3: Preparation of High Density Plugs Protocol B). Isolating the YAC DNA from the plugs using the remainder of the existing protocol (described in the Appendix, Protocol 2: Preparation of YAC DNA for Pronuclear Injection Protocol) resulted in no intact DNA being purified.

In tandem a different agarose plug protocol suggested by Dr Clare Huxley (Imperial College School of Medicine) was tried and that also resulted in better resolution of bands. But again, isolating the YAC DNA from the plugs using the remainder of the existing DNA isolation protocol (see Appendix, Protocol 2: Preparation of YAC DNA for Pronuclear Injection Protocol) resulted in no intact DNA being purified. Dr Huxley's protocol also leaves out the proteinase K and uses the detergent 1% lithium dodecyl sulphate. The complete plug preparation protocol is in the Appendix, Protocol 4: Preparation of High Density Plugs Protocol C.

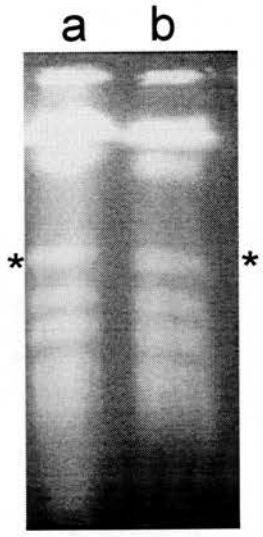

Figure 3.4. Comparison of different plug making techniques. (a) Plugs made using plug protocol A. (b) Plugs made using plug protocol B.

d) Possibility of DNA degrading factor present in PFG equipment. Previously the equipment was rarely cleaned and was often left for long periods of time full of old running buffer exposed to sunlight. The equipment was washed with reagents suggested by the manufacturer but there was no obvious improvement in DNA preparation. The equipment was primarily being used for analytical work and so any DNA degradation was less important. This protocol required equipment for preparative work. Therefore another group was identified that maintained their equipment at a higher standard. From this point onwards it seemed prudent to use this equipment.

With all these changes intact DNA was still not being purified. The systematic examination of the protocol had identified that the DNA was being lost during the agarose melting stage. Even though the modifications discussed above had failed to identify the factor that was causing this, these adjustments had resulted in the bands on the PFG being distinctly clearer and sharper. It seemed better to have this than more diffuse bands with a high amount of background smear.

DNA concentration

It was also a possibility that even with the heating and melting optimised, and the prior preparation optimised the concentration of the DNA to begin with was too low. That is, the melting and heating steps even when optimised may always lose a certain unavoidable percentage and so if the initial DNA concentration was too low the protocol would fail.

The protocol specifies the number of yeast cells to be used in making the plugs. Each haploid yeast cell contains one copy of the YAC. Therefore the DNA concentration in the separated YAC DNA band in the first PFG (Figure 3.2 step 2) was predictable. This prediction assumed that the number of yeast cells being lysed and releasing their DNA was consistent. According to the manufacturer of the Zymolyase the extent of yeast cell lysis will vary with yeast growth and cultural conditions and so the yeast growing conditions can have a detrimental effect on the amount of DNA produced. However, the growing conditions of the yeast colonies had previously been examined, see above, and so it was considered probable that the Zymolyase was working correctly.

The next step in the scheme was to excise the DNA. The slice was cut as small as possible with the least amount of surrounding gel to ensure the DNA concentration was as high as possible. After this the DNA was concentrated into a smaller band (concentrator gel, step 3) and again the gel slice cut as close as possible to this so as to maintain a high DNA concentration. At neither of these points was the actual isolated DNA visualised. As explained above, the position of the DNA had to be estimated by dividing up the gel and using EtBr stained markers. Therefore, there was the possibility that the concentration was not as high as anticipated. Post staining the gels with EtBr after the slices had been removed gave some indication as to how effectively the DNA band had been excised. If it was felt too much DNA had been missed the protocol could be aborted.

Running an aliquot of the DNA sample collected prior to the 68°C melting step demonstrated there was some DNA present; however, the exact concentration of the DNA was unknown. Unfortunately the expected DNA concentration at this stage was not discussed in the protocols. The concentration of DNA in the agarose gel prior to the 68°C melting step can be established by examining the intensity of the DNA band if a known standard molecular marker of a similar size is available. High molecular weight markers are commercially available, but the concentration of each band in the marker is unknown, and so the concentration of DNA can not be calculated from them.

Since the concentration of DNA prior to the melting step is unknown but the final product is no or very little intact injection quality DNA and there are several different alternative methods to isolate YAC DNA, it seemed a good idea to examine the alternatives. Most of the schemes use the same growing and similar plug manufacture processes to the ones described above. The major difference in the approaches is the way the DNA is concentrated. In the original protocol a 4% concentrator gel is used. One alternative protocol suggested by Dr Lluis Montoliu (Campus de la Universidad Autónoma de Madrid, Spain) is to place the DNA solution in a spin column and briefly centrifuge. A brief outline of the changes is discussed below, also see figure 3.5. The complete protocol appears in the Appendix, Protocol 5: Preparation of YAC DNA for Pronuclear Injection.

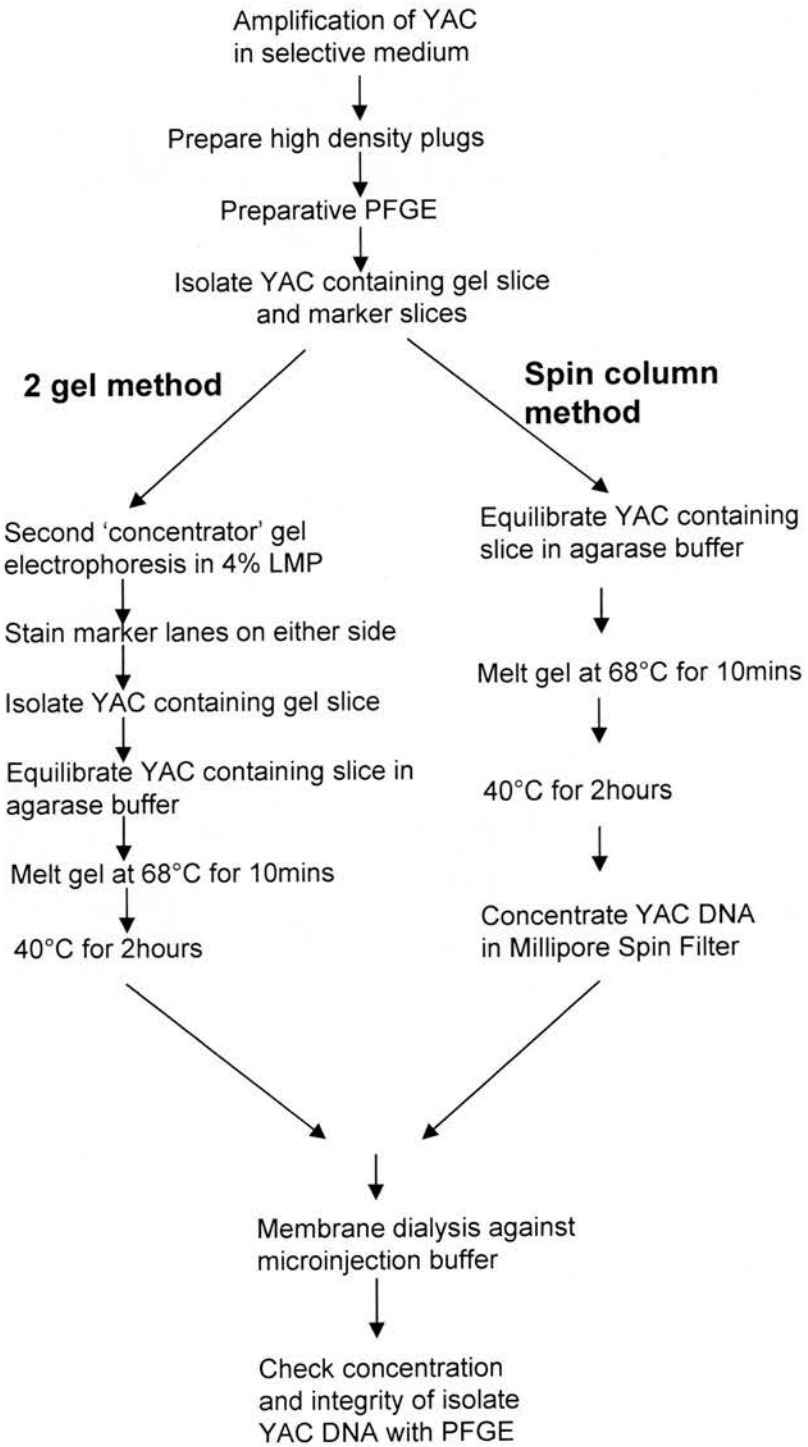

Figure 3.5. Schematic of the different protocols.

1. High concentration plugs

This was conducted in a similar manner to Dr Clare Huxley's plug preparation protocol.

2. Separation of YAC DNA from yeast endogenous chromosomes.

This was conducted in the same manner as before but a 1% low melting point agarose TBE gel was used because the final equilibration of the excised band is into agarase buffer (10mM Bis-Tris-HCl pH 6.5, 0.1 mM EDTA, 100mM NaCl, 30 μM Spermine, 70 μM Spermidine). The equilibration was done at least overnight. Part of this equilibration will dilute any boric acid and so prevents the boric acid from inhibiting subsequent agarase reactions.

3. Melting the agarose gel.

Conducted the same as before

4. Concentrate the isolated DNA using a filter column.

The YAC DNA was pipetted onto a Millipore Ultrafree-MC 30,000 NMWL Filter Unit (Millipore Cat # UFC3 TTK 00). The filter unit is filled with the DNA solution and centrifuged at 3000 g in a microcentrifuge for 5 min. The liquid that had passed through the filter was discarded. The 5 min centrifugation was repeated until 200 to 300 μl of the liquid had passed through the filter. This gave a 2 to 4 x concentration. Generally the centrifugation had to be repeated 5-10 times. Once concentrated, the remaining DNA solution was removed by pipetting up and down once or twice slowly to dislodge the DNA from the surface of the filter.

5. Dialyse the DNA into injection buffer.

This was conducted in the same manner as before.

The new protocol was attempted a few times without success. The protocol was then repeated removing samples at every step and analysing them on a PFG. Again the DNA was found to be lost at the step where the agarose was melted at 68°C and incubated at 40°C.

Alternatives to heating at 68°C and incubating at 40°C for two hours

Examination of the literature on high molecular weight DNA revealed that most protocols are based on either this new protocol (spin columns) or are based on the original protocol (concentrator gel). Both types of protocol required the agarose to be melted at 68°C at some point to isolate the DNA from the agarose. It is possible to use electroelution to isolate the DNA from the agarose (Strong *et al.* 1997). The rest of the protocol was similar to either of the two already tried. Electroelution devices are available commercially and ElutaTube™ (Fermentas, Lithuania) was purchased and tried but with no success.

Ingredients in solutions added to protect the high molecular weight DNA from degradation.

A number of different schemes have been tried to protect high molecular weight DNA from breakage. A review of the different schemes reveals a large degree of conflicting empirical evidence.

Additives used to compact the DNA to reduce shearing forces

The salts commonly used for protecting high molecular weight DNA in this way can be broken down into three classes: Polyamines such as spermidine and spermine; Na^+; or combinations using both polyamines and Na^+. These approaches are believed to reduce the radius of gyration of large linear DNAs by compacting them in these various salts (Bauchwitz and Costantini 1998). It has also been suggested that they might protect the DNA by forming inter as well as intra-molecular bridges (Schedl *et al.*).

Comparing protocols that include and exclude polyamines, it was found that the presence of polyamines, specifically 5mM spermine, was essential for the isolation of intact 280kb YAC DNA (Couto *et al.* 1989). Analysis of another protocol that excluded polyamines found that the average size of recovered YAC DNA was approximately 150kb, whereas including polyamines (750 μM spermidine and 300 μM spermine) in the protocol the average size increased to greater than 400kb(McCormick *et al.* 1989).

Using commercial yeast chromosomes as a source of high molecular weight DNA, another group identified that high molecular weight DNA prepared in agarose was degraded when heated to 68°C in the presence of 30mM NaCl but with no polyamines (Larin *et al.* 1991).They found that to eliminate this effect it was necessary to include 750μM spermidine and 300μM spermine to prevent degradation of large (in this case greater than 620kb) DNA fragments (Larin *et al.* 1991)

Later it was confirmed that the presence of polyamines (750 μM spermidine and 300 μM spermine) enabled the recovery of intact 250kb YAC DNA (Gnirke *et al.* 1993). In addition, Gnirke *et al.* (1993) found that without NaCl or polyamines the yeast chromosomes degraded during agarase treatment (Gnirke *et al.* 1993). However, in their hands the DNA prepared sedimented too much to be used for microinjection (Gnirke *et al.* 1993). They found that polyamines precipitated the DNA at NaCl concentrations of 60 mM or less (Gnirke *et al.* 1993). Interestingly, they found NaCl concentrations as low as 30 mM in the absence of polyamines protect the DNA from being sheared (Gnirke *et al.* 1993). Furthermore, at NaCl concentrations of 100 mM or more they found that polyamines appeared to have no effect (Gnirke *et al.* 1993). Therefore they used NaCl at 100mM with no polyamines to isolate YAC DNA.

However, another group found, that the reliance on Na^+, either alone or in combination with polyamines, will not provide protection of YACs comparable to that from polyamines alone (Bauchwitz and Costantini 1998). In addition, they found that the presence of sodium will antagonize the protective effects of the polyamines on YAC DNA (Bauchwitz and Costantini 1998).

Other possible additives

It has been discussed above that metal ions from metal blades can lead to degradation of high molecular weight DNA. Previously it had been shown that Fe^{2+} complexed with EDTA bound strongly to DNA and caused cleavage of single and double stranded DNA when heated to 68°C in the presence of reducing agents(Schultz and Dervan 1983). It had also been observed that high levels of Mg^{2+} protected DNA in agarose from degradation when heated to 68°C (Larin *et al.* 1991). This may be due to the high ionic strength of Mg^{2+}, preventing DNA from denaturing, or because Mg^{2+} forms a complex with EDTA and competes with any metal ions (found in commercial agarose) for the chelation site (Larin *et al.* 1991). Therefore Larin *et al.* (1991) supplemented their solutions with 10mM $MgCl_2$.

It is impossible to satisfy all of the above conditions since some are contradictory. Also it is important to remember the aim of this project, is to generate a '*Pax6* Reporter' mouse, and not to explain the inter-molecular dynamics of high molecular weight DNA. It seemed that the remedy was to find a complete scheme that worked in my hands with this particular YAC; Up until this point two protocols based on using 100mM NaCl and polyamines to protect the DNA had been unsuccessfully used. One used a 4% gel to concentrate the DNA and one used brief centrifugation. Parts of these protocols had been modified, specifically the way the agarose plugs were made, but with no success. Therefore it seemed logical to try a protocol that did not use the same salts to protect the DNA. Dr Clare Huxley suggested a protocol for isolating high molecular weight DNA (included in full in the Appendix, Protocol 6)

that omitted polyamines, maintained a high NaCl concentration, and used commercially available embryo quality water throughout rather than deionised water made in the laboratory. The protocol used the spin column method of concentrating the DNA, and prior to the agarose melting step the agarose gel slice was equilibrated into a solution that was not supplemented with polyamines. This protocol was tried and after a few attempts worked satisfactorily, see Figure 3.6. The recovered intact DNA was resuspended in 10mM Tris, 0.2mM EDTA, 100mM NaCl made in embryo grade water. The DNA appeared stable at 4°C for several months.

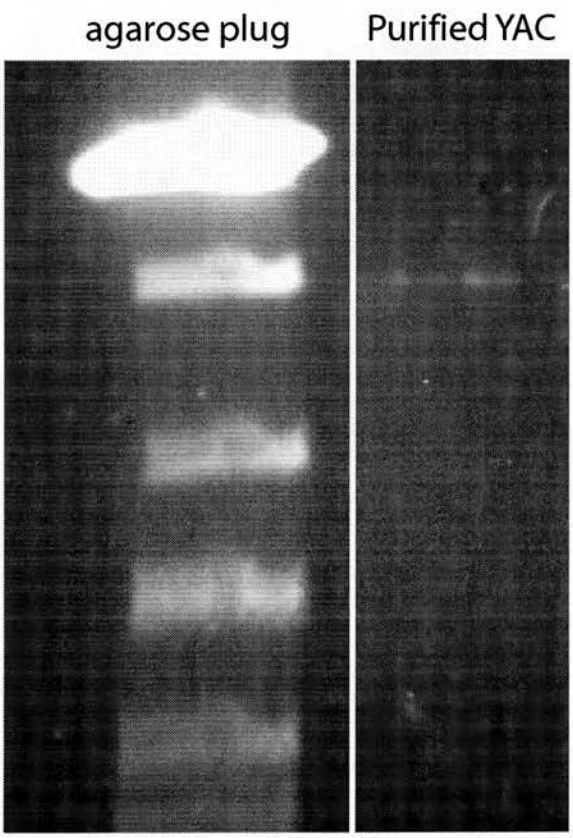

Figure 3.6. Photograph of a PFG of the purified YAC DNA alongside a yeast plug.

Chapter 4. Microinjection of YAC DNA into one cell embryos.

Introduction

The description of the production of the '*Pax6* reporter' mouse has been broken down into four parts. Chapter 2 described the modification of the original Y593 YAC with a bacterial targeting construct pDT1. Chapter 3 described the optimisation of an appropriate protocol to isolate and purify the YAC DNA from the yeast endogenous chromosomes. This Chapter describes the microinjection of the isolated YAC DNA into mouse one cell embryos, and the next Chapter analyses the expression pattern of the generated lines of transgenic mice.

Materials and methods

Microinjection is a highly specialised skill and it was decided to enlist the expertise of a specialist microinjection facility. After identifying and contacting a few places it was arranged that the work would be carried out by two groups. Group One was a specialist microinjection group at the University of Manchester and they would inject YAC Y1123. Group Two was Dr Dirk A Kleinjan and Prof. Veronica van Heyningen at the MRC Human Genetics Unit (Edinburgh) and they injected YAC Y374.

Group One: University of Manchester, UK

This work was conducted by technicians at the University of Manchester, UK. We supplied the DNA at three different concentrations and they injected approximately 200 one cell embryos with each concentration. Table 4.1 summarises the details of

Concentration of YAC DNA	Number of embryos injected	Number replaced	Number born	Number transgenic	Founder ID
1.5ng/µl	305	240	41	2	9† 22
1.0ng/µl	245	195	37	0	0
0.5ng/µl	276	190	25	2	42 54
TOTAL	826	625	103	4	

Table 4.1

This table summarises the injection performed by Group One. † Founder 9 is not transmitting.

the injections. It was decided to try different concentrations of DNA because in the YAC literature and from talking to groups that have successfully generated YAC transgenics by microinjection, they generally isolate about 1 to 5 ng/μl and subsequently inject at concentrations of 0.3 to 5 ng/μl.

The oocytes used for microinjection were isolated from crosses of C57Bl/6 and CBA.

Group Two: MRC Human Genetics Unit, Edinburgh, UK.

Several aliquots of DNA were supplied at a concentration within the recommended range for injection concentration (0.3 to 5 ng/μl). Table 4.2 summarises the details of the injections.

The oocytes used for microinjection were obtained from crossing B6CBAF1/JIcoCrl females to B6CBAF1/JIcoCrl males. The recipient females used were Crl:CD-1(ICR).

Injection round	Number of embryos injected	Number replaced	Number born	Number transgenic	Transgenic ID
17 June	145	21	2	0	
19 June	183	23	4	1	001
26 June	nr	45	0	0	
14 July	nr	nr	3	1	028
21 July	145	24	2	0	
16 Sept	258	28	6	3§	223‡ 226 227§
TOTAL	731†	141†	17	5§	

Table 4.2. Summary of injection of Y374 carried out by Group Two. nr indicates not recorded. † indicates incomplete data because some of the data were not recorded. ‡ Founder 223 died before breeding. § Unclear if Founder 227 is transgenic.

Outline of injection and embryo transfer procedure

Generally speaking similar protocols were used by both groups. 25µl of isolated YAC DNA is enough to inject 200-250 one-cell embryos. The groups also used exactly the same needles to inject the YACs as they use for plasmid DNA, although they aimed for larger diameter holes at the end of the needles. Furthermore, they loaded the needles by capillary action from the back of the needle, not by aspiration of the DNA through the needle end because this leads to unnecessary degradation of the DNA. The microinjection itself was typically performed using a balance pressure setting high enough to ensure continuous outflow of DNA.

Another difficulty was that the efficiency rate with YAC transgenics is somewhat lower than with plasmids and a reasonable estimate was that 5% of injected one-cell embryos will ultimately be born. Thus the number of injections needed would be higher than for plasmid injections.

Once injected the one cell embryos were either replaced immediately into a pseudopregnant female mouse or cultured overnight until two-cell and then transferred to pseudopregnant female mice. Mice typically have litter sizes of 10 pups and it was expected that many of the embryos would not make it to full term; therefore, more than 10 one cell embryos were returned to each female. As well as using fewer mice it also meant that the actual live litter size was larger and closer to 10. It has been reported anecdotally that female mice that give birth to litters with far less than this can destroy the litter. It was therefore prudent to engineer it so that the females would give birth to numbers closer to 10.

Once the transgenic pups were born they were left until weaning (about three-weeks old) when they were ear punched for identification. The tissue biopsies from the ear punching were digested with proteinase K and DNA isolated using standard molecular biology techniques. The DNA was then used in a PCR with primers specific for mouse *Pax6* and Human *PAX6* (details of the primers in the Appendix). Transgenic mice were identified by having both a mouse specific band and a human one.

Results

In total nine transgenic founders were identified. Four were identified from the YAC Y1123 (see Table 4.1) and five from YAC Y374 (see Table 4.2). Each identified founder was bred with CD1 mice to establish nine lines. The nine lines were each denoted by the original number assigned to the founder plus the name of the YAC. Hence, the four Y1123 lines are DTy1123.9, DTy1123.22, DTy1123.42, and DTy1123.54. The five Y374 lines are DTy374.001, DTy374.028, DTy374.223, DTy374.226, and DTy374.227. Unfortunately, founder 1123.9 appeared to be sterile and so did not pass on the transgene, 374.223 died before breeding, and it was unclear if 374.227 was actually transgenic or not. It is possible that 374.227 was a very low percentage mosaic and this may make it difficult to be conclusive. Breeding of the line should establish if it is transgenic or not.

Summary

This Chapter has described the microinjection of the two YACs Y1123 and Y374 by two different groups. A total of nine transgenic founders were identified and transgenic lines were established by crossing these founders with CD1 mice. Further analysis on these lines was done to confirm the extent of the YAC that has been integrated, the copy number, and the GFP expression pattern. This is described in Chapter 5.

Chapter 5. Analysis of '*Pax6* reporter' mice.

Summary

Chapter 5 describes the characterisation of the nine lines of the '*Pax6* reporter' mice, whose generation was described in Chapters 2, 3, and 4. This analysis shows that the GFP expression is largely the same in some of the lines as the previously reported *Pax6* expression pattern. In other lines that were analysed the GFP expression was incomplete and seen in only a subset of where *Pax6* expression has been previously reported.

Introduction

PCR was used to initially identify transgenic founders (described in Chapter 4). The GFP expression has been analysed at a range of developmental stages by imaging appropriate mouse embryos. In addition, the calculation of the copy number and extent of the YAC incorporated in each of the nine lines is described.

Materials and Methods

Extent of YAC Y1123 and YAC Y374 incorporated in the transgenic founders

The extent of each YAC that incorporated into the transgenic founder was investigated using PCR. From each founder DNA was isolated from ear notches that had been made for the purpose of identification of the mice. PCR reactions were set up with 500ng of the ear notch DNA and pairs of human *PAX6* specific primers. The primer sets span the length of the YAC and location is shown in Figure 5.1. The primer sequences are given in Appendix A.

Number of copies of the YAC that incorporated in the transgenic founders

The number of copies of the YAC that incorporated was established by using quantified real time PCR (qPCR). A QIAGEN QuantiTect SYBR Green PCR Kit (Qiagen) was used according to the manufacturer's instructions. Briefly, the kit contains an optimized fluorescent dye SYBR Green 1. This dye binds all double-stranded DNA molecules, emitting a fluorescent signal on binding. This signal can be detected using a real time PCR machine (MJ Research, San Francisco, USA) and the amount of original target material calculated.

The number of copies of the YAC incorporated in four (DTy1123.22, DTy1123.42, DTy1123.54, and DyY374.001) of the lines was calculated. From each line DNA was isolated from ear notches that had been made for the purpose of identification of the mice. DNA was collected from at least six mice from each line.

300ng of the isolated ear notch DNA was added to each of the qPCR reactions. The qPCR reactions were set up according to the SYBR Green manufacture's instructions. Each reaction contained the template DNA, primers, and the SYBR Green mix supplied by the manufacturer. Three sets of qPCR were set up with different sets of primers. Set one used the human *PAX6* specific primers previously used in identifying the transgenic founders. Set two used the mouse *Pax6* specific

Figure 5.1. Diagram of the locations of primers along YAC Y593. The primer set location is indicated by a grey vertical line and the name of the primer set is written above. Red boxes are the *PAX6* exons. The green box is the GFP-neo^{R} reporter cassette. The yellow box is exon 5a. Blue boxes are the 3' exons of the antisense neighbour gene ELP4. E100+ (Box 123) and HS234 are long range highly evolutionary conserved elements. SIMO is the most distant human patient breakpoint. The approximate minimum extent of the YAC incorporated in the nine transgenic founders is indicated by the dashed lines.

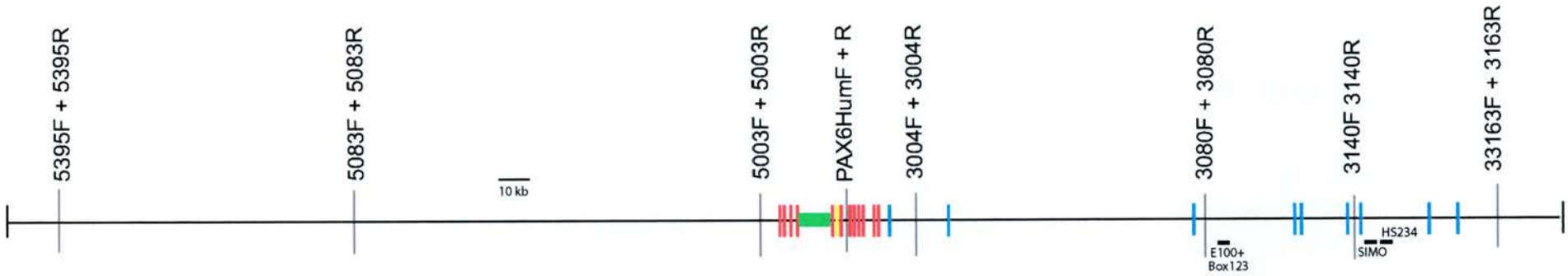

1123.9
1123.22
1123.42
1123.54

374.001
374.028
374.223
374.226
374.227

primers used in identifying the transgenic founders. Set three used mouse specific *Pax3* primers. The sequences of all the primers are given in the Appendix A.

Sets two and three are controls and will produce a predicable amount of SYBR Green fluorescence since the gene copy number of both is known to be two. By comparing the fluorescence generated against the fluorescence generated when the same amount of DNA is used in set one the number of *PAX6* gene copies can be calculated. This assumes that the DNA is homogenously mixed. The strategy was recommended by the manufacturers of the real time machine, see Figure 5.17 for a diagram explaining the calculation. Each qPCR was standardised against the same set of serial dilutions of known quantities of DNA. In all reactions the samples appeared on the standard curve within a confidence of >95%. Each reaction was repeated three times.

Tissue processing for Vibratome sections

Embryos or tissues were fixed in ice cold 4% paraformaldehyde in phosphate buffered saline (PBS) overnight and embedded in 4% low melting point agarose. Embryos were obtained from natural matings of transgenic mice and CD1 mice and the day of the vaginal plug was designated day E0.5.

Sections (200μM) were cut on a Vibratome in ice cold water. Some sections were counterstained with 0.5μM of TOPRO3 (Molecular Probes, NL). TOPRO3 binds nucleic acids. Sections were then mounted on glass slides.

Figure 5.17. Graph for qPCR calculations. A step by step example of calulating the number of copies of the YAC with founder x is:

1) For each founder sample 300ng of homogenous DNA was used. Containing N copies of the genome. However, as this is a homogenous solution the number of copies of genome is proportional to the mass of DNA used and the amount of DNA used is the same for each set of primer. Hence N is the same for all the samples.

2) With founder x

F_{x1} is the fluorescence intensity with Pax6 primers = 91
(from N numbers of genome each with 2 copies of Pax6)

F_{x2} is the fluorescence intensity with Pax3 primers = 76 (from 2 initial copies)
(from N numbers of genome each with 2 copies of Pax3)

F_{x3} is the fluorescence intensity with PAX6 primers = 42
(from N numbers of genome each with ? copies of PAX6)

There is a linear relationship between SYBR green fluorescence and amount of DNA. So:

$$\frac{\text{no. of initial copies of fragment amplified by PAX6 primers} \times \text{PCR amplification}}{\text{no. of initial copies of fragmnt amplified by Pax3 (or Pax6) primers} \times \text{PCR amplification}} = \frac{\text{fluorescence intensity with PAX6 primers}}{\text{fluorescence intensity with Pax6 (or Pax3) primers}}$$

The fragment sizes are very similar so the PCR amplification is assumed to be the same and so cancels out, and:

no. of initial copies of fragment amplified by Pax6 primers = N genomes x 2 copies in each genome

no. of initial copies of fragment amplified by Pax3 primers = N genomes x 2 copies in each genome

no. of initial copies of fragment amplified by PAX6 primers = N genomes x ? copies in each genome

4) This leaves:

no. of genome copies based on Pax6 primers:

$$\frac{?N}{2N} = \frac{42}{91}$$

$$\frac{?}{2} = \frac{42}{91}$$

$$\text{Therefore } ? = \frac{2 \times 42}{91} = \underline{\underline{0.9 \text{ copies}}}$$

and

no. of genome copies based on Pax3 primers:

$$\frac{?N}{2N} = \frac{42}{76}$$

$$\frac{?}{2} = \frac{42}{76}$$

$$\text{Therefore } ? = \frac{2 \times 42}{76} = \underline{\underline{1.1 \text{ copies}}}$$

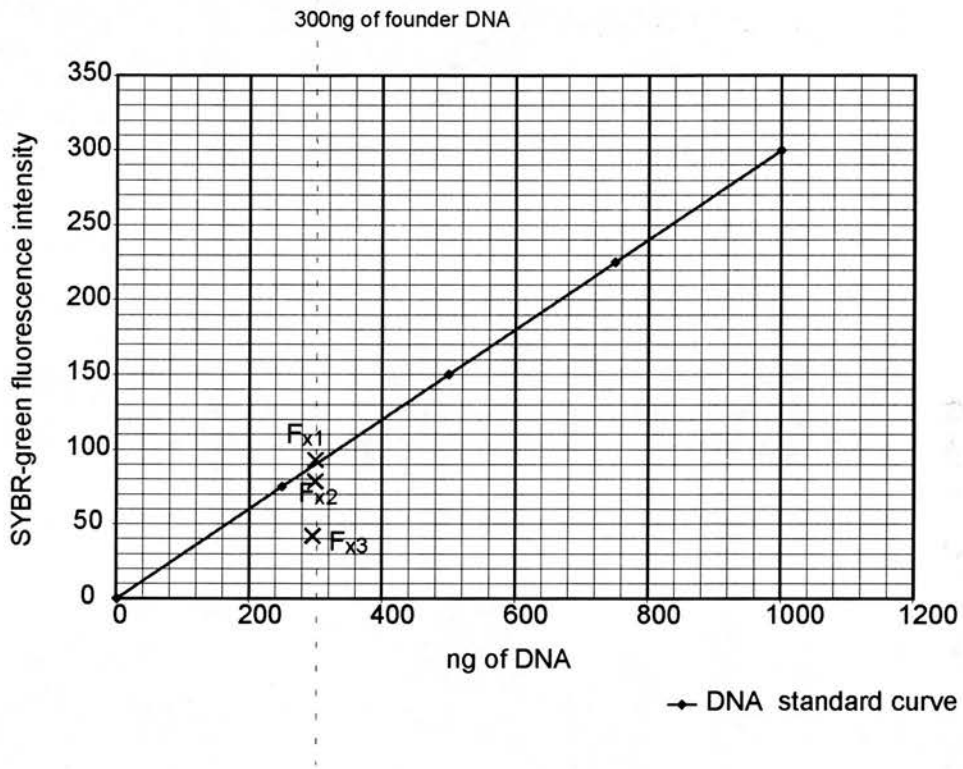
300ng of founder DNA
SYBR-green fluorescence intensity
350
300
250
200
150
100
50
0
0
200
400
600
800
1000
1200
ng of DNA
F_{x1}
F_{x2}
F_{x3}
DNA standard curve

Confocal microscopy

Cells and tissue were imaged using a Leica TCS NT confocal system and associated software with DMIRBE (inverted) or DMRE (compound) microscope in a facility run by Linda Wilson. Corresponding bright field images were collected in the transmitted channel. GFP was detected in the FITC channel. With the counterstained sections the TOPRO3 was detected in the TRITC channel.

Results

Most of the nine transgenic founders bred and passed on the transgene successfully. However, DTy374.223 died before it was mated and so the line was lost and DTy1123.9 was sterile. In both cases no analysis of the expression pattern was possible although the extent of the YAC incorporated in the founder was investigated in both lines as well as in the other seven remaining lines. With line DTy374.227 it was inconclusive if it is transgenic or not. Some of the results with DTy374.227 were positive, some were negative. A possible explanation is that it was a very low percentage mosaic and that repeated breeding would establish the line.

Number and extent of incorporation of YAC Y1123 and YAC Y374 in the transgenic founders

The results of the PCR to establish the extent of the incorporation of the YAC are summarised in Figure 5.1. The diagram has horizontal dashed lines indicating the minimum amount of transgene that is present. It is not necessarily the maximum amount present since the truncation does not necessarily have to have occurred

immediately next to the last set of primers that worked. The extent of the YAC incorporated in the nine lines of transgenic founders was found to be different in each line. Some (DTy1123.54, DTy374.001, DTy374.223) had incorporated the majority (at least 300kb) of the 424kb YAC. The exact 5′ end of the incorporated transgene was hard to identify. The 5′ end contains many repeats and may potentially be a region of variability from the published human sequence and so the primers used may not work. The other six founders had incorporated smaller lengths. DTy1123.22 and DTy1123.42 were the most truncated and did not seem to have even incorporated all of the *PAX6* exons.

The number of copies of the YAC incorporated in some of the lines is summarised in Table 5.1. In all cases examined the copy number was found to be low. The results are shown from each set of standards (*Pax6* or *Pax3*). There is a small mean difference between the copy numbers calculated from each standard but it is less than half a copy number. The standard errors are all less than one copy number. Since only whole copy numbers are possible I am confident that for line DTy1123.54 the copy number is one. For lines DTy1123.22, DTy1123.42, and DTy374.001 the copy number is either one or two.

Line	Standard		n
	Pax3	*Pax6*	
	Mean copy number ± SD	**Mean copy number ± SD**	
DTy1123.22	1.3 ± 0.5	1.0 ± 0.5	6
DTy1123.42	1.4 ± 0.5	1.2 ± 0.5	8
DTy1123.54	0.8 ± 0.2	0.9 ± 0.4	7
DTy374.001	1.4 ± 0.5	1.8 ± 0.8	11

Table 5.1. Real-time quantitative PCR to determine transgene copy number. n is the number of different animals analysed from each line.

Initial analysis of GFP expression in the transgenic animals

Six lines (DTy1123.22, DTy1123.42, DTy1123.54, DTy374.001, DTy374.028, and DTy374.226) were identified as able to successfully pass on the transgene and therefore could be used to establish transgenic colonies. All six lines are potentially very interesting since the truncated versions include some but not the entire set of regulatory elements of *PAX6*. However, analysing the GFP expression pattern in all six lines is a huge undertaking. Therefore, only a selection was examined in detail.

Initially, DTy1123.22, DTy1123.42, DTy1123.54, and DTy374.001 were investigated. This was done by looking at GFP expression in the eyes of live adult transgenic mice. *Pax6* has been previously reported to be expressed in the eyes of adult mice (Walther and Gruss 1991; Ton *et al.* 1992; Beimesche *et al.* 1999). This analysis was performed by shining a blue LED torch (Inova™ X5™, Emissive Energy, RI, USA) into the eyes of the live animals. The light is only in the visible spectrum and so does not harm the animal. The torch emits blue light at the correct wavelength to excite the GFP. The emitted light was visualized using an appropriate filter (Tyas *et al.* 2003). The GFP was clearly evident in the eyes of some of the transgenic animals. Any pigmentation of the eye made it difficult to be conclusive in all of the animals. In addition, it is technically very difficult to take a photograph of this to report the result. Therefore, the eyes from dead transgenic adults were imaged using confocal microscopy. The eyes were counterstained using TOPRO3. The results are shown in Figure 5.2. All of the four transgenic lines had GFP expression

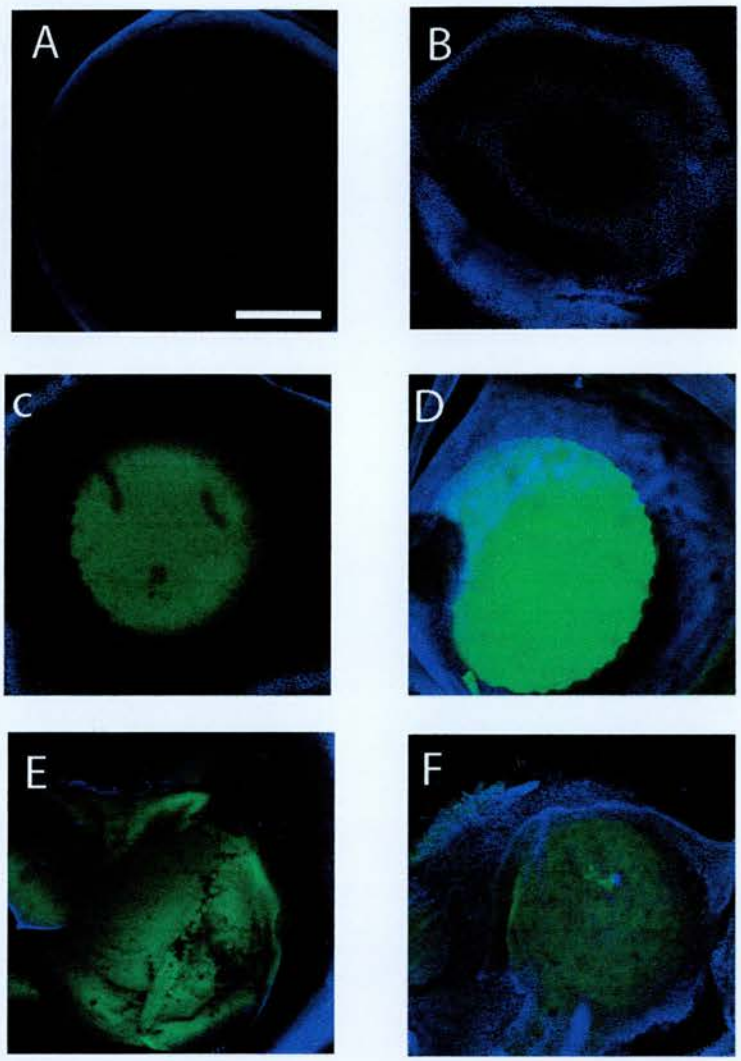

Figure 5.2. Confocal images of whole mount adult eyes. (A-F) are merged green fluorescent and TOPRO3 images. (A) Wild type. (B) Y1123.22. (C) Y1123.42. (D) Y1123.54. (E) Y374.001. (F) Y374.001/Pax6$^{+/Sey}$. Bar is 400μm.

in the adult eye. DTy1123.22 had very faint expression. The greatest level of GFP expression was seen in DTy1123.54 eyes.

Analysis of GFP expression in a developmental time series in lines DTy1123.54 and DTy374.001

DTy1123.54 and DTy374.001 both had incorporated the largest extent of the YAC. Therefore, the GFP expression in these animals was investigated in greater detail. Embryos were collected from both lines at several developmental stages. With line DTy1123.54 embryos were collected at ages E9.5, E10.5, and E14.5. With line DTy374.001 embryos were collected at ages E8, E10.5, and E16. A summary of the development stages examined and index to the corresponding figures is given in Table 5.2. Some of the embryos were imaged whole mount, with the older ones appropriate vibratome section were cut and imaged. GFP expression was seen at all six time points analysed.

a) DTy1123.54 developmental series

At age E9.5 it is possible to confocal image the whole embryo. Figure 5.3 is a confocal image of a E9.5 DTy1123.54 embryo along side a wild type litter mate. The wild type litter mate has some green colour; however, when viewing the embryo with the microscope the mouse looks more 'yellowish green', which is typical of auto-fluorescence, rather than the 'bluer' green of GFP. It is difficult to capture a whole mount image that can clearly distinguish the two as there is a lot of surrounding tissue. However, the eye clearly has GFP signal in the transgenic (see Figure 5.3A). In the wild type litter mate (see Figure 5.3B) there is no signal there.

Age	DTY1123.22	DTY1123.42	DTY1123.54	DTY374.001	WILD TYPE
E8.0				Data not shown	
E9.5			Figure 5.3		Figure 5.3
E10.5			Figures 5.4 and 5.5	Figure 5.9	Figure 5.12
E14.5	Figure 5.11	Figure 5.13	Figures 5.6, 5.7, and 5.8		
E16				Figure 5.10	
Adult (eye)	Figure 5.2	Figure 5.2	Figure 5.2	Figure 5.2	Figure 5.2

Table 5.2. Summary of Figures in this Chapter of GFP expression analysed in the different '*Pax6* reporter' lines.

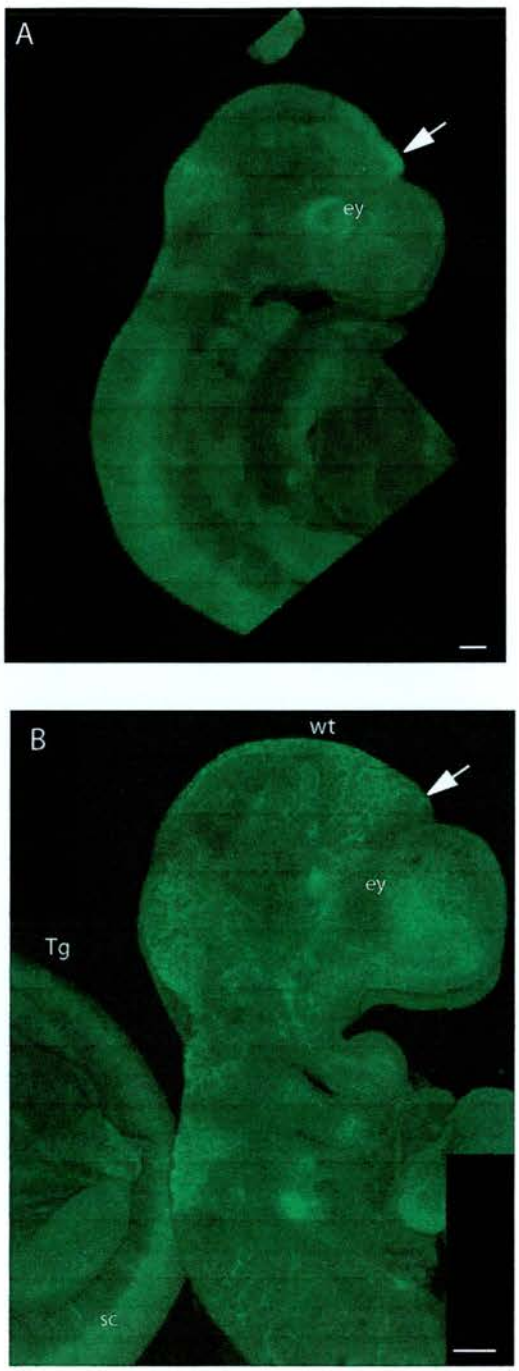

Figure 5.3. Confocal images of whole mount embryos, imaged through only the GFP channel. (A) Y1123.54 at E9.5. (B) Part of Y1123.54 (Tg) and wild-type (wt) litter mate at E9.5. Eye (ey), spinal cord (sc). The arrow indicates the diencephalon. Bars are 200 µm.

Later stage DTy1123.54 embryos had to be sectioned before imaging. This significantly reduced background auto-fluorescence. Some of these sections were counter stained with TOPRO3 which is a nucleic acid stain and marks the nuclei of cells and appears blue in the sections presented here.

At E10.5 (Figure 5.4) GFP expression was seen in the neural tube and the pons. Expression was also seen in the diencephalon. There was also GFP expression in the cerebral cortex and it appears to be in a rostral (high) to caudal (low) gradient. Figure 5.12 is a wild type litter mate for comparison. GFP expression was also seen in the lens, neural retina, and optic nerve (see Figure 5.5).

Coronal sections through heads of DTy1123.54 at E14.5 clearly show that the GFP expression (see Figure 5.6) is in the epithalamus, pineal, ventral thalamus, parts of the ganglionic eminence, eminentia thalami, and cerebral cortex. In addition, the retina and lens is expressing GFP (Figure 5.6). Figure 5.7 shows a magnified confocal image of an E14.5 eye of a DTy1123.54 embryo. Figure 5.6 shows that the optic nerve is clearly expressing GFP at E14.5.

Figure 5.4. Confocal image of a 200μM central sagittal section through a DTy1123.54 E10.5 embryo. (A) and (B) are both merged GFP and TOPRO3 images. (A) Embryo head and trunk, scale bar is 200μM. (B) Enlargement of boxed red area in (A), scale bar is 20μM. (C) Diagram showing a red line that indicates the plane of section of (A). Cerebral cortex (cc), basal plate of pons (po), diencephalon (di), neural tube (nt), and tongue (tg).

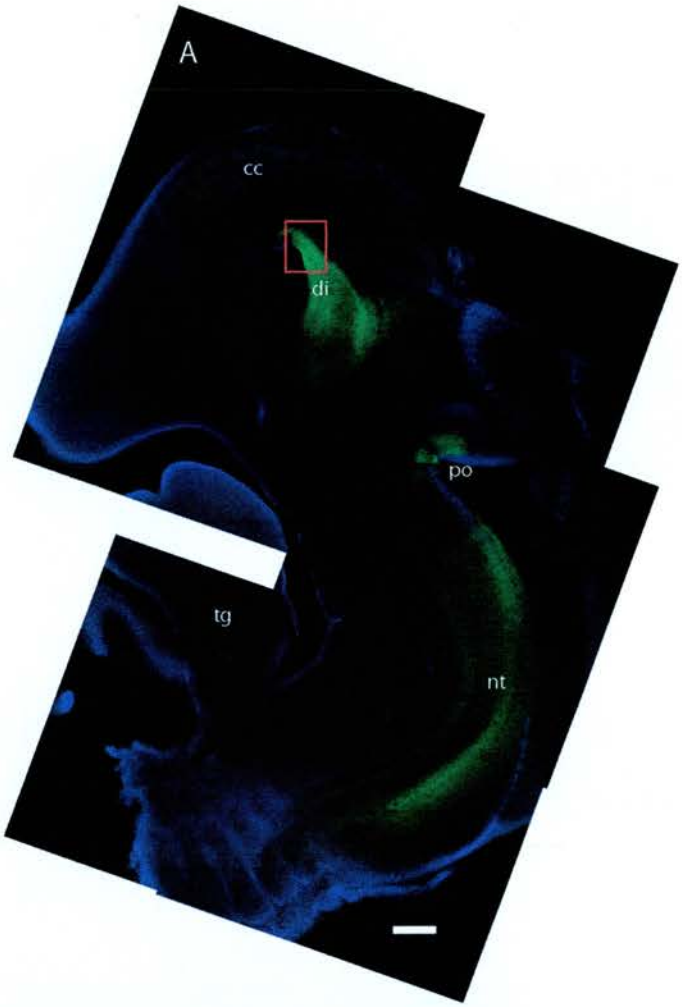
A
cc
di
po
tg
nt

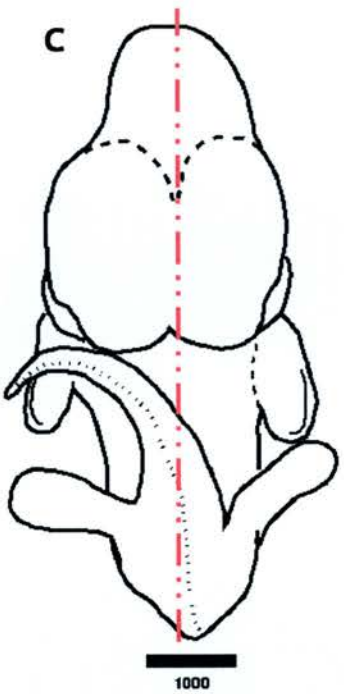
C
1000

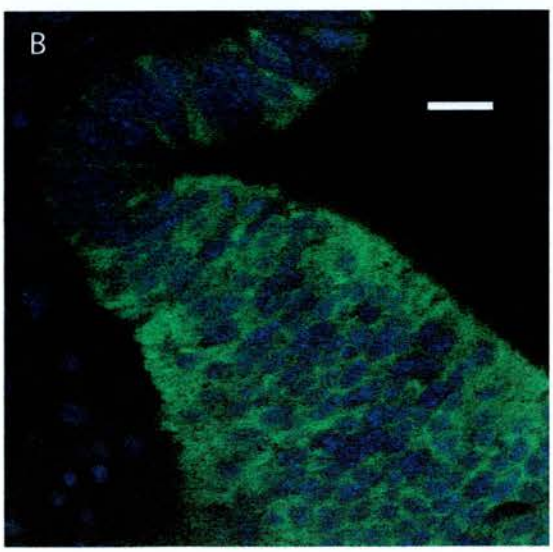
B

Figure 5.12. Confocal image of 200μM coronal section through the head of an E10.5 wild type littermate. Image is a merged GFP and TOPRO3.

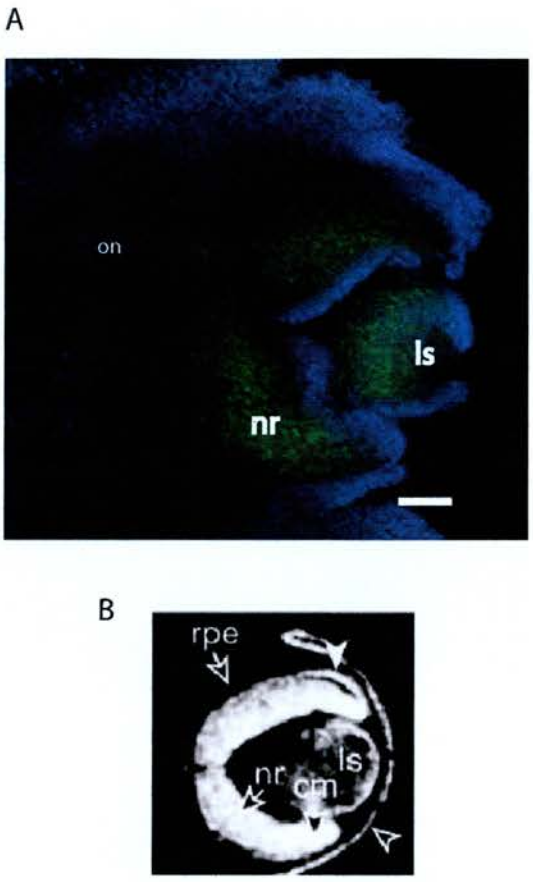

Figure 5.5. Confocal image of a 200µM section through an E10.5 DTy1123.54 eye. The image is a merged GFP and TOPRO3. (B) *Pax6* mRNA *in situ* of E10.5 eye (taken from Fig. 3 Bernier *et al.*, 2001). Retinal pigmented epithelium (rpe), lens (ls), distal portion of retina - ciliary margin (cm), neural retina (nr). (on) optic nerve. The scale bar is 200µm.

Figure 5.6. Confocal image of 200 µm coronal sections through head of Y1123.54 E14.5 embryos. Section (B) is more caudal than (A). (C) Diagram showing the planes of section. (D) Pax6 in situ mRNA hybridization at e14.5 (Actual size figure from Fig3, Stoykova, A. et al., 1996). (E) Pax6 immuno histochemistry at E16.5 (Figure from Fig1, Toresson, H. et al., 2000). The arrow heads in (E) point to a stream of Pax6-positive cells in the lateral LGE. Epithalamus (et), pineal (pi), ventral thalamus (vt), dorsal thalamus (dt), retina (r), optic nerve (on), optic tract (ot), ganglionic eminence (ge), eminentia thalami (emt), hypothalamus (HT), neocortex (NCX), paraventricular nucleus (PA), ventricular zone (VZ), lateral ganglionic eminence (LGE), medial ganglionic eminence (MGE). Bar is 200 µm in both (A) and (B).

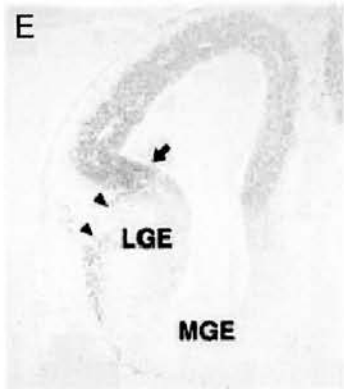

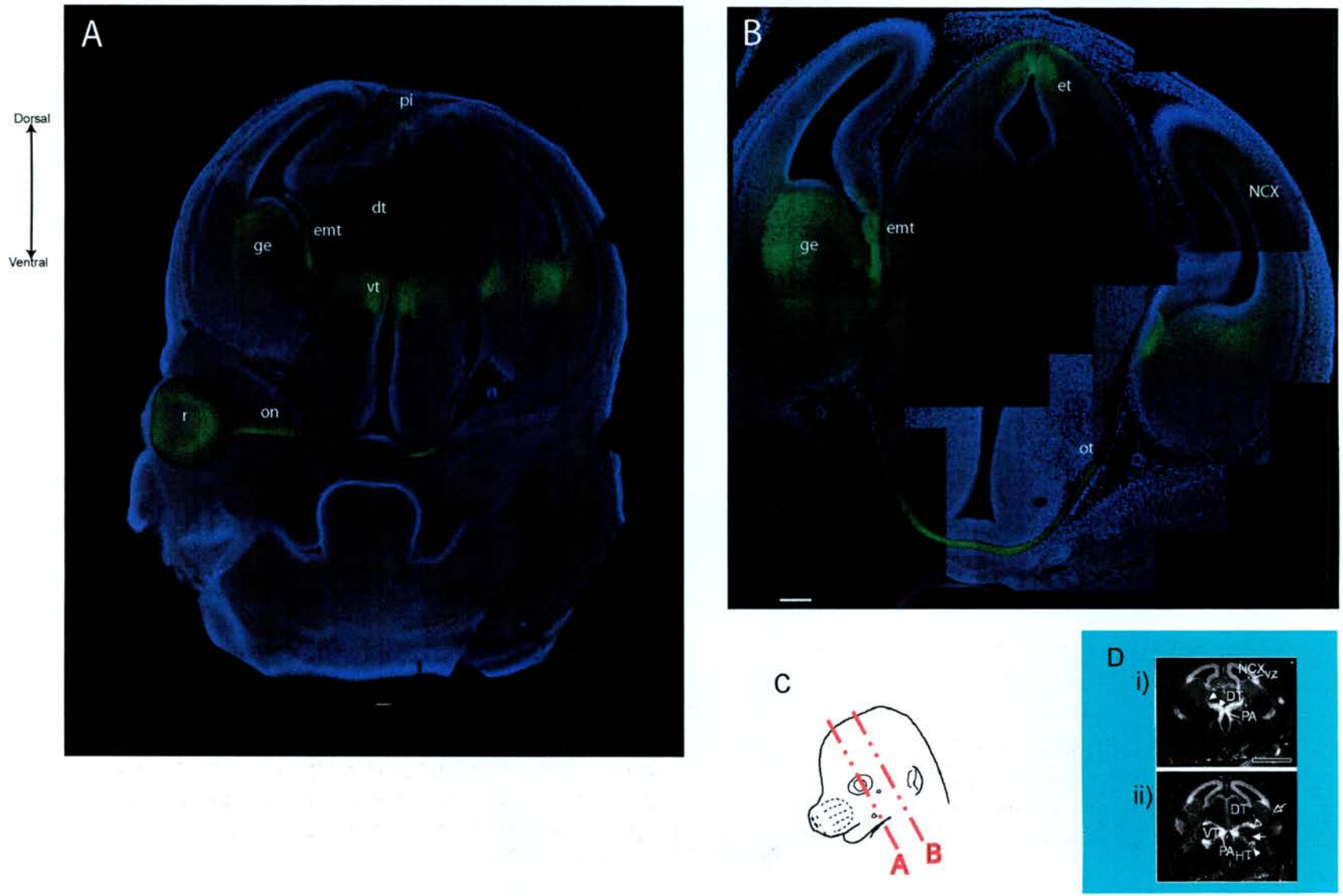
A
Dorsal
Ventral
pi
dt
emt
ge
vt
r
on
B
et
NCX
emt
ge
ot
C
A
B
D
i)
NCX
VZ
DT
PA
ii)
DT
VT
PA
HT

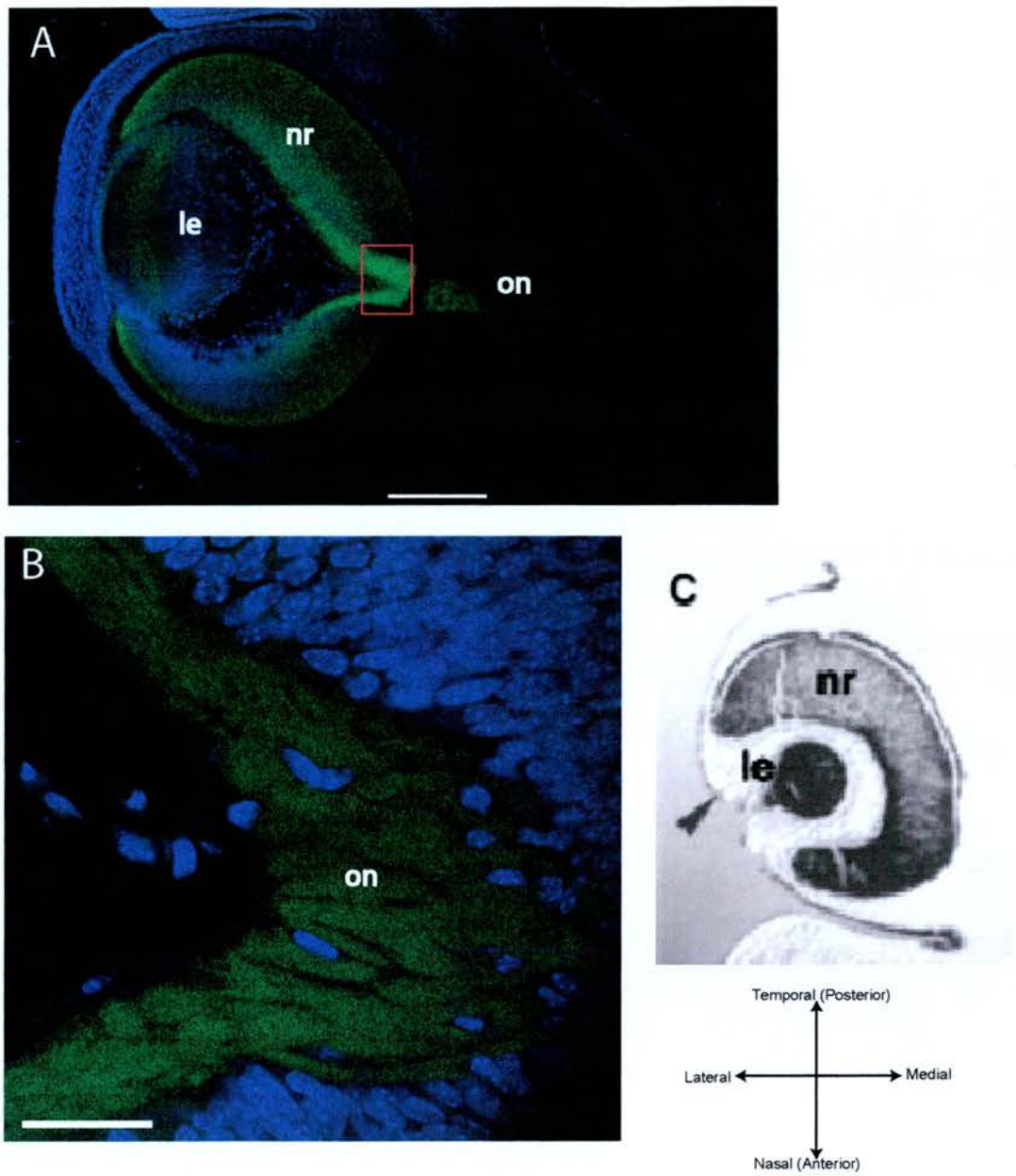

Figure 5.7. Confocal image of 200 µm sections through eye of Y1123.54 E14.5 embryo. (B) is a magnified view of the boxed area in (A). Both images are merged GFP and TOPRO3. (C) *Pax6* mRNA *in situ* of E13.5 eye (taken from Fig. 5 Callaerts *et al.*, 1997). Neural retina (nr), lens (le), optic nerve (on). Bar is 200 µm in (A) and 20 µm in (B).

Cutting DTy1123.54 E14.5 in the sagittal plane (Figure 5.8) allows the GFP expression to be confirmed in the locations already identified; the basal plate of the pons, the epithalamus, cerebellum, ventral thalamus, and optic tract.

b) DTy374.001 developmental series.

The earliest embryonic developmental stage looked at with any of the transgenic lines was with DTy374.001 at E8.0, data not shown. The dissection at the stage was difficult and only conducted on one litter. There was potential GFP signal, however, it was difficult to identify the exact location. Therefore, this needs to be repeated and with carefully cut thin sections in order to fully demonstrate the expression.

E10.5 whole mount DTy374.001 was imaged, see Figure 5.9. As with other whole mount embryos there is a lot of tissue and so imaging is difficult because of the auto-fluorescence. However, the eye is clearly labelled with GFP. Parts of the brain are also possibly expressing GFP but it is difficult to be certain because of the auto-fluorescence.

Cutting sections from E16 embryos allowed GFP expressing tissues to be clearly identified. Figure 5.10 is a transverse section through the head of a DTy374.001 embryo. The eye, optic nerve, optic tract, and telencephalon are clearly expressing GFP. The olfactory epithelium is also possibly expressing GFP.

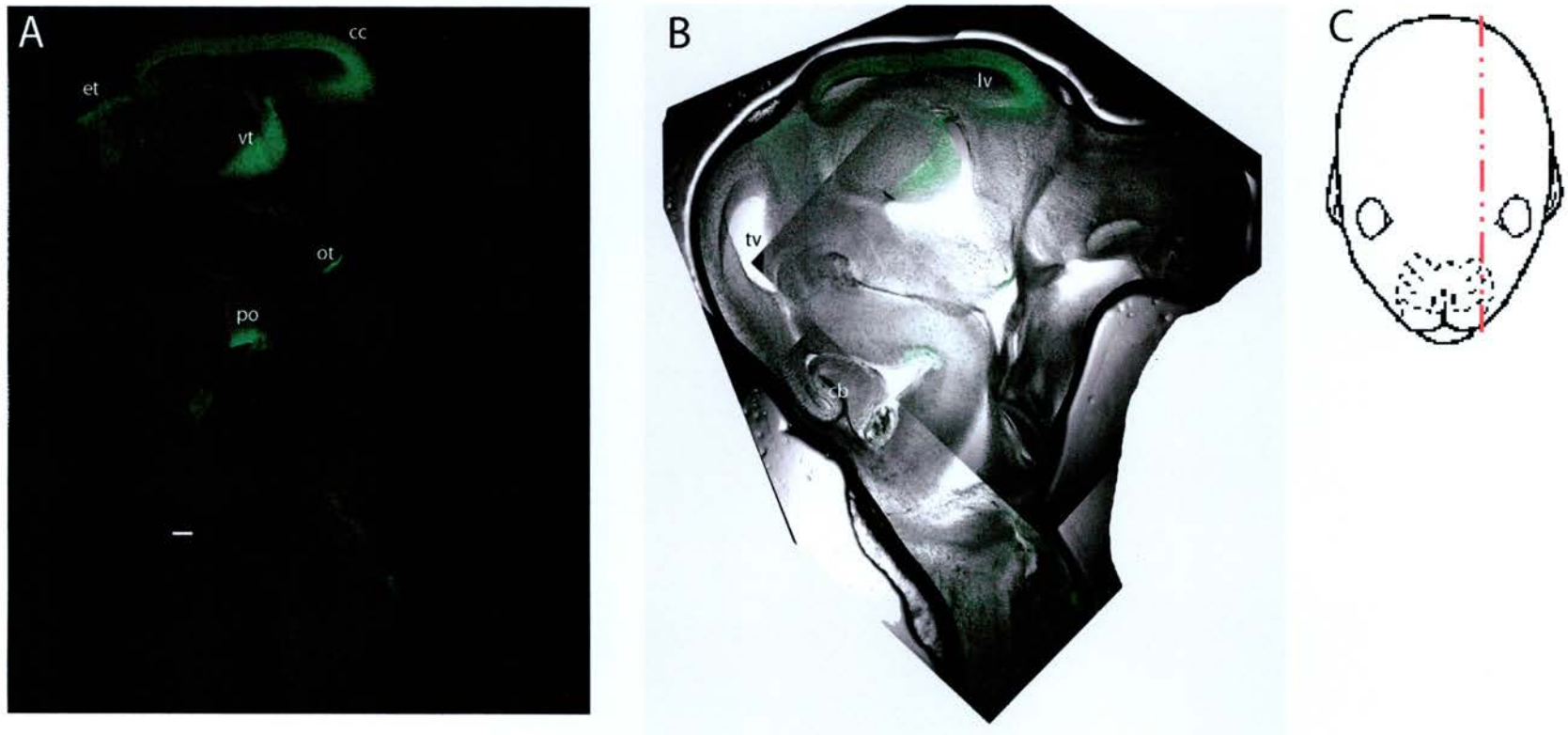

Figure 5.8. Confocal image of a 200 µm sagittal section through head of Y1123.54 E14.5 embryo. Epithalamus (et), ventral thalamus (vt), cerebral cortex (cc), third ventricle (tv), lateral ventricle (lv), basal plate of pons (po), optic tract (ot), and cerebellum (cb). (A) GFP. (B) Merged GFP and bright field image. (C) Drawing with a red line indicating the plane of section of (A) and (B). Bar is 200 µm.

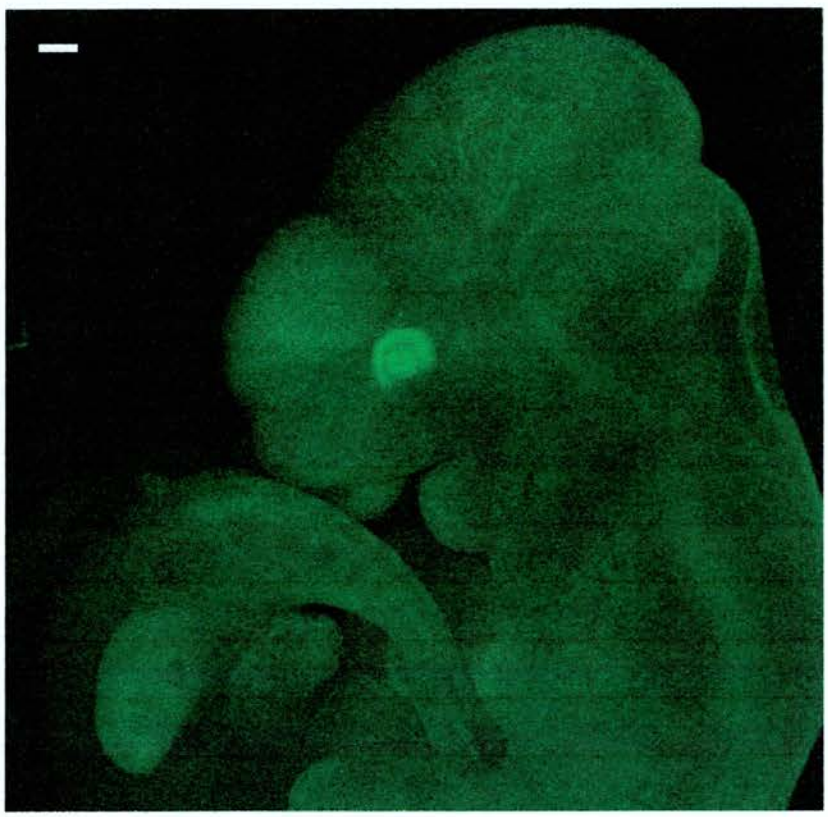

Figure 5.9. Confocal image of whole mount embryo Y374.001 at E10.5. Image is GFP channel only. Bar is 200 μm.

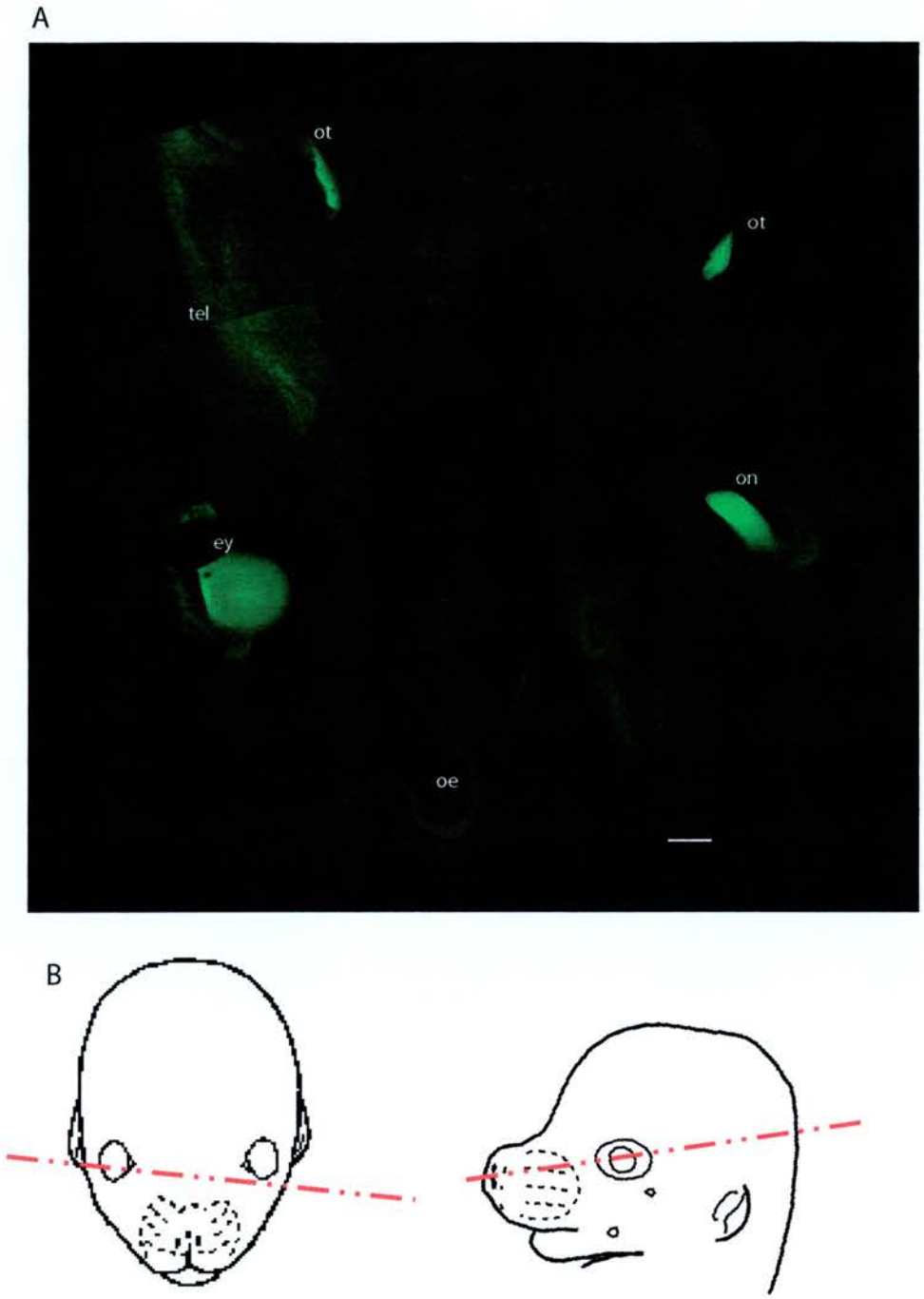

Figure 5.10. Confocal image of a 200 µm transverse section of E16 Y374.001 embryo. (A) Image is GFP channel only. (B) Diagrams showing the plane of section. Eye (ey), telencephalon (tel), olfactory epithelium (oe), optic tract (ot), and optic nerve (on). Bar is 200 µm.

Analysis of GFP expression in E14.5 DTy1123.22 and DTy1123.42

From the PCR analysis it was believed that lines DTy1123.22 and DTy1123.42 only incorporated a small part of the YAC Y1123. Interestingly, neither of these two lines appeared to have incorporated all of the *PAX6* exons. Therefore, one developmental stage (E14.5) was selected to analyse the GFP expression of these two lines.

Figure 5.11 shows the expression in two coronal sections of the head of an E14.5 DTy1123.22 embryo. GFP expression was seen in the ventral thalamus and parts of the ganglionic eminence, amygdala, prospective entopeduncular nucleus, and the cerebral cortex. However, GFP expression was absent in the eye at E14.5. There was no apparent ectopic GFP expression seen in any of the sections.

Figure 5.13 shows the GFP expression in a coronal section of the head of a DTy1123.42 embryo. Some GFP expression was seen in the retinal pigmented epithelium in the E14.5 eye (see Figure 5.13B for an enlargement of the eye) and possibly parts of the brain, such as the pineal gland and the dorsal thalamus. However, the level of brain expression is only slightly above background auto-fluorescence and appears to be ectopic, such as in the basal telencephalon, Figure 5.13. Compare this expression level to the potential GFP expression in the extraocular muscles (Figure 5.13) and the actual GFP expression verses auto-fluorescence is questionable. There is also a very low level of expression in the lens.

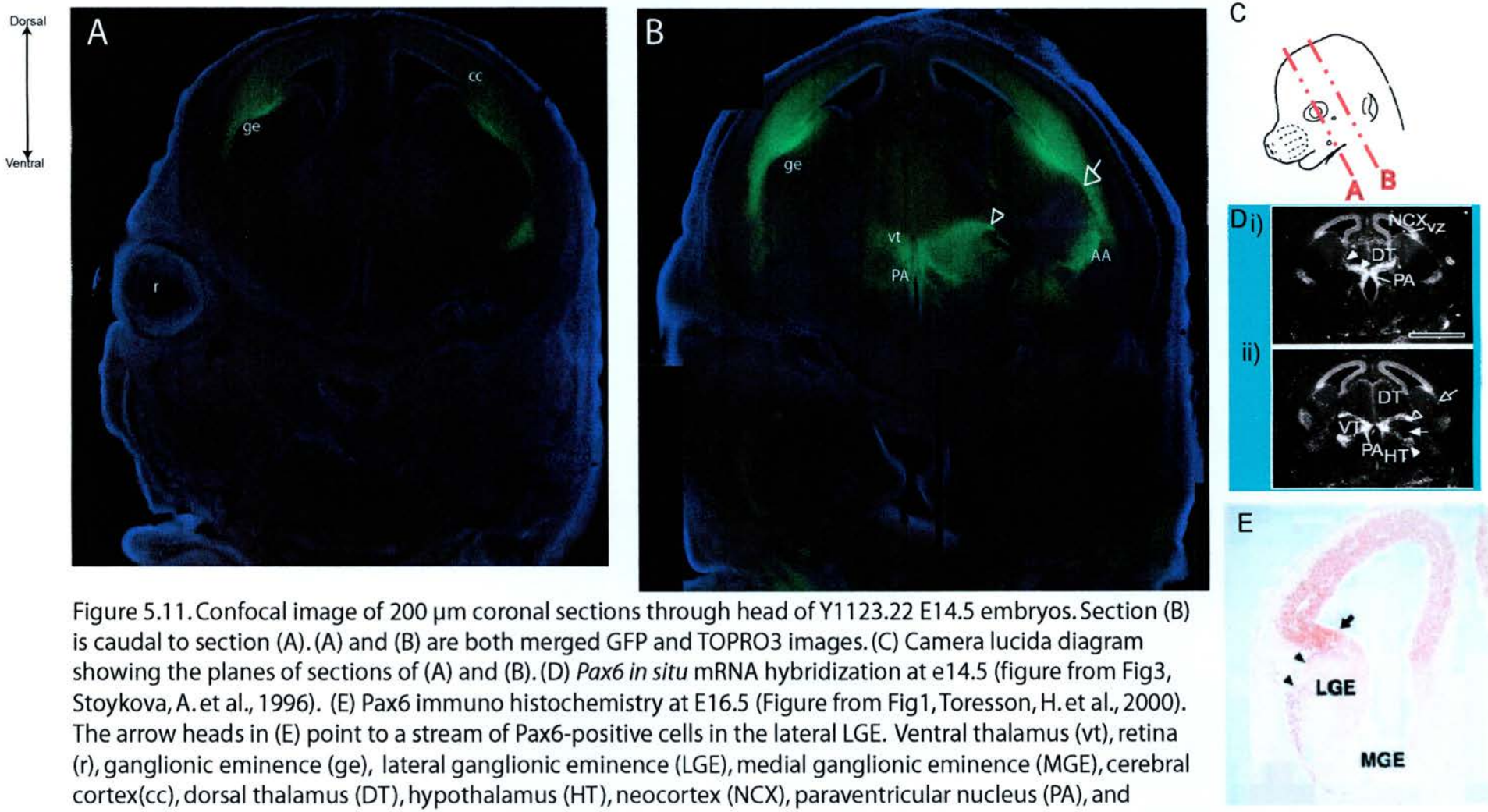

Figure 5.11. Confocal image of 200 µm coronal sections through head of Y1123.22 E14.5 embryos. Section (B) is caudal to section (A). (A) and (B) are both merged GFP and TOPRO3 images. (C) Camera lucida diagram showing the planes of sections of (A) and (B). (D) *Pax6 in situ* mRNA hybridization at e14.5 (figure from Fig3, Stoykova, A. et al., 1996). (E) Pax6 immuno histochemistry at E16.5 (Figure from Fig1, Toresson, H. et al., 2000). The arrow heads in (E) point to a stream of Pax6-positive cells in the lateral LGE. Ventral thalamus (vt), retina (r), ganglionic eminence (ge), lateral ganglionic eminence (LGE), medial ganglionic eminence (MGE), cerebral cortex(cc), dorsal thalamus (DT), hypothalamus (HT), neocortex (NCX), paraventricular nucleus (PA), and ventricular zone (VZ), amygdala (AA).

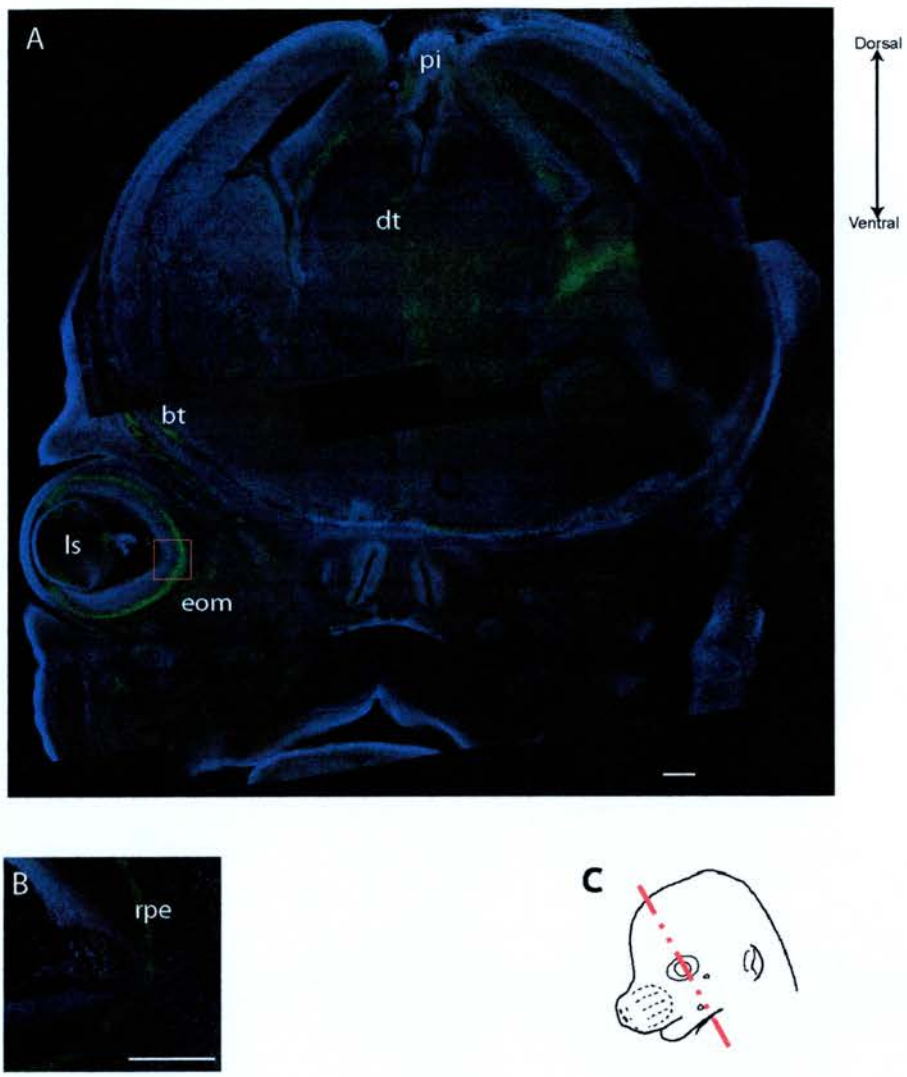

Figure 5.13. Confocal image of 200 µm coronal section through the head of an Y1123.42 E14.5 embryo. Both images are merged GFP and TOPRO3. (B) is an enlargement of the red box in (A). (C) Camera lucida diagram showing the plane of section of (A). Retinal pigmented epithelium (rpe), dorsal thalamus (dt), lens (ls), basal telencephalon (bt), extraocular muscles (eom), and pineal (pi). Scale bar is 200 µM in both.

Discussion

Extent of the YAC integrated in the '*Pax6* Reporter' mice

Using PCR primers to establish the extent of the incorporation of the YAC revealed that a varying amount was integrated in each line. PCR is not a conclusive method of establishing the extent of the integration since it will only identify short pieces and I have to assume that if corresponding flanking short sequences are present then the in-between sequence (that is not included in the PCR) is also present. In addition, the 5′ most primer pair (5395F and 5395R) failed to produce a band with any of the founders, and the next set of primers (5083F and 5083R) produced a band with some of the founders (for example DTy1123.54). I can not conclude that the YAC necessarily truncates at this point. The primers are 90kb apart and so the truncation could be anywhere between them.

The YAC is 424kb long and so sequencing is not an option. The PCR analysis shows that lines DTy1123.54, DTy374.001, and DTy374.226 have incorporated the majority of the YAC. Furthermore, GFP expression was seen in lines DTy1123.54 and DTy374.001 in locations appropriate for *Pax6* expression, discussed below. The GFP expression in line DTy374.226 was never examined. The fact that the GFP was seen in areas consistent with previously reported *Pax6* expression is evidence that the regulatory elements are probably all present since the expression appears correct.

GFP expression in DTy1123.54 and DTy374.001

Looking at the various DTy1123.54 and DTy374.001 embryos (see Table 5.2 for index of figures) it is clear that the GFP expression pattern seen is the same in both at the developmental stages when both lines were examined.

a) E9.5

GFP expression at E9.5 was only examined in line DTy1123.54 (Figure 5.3). This Figure is a whole mount embryo and so the background auto-fluorescence is high. However, in Figure 5.3B the spinal cord of a DTy1123.54 embryo is shown next to the wild-type. Comparing the spinal cord of the transgenic against the wild type litter mate it is clear that the spinal cord has specific GFP expression. *Pax6* mRNA has been detected in the spinal cord of E9.5 embryos before (Filosa *et al.* 1997; Bernier *et al.* 2001). Also see Figure 1.6 in Chapter 1.

The clearest GFP expression is in the eye. In the transgenics the eye appears as a bright green ring, in the wild type it does not. *Pax6* mRNA expression in the eye at E.9.5 has been previously shown (Walther and Gruss 1991; Bernier *et al.* 2001).

The forebrain, probably the diencephalon, indicated by the arrow in Figure 5.3 seems to have a defined GFP expression in the transgenic DTy1123.54. This is consistent with *Pax6* mRNA expression that has been seen in E9.5 forebrains before (Bernier *et al.* 2001; Ohtoshi *et al.* 2002).

b) E10.5

GFP expression at E10.5 was examined in both DTy1123.54 and DTy374.001.

Figure 5.5 shows that GFP was clearly expressed in the neural retina and lens of the eye of E10.5 DTy1123.54 embryos. At this age the lens pit, optic cup, and presumptive retina have been shown to express Pax6 protein (Faber *et al.* 2001).*Pax6* mRNA expression has also been previously detected at this age in the retinal pigmented epithelium, iris, distal portion of the retina, and the lens (see Figure 5.5 B for Figure from Bernier et al., 2001)(Bernier *et al.* 2001), the lens pit and surface ectoderm of the eye (Grindley *et al.* 1995), and the lens and neural retina (van Raamsdonk and Tilghman 2000). Expression in the eye was also easily seen in E10.5 DTy374.001 whole mount embryos, see Figure 5.9. However, as with other whole mount embryos there is a lot of tissue and so imaging is difficult without a lot of auto-fluorescence.

Whole mount E10.5 DTy374.001 embryos also appeared to have specific GFP expression in the brain (see Figure 5.9). A sagittal section of a DTy1123.54 embryo at this age reveals the specific GFP expression in the brain. It appears to be localised to the diencephalon, both the ventral and dorsal thalamus (see Figure 5.4A and B). This is consistent with previously reported *Pax6* expression (Walther and Gruss 1991; Warren and Price 1997). The enlargement in Figure 5.4 demonstrates the expression is cellular rather than from axon tracts. The cerebral cortex is also expressing GFP, (Figure

5.4). In addition the expression appears to be in a rostral (high) –caudal (low) gradient. GFP expression was also clearly seen in the neural tube. All of these observations fit with previously reported *Pax6* expression at E10.5 (Walther and Gruss 1991).

c) E14.5

This developmental stage was only examined in DTy1123.54 but it was examined in two different planes of section.

Coronal sections through heads of DTy1123.54 E14.5 clearly show that the GFP expression is the same as previously reported *Pax6* expression. More precisely, in Figure 5.6 the epithalamus, pineal, ventral thalamus, eminentia thalami, and cerebral cortex express GFP. All of these structures have previously been shown to have *Pax6* mRNA expression at E14.5 (Stoykova *et al.* 1996; Warren *et al.* 1999). In addition, the retina is expressing GFP (Figure 5.6). It has been previously shown at age E12.5 (Grindley *et al.* 1995) and E13.5 (Callaerts *et al.* 1997; Bernier *et al.* 2001) that *Pax6* is expressed in the neural retina, lens and optic stalk of DTy1123 at E14.5 (see Figure 5.7 A and B, also see Figure 5.7C for a comparative Pax6 mRNA E13.5 expression pattern from Callaerts et al., 1997). At E17.5 Pax6 expression has been detected in the ciliary body and iris(Bernier *et al.* 2001). Figure 5.6 and Figure 5.7A and B show that the optic nerve and optic tract are clearly expressing GFP at E14.5. In addition, Figure 5.7B is a magnified image of the optic nerve and the GFP is clearly not co-localised with the nuclear

TOPRO3 counter stain, hence demonstrating that the GFP is expressed in the cell body. More specifically, the cell body appears to be fibrous, this is consistent with the GFP expression being in the optic nerve. The optic stalk has been shown to slightly label for *Pax6* mRNA before (Callaerts *et al.* 1997). It is thought that since the cell body and nucleus for these cells is in the retina of the eye that there may be some *Pax6* mRNA and protein in the cell body (the optic stalk and optic nerve) that will label. In this thesis the GFP used is tauGFP so it is expected that the microtubule containing elements, such as axons, would contain the GFP. Hence, these structures are labelled with GFP. This is also seen in coronal sections of DTy1123.54 E14.5 embryos (see Figure 5.6). This does provide a useful way of identifying possible target sites of *Pax6* expressing cells.

The ganglionic eminence also appears to express GFP. Previously the reporting of *Pax6* expression in this area is a little mixed. It has been previously reported that *Pax6* expression is in the ventricular zone of the cortex but specifically not in the medial and lateral ganglionic eminence(Stoykova *et al.* 1996). See Figure 5.14 for a reproduction of the figure from the publication, one of the Stoykova et al., 1996 figures is also included in Figure 5.6 as panel D for easy comparison with the Y1123.54 expression in Figure 5.6 panels A and B. However, more recently it has been reported that *Pax6* mRNA is expressed in the dLGE and vLGE (see Figure 5.14 for reproduction of the published figure(Yun *et al.* 2001)). In addition,

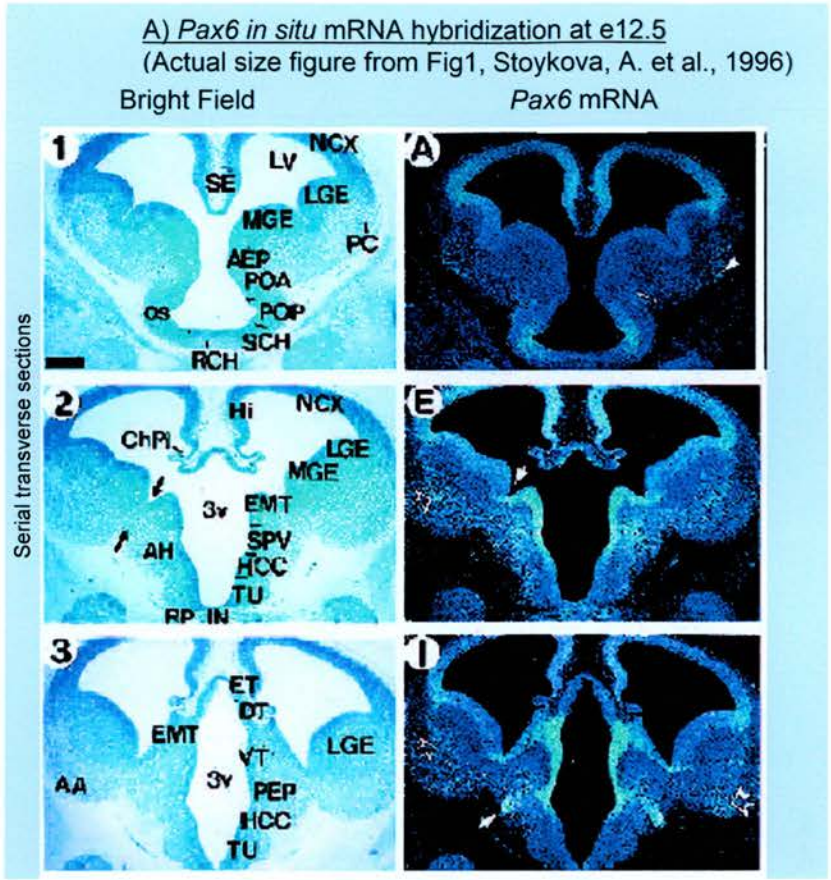

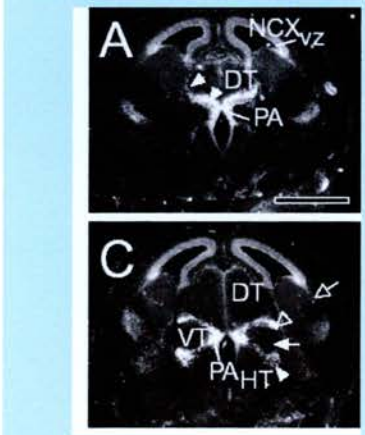

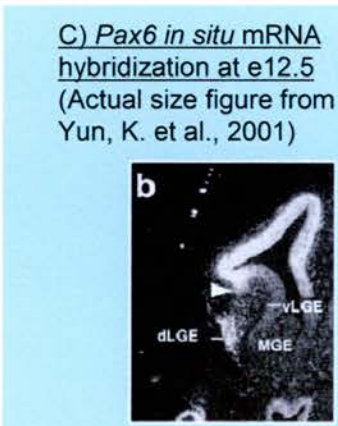

Figure 5.14. Previous published figures of *Pax6* expression in the sections of the developing mouse embryo. Amygdale (AA), anterior entopeduncular area (AEP), anterior hypothalamus (AH), chorioid plexus (ChPl), dorsal lateral ganglionic eminence (dLGE), dorsal thalamus (DT), eminentia thalami (EMT), epithalamus (ET), hippocampal primordium (Hi), hypothalamic cell cord (HCC), hypothalamus (HT), infundibulum (IN), lateral ganglionic eminence (LGE), lateral ventricle (LV), medial ganglionic eminence (MGE), neocortex (NCX), optic stalk (OS), paraventricular nucleus (PA), piriform cortex (PC), posterior entopeduncular area (PEP), anterior preoptic area (POA), posterior preoptic area (POP), posterior commissure (PC), retrochiasmatic area (RCH), rathke's pouch (RP), septum (SE), suprachiasmatic area (SCH), supraoptic/paraventricular area (SPV), tuberal hypothalamus (TU), ventral lateral ganglionic eminence (VLGE), ventricular zone (VZ), ventral thalamus (VT), and third ventricle (3V).

this has been confirmed that Pax6 protein is seen in the LGE (see Figure 5.6 E (Toresson *et al.* 2000), the Toresson et al., 2000 Figure is also included in panel E of Figure 5.6 for easy comparison). The expression in the LGE is identical to the expression in Line Y1123.54 shown in Figure 5.6 part (A), left cerebral hemisphere. Also unpublished data, see Figure 5.15, indicates there may be Pax6 positive cells in the ventricular zone of the ganglionic eminence. In addition, close inspection of the ventricular area of the ganglionic eminence of Figure 5.14 panel A of the work presented by Stoyoka et al., 1996 there is a definite difference in colour that could be interpreted as low level *Pax6* expression. This band of colour is not discussed by the original authors. In conclusion, the present work and the more recent publication have demonstrated that there clearly is some *Pax6* expression in parts of the ganglionic eminence.

As was discussed in Chapter 1 there is a body of literature investigating the role of *Pax6* in specifying the regionalisation of the telencephalon. Fully reconciling the results presented in this thesis with the body of literature will require further work. However, it is also worth remembering this is a reporter mouse that has tauGFP expression controlled by PAX6 regulatory elements and therefore, will not necessarily have an identical expression pattern as an mRNA *in situ* or a Pax6 immunohistochemistry (this is discussed later in this discussion). In addition, there are sensitivity differences in mRNA *in situ* and Pax6 protein immuno studies and there is no reason why the reporter mouse will not have a different sensitivity to both of these. All of these factors mean

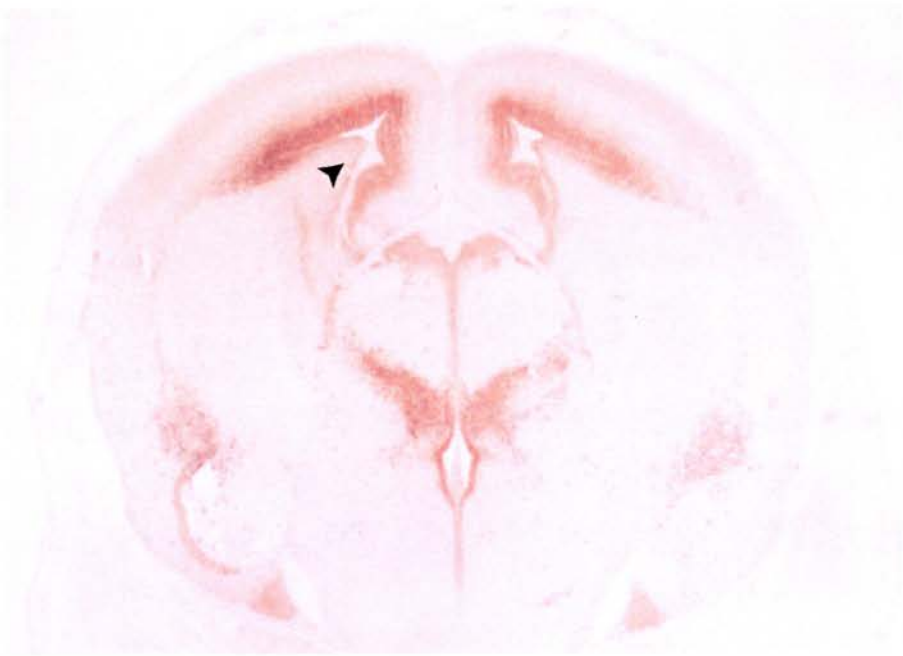

Figure 5.15. Pax6 Immuno histochemistry of a coronal section of an e15.5 embryo. The arrow head marks where that Pax6 expression extends along the ventricular zone of the ganglionic eminence. Figure courtesy of Tom Pratt, unpublished data.

there may be some differences in details of the expression pattern depending upon the method of analysis.

In addition the DNA sequence for the Y1123 is human PAX6 and not mouse Pax6. There are some differences in the sequences and it is possible that the difference in expression pattern is due to the difference in regulatory elements between mouse and human PAX6. Also it is currently unknown what the half-life for tauGFP is compared to Pax6 protein and this may complicate analysis of the expression pattern. Interestingly, in the Y1123.22 line (See Figure 5.11 panels A and B, this Figure also contains the Stoykova et al., 1996 in panel D, and the Toresson et al., 2000 Figure for easy comparison) that carries a truncated version of the YAC1123 the expression pattern in the ganglionic eminence at this age is different to the one seen with the Y1123.54 line. It is unknown without further work which is correct. In line Y373.001 that has also incorporated the full length YAC, expression analysis of the ganglionic eminence has not been done. The difference in expression pattern seen in Y1123.22 and Y1123.54 could be a position effect or subtle alteration in the regulation of Y1123.54 that is leading to the ganglionic eminence GFP expression to be different.

The only way to answer this is further work. Initially I would label some of the sections from the Pax6 Reporter for Pax6 mRNA and others for Pax6 protein. Then use confocal microscopy to look for coincidence of labelling between the GFP and the immuno or GFP and the mRNA *in situ*. As well as

addressing the issue of establishing the Pax6 expression pattern in the ganglionic eminence these comparative analysis will potentially help to understand the role of Pax6 in the telencephalon; particularly its role in establishing the pallial-subpallial boundary.

Further work also needs to establish if the tauGFP in the ganglionic eminence is nuclear or axonal projections. Pax6 is a nuclear protein, and therefore Pax6 immunos will show nuclei staining. tauGFP is designed to label cytoskeletal projections, such as the ones found in axons, and is specifically excluded from the nucleus. In cells that do not have axons it is expected the cytoplasm will be labelled. However, further work such as higher magnification confocal microscopy with the nuclear co-stain TOPRO3 will help.

Sagittal sections of DTy1123.54 (Figure 5.8) reveal expression in the basal plate of the pons. This area has been described previously to express Pax6 protein (Vitalis *et al.* 2000). In addition, expression in the epithalamus, cerebellum, ventral thalamus, and optic tract is again seen.

d) E16

The latest developmental stage examined was at E16 in DTy374.001 embryos. Figure 5.10 is a transverse section through the head of a transgenic embryo. The eye is clearly labelled along with the optic nerve, and optic tract. This has been discussed above. *Pax6* expression has been detected in the ciliary body and iris at E17.5 (Bernier *et al.* 2001). The telencephalon is also

labelled with GFP. *Pax6* mRNA expression in the telencephalon has been observed previously at E16 (Toresson and Campbell 2001). The olfactory epithelium is also possibly expressing GFP. This is consistent with previously reported *Pax6* expression at E16 in the olfactory epithelium (Walther and Gruss 1991).

In summary, the GFP expression mostly matches the *Pax6* mRNA and protein expression seen before at this range of ages in both DTy1123.54 and DTy374.001. The only expression that needs further investigation is in the ganglionic eminence, and the further work that I would suggest has been discussed above.

In terms of developmental age of expression, GFP was clearly visible in the correct places at age E9.5 and potentially at E8.0 (data not shown). This is consistent with the point when *Pax6* is first expressed in the mouse.

Partial GFP expression in E14.5 DTy1123.22 embryos

Figure 5.11 shows that some of the GFP is expressed in regions that are appropriate for *Pax6* expression. In Figure 5.11 panels D and E are examples of published Pax6 expression in the brain for comparison. The cortex, ventral thalamus, amygdala, and ganglionic eminence GFP expression seems to be as expected for this age(Stoykova *et al.* 1996; Toresson *et al.* 2000). The open arrow heads in Figure 5.11 B and the Stoykova et al., 1996 figure in panel D (ii) are a positive stream of Pax6 positive cells all along the external medullary lamina and are believed to contribute to part of the ventral lateral geniculate body (VLG)(Stoykova *et al.* 1996). The open arrow

head in Figure 5.11 B and D (ii) is the prospective entopeduncular nucleus (EP) which has been previously shown to strongly express *Pax6*(Stoykova *et al.* 1996).

The interesting aspect of the GFP expression is in the eye. Figure 5.6 shows that GFP expression was very clearly evident in the eye of DTy1123.54 E14.5 embryos. However, with DTy1123.22 this was not the case. Several sections were examined and the GFP expression level was always very similar to background auto-fluorescence.

This is a truncated YAC so there are several possibilities why this could have occurred. Firstly, the truncated YAC might not include a necessary eye regulatory element. Figure 5.2 shows that in adult DTy1123.22 GFP is also expressed at a very low level. This is possibly due to the truncated YAC not containing the regulatory element required for GFP expression. Secondly, the truncated YAC could be as small as 65kb. This might be small enough that the position where it has integrated has an effect on the expression, such as tissue specific silencing of the truncated YAC. Detailed Southern blot analysis and fluorescent *in situ* hybridisation will have to be done to elucidate the exact extent of the YAC integrated and the location of the insertion site, this is described below. In addition, detailed analysis of developmental stages of DTy1123.22 would have to be examined in order to understand the GFP expression. The truncation may have resulted in the loss of a regulatory element required for E14.5 and adult expression or it could be more general and mean that GFP is never expressed in the embryonic eye.

Partial GFP expression in E14.5 DTy1123.42 embryos

GFP expression in E14.5 DTy1123.42 embryos was also very interesting. The GFP expression was seen at a low level in the pigmented retinal epithelium, (Figure 5.13). The presumptive pigment epithelium has been previously shown to expresses a low level of *Pax6* (Walther and Gruss 1991).

GFP was also possibly expressed in parts of the brain; however, it is difficult to establish what is auto-fluorescence and what is GFP expression.

Interestingly, Figure 5.2C shows the GFP was expressed clearly in the eye of adult DTy1123.42 mice. The level of GFP expression in the eye is possibly lower in DTy1123.42 compared to DTy1123.54 (compare the adult eyes in Figure 5.2C and Figure 5.2D and the E14.5 embryonic eyes in Figure 5.13B and Figure 5.6).

Comparing Figure 5.13B against Figure 5.7B it seems that in E14.5 DTy1123.42 embryos the optic tract and nerve do not express GFP. As discussed above the GFP expression in the optic nerve and tract are probably due to expression in the cell bodies of the axons in the retina. Since there appears to be very low expression in the eye in general it seems reasonable that there is low or no GFP expression in the optic nerve and tract.

From the PCR analysis it was known that the YAC integrated in DTy1123.42 was truncated. As discussed above for DTy1123.22 there are many reasons why this truncation could result in unexpected GFP expression. What is more interesting is that from the PCR analysis both DTy1123.22 and DTy1123.42 seem to have

integrated at least 65kb of the YAC but probably less than 150kb, but the expression pattern is completely different in the two lines. DTy1123.22 seems to express in the correct areas of the brain in E14.5 embryos but has very low expression in the eye. On the other hand DTy1123.42 seems to have some expression specifically in the retinal pigment epithelium and possibly some in the brain. This difference could be due to the truncation being different and including different regulatory elements or due to the position the YAC integrated, or a combination of both.

An important conclusion is that in lines DTy1123.54 and DTy374.001, which have both incorporated at least 300kb of the 424kb YAC the GFP expression is largely consistent with previously seen *Pax6* expression over the developmental time series examined (E8.0 to E16). However, truncated YACs, that is the ones incorporated in lines DTy1123.22 and DTy1123.42, do not recapitulate the complete *Pax6* expression. Therefore, using a vector containing many hundred kilobases of the *PAX6* locus, for example a YAC, is the only way of correctly describing the expression pattern of *Pax6* in addition transgenic reporter mice. As discussed in Chapter 1 the alternative method of generating a reporter mouse by homologous recombination in ES cells to introduce the reporter gene (more commonly known as "knock-in") could not be used in this case because it would disturb one of the endogenous *Pax6* loci, resulting in the *small eye* phenotype,

Further analysis of the truncated lines

From the PCR analysis both DTy1123.22 and DTy1123.42 seem to have integrated at least 65kb of the YAC but probably less than 150kb. The exact truncations in both

case need to be established. I would suggest using southern blot analysis with first a *Pax6* cDNA probe to confirm all of the PAX6 locus has incorporated. Genomic DNA isolated from the founder will contain both the endogenous *Pax6* DNA and the YAC DNA. Comparing the sequences of the two reveals that there are differences in the distribution of restriction enzyme sites in the intronic regions. Digestion of the founder genomic DNA with these restriction enzymes prior to Southern blotting with the *Pax6* cDNA will reveal two distinct patterns. One for the endogenous *Pax6* and one for the human *PAX6*. Analysis of this will confirm if all of the *Pax6* locus is there. Once it is established the extent of the PAX6 locus that has been integrated short probes spaced every 50kb from the 5′ and 3′ ends should be used to establish the extent of the incorporated YAC. Once this is established finer tuning could be used to find the exact amount of the YAC integrated..

In line Y1123.22, no GFP expression was observed in the eye. There are several eye enhancers and regulatory elements with the Pax6 locus, e.g. NRE (Kammandel *et al.* 1999; Xu *et al.* 1999). If the Southern analysis confirms that most of the PAX6 locus has incorporated then it must be assumed that these particular eye regulatory elements are present. As was discussed in Chapter 1 there are several long range elements that have been identified. These have mostly been identified in the human, (Fantes *et al.* 1995; Crolla *et al.* 1996; Lauderdale *et al.* 2000). Aniridia is typically diagnosed by an eye phenotype. Hence, all of these cases will have an eye phenotype. However, the fact that there are humans with eye phenotypes who have mutations, in some case several hundred kb 3′ demonstrates there are eye regulatory elements this far away. Box123 that is 100kb away from the 3′ end of *Pax6* has been

shown to contain an 800bp regulatory element, Box3 that directs *LacZ* expression in transgenic mice specifically in the neural retina(Griffin *et al.* 2002). Interestingly, it did not have expression in the lens or cornea(Griffin *et al.* 2002). Box123 also contains regulatory elements that have been shown to direct *LacZ* in other subparts of the *Pax6* expression pattern (Griffin *et al.* 2002). It is possible that there is redundancy with control elements, which is why the central nervous system expression seemed intact. However, further more detail analysis of this expression pattern may identify sub sets of cells (possibly at particular developmental time points) that are missing. It would also be interesting to look at the olfactory system in the truncated lines since Box 123 also contains an olfactory regulatory element(Griffin *et al.* 2002).

Pax6 Reporter mouse might not report all *Pax6* expression

It is important to realise that the '*Pax6* reporter' mouse might not report all *Pax6* expressing cells. The GFP was placed into the protein translation start site in exon 4. So it will work with mRNA transcripts produced from the promoters P0 and P1 that begin transcription in exon 4. However, there is some evidence emerging that *Pax6* may have several different mRNA transcripts that contain different potential protein translation start sites. The putative additional possible ATG translation start sites are downstream from the ATG in exon 4(Carriere *et al.* 1995). As discussed in Chapter 1 some of the putative start sites have been demonstrated to make potential protein using *in vitro* translation assays. However, this has still not been demonstrated *in vivo*. In addition, there is also the recently identified potential antisense transcript (Anderson *et al.* 2002).

The putative sense translation start sites that are downstream from exon 4 would all produce potential protein that initiates after the reporter construct. This means firstly, the reporter would probably fail to report cells that are producing protein only using one or a combination of these downstream translation start sites. Secondly, the modified YAC has been designed to not produce Pax6 protein (the exact mechanism by which this works is discussed in Chapter 2) when a protein is initiated from the translational start site in exon 4. If translation was to occur from the putative downstream translational start sites then protein would be produced. This protein could rescue part of the *Small eye* phenotype in *Pax6* $^{SeyEd/SeyEd}$ mice. However, firstly the possible ATG sites have not been demonstrated to work *in vivo* yet and it would have been too complicated to address all of these sites. To design the YAC so that there is no possibility of PAX6 being produced would mean introducing many translational stop sites. This would have made an already ambitious transgenic project harder. It would have also meant changing the coding sequence to make the stop sites and this would have had possible effect on *Pax6* regulation. Secondly, it is important to remember that all of the *Pax6* reporter transgenic lines generated, apart from the GFP, have a normal eye phenotype.

New experimental avenues made available by the reporter mouse

The primary goal of this study, as set out in the aims section of Chapter 1, was to be able to identify discrete *Pax6* expressing cells *in vivo* that were able to express *Pax6* irrespective of the status of the endogenous *Pax6* gene and use these to identify *Pax6* downstream targets. As a prerequisite I have generated a novel transgenic mouse, a "Pax6 reporter" mouse that is designed to serve this purpose.

Aim 1: Demonstrate that using a 420kb YAC containing the human *PAX6* contains enough of the regulatory Pax6 elements to drive GFP expression to recapitulate the *Pax6* expression pattern in developing mouse embryos.

The GFP expression mostly matches the *Pax6* mRNA and protein expression seen before at this range of ages in both DTy1123.54 and DTy374.001. The only expression that needs further investigation is in the ganglionic eminence, and the further work that I would suggest has been discussed above. Once I had identified a suitable Pax6 reporter line I intended to study the characteristics of these cells, and in the aims section of Chapter 1 I described a list of hypotheses based on these cells. However, due to time constraints I have been unable to address these hypotheses. Some of the initial avenues now available have already been discussed above. With regard to the aims set out in the introduction I will speculate what can now be undertaken.

Aim 2: Examine changes in target gene expression using micro arrays in discrete FACS sorted populations of *Pax6* expressing cells depending on changes to *Pax6* status.

Initially I would cross the reporter mouse with $Pax6^{SeyEd/+}$. Then I would cross the combined (Pax6 Reporter: $Pax6^{SeyEd/+}$) heterozygotes with $Pax6^{SeyEd/+}$ and collect embryos over developmental stages. The reason for not intercrossing the combined heterozygotes is it will increase the number of reporter YACs. By having a range of number of YACs in each mouse this has the possibility of interfering with the analysis. Primarily I am interested in changes in gene expression in the central nervous system. This could be approached by discretely dissecting parts of the central nervous tissue, e.g. telencephalon, or using the whole central nervous system. Simultaneously I would collect one of the limbs separately, this tissue will be used to isolate DNA and confirm the genotype of the embryo. With the isolated tissue, e.g. the whole central nervous system I would dissociate the cells, a potential protocol is the *Worthington Papain dissociation system* (Lakewood, NJ, USA). This system uses proteolytic enzymes to dissociate the tissue, this have been widely used in cell dissociation previously(Huettner and Baughman 1986). Once a solution of suspended cells has been isolated separately from each embryo I would run it through a FACS to cell sort the cells into bins of cells. The FACS machine will be optimised to generate two bins of cells. One is GFP positive. The other is not. In the embryos that do not have the Pax6 reporter only one bin will be generated, GFP negative. The exact setting of

the forward and reverse scatter and the gates on the FACS machine will have to be optimised empirically. I would not fix the cells because I think the fixing process could interfere with the GFP signal. Once a FACS protocol has been established I would use it for the entire litter, and subsequent litters. A cross of $Pax6^{SeyEd/+}$:Pax6 Reporter with $Pax6^{SeyEd/+}$ will yield embryos with several genotypes, see Table 5.3 for a summary.

Pax6 reporter status	Endogenous *Pax6* status	Expected Percentage in one litter	Average number in one litter (assuming 12 embryos in total)
Not present	*Pax6* $^{+/+}$	12.5%	1.5
Not present	*Pax6* $^{+/-}$	25%	3
Not present	**Pax6* $^{-/-}$	12.5%	1.5
One copy	*Pax6* $^{+/+}$	12.5%	1.5
One copy	*Pax6* $^{+/-}$	25%	3
One copy	*Pax6* $^{-/-}$	12.5%	1.5

Table 5.3. Table of the expected outcomes of a *Pax6*$^{SeyEd/+}$:Pax6 Reporter cross with *Pax6*$^{SeyEd/+}$. (* Analysis possible until near birth.)

The Pax6 status of the embryo is established from DNA isolated from the limb that is simultaneously isolated prior to papain dissociation. Once the bins are isolated I would collect mRNA from them and use it to hybridise to micro arrays to analyse changes in gene expression. Depending on the status of Pax6 the gene expression is expected to change. A number of litters would have to be collected to get statistically significant numbers. However, I would run each embryo as a separate sample rather than pool embryos with the same genotype, and then identify genes that have changes in expression in all of the embryos with the same genotype. The embryos that do not have the Pax6 reporter are controls for the ones that do. If the initially dissections do not yield significant results I would consider doing dissections of individual tissues, parts of the cortex, etc.

The experiment I would first like to use these crosses for is to investigate the general role of Pax6 in the developing cortex. I would dissect the cortex from E14.5 embryos and collect bins of cells as described in Table 5.4. Examining the global changes of downstream gene expression by micro array between 1A, 2A, and 3A will identify what are the downstream targets of Pax6 protein in the E14.5 cortex. This will help to understand what the role of Pax6 is in the developing cortex. It would also be interesting to collect the cortex from earlier embryos and contrast the changes since it has already been shown that in $Pax6^{-/-}$ E11 embryos there is already a dorsal to ventral transformation in the telencephalon (Muzio and Mallamaci 2003). However, if the dissection is

Embryo	Genotype of embryo	Endogenous *Pax6* status	Description of bins of cells generated from each embryo by FACS sort by GFP signal			Bin number
			GFP +ve or - ve cells	Cells able to express Pax6?	Cells actually producing Pax6 protein?	
1	$Pax6^{+/+}$:Pax6 Reporter	$Pax6^{+/+}$	+ve	Yes	Yes	1a
			-ve	No	No	1b
2	$Pax6^{+/-}$:Pax6 Reporter	$Pax6^{+/-}$	+ve	Yes but heterozygous mutants	Yes but from heterozygous cells	2a
			-ve	No	No	2b
3	$Pax6^{-/-}$:Pax6 Reporter	$Pax6^{-/-}$	+ve	Yes but homozygous mutants	No*	3a
			-ve	No	No*	3b

Table 5.4 Table of bins of cells of interest from the cross of $Pax6^{+/-}$:Pax6 Reporter mice and $Pax6^{+/-}$ mice. (* Analysis possible until near birth).

too difficult at the ages before E11 then I will have to accept that a certain amount of regionalisation has already taken place by E14.5.

Alternatively, this could also be used to examine a few specific down stream targets of *Pax6*, for instance investigating the downstream targets in determining neurogenic potential in the developing cortex. It has been previously suggested that the neurogenic potential in *Pax6* mutant cortices is reduced and that cortical radial glial cells express *Pax6*(Heins *et al.* 2002). By collecting the cortex from E14.5 embryos a change in the radial glial "markers" such as RC2 and the astrocyte-specific glutamate transporter (GLAST) verses neuron "specific" markers such as β-tubulin III could be investigated. The bin 1a cells will have upstream signals activating *Pax6* which in turn leads to the Pax6 protein potentially altering the expression of RC2, GLAST, and β-tubulin III consistent with a cell lineage fate. The bin 3a cells will have the upstream signals activating *Pax6*, however the Pax6 protein will not able to alter RC2, GLAST, and β-tubulin III gene expression consistent with the lineage fate. Hence, this will enable me to investigate if Pax6 has a role in neurogenic lineage fate determination in the developing cortex.

Aim 3: Demonstrate auto regulation in discrete isolated cells that are expressing *Pax6* using FACS to identify and sort the cells capable of *Pax6* expression and to quantify the number and amount of fluorescence.

I would use similar crosses that were designed for Aim 2, see Table 5.3. Primarily I am interested in autoregulation in the central nervous system, but autoregulation of Pax6 has only ever been previously reported in the eye so it would be prudent to start with just the eye. Once I have established this system works in the eye I could continue by discretely dissecting other tissue, or using the whole head. For very early embryos the whole embryo could be used. Similar to Aim 2 I would simultaneously collect unwanted tissue, such as one of the limbs, separately to use to confirm the genotype of the embryo and I would use the same dissociation system. However, once a solution of suspended cells has been isolated I would run it through a FACS system to analyse the cells but this time I wouldn't collect the cells I would just count them. I would set the FACS machine to plot the forward scatter of the cells against fluorescence intensity. Initially I would calibrate the machine to subtract autofluorescence, so the fluorescence measured is the GFP signal. These exact setting of the forward and reverse scatter and the gates will have to be optimised empirically. Again I would not fix the cells because I think the fixing process could interfere with the GFP signal. Once a FACS protocol has been established I would use it for the entire litter and subsequent litters.

Again the embryos that do not have the Pax6 reporter are controls for the ones that do. With this whole range of Pax6 status I will be able to establish:

a) If the absolute number of cells expressing *Pax6* changes with Pax6 status.
b) If the same number of cells are expressing *Pax6* but at a different expression level.

If these dissections do not yield significant results I would consider doing dissections of individual tissues, part of the forebrain, etc. In addition, I would consider crossing the Pax6 reporter with PAX77. This transgenic line contains 5-10 copies of the YAC Y593 containing human PAX6(Schedl *et al.* 1996). When PAX77 transgenic mice were crossed with *Small eye* mice it rescued the eye phenotype in mice that were heterozygous and homozygous mutants for endogenous *Pax6*. In addition, analysis of the offspring of the cross that have the genotype PAX77:Pax6$^{+/+}$ demonstrated a similar eye phenotype to *Small eye*(Schedl *et al.* 1996). This suggests the number of copies of *Pax6*, both a minimum and a maximum, is important for correct eye development. Once I had generated the mice with the genotype PAX77:Pax6 Reporter I would cross these onto a Pax6$^{+/-}$ background. And finally once these were established I would cross this *PAX77: Pax6* $^{+-}$*:Pax6 Reporter* with *PAX77: Pax6* $^{+-}$ this would give mice with a complete range of different numbers of Pax6 and PAX77, Table 5.5 has a summary of the genotypes required.

Genotype of embryo (all the ones in this table have the Pax6 reporter)	*Pax6* reporter status	Endogenous *Pax6* status	PAX77 status	Number of functional copies of *Pax6* and *PAX6*
PAX77$^{-/-}$:*Pax6* $^{-/-}$	One copy	**Pax6* $^{-/-}$	Not present	0
PAX77$^{-/-}$:*Pax6*$^{+/-}$	One copy	*Pax6* $^{+/-}$	Not present	1
PAX77$^{-/-}$:*Pax6*$^{+/+}$	One copy	*Pax6* $^{+/+}$	Not present	2
PAX77$^{+/-}$:*Pax6* $^{-/-}$	One copy	*Pax6* $^{-/-}$	PAX77 heterozygous	5
PAX77$^{+/-}$:*Pax6*$^{+/-}$	One copy	*Pax6* $^{+/-}$	PAX77 heterozygous	6
PAX77$^{+/}$:*Pax6*$^{+/+}$	One copy	*Pax6* $^{+/+}$	PAX77 heterozygous	7
PAX77$^{+/+}$:*Pax* $^{-/-}$	One copy	*Pax6* $^{-/-}$	PAX77 homozygous	10
PAX77$^{+/+}$:*Pax6*$^{+/-}$	One copy	*Pax6* $^{+/-}$	PAX77 homozygous	11
PAX77$^{+/+}$:*Pax6*$^{+/+}$	One copy	*Pax6* $^{+/+}$	PAX77 homozygous	12

Table 5.5. Table of the number of copies of *Pax6* and *PAX77* from crosses of *PAX77: Pax6* $^{+-}$*:Pax6 Reporter* with *PAX77: Pax6* $^{+-}$. For convenience only the embryos that have the Pax6 reporter are given. The controls would have identical genotypes but without the Pax6 reporter (* Analysis possible until near birth.).

Once these embryos were available I would investigate autoregulation for each genotype and see how it fits with the number of functional Pax6 and PAX6 genes. Again litter mates with identical genotypes except for the presence of the Pax6 reporter would be identified and used as controls.

It is important to note that YAC Y593 was the starting point for the Pax6 reporter mouse so in order to genotype the crosses between PAX77 and the Pax6 reporter I would design PCR primers that span where the reporter cassette pDT1 is inserted. I would use a second set of genotyping primers for GFP. This should enable the genotypes of all the embryos to be identified. In addition, the primers would be designed to produce a product of approximately 250bp, thus they could be used with qPCR to genotyping the number of copies of PAX77.

Conclusion

Two of the nine transgenic lines generated (DTy1123.54 and DTy374.001) have incorporated the majority of the YAC and predominantly successfully report the *Pax6* expression pattern at the developmental stages investigated. Therefore, these two lines can be used as '*Pax6* reporters' to investigate the function of *Pax6*.

Two of the lines (DTy1123.22 and DTy1123.42) incorporated part of the YAC. Both of these incorporated a functional GFP reporter cassette and both express some GFP. As discussed above it would be interesting to further investigate these lines and see where the truncation in the YAC is and the chromosomal location of the incorporated YAC.

Further analysis of the three remaining viable lines is still necessary (DTy374.028, DTy374.226, and DTy374.227). It is anticipated that DTy374.226, which appears to have incorporated the majority of the YAC, will have a GFP expression pattern similar to DTy1123.54 and DTy374.001.

A major difference was observed in GFP expression between DTy1123.22 and DTy1123.42 which both have incorporated truncated YACs. Therefore, it seems likely that the GFP expression in DTy374.028 and DTy374.227, which have both incorporated truncated YACs, the GFP expression will be unpredictable. However, it is none the less still very interesting. The mechanisms behind why some of these transgenic lines that lack the majority of the YAC fail to fully report *Pax6* expression could give insights into the regulation of the *Pax6* gene.

Bibliography

Altmann, C. R., R. L. Chow, R. A. Lang and A. Hemmati-Brivanlou (1997). Lens induction by Pax-6 in Xenopus laevis. *Dev Biol* **185**(1): 119-23.

Anderson, T. R., E. Hedlund and E. M. Carpenter (2002). Differential Pax6 promoter activity and transcript expression during forebrain development. *Mech Dev* **114**(1-2): 171-5.

Aota, S., N. Nakajima, R. Sakamoto, S. Watanabe, N. Ibaraki and K. Okazaki (2003). Pax6 autoregulation mediated by direct interaction of Pax6 protein with the head surface ectoderm-specific enhancer of the mouse Pax6 gene. *Dev Biol* **257**(1): 1-13.

Ashery-Padan, R. and P. Gruss (2001). Pax6 lights-up the way for eye development. *Curr Opin Cell Biol* **13**(6): 706-14.

Ashery-Padan, R., T. Marquardt, X. Zhou and P. Gruss (2000). Pax6 activity in the lens primordium is required for lens formation and for correct placement of a single retina in the eye. *Genes & Development* **14**: 2701-2711.

Aubert, J., M. P. Stavridis, S. Tweedie, M. O'Reilly, K. Vierlinger, M. Li, P. Ghazal, T. Pratt, J. O. Mason, D. Roy and A. Smith (2003). Screening for mammalian neural genes via fluorescence-activated cell sorter purification of neural precursors from Sox1-gfp knock-in mice. *Proc Natl Acad Sci U S A* **100 Suppl 1**: 11836-41.

Barth, K. A. and S. W. Wilson (1995). Expression of zebrafish nk2.2 is influenced by sonic hedgehog/vertebrate hedgehog-1 and demarcates a zone of neuronal differentiation in the embryonic forebrain. *Development* **121**(6): 1755-68.

Bauchwitz, R. and F. Costantini (1998). YAC transgenesis: a study of conditions to protect YAC DNA from breakage and a protocol for transfection. *Biochim Biophys Acta* **1401**(1): 21-37.

Beimesche, S., A. Neubauer, S. Herzig, R. Grzeskowiak, T. Diedrich, I. Cierny, D. Scholz, T. Alejel and W. Knepel (1999). Tissue-specific transcriptional activity of a pancreatic islet cell-specific enhancer sequence/Pax6-binding site determined in normal adult tissues in vivo using transgenic mice. *Mol Endocrinol* **13**(5): 718-28.

Bernier, G., W. Vukovich, L. Neidhardt, B. G. Herrmann and P. Gruss (2001). Isolation and characterization of a downstream target of Pax6 in the mammalian retinal primordium. *Development* **128**(20): 3987-94.

Bishop, K. M., G. Goudreau and D. D. O'Leary (2000). Regulation of area identity in the mammalian neocortex by Emx2 and Pax6. *Science* **288**(5464): 344-9.

Bishop, K. M., J. L. Rubenstein and D. D. O'Leary (2002). Distinct actions of Emx1, Emx2, and Pax6 in regulating the specification of areas in the developing neocortex. *J Neurosci* **22**(17): 7627-38.

Blank, V. and N. C. Andrews (1997). The Maf transcription factors: regulators of differentiation. *Trends Biochem Sci* **22**(11): 437-41.

Bloemendal, H. and W. W. de Jong (1991). Lens proteins and their genes. *Prog Nucleic Acid Res Mol Biol* **41**: 259-81.

Boeke, J. D., J. Trueheart, G. Natsoulis and G. R. Fink (1987). 5-Fluoroorotic acid as a selective agent in yeast molecular genetics. *Methods Enzymol* **154**: 164-75.

Botstein, D., S. C. Falco, S. E. Stewart, M. Brennan, S. Scherer, D. T. Stinchcomb, K. Struhl and R. W. Davis (1979). Sterile host yeasts (SHY): a eukaryotic system of biological containment for recombinant DNA experiments. *Gene* **8**(1): 17-24.

Burrill, J. D., L. Moran, M. D. Goulding and H. Saueressig (1997). PAX2 is expressed in multiple spinal cord interneurons, including a population of EN1+ interneurons that require PAX6 for their development. *Development* **124**(22): 4493-503.

Callaerts, P., G. Halder and W. J. Gehring (1997). PAX-6 in development and evolution. *Annu Rev Neurosci* **20**: 483-532.

Campbel, I. and J. Duffus (1988). Yeast: a practical approach. Oxford, UK, IRL Press.

Campbell, K. and M. Gotz (2002). Radial glia: multi-purpose cells for vertebrate brain development. *Trends Neurosci* **25**(5): 235-8.

Caric, D., D. Gooday, R. E. Hill, S. K. McConnell and D. J. Price (1997). Determination of the migratory capacity of embryonic cortical cells lacking the transcription factor Pax-6. *Development* **124**(24): 5087-96.

Carriere, C., S. Plaza, J. Caboche, C. Dozier, M. Bailly, P. Martin and S. Saule (1995). Nuclear localization signals, DNA binding, and transactivation properties of quail Pax-6 (Pax-QNR) isoforms. *Cell Growth Differ* **6**(12): 1531-40.

Casarosa, S., C. Fode and F. Guillemot (1999). Mash1 regulates neurogenesis in the ventral telencephalon. *Development* **126**(3): 525-34.

Chalepakis, G., F. S. Jones, G. M. Edelman and P. Gruss (1994). Pax-3 contains domains for transcription activation and transcription inhibition. *Proc Natl Acad Sci U S A* **91**(26): 12745-9.

Chapouton, P., A. Gartner and M. Gotz (1999). The role of Pax6 in restricting cell migration between developing cortex and basal ganglia. *Development* **126**(24): 5569-79.

Chauhan, B. K., N. A. Reed, Y. Yang, L. Cermak, L. Reneker, M. K. Duncan and A. Cvekl (2002). A comparative cDNA microarray analysis reveals a spectrum of genes regulated by Pax6 in mouse lens. *Genes Cells* **7**(12): 1267-83.

Chauhan, B. K., N. A. Reed, W. Zhang, M. K. Duncan, M. Kilimann and A. Cvekl (2002). Identification of genes downstream of Pax6 in the mouse lens using cDNA microarrays. *J Biol Chem*.

Chiang, C., Y. Litingtung, E. Lee, K. E. Young, J. L. Corden, H. Westphal and P. A. Beachy (1996). Cyclopia and defective axial patterning in mice lacking Sonic hedgehog gene function. *Nature* **383**(6599): 407-13.

Chow, R., C. Altmann, R. Lang and A. Hemmati-Brivanlou (1999). Pax6 induces ectopic eyes in a vertebrate. *Development* **126**: 4213-4222.

Chu, G., D. Vollrath and R. W. Davis (1986). Separation of large DNA molecules by contour-clamped homogeneous electric fields. *Science* **234**(4783): 1582-5.

Collinson, J. M., R. E. Hill and J. D. West (2000). Different roles for Pax6 in the optic vesicle and facial epithelium mediate early morphogenesis of the murine eye. *Development* **127**(5): 945-56.

Couto, L., E. Spangler and E. Rubin (1989). A method for the preparative isolation and concentration of intact yeast artificial chromosmes. *Nucleic Acids Res* **17**(19): 8010.

Crolla, J. A., I. Cross, N. Atkey, M. Wright and C. A. Oley (1996). FISH studies in a patient with sporadic aniridia and t(7;11) (q31.2;p13). *J Med Genet* **33**(1): 66-8.

Crossley, P. H. and G. R. Martin (1995). The mouse Fgf8 gene encodes a family of polypeptides and is expressed in regions that direct outgrowth and patterning in the developing embryo. *Development* **121**(2): 439-51.

Cvekl, A., F. Kashanchi, J. N. Brady and J. Piatigorsky (1999). Pax-6 interactions with TATA-box-binding protein and retinoblastoma protein. *Invest Ophthalmol Vis Sci* **40**(7): 1343-50.

Cvekl, A., F. Kashanchi, C. M. Sax, J. N. Brady and J. Piatigorsky (1995). Transcriptional regulation of the mouse alpha A-crystallin gene: activation dependent on a cyclic AMP-responsive element (DE1/CRE) and a Pax-6-binding site. *Mol Cell Biol* **15**(2): 653-60.

Cvekl, A., C. M. Sax, X. Li, J. B. McDermott and J. Piatigorsky (1995). Pax-6 and lens-specific transcription of the chicken delta 1-crystallin gene. *Proc Natl Acad Sci U S A* **92**(10): 4681-5.

Czerny, T. and M. Busslinger (1995). DNA-binding and transactivation properties of Pax-6: three amino acids in the paired domain are responsible for the different sequence recognition of Pax-6 and BSAP (Pax-5). *Mol Cell Biol* **15**(5): 2858-71.

Davies, N. P., I. R. Rosewell, J. C. Richardson, G. P. Cook, M. S. Neuberger, B. H. Brownstein, M. L. Norris and M. Bruggemann (1993). Creation of mice expressing human antibody light chains by introduction of a yeast artificial chromosome containing the core region of the human immunoglobulin kappa locus. *Biotechnology (N Y)* **11**(8): 911-4.

Dehay, C., P. Giroud, M. Berland, I. Smart and H. Kennedy (1993). Modulation of the cell cycle contributes to the parcellation of the primate visual cortex. *Nature* **366**(6454): 464-6.

Dominguez, M., D. Ferres-Marco, F. J. Gutierrez-Avino, S. A. Speicher and M. Beneyto (2004). Growth and specification of the eye are controlled independently by Eyegone and Eyeless in Drosophila melanogaster. *Nat Genet* **36**(1): 31-9.

Donoghue, M. J. and P. Rakic (1999). Molecular evidence for the early specification of presumptive functional domains in the embryonic primate cerebral cortex. *J Neurosci* **19**(14): 5967-79.

Dou, C. L., S. Li and E. Lai (1999). Dual role of brain factor-1 in regulating growth and patterning of the cerebral hemispheres. *Cereb Cortex* **9**(6): 543-50.

Dozier, C., C. Carriere, D. Grevin, P. Martin, B. Quatannens, D. Stehelin and S. Saule (1993). Structure and DNA-binding properties of Pax-QNR, a paired box- and homeobox-containing gene. *Cell Growth Differ* **4**(4): 281-9.

Duncan, M. K., J. I. Haynes, 2nd, A. Cvekl and J. Piatigorsky (1998). Dual roles for Pax-6: a transcriptional repressor of lens fiber cell-specific beta-crystallin genes. *Mol Cell Biol* **18**(9): 5579-86.

Duncan, M. K., Z. Kozmik, K. Cveklova, J. Piatigorsky and A. Cvekl (2000). Overexpression of PAX6(5a) in lens fiber cells results in cataract and upregulation of (alpha)5(beta)1 integrin expression. *J Cell Sci* **113 (Pt 18)**: 3173-85.

Echelard, Y., D. J. Epstein, B. St-Jacques, L. Shen, J. Mohler, J. A. McMahon and A. P. McMahon (1993). Sonic hedgehog, a member of a family of putative signaling molecules, is implicated in the regulation of CNS polarity. *Cell* **75**(7): 1417-30.

Epstein, J., J. Cai, T. Glaser, L. Jepeal and R. Maas (1994). Identification of a Pax paired domain recognition sequence and evidence for DNA-dependent conformational changes. *J Biol Chem* **269**(11): 8355-61.

Ericson, J., J. Muhr, M. Placzek, T. Lints, T. M. Jessell and T. Edlund (1995). Sonic hedgehog induces the differentiation of ventral forebrain neurons: a common signal for ventral patterning within the neural tube. *Cell* **81**(5): 747-56.

Ericson, J., P. Rashbass, A. Schedl, S. Brenner-Morton, A. Kawakami, V. van Heyningen, T. M. Jessell and J. Briscoe (1997). Pax6 controls progenitor cell identity and neuronal fate in response to graded Shh signaling. *Cell* **90**(1): 169-80.

Estivill-Torrus, G., H. Pearson, V. van Heyningen, D. J. Price and P. Rashbass (2002). Pax6 is required to regulate the cell cycle and the rate of progression from symmetrical to asymmetrical division in mammalian cortical progenitors. *Development* **129**(2): 455-66.

Faber, S. C., P. Dimanlig, H. P. Makarenkova, S. Shirke, K. Ko and R. A. Lang (2001). Fgf receptor signaling plays a role in lens induction. *Development* **128**(22): 4425-38.

Fantes, J., B. Redeker, M. Breen, S. Boyle, J. Brown, J. Fletcher, S. Jones, W. Bickmore, Y. Fukushima, M. Mannens and et al. (1995). Aniridia-associated cytogenetic rearrangements suggest that a position effect may cause the mutant phenotype. *Hum Mol Genet* **4**(3): 415-22.

Filosa, S., J. A. Rivera-Perez, A. P. Gomez, A. Gansmuller, H. Sasaki, R. R. Behringer and S. L. Ang (1997). Goosecoid and HNF-3beta genetically interact to regulate neural tube patterning during mouse embryogenesis. *Development* **124**(14): 2843-54.

Fode, C., Q. Ma, S. Casarosa, S. L. Ang, D. J. Anderson and F. Guillemot (2000). A role for neural determination genes in specifying the dorsoventral identity of telencephalic neurons. *Genes Dev* **14**(1): 67-80.

Fujita, S. (1964). Analysis of neuron differentiation in the central nervous system by tritiated thymidine autoradiography. *J Comp Neurol* **122**: 311-328.

Fukuchi-Shimogori, T. and E. A. Grove (2001). Neocortex patterning by the secreted signaling molecule FGF8. *Science* **294**(5544): 1071-4.

Fukuda, T., H. Kawano, N. Osumi, K. Eto and K. Kawamura (2000). Histogenesis of the cerebral cortex in rat fetuses with a mutation in the Pax-6 gene. *Brain Res Dev Brain Res* **120**(1): 65-75.

Furuta, Y., D. W. Piston and B. L. Hogan (1997). Bone morphogenetic proteins (BMPs) as regulators of dorsal forebrain development. *Development* **124**(11): 2203-12.

Ganzler, S. I. and C. Redies (1995). R-cadherin expression during nucleus formation in chicken forebrain neuromeres. *J Neurosci* **15**(6): 4157-72.

Gillies, K. and D. J. Price (1993). Cell migration and subplate loss in explant cultures of murine cerebral cortex. *Neuroreport* **4**(7): 911-4.

Glaser, T., L. Jepeal, J. G. Edwards, S. R. Young, J. Favor and R. L. Maas (1994). PAX6 gene dosage effect in a family with congenital cataracts, aniridia, anophthalmia and central nervous system defects. *Nat Genet* **7**(4): 463-71.

Glaser, T., J. Lane and D. Housman (1990). A mouse model of the aniridia-Wilms tumor deletion syndrome. *Science* **250**(4982): 823-7.

Glaser, T., D. S. Walton and R. L. Maas (1992). Genomic structure, evolutionary conservation and aniridia mutations in the human PAX6 gene. *Nat Genet* **2**(3): 232-9.

Gleeson, J. G. and C. A. Walsh (2000). Neuronal migration disorders: from genetic diseases to developmental mechanisms. *Trends Neurosci* **23**(8): 352-9.

Gnirke, A., C. Huxley, K. Peterson and M. V. Olson (1993). Microinjection of intact 200- to 500-kb fragments of YAC DNA into mammalian cells. *Genomics* **15**(3): 659-67.

Golden, J. A., A. Bracilovic, K. A. McFadden, J. S. Beesley, J. L. Rubenstein and J. B. Grinspan (1999). Ectopic bone morphogenetic proteins 5 and 4 in the chicken forebrain lead to cyclopia and holoprosencephaly. *Proc Natl Acad Sci U S A* **96**(5): 2439-44.

Gopal-Srivastava, R., A. Cvekl and J. Piatigorsky (1996). Pax-6 and alphaB-crystallin/small heat shock protein gene regulation in the murine lens. Interaction with the lens-specific regions, LSR1 and LSR2. *J Biol Chem* **271**(38): 23029-36.

Gotz, M., A. Stoykova and P. Gruss (1998). Pax6 controls radial glia differentiation in the cerebral cortex. *Neuron* **21**(5): 1031-44.

Green, L. L., M. C. Hardy, C. E. Maynard-Currie, H. Tsuda, D. M. Louie, M. J. Mendez, H. Abderrahim, M. Noguchi, D. H. Smith, Y. Zeng and et al. (1994). Antigen-specific human monoclonal antibodies from mice engineered with human Ig heavy and light chain YACs. *Nat Genet* **7**(1): 13-21.

Griffin, C., D. A. Kleinjan, B. Doe and V. van Heyningen (2002). New 3[prime prime or minute] elements control Pax6 expression in the developing pretectum, neural retina and olfactory region. *Mech Dev* **112**(1-2): 89-100.

Grindley, J. C., D. R. Davidson and R. E. Hill (1995). The role of Pax-6 in eye and nasal development. *Development* **121**(5): 1433-42.

Grove, E. A., S. Tole, J. Limon, L. Yip and C. W. Ragsdale (1998). The hem of the embryonic cerebral cortex is defined by the expression of multiple Wnt genes and is compromised in Gli3-deficient mice. *Development* **125**(12): 2315-25.

Grove, E. A., B. P. Williams, D. Q. Li, M. Hajihosseini, A. Friedrich and J. Price (1993). Multiple restricted lineages in the embryonic rat cerebral cortex. *Development* **117**(2): 553-61.

Guillemot, F. (1999). Vertebrate bHLH genes and the determination of neuronal fates. *Exp Cell Res* **253**(2): 357-64.

Gulisano, M., V. Broccoli, C. Pardini and E. Boncinelli (1996). Emx1 and Emx2 show different patterns of expression during proliferation and differentiation of the developing cerebral cortex in the mouse. *Eur J Neurosci* **8**(5): 1037-50.

Halder, G., P. Callaerts and W. J. Gehring (1995). Induction of ectopic eyes by targeted expression of the eyeless gene in Drosophila. *Science* **267**(5205): 1788-92.

Hallonet, M., T. Hollemann, R. Wehr, N. A. Jenkins, N. G. Copeland, T. Pieler and P. Gruss (1998). Vax1 is a novel homeobox-containing gene expressed in the developing anterior ventral forebrain. *Development* **125**(14): 2599-610.

Hamer, L., M. Johnston and E. D. Green (1995). Isolation of yeast artificial chromosomes free of endogenous yeast chromosomes: construction of alternate hosts with defined karyotypic alterations. *Proc Natl Acad Sci U S A* **92**(25): 11706-10.

Hanson, I., A. Churchill, J. Love, R. Axton, T. Moore, M. Clarke, F. Meire and V. van Heyningen (1999). Missense mutations in the most ancient residues of the PAX6 paired domain underlie a spectrum of human congenital eye malformations. *Hum Mol Genet* **8**(2): 165-72.

Heard, J. M., P. Herbomel, M. O. Ott, A. Mottura-Rollier, M. Weiss and M. Yaniv (1987). Determinants of rat albumin promoter tissue specificity analyzed by an improved transient expression system. *Mol Cell Biol* **7**(7): 2425-34.

Hebert, J. M., Y. Mishina and S. K. McConnell (2002). BMP signaling is required locally to pattern the dorsal telencephalic midline. *Neuron* **35**(6): 1029-41.

Heins, N., P. Malatesta, F. Cecconi, M. Nakafuku, K. L. Tucker, M. A. Hack, P. Chapouton, Y. A. Barde and M. Gotz (2002). Glial cells generate neurons: the role of the transcription factor Pax6. *Nat Neurosci* **5**(4): 308-15.

Hill, R. E., J. Favor, B. L. Hogan, C. C. Ton, G. F. Saunders, I. M. Hanson, J. Prosser, T. Jordan, N. D. Hastie and V. van Heyningen (1991). Mouse small eye results from mutations in a paired-like homeobox-containing gene. *Nature* **354**(6354): 522-5.

Hogan, B. L., G. Horsburgh, J. Cohen, C. M. Hetherington, G. Fisher and M. F. Lyon (1986). Small eyes (Sey): a homozygous lethal mutation on chromosome 2 which affects the differentiation of both lens and nasal placodes in the mouse. *J Embryol Exp Morphol* **97**: 95-110.

Holst, B. D., Y. Wang, F. S. Jones and G. M. Edelman (1997). A binding site for Pax proteins regulates expression of the gene for the neural cell adhesion molecule in the embryonic spinal cord. *Proc Natl Acad Sci U S A* **94**(4): 1465-70.

Honig, M. G., S. J. Camilli and Q. S. Xue (2002). Effects of L1 blockade on sensory axon outgrowth and pathfinding in the chick hindlimb. *Dev Biol* **243**(1): 137-54.

Huettner, J. E. and R. W. Baughman (1986). Primary culture of identified neurons from the visual cortex of postnatal rats. *J Neurosci* **6**(10): 3044-60.

Hugerat, Y., F. Spencer, D. Zenvirth and G. Simchen (1994). A versatile method for efficient YAC transfer between any two strains. *Genomics* **22**(1): 108-17.

Huh, S., V. Hatini, R. C. Marcus, S. C. Li and E. Lai (1999). Dorsal-ventral patterning defects in the eye of BF-1-deficient mice associated with a restricted loss of shh expression. *Dev Biol* **211**(1): 53-63.

Hussain, M. A. and J. F. Habener (1999). Glucagon gene transcription activation mediated by synergistic interactions of pax-6 and cdx-2 with the p300 co-activator. *J Biol Chem* **274**(41): 28950-7.

Huxley, C. (1998). Exploring gene function: use of yeast artificial chromosome transgenesis. *Methods* **14**(2): 199-210.

Jakobovits, A., A. L. Moore, L. L. Green, G. J. Vergara, C. E. Maynard-Currie, H. A. Austin and S. Klapholz (1993). Germ-line transmission and expression of a human-derived yeast artificial chromosome. *Nature* **362**(6417): 255-8.

Jaworski, C., S. Sperbeck, C. Graham and G. Wistow (1997). Alternative splicing of Pax6 in bovine eye and evolutionary conservation of intron sequences. *Biochem Biophys Res Commun* **240**(1): 196-202.

Jordan, T., I. Hanson, D. Zaletayev, S. Hodgson, J. Prosser, A. Seawright, N. Hastie and V. van Heyningen (1992). The human PAX6 gene is mutated in two patients with aniridia. *Nat Genet* **1**(5): 328-32.

Jun, S. and C. Desplan (1996). Cooperative interactions between paired domain and homeodomain. *Development* **122**(9): 2639-50.

Kamachi, Y. and H. Kondoh (1993). Overlapping positive and negative regulatory elements determine lens-specific activity of the delta 1-crystallin enhancer. *Mol Cell Biol* **13**(9): 5206-15.

Kamachi, Y., S. Sockanathan, Q. Liu, M. Breitman, R. Lovell-Badge and H. Kondoh (1995). Involvement of SOX proteins in lens-specific activation of crystallin genes. *Embo J* **14**(14): 3510-9.

Kamachi, Y., M. Uchikawa, A. Tanouchi, R. Sekido and H. Kondoh (2001). Pax6 and SOX2 form a co-DNA-binding partner complex that regulates initiation of lens development. *Genes Dev* **15**(10): 1272-86.

Kammandel, B., K. Chrowdhury, A. Stoykova, S. Aparicio, S. Brenner and P. Gruss (1999). Distinct cis-Essential Modules Direct the Time-Space Pattern of the Pax6 Gene Activity. *Developmental Biology* **205**: 79-97.

Kiecker, C. and C. Niehrs (2001). The role of prechordal mesendoderm in neural patterning. *Curr Opin Neurobiol* **11**(1): 27-33.

Kioussi, C., S. O'Connell, L. St-Onge, M. Treier, A. S. Gleiberman, P. Gruss and M. G. Rosenfeld (1999). Pax6 is essential for establishing ventral-dorsal cell boundaries in pituitary gland development. *Proc Natl Acad Sci U S A* **96**(25): 14378-82.

Kisseberth, W. C., N. T. Brettingen, J. K. Lohse and E. P. Sandgren (1999). Ubiquitous expression of marker transgenes in mice and rats. *Dev Biol* **214**(1): 128-38.

Kitamura, K., T. Kaneko and Y. Yamamoto (1971). Lysis of viable yeast cells by enzymes of Arthrobacter luteus. *Arch Biochem Biophys* **145**(1): 402-4.

Kleinjan, D. A., A. Seawright, A. J. Childs and V. van Heyningen (2004). Conserved elements in Pax6 intron 7 involved in (auto)regulation and alternative transcription. *Dev Biol* **265**(2): 462-77.

Kleinjan, D. A., A. Seawright, A. Schedl, R. A. Quinlan, S. Danes and V. van Heyningen (2001). Aniridia-associated translocations, DNase hypersensitivity, sequence comparison and transgenic analysis redefine the functional domain of PAX6. *Hum Mol Genet* **10**(19): 2049-59.

Kozak, M. (2003). Alternative ways to think about mRNA sequences and proteins that appear to promote internal initiation of translation. *Gene* **318**: 1-23.

Kozmik, Z., T. Czerny and M. Busslinger (1997). Alternatively spliced insertions in the paired domain restrict the DNA sequence specificity of Pax6 and Pax8. *Embo J* **16**(22): 6793-803.

Kralova, J., T. Czerny, H. Spanielova, V. Ratajova and Z. Kozmik (2002). Complex regulatory element within the gammaE- and gammaF-crystallin enhancers mediates Pax6 regulation and is required for induction by retinoic acid. *Gene* **286**(2): 271-82.

Larin, Z., A. P. Monaco and H. Lehrach (1991). Yeast artificial chromosome libraries containing large inserts from mouse and human DNA. *Proc Natl Acad Sci U S A* **88**(10): 4123-7.

Lauderdale, J. D., J. S. Wilensky, E. R. Oliver, D. S. Walton and T. Glaser (2000). 3' deletions cause aniridia by preventing PAX6 gene expression. *Proc Natl Acad Sci U S A* **97**(25): 13755-9.

Lebrand, C., O. Cases, R. Wehrle, R. D. Blakely, R. H. Edwards and P. Gaspar (1998). Transient developmental expression of monoamine transporters in the rodent forebrain. *J Comp Neurol* **401**(4): 506-24.

Lee, K. J. and T. M. Jessell (1999). The specification of dorsal cell fates in the vertebrate central nervous system. *Annu Rev Neurosci* **22**: 261-94.

Lee, M. K., J. B. Tuttle, L. I. Rebhun, D. W. Cleveland and A. Frankfurter (1990). The expression and posttranslational modification of a neuron-specific beta-tubulin isotype during chick embryogenesis. *Cell Motil Cytoskeleton* **17**(2): 118-32.

Lee, S. M., S. Tole, E. Grove and A. P. McMahon (2000). A local Wnt-3a signal is required for development of the mammalian hippocampus. *Development* **127**(3): 457-67.

Levers, T. E., J. M. Edgar and D. J. Price (2001). The fates of cells generated at the end of neurogenesis in developing mouse cortex. *J Neurobiol* **48**(4): 265-77.

Liu, J. J., W. W. Kao and S. E. Wilson (1999). Corneal epithelium-specific mouse keratin K12 promoter. *Exp Eye Res* **68**(3): 295-301.

Lotto, R. B., P. Asavaritikrai, L. Vali and D. J. Price (2001). Target-derived neurotrophic factors regulate the death of developing forebrain neurons after a change in their trophic requirements. *J Neurosci* **21**(11): 3904-10.

Luskin, M. B., J. G. Parnavelas and J. A. Barfield (1993). Neurons, astrocytes, and oligodendrocytes of the rat cerebral cortex originate from separate progenitor

cells: an ultrastructural analysis of clonally related cells. *J Neurosci* **13**(4): 1730-50.

Lyon, M. F., D. Bogani, Y. Boyd, P. Guillot and J. Favor (2000). Further genetic analysis of two autosomal dominant mouse eye defects, Ccw and Pax6(coop). *Mol Vis* **6**: 199-203.

Marin, O. and J. L. Rubenstein (2001). A long, remarkable journey: tangential migration in the telencephalon. *Nat Rev Neurosci* **2**(11): 780-90.

Marquardt, T., R. Ashery-Padan, N. Andrejewski, R. Scardigli, F. Guillemot and P. Gruss (2001). Pax6 is required for the multipotent state of retinal progenitor cells. *Cell* **105**(1): 43-55.

Mastick, G. S., N. M. Davis, G. L. Andrew and S. S. Easter, Jr. (1997). Pax-6 functions in boundary formation and axon guidance in the embryonic mouse forebrain. *Development* **124**(10): 1985-97.

Matise, M. P., D. J. Epstein, H. L. Park, K. A. Platt and A. L. Joyner (1998). Gli2 is required for induction of floor plate and adjacent cells, but not most ventral neurons in the mouse central nervous system. *Development* **125**(15): 2759-70.

Matsunami, H. and M. Takeichi (1995). Fetal brain subdivisions defined by R- and E-cadherin expressions: evidence for the role of cadherin activity in region-specific, cell-cell adhesion. *Dev Biol* **172**(2): 466-78.

McCormick, M. K., J. H. Shero, M. C. Cheung, Y. W. Kan, P. A. Hieter and S. E. Antonarakis (1989). Construction of human chromosome 21-specific yeast artificial chromosomes. *Proc Natl Acad Sci U S A* **86**(24): 9991-5.

Meech, R., P. Kallunki, G. M. Edelman and F. S. Jones (1999). A binding site for homeodomain and Pax proteins is necessary for L1 cell adhesion molecule gene expression by Pax-6 and bone morphogenetic proteins. *Proc Natl Acad Sci U S A* **96**(5): 2420-5.

Mendez, M. J., H. Abderrahim, M. Noguchi, N. E. David, M. C. Hardy, L. L. Green, H. Tsuda, S. Yoast, C. E. Maynard-Currie, D. Garza and et al. (1995). Analysis of the structural integrity of YACs comprising human immunoglobulin genes in yeast and in embryonic stem cells. *Genomics* **26**(2): 294-307.

Mendez, M. J., L. L. Green, J. R. Corvalan, X. C. Jia, C. E. Maynard-Currie, X. D. Yang, M. L. Gallo, D. M. Louie, D. V. Lee, K. L. Erickson, J. Luna, C. M. Roy, H. Abderrahim, F. Kirschenbaum, M. Noguchi, D. H. Smith, A. Fukushima, J. F. Hales, S. Klapholz, M. H. Finer, C. G. Davis, K. M. Zsebo and A. Jakobovits (1997). Functional transplant of megabase human immunoglobulin loci recapitulates human antibody response in mice. *Nat Genet* **15**(2): 146-56.

Miyashita-Lin, E. M., R. Hevner, K. M. Wassarman, S. Martinez and J. L. Rubenstein (1999). Early neocortical regionalization in the absence of thalamic innervation. *Science* **285**(5429): 906-9.

Monuki, E. S., F. D. Porter and C. A. Walsh (2001). Patterning of the dorsal telencephalon and cerebral cortex by a roof plate-Lhx2 pathway. *Neuron* **32**(4): 591-604.

Monuki, E. S. and C. A. Walsh (2001). Mechanisms of cerebral cortical patterning in mice and humans. *Nat Neurosci* **4 Suppl**: 1199-206.

Morrison, S. J. (2000). The last shall not be first: the ordered generation of progeny from stem cells. *Neuron* **28**(1): 1-3.

Mountford, P., B. Zevnik, A. Duwel, J. Nichols, M. Li, C. Dani, M. Robertson, I. Chambers and A. Smith (1994). Dicistronic targeting constructs: reporters and modifiers of mammalian gene expression. *Proc Natl Acad Sci U S A* **91**(10): 4303-7.

Muller, U., N. Cristina, Z. W. Li, D. P. Wolfer, H. P. Lipp, T. Rulicke, S. Brandner, A. Aguzzi and C. Weissman (1996). Mice homozygous for a modified beta-amyloid precursor protein (beta APP) gene show impaired behavior and high incidence of agenesis of the corpus callosum. *Ann N Y Acad Sci* **777**: 65-73.

Muller, U., N. Cristina, Z. W. Li, D. P. Wolfer, H. P. Lipp, T. Rulicke, S. Brandner, A. Aguzzi and C. Weissmann (1994). Behavioral and anatomical deficits in mice homozygous for a modified beta-amyloid precursor protein gene. *Cell* **79**(5): 755-65.

Muzio, L. and A. Mallamaci (2003). Emx1, emx2 and pax6 in specification, regionalization and arealization of the cerebral cortex. *Cereb Cortex* **13**(6): 641-7.

Nadarajah, B. and J. G. Parnavelas (2002). Modes of neuronal migration in the developing cerebral cortex. *Nat Rev Neurosci* **3**(6): 423-32.

Nakagawa, Y., J. E. Johnson and D. D. O'Leary (1999). Graded and areal expression patterns of regulatory genes and cadherins in embryonic neocortex independent of thalamocortical input. *J Neurosci* **19**(24): 10877-85.

Nanjo, Y., S. Kawasaki, K. Mori, C. Sotozono, T. Inatomi and S. Kinoshita (2004). A novel mutation in the alternative splice region of the PAX6 gene in a patient with Peters' anomaly. *Br J Ophthalmol* **88**(5): 720-1.

Naylor, L. H. (1999). Reporter gene technology: the future looks bright. *Biochem Pharmacol* **58**(5): 749-57.

Ohtoshi, A., I. Nishijima, M. J. Justice and R. R. Behringer (2002). Dmbx1, a novel evolutionarily conserved paired-like homeobox gene expressed in the brain of mouse embryos. *Mech Dev* **110**(1-2): 241-4.

O'Leary, D. D. (1989). Do cortical areas emerge from a protocortex? *Trends Neurosci* **12**(10): 400-6.

Osumi, N., A. Hirota, H. Ohuchi, M. Nakafuku, T. Iimura, S. Kuratani, M. Fujiwara, S. Noji and K. Eto (1997). Pax-6 is involved in the specification of hindbrain motor neuron subtype. *Development* **124**(15): 2961-72.

Park, H. L., C. Bai, K. A. Platt, M. P. Matise, A. Beeghly, C. C. Hui, M. Nakashima and A. L. Joyner (2000). Mouse Gli1 mutants are viable but have defects in SHH signaling in combination with a Gli2 mutation. *Development* **127**(8): 1593-605.

Pera, E. M. and M. Kessel (1997). Patterning of the chick forebrain anlage by the prechordal plate. *Development* **124**(20): 4153-62.

Peterson, K. R., C. H. Clegg, Q. Li and G. Stamatoyannopoulos (1997). Production of transgenic mice with yeast artificial chromosomes. *Trends Genet* **13**(2): 61-6.

Piatigorsky, J. (1998). Multifunctional lens crystallins and corneal enzymes. More than meets the eye. *Ann N Y Acad Sci* **842**: 7-15.

Pichaud, F. and C. Desplan (2002). Pax genes and eye organogenesis. *Curr Opin Genet Dev* **12**(4): 430-4.

Planque, N., L. Leconte, F. M. Coquelle, S. Benkhelifa, P. Martin, M. P. Felder-Schmittbuhl and S. Saule (2001). Interaction of Maf transcription factors with Pax-6 results in synergistic activation of the glucagon promoter. *J Biol Chem* **276**(38): 35751-60.

Plaza, S., C. Dozier, M. C. Langlois and S. Saule (1995). Identification and characterization of a neuroretina-specific enhancer element in the quail Pax-6 (Pax-QNR) gene. *Mol Cell Biol* **15**(2): 892-903.

Plaza, S., C. Dozier and S. Saule (1993). Quail Pax-6 (Pax-QNR) encodes a transcription factor able to bind and trans-activate its own promoter. *Cell Growth Differ* **4**(12): 1041-50.

Plaza, S., N. Turque, C. Dozier, M. Bailly and S. Saule (1995). C-Myb acts as transcriptional activator of the quail PAX6 (PAX-QNR) promoter through two different mechanisms. *Oncogene* **10**(2): 329-40.

Pratt, T., T. Vitalis, N. Warren, J. M. Edgar, J. O. Mason and D. J. Price (2000). A role for Pax6 in the normal development of dorsal thalamus and its cortical connections. *Development* **127**(23): 5167-78.

Price, M., D. Lazzaro, T. Pohl, M. G. Mattei, U. Ruther, J. C. Olivo, D. Duboule and R. Di Lauro (1992). Regional expression of the homeobox gene Nkx-2.2 in the developing mammalian forebrain. *Neuron* **8**(2): 241-55.

Qiu, M., K. Shimamura, L. Sussel, S. Chen and J. L. Rubenstein (1998). Control of anteroposterior and dorsoventral domains of Nkx-6.1 gene expression relative to other Nkx genes during vertebrate CNS development. *Mech Dev* **72**(1-2): 77-88.

Quinn, J. C., J. D. West and R. E. Hill (1996). Multiple functions for Pax6 in mouse eye and nasal development. *Genes Dev* **10**(4): 435-46.

Quiring, R., U. Walldorf, U. Kloter and W. J. Gehring (1994). Homology of the eyeless gene of Drosophila to the Small eye gene in mice and Aniridia in humans. *Science* **265**(5173): 785-9.

Ragsdale, C. W. and E. A. Grove (2001). Patterning the mammalian cerebral cortex. *Curr Opin Neurobiol* **11**(1): 50-8.

Rakic, P. (1988). Specification of cerebral cortical areas. *Science* **241**(4862): 170-6.

Rakic, P. (1995). A small step for the cell, a giant leap for mankind: a hypothesis of neocortical expansion during evolution. *Trends Neurosci* **18**(9): 383-8.

Rallu, M., J. G. Corbin and G. Fishell (2002). Parsing the prosencephalon. *Nat Rev Neurosci* **3**(12): 943-51.

Rayner, J. C. and S. Munro (1998). Identification of the MNN2 and MNN5 mannosyltransferases required for forming and extending the mannose branches of the outer chain mannans of Saccharomyces cerevisiae. *J Biol Chem* **273**(41): 26836-43.

Reid, C. B., I. Liang and C. Walsh (1995). Systematic widespread clonal organization in cerebral cortex. *Neuron* **15**(2): 299-310.

Richardson, J., A. Cvekl and G. Wistow (1995). Pax-6 is essential for lens-specific expression of zeta-crystallin. *Proc Natl Acad Sci U S A* **92**(10): 4676-80.

Ritz-Laser, B., A. Estreicher, N. Klages, S. Saule and J. Philippe (1999). Pax-6 and Cdx-2/3 interact to activate glucagon gene expression on the G1 control element. *J Biol Chem* **274**(7): 4124-32.

Rubenstein, J. L. and P. A. Beachy (1998). Patterning of the embryonic forebrain. *Curr Opin Neurobiol* **8**(1): 18-26.

Rubenstein, J. L., K. Shimamura, S. Martinez and L. Puelles (1998). Regionalization of the prosencephalic neural plate. *Annu Rev Neurosci* **21**: 445-77.

Sakai, M., M. S. Serria, H. Ikeda, K. Yoshida, J. Imaki and S. Nishi (2001). Regulation of c-maf gene expression by Pax6 in cultured cells. *Nucleic Acids Res* **29**(5): 1228-37.

Scardigli, R., C. Schuurmans, G. Gradwohl and F. Guillemot (2001). Crossregulation between Neurogenin2 and Pathways Specifying Neuronal Identity in the Spinal Cord. *Neuron* **31**(2): 203-17.

Schedl, A., B. Grimes and L. Montoliu (1996). YAC Protocols. Totowa, NJ, Humana Press Inc.

Schedl, A., A. Ross, M. Lee, D. Engelkamp, P. Rashbass, V. van Heyningen and N. D. Hastie (1996). Influence of PAX6 gene dosage on development: overexpression causes severe eye abnormalities. *Cell* **86**(1): 71-82.

Schlaggar, B. L. and D. D. O'Leary (1991). Potential of visual cortex to develop an array of functional units unique to somatosensory cortex. *Science* **252**(5012): 1556-60.

Schmahl, W., M. Knoedlseder, J. Favor and D. Davidson (1993). Defects of neuronal migration and the pathogenesis of cortical malformations are associated with Small eye (Sey) in the mouse, a point mutation at the Pax-6-locus. *Acta Neuropathol (Berl)* **86**(2): 126-35.

Schultz, P. G. and P. B. Dervan (1983). Sequence-specific double-strand cleavage of DNA by penta-N-methylpyrrolecarboxamide-EDTA X Fe(II). *Proc Natl Acad Sci U S A* **80**(22): 6834-7.

Schuurmans, C. and F. Guillemot (2002). Molecular mechanisms underlying cell fate specification in the developing telencephalon. *Curr Opin Neurobiol* **12**(1): 26-34.

Sharp, P. A., B. Sugden and J. Sambrook (1973). Detection of two restriction endonuclease activities in Haemophilus parainfluenzae using analytical agarose--ethidium bromide electrophoresis. *Biochemistry* **12**(16): 3055-63.

Shimamura, K., D. J. Hartigan, S. Martinez, L. Puelles and J. L. Rubenstein (1995). Longitudinal organization of the anterior neural plate and neural tube. *Development* **121**(12): 3923-33.

Shimamura, K. and J. L. Rubenstein (1997). Inductive interactions direct early regionalization of the mouse forebrain. *Development* **124**(14): 2709-18.

Sidman, R. L., I. L. Miale and N. Feder (1959). Cell proliferation and migration in the primitive ependymal zone: an autoradiographic study of histogenesis in the nervous system. *Exp Neurol* **1**: 322-333.

Simpson, T. I. and D. J. Price (2002). Pax6; a pleiotropic player in development. *Bioessays* **24**(11): 1041-51.

Singh, S., R. Mishra, N. A. Arango, J. M. Deng, R. R. Behringer and G. F. Saunders (2002). Iris hypoplasia in mice that lack the alternatively spliced Pax6(5a) isoform. *Proc Natl Acad Sci U S A* **99**(10): 6812-5.

Sivak, J. M., J. A. West-Mays, A. Yee, T. Williams and M. E. Fini (2004). Transcription Factors Pax6 and AP-2alpha Interact To Coordinate Corneal Epithelial Repair by Controlling Expression of Matrix Metalloproteinase Gelatinase B. *Mol Cell Biol* **24**(1): 245-57.

Smith, C., S. Klco and C. Cantor (1988). Genome Analysis: A Practical Approach. Oxford, IRL Press.

Soderholm, J., B. J. Bevis and B. S. Glick (2001). Vector for pop-in/pop-out gene replacement in Pichia pastoris. *Biotechniques* **31**(2): 306-10, 312.

Spencer, F., Y. Hugerat, G. Simchen, O. Hurko, C. Connelly and P. Hieter (1994). Yeast kar1 mutants provide an effective method for YAC transfer to new hosts. *Genomics* **22**(1): 118-26.

Stables, J., A. Green, F. Marshall, N. Fraser, E. Knight, M. Sautel, G. Milligan, M. Lee and S. Rees (1997). A bioluminescent assay for agonist activity at potentially any G-protein-coupled receptor. *Anal Biochem* **252**(1): 115-26.

Stanfield, B. B. and D. D. O'Leary (1985). Fetal occipital cortical neurones transplanted to the rostral cortex can extend and maintain a pyramidal tract axon. *Nature* **313**(5998): 135-7.

St-Onge, L., B. Sosa-Pineda, K. Chowdhury, A. Mansouri and P. Gruss (1997). Pax6 is required for differentiation of glucagon-producing alpha-cells in mouse pancreas. *Nature* **387**: 406-409.

Storm, E. E., J. L. Rubenstein and G. R. Martin (2003). Dosage of Fgf8 determines whether cell survival is positively or negatively regulated in the developing forebrain. *Proc Natl Acad Sci U S A* **100**(4): 1757-62.

Stoykova, A., R. Fritsch, C. Walther and P. Gruss (1996). Forebrain patterning defects in Small eye mutant mice. *Development* **122**(11): 3453-65.

Stoykova, A., M. Gotz, P. Gruss and J. Price (1997). Pax6-dependent regulation of adhesive patterning, R-cadherin expression and boundary formation in developing forebrain. *Development* **124**(19): 3765-77.

Stoykova, A. and P. Gruss (1994). Roles of Pax-genes in developing and adult brain as suggested by expression patterns. *J Neurosci* **14**(3 Pt 2): 1395-412.

Stoykova, A., D. Treichel, M. Hallonet and P. Gruss (2000). Pax6 modulates the dorsoventral patterning of the mammalian telencephalon. *J Neurosci* **20**(21): 8042-50.

Strong, S. J., Y. Ohta, G. W. Litman and C. T. Amemiya (1997). Marked improvement of PAC and BAC cloning is achieved using electroelution of pulsed-field gel-separated partial digests of genomic DNA. *Nucleic Acids Res* **25**(19): 3959-61.

Sussel, L., O. Marin, S. Kimura and J. L. Rubenstein (1999). Loss of Nkx2.1 homeobox gene function results in a ventral to dorsal molecular respecification within the basal telencephalon: evidence for a transformation of the pallidum into the striatum. *Development* **126**(15): 3359-70.

Szucsik, J. C., D. P. Witte, H. Li, S. K. Pixley, K. M. Small and S. S. Potter (1997). Altered forebrain and hindbrain development in mice mutant for the Gsh-2 homeobox gene. *Dev Biol* **191**(2): 230-42.

Takahashi, M. and N. Osumi (2002). Pax6 regulates specification of ventral neurone subtypes in the hindbrain by establishing progenitor domains. *Development* **129**(6): 1327-38.

Tan, S. S., M. Kalloniatis, K. Sturm, P. P. Tam, B. E. Reese and B. Faulkner-Jones (1998). Separate progenitors for radial and tangential cell dispersion during development of the cerebral neocortex. *Neuron* **21**(2): 295-304.

Tao, W. and E. Lai (1992). Telencephalon-restricted expression of BF-1, a new member of the HNF-3/fork head gene family, in the developing rat brain. *Neuron* **8**(5): 957-66.

Theil, T., G. Alvarez-Bolado, A. Walter and U. Ruther (1999). Gli3 is required for Emx gene expression during dorsal telencephalon development. *Development* **126**(16): 3561-71.

Ton, C. C., H. Miwa and G. F. Saunders (1992). Small eye (Sey): cloning and characterization of the murine homolog of the human aniridia gene. *Genomics* **13**(2): 251-6.

Toresson, H. and K. Campbell (2001). A role for Gsh1 in the developing striatum and olfactory bulb of Gsh2 mutant mice. *Development* **128**(23): 4769-80.

Toresson, H., S. S. Potter and K. Campbell (2000). Genetic control of dorsal-ventral identity in the telencephalon: opposing roles for Pax6 and Gsh2. *Development* **127**(20): 4361-71.

Tyas, D. A., T. Pratt, T. I. Simpson, J. O. Mason and D. J. Price (2003). Identifying GFP-transgenic animals by flashlight. *Biotechniques* **34**(3): 474-6.

Vagner, S., B. Galy and S. Pyronnet (2001). Irresistible IRES. Attracting the translation machinery to internal ribosome entry sites. *EMBO Rep* **2**(10): 893-8.

Valerius, M. T., H. Li, J. L. Stock, M. Weinstein, S. Kaur, G. Singh and S. S. Potter (1995). Gsh-1: a novel murine homeobox gene expressed in the central nervous system. *Dev Dyn* **203**(3): 337-51.

Van Heyningen, V. and K. A. Williamson (2002). PAX6 in sensory development. *Hum Mol Genet* **11**(10): 1161-7.

van Raamsdonk, C. D. and S. M. Tilghman (2000). Dosage requirement and allelic expression of PAX6 during lens placode formation. *Development* **127**(24): 5439-48.

Vitalis, T., O. Cases, D. Engelkamp, C. Verney and D. Price (2000). Defects of Tyrosine Hydroxylase-Immunoreactive Neurons in the Brains of Mice Lacking the Transcription Factor Pax6. *J Neuroscience* **20**(17): 6501-6516.

Vollrath, D., R. W. Davis, C. Connelly and P. Hieter (1988). Physical mapping of large DNA by chromosome fragmentation. *Proc Natl Acad Sci U S A* **85**(16): 6027-31.

Walther, C. and P. Gruss (1991). Pax-6, a murine paired box gene, is expressed in the developing CNS. *Development* **113**(4): 1435-49.

Warren, N., D. Caric, T. Pratt, J. Clausen, P. Asavaritikrai, J. Mason, R. Hill and D. Price (1999). The Transcription Factor, PAx6, is required for Cell Proliferation and Differentiation in the Developing Cerebral Cortex. *Cerebral Cortex* **9**: 627-635.

Warren, N. and D. Price (1997). Roles of Pax-6 in murine diencephalic development. *Development* **124**: 1573-1582.

Williams, S. C., C. R. Altmann, R. L. Chow, A. Hemmati-Brivanlou and R. A. Lang (1998). A highly conserved lens transcriptional control element from the Pax-6 gene. *Mech Dev* **73**(2): 225-9.

Wilson, D. S., G. Sheng, S. Jun and C. Desplan (1996). Conservation and diversification in homeodomain-DNA interactions: a comparative genetic analysis. *Proc Natl Acad Sci U S A* **93**(14): 6886-91.

Xu, H. E., M. A. Rould, W. Xu, J. A. Epstein, R. L. Maas and C. O. Pabo (1999). Crystal structure of the human Pax6 paired domain-DNA complex reveals

specific roles for the linker region and carboxy-terminal subdomain in DNA binding. *Genes Dev* **13**(10): 1263-75.

Xu, P. X., X. Zhang, S. Heaney, A. Yoon, A. M. Michelson and R. L. Maas (1999). Regulation of Pax6 expression is conserved between mice and flies. *Development* **126**(2): 383-95.

Xu, Z. P. and G. F. Saunders (1997). Transcriptional regulation of the human PAX6 gene promoter. *J Biol Chem* **272**(6): 3430-6.

Xu, Z. P. and G. F. Saunders (1998). PAX6 intronic sequence targets expression to the spinal cord. *Dev Genet* **23**(4): 259-63.

Xuan, S., C. A. Baptista, G. Balas, W. Tao, V. C. Soares and E. Lai (1995). Winged helix transcription factor BF-1 is essential for the development of the cerebral hemispheres. *Neuron* **14**(6): 1141-52.

Yamada, T., M. Placzek, H. Tanaka, J. Dodd and T. M. Jessell (1991). Control of cell pattern in the developing nervous system: polarizing activity of the floor plate and notochord. *Cell* **64**(3): 635-47.

Yun, K., S. Potter and J. L. Rubenstein (2001). Gsh2 and Pax6 play complementary roles in dorsoventral patterning of the mammalian telencephalon. *Development* **128**(2): 193-205.

Zaki, P. A., J. C. Quinn and D. J. Price (2003). Mouse models of telencephalic development. *Curr Opin Genet Dev* **13**(4): 423-37.

Zheng, J. B., Y. H. Zhou, T. Maity, W. S. Liao and G. F. Saunders (2001). Activation of the human PAX6 gene through the exon 1 enhancer by transcription factors SEF and Sp1. *Nucleic Acids Res* **29**(19): 4070-8.

Appendix A.

Molecular Biology Materials and Reagents.

General purpose molecular biology reagents were purchased from Sigma UK, Fisher UK, and Merck UK.

Agarose for gel electrophoresis

Seakem LE Agarose Cambrex Bioscience, UK)

Bacterial culture media and antibiotics

LB tablets (Sigma UK)

Ampicillin (Roche UK)

50mg/ml dissolved in ddH_2O and stored at -20°C. It was diluted 1000 fold to working concentration of 50µg/ml in LB or LB-agar.

Enzymes for molecular biology

DNA Restriction enzymes

These were purchased from New England Biolabs (US), Roche UK, and Amersham Pharmacia UK and used according to manufacturers guidelines.

DNA modifying enzymes

Cloned Pfu polymerase (Stratagene, La Jolla, CA, USA)

T4 DNA ligase (New England Biolabs)

Other enzymes

Proteinase K (Roche)

Molecular biology kits

Plasmid mini prep kit (Qiagen, UK)

Plasmid midi prep kit (Qiagen)

Qiaex II gel extraction system (Qiagen)

High Prime DNA labelling kit (Roche)

Oligonucleotides

The oligonucleotides were designed using PRIMER3 software (Whitehead Institute for Biomedical Research US) and purchased form MWG-biotech, Germany

Generation of pDT1

C2MAZFor	ACTGTCTAGAGGATCCCTTGGGGGAGGGGGA
C2MAZRev	ACGAGCTCACTAGTCAGCTCACTCCCCTGTTGA
neoFOR	CACCTCGAGATGGGATCGGCCATTG
neoREV	ATCACTAGTTCAGAAGAACTCGTCAAGAAGG
IRESkzFor	ACTGTCTAGAACTAGTGGGATCCGCCCCTCTC
IRESkzRev	AGATCTCGAGCATGGTTGTGGCCATATTATCA
PAX6_5F	AAAGCAGTGAGGCGAGG
PAX6_5R	CATGCTGGCTCTGGCTGG

PAX6_3F	GAATTCAGAACAGTAAGTGCCTCTGGTCTTTC
PAX6_3F	GAATTCCAGCGACAAACGCTCAGG
TauGFPfor	CATGGCTGAGCCCCGCC
TauGFPrev	TGCTCGAGGAGCTCTTATTTGTATAGTTCATCCATGCCATGT

Primers to check PAX6 5′ homology arm joins TauGFP correctly

FUSIONFOR	ACTTTGTTTCAAGCCCCAAA
FUSIONREV	CCCTGAGCATGATCTTCCAT

Sequencing primers for checking pDT1

DTA	TCAAATGGCTCTCCTCAAGC
DTB	ATACTTTCTCGGCAGGAGCA
DTC	CCTGAAACATAAAATGAATGCAA
DTD	TTGGCGGATAATGCCTTTAG
DTE	ATCTAATTCAACAAGAATTGGGACA
DTF	CGTATACATCATGGCCGACAAG
DTG	CAGACCCAGTAAACCGTGCT
DTH	AGTCACTCTCAGGGCAGCTC
DTI	CAGGTATTGTTAGCGGTTTGA
DTJ	CAAGCCCCAAAGGGTAGATT
DTK	TTCAGAGCCTGGTTCCTCAG
DTL	AGTCCCTTCCCGCTTCAG
DTM	CTCGCGCCAGCCGAAC
DTN	ACTGCACAGAACAAAAACCT

DTO	CAATGAAGCACACAAGTTT

Southern Probes

SouProbe2F	GCTTCCTGTGCCTAGAGGTG
SouProbe2R	AATTGCATCGTCACGACAAA

Primers to confirm pDT1 has integrated correctly in YAC

Targ1.1	TGTAATTGGGGGAAATGGAG
Targ2.1	CAAGGCCATTCCTGGTCTAC
Targ3.1	GTACAGAGCCTCGGGCTGA
Targ4.1	GGGCAAGCCCAACTTTTTAT

Genotyping Y1123 and Y374 transgenic mice

PAX6HumF	CCGTGTGCCTCAACCGTA
PAX6HumR	CACGGTTTACTGGGTCTGG
PAX6MouF	CGCAAATACACCTTTGCTCA
PAX6MouR	GAGGGTTTCCTGGATCTGG

Checking extent of integration of YACs Y1123 and Y374

3163F	AAGCCATTTTGTTGGTGAGC
3163R	TTCCAGTTATACAGGGGCTGA
3140F	AAGGTGCCCAGCCTAATTCT
3140R	TCGTCTCGATCTCCTGACCT
5003F	CAGAGGGAGGACCTCTCAGG

5003R	TTTGCCTTTAGGGCTCACTG
3207F	CAGGGGGTTTTGGCTTTTA
3207R	TCATACACATGCCCCAAGAA
3004F	CTTCCCTGGCTACCATGTCT
3004R	CGGCCCAGTGAATTAGAAAA
3080F	TGAAAATGCAAACAGGTTCC
3080R	AAGCCGTCAGACCACTTTTG
5083F	TGAGAGCTGTGCAGAGCAGA
5083R	GAAAGCAAAACCCTGGACAA
5405F	GCCATCTGAAAGCTGAGGAG
5405R	CCAGCCTACCTTGACATGCT
5395F	GACACGCTGGTCACCAAGTA
5395R	TTACAGCGGACCCCTCTTC

Checking the copy number of the integrated YACs Y1123 and Y374

Pax3F	AAGCAGCGCAGGAGCAGAACC
Pax3R	CCTCGGTAAGCTTCGCCCTCT

Mouse genomic DNA

Tail tip lysis buffer (TTLB): 200mM Tris pH 8, 200mM NaCl, 5mM EDTA, 0.2% SDS

Southern Blotting and hybridisation

^{32}P-α-dCTP for radiolabeled probe preparation was purchased from ICN (Ohio US)

Southern denaturing solution: 0.5M NaOH

Southern neutralising solution: 0.5M Tris, 3M NaCl, pH 7.0

20xSSC: 3M NaCl, 0.3M sodium citrate

Church Solution: 0.5M $NaP0_4$, 7% SDS, 1mM EDTA, 1% BSA, pH7.2

Church Wash: 40mM $NaP0_4$, 1% SDS, 1mM EDTA, pH7.2

Nylon membrane (positively charged) (Roche)

Yeast reagents

-AT drop out yeast medium

6.7 g	Yeast Nitrogen Base
50ml	40% glucose
43mg	arginine
69mg	aspartic acid
17mg	histidine
43mg	isoleucine
86mg	leucine
43mg	lysine
17mg	methionine
43mg	phenylalanine
86mg	threonine
43mg	tyrosine
17mg	uracil
120mg	valine

Make up to 1 litre, autoclave, and store protected from the light at 4°C.

Appendix B.

YAC purification and isolation protocols.

Protocol 1: Preparation of High Density Plugs Protocol A

(Protocol from Dr Andreas Schedl, Institute of Human Genetics, University of Newcastle upon Tyne)

1. 10ml of -AT drop out medium was inoculated with the frozen stock of the yeast colony containing the YAC and incubated at 30°C for 16 hours in a shaking incubator.
2. The 10ml starter culture was poured into 500ml of -AT drop out medium and incubated for 2-3 days at 30°C in a shaking incubator.
3. A 2.5ml solution of 1% Seaplaque GTG LMP agarose in SE buffer was prepared. SE buffer was 1M sorbitol, 20mM EDTA pH 8.0, 14mM β-mercapto-ethanol was added. The agarose solution was kept at 42°C until use. 2mg/ml Zymolyase was added immediately before use.
4. The yeast culture was centrifuged at 3000g for 5 min to pellet the cells. The supernatant was discarded and the pellet was resuspended in 50ml SE buffer. This was repeated 3 times.
5. After the last washing step, the supernatant was discarded and all liquid was carefully removed. The cell pellet was approximately 1 to 1.5 ml.
6. 200µl of SE buffer was added to the pellet and mixed.
7. The yeast cell suspension was heated to 37°C and added 50:50 to the LMP agarose and mixed by pipetting up and down using a blue cut off tip. The solution was kept at 42°C at all times to avoid setting of the agarose.

8. The plug moulds were prepared and placed on ice.
9. Using a cut off yellow tip pipette 100 µl aliquots of the mixture was added to the plug mould. The mixture was left for 30 mins to allow the agarose to set.
10. The plugs were transferred into SE buffer containing 14mM β-mercapto-ethanol and 1 mg/ml Zymolyase and incubated at 37°C for 4 to 6h.
11. The buffer was replaced with 0.2M EDTA, 0.1M Tris pH8.0, 0.5M NaCl, 1% SDS, 0.5M β-mercapto-ethanol and 1 mg/ml proteinase K using 0.5 ml/ plug and incubated at 37°C overnight.
12. The following day the plugs were washed extensively in TE pH8.0 until no more bubbles (from the SDS solution) could be seen. The plugs were stored in 0.5 M EDTA at 4^{o}C until needed.

Protocol 2: Preparation of YAC DNA for Pronuclear Injection Protocol (4% Concentrator Gel Method)

(Protocol from Dr Andreas Schedl, Institute of Human Genetics, University of Newcastle upon Tyne)

1. A 1% agarose gel made in 0.5xTAE was poured with a long continuous slot for a well.
2. The agarose plugs were loaded end-to-end in the well. Any trapped air bubbles were released using a pipette tip.
3. The plugs were covered with 1% agarose made in 0.5% TAE.
4. Once the agarose had solidified the PFG was run. The optimal settings were worked out by trial and error to separate the YAC from the endogenous chromosomes. For the 426 kb Y1123 and Y374 YACs, the running buffer was 0.5% TAE, kept at 4°C, running at 200 V, with an initial pulse of 23 seconds and a final pulse of 40 seconds. The gel was run for 24 hours.
5. Once the gel had finished. A small amount of the two edges of the gel were removed and stained with 50µl of 10mg/ml Ethidium Bromide for 30 minutes with very gentle agitation at room temperature.
6. Under UV light the precise location of the YAC chromosomal, upper, and lower chromosome bands were marked with a blade.
7. The PFG was reassembled using the marks to identify the location of the YAC, upper, and lower chromosomes. Three agarose slices containing the three chromosomes were excised using a clean glass cover slip as a blade.

8. The isolated gel slices containing the YAC, the upper and lower chromosomes were turned through 90° and a 4% low melting point agarose gel cast around them.
9. This concentrating gel was run overnight at 30 V in 0.5% TAE at 4°C with the buffer re-circulated.
10. The gel was then cut into three longitudinal sections and the upper and lower chromosomes stained with EtBr.
11. Visualisation with UV light showed the location of the compacted bands of the upper and lower chromosomes.
12. Using these as markers the location of the compacted YAC DNA was identified and the band excised.
13. The agarose slice was equilibrated in the following buffer for 2 hours at 4°C (10mM Tris-HCl pH7.5, 1mM EDTA, 100mM NaCl, 30µM spermine, 70µM spermidine).
14. The buffer was removed and the gel slice weighed.
15. The slice was melted at 68°C for 5 minutes.
16. Then the gel slice was placed at 40°C for 5 minutes.
17. 2U agarase (NEB) per 100mg of agarose slice was added.
18. The gel slice was incubated at 40°C for 3 hours.
19. The tube containing the digested agarose was placed at 4°C for several hours. If the slice was not completely digested it was re-melted.
20. A Petri dish with 40 ml of Microinjection Buffer (10mM Tris-HCl pH7.5, 0.1mM EDTA, 100mM NaCl, 30µM spermine, 70µM spermidine) was prepared.

21. The YAC DNA solution was carefully pipetted into the centre of the filter by transferring with a yellow cut off tip.
22. The solution was dialyzed for 1 hour at 4°C.
23. The YAC DNA solution was removed with a cut off yellow tip and stored at 4°C.
24. The integrity of the YAC DNA was verified by running an aliquot of the DNA on a PFG alongside a yeast plug.

Protocol 3: Preparation of High Density Plugs Protocol B

(Protocol from Dr Simon Fisher, Oxford University)

1. 10ml of -AT drop out medium was inoculated with the frozen stock of the yeast colony containing the YAC and incubated at 30°C for 16 hours in a shaking incubator.
2. The 10ml starter culture was poured into 500ml of -AT drop out medium and incubated for 2-3 days at 30°C in a shaking incubator.
3. A 1.2% Seaplaque GTG LMP agarose solution was prepared in buffer containing (1M sorbitol, 20mM EDTA, 14.4mM β-mercaptoethanol) and kept at 42°C until used.
4. The culture was centrifuged at 3000g for 5 min to pellet the cells. The supernatant was discarded and the pellet was resuspend in 20ml of 50mM EDTA pH8.0.
5. The cells were centrifuged again at 3000g for 5 min to pellet the cells and the supernatant was discarded.
6. The cells were resuspended in 2ml buffer (1M sorbitol, 20mM EDTA, 14.4mM β-mercaptoethanol, 2mg/ml Zymolyase).
7. The plug moulds were prepared and placed on ice.
8. The cell suspension solution was mixed 50:50 with the LMP agarose solution.
9. This solution was transferred into the plug moulds and left on ice to allow the agarose to set.

10. The plugs were transferred into a buffer containing (1M sorbitol, 20mM EDTA, 14.4mM β-mercaptoethanol, 10mM Tris-Cl pH7.5, 2mg/ml Zymolyase) and incubated at 37°C for 2h with gentle shaking.
11. The solution was replaced with 25ml of the buffer (100mM EDTA, 10mM Tris-Cl pH8.0, 1% lithium dodecyl sulphate) and incubated at 37°C for 30-60mins.
12. The solution was replaced with 25ml of fresh buffer (100mM EDTA, 10mM Tris-Cl pH8.0, 1% lithium dodecyl sulphate) and incubated at 37°C overnight.
13. The next day the solution was replaced with 25ml of the buffer (100mM EDTA, 10mM Tris-Cl pH8.0, 1% lithium dodecyl sulphate) and stored at room temperature until needed.

Protocol 4: Preparation of High Density Plugs Protocol C

(Protocol from Dr Clare Huxley, Imperial College School of Medicine)

1. 10ml of -AT drop out medium was inoculated with the frozen stock of the yeast colony containing the YAC and incubated at 30°C for 16 hours in a shaking incubator.
2. The 10ml starter culture was poured into 500ml of -AT drop out medium and incubated for 2-3 days at 30°C in a shaking incubator.
3. The culture was centrifuged at 1000 g for 5 minutes and the supernatant discarded.
4. The cells were resuspended in 40 ml of 50 mM EDTA.
5. The cells were then again centrifuged at 1000 g for 5 minutes and the supernatant discarded.
6. The pellet was resuspended in 100 ml of 1M sorbitol, 20 mM EDTA pH 8.0, 4 mM β-mercaptoethanol.
7. The cells were centrifuged at 1000 g for 5 minutes and all the supernatant carefully discarded.
8. Enzyme solution (1M sorbitol, 20 mM EDTA pH 8.0, 4 mM β-mercaptoethanol, 2 mg/ml Zymolyase) was added. This was mixed well and warmed briefly to 40°C.
9. Agarose Solution (2% SeaPlaque GTG LMP agarose in 1M sorbitol, 20 mM EDTA pH 8.0 was prepared. 14mM β-mercaptoethanol was added to the agarose solution once it was melted.

10. The molten agarose solution was added to the yeast cell solution at a ratio of 40:60 and mixed.
11. The solution was poured into the pre-chilled plug mould.
12. The plugs were allowed to set for 1 hour on ice.
13. The plugs were transferred to 50ml 1 M sorbitol, 20 mM EDTA pH 8.0, 10 mM Tris pH 7.5, 14 mM β-mercaptoethanol, 2 mg/ml Zymolyase and incubated at 37°C for 2 hours with agitation.
14. The solution was replaced with 50ml 1% lithium dodecyl sulphate, 100 mM EDTA pH 8.0, 10 mM Tris pH 8.0 and incubated at 37°C for 1 hour with agitation.
15. The solution was replaced with 1% lithium dodecyl sulphate, 100 mM EDTA pH 8.0, 10 mM Tris pH 8.0 and incubated at 37°C overnight with agitation.
16. The next day the solution was replace with fresh 1% lithium dodecyl sulphate, 100 mM EDTA pH 8.0, 10 mM Tris pH 8.0for several hours, and incubated at 37°C with agitation.
17. The plugs were washed in 50 ml of NDS solution (100mM EDTA, 1.7mM Tris-Base, 68mM N-laurylsarcosine (Sigma), pH 8.0) for 2 hrs at room temperature with agitation.
18. This wash was repeated three times.
19. The plugs were stored at 4°C in NDS solution. Prior to use the plugs were washed in 1x for several hours.

Protocol 5: Preparation of YAC DNA for Pronuclear Injection (Spin Column method)

Dr Lluís Montoliu (Campus de la Universidad Autónoma de Madrid, Spain)

Part I: Preparation of high density plugs

1. 10ml of -AT drop out medium was inoculated with the frozen stock of the yeast colony containing the YAC and incubated at 30°C for 16 hours in a shaking incubator.
2. The 10ml starter culture was poured into 500ml of -AT drop out medium and incubated for 2-3 days at 30°C in a shaking incubator.
3. The culture was centrifuged at 600 g for 5 minutes and the supernatant discarded.
4. The cells were resuspended in 50 mM EDTA.
5. The cells were then again centrifuged at 600 g for 5 minutes and the supernatant discarded. The pellet was resuspended again in 10 ml 50 mM of EDTA.
6. The culture was centrifuged at 600 g for 5 minutes and the supernatant discarded.
7. The pellet was warmed briefly to 37°C and enough prewarmed enzyme solution (1M sorbitol, 20mM EDTA pH 8.0, 14 mM β-mercaptoethanol, 2 mg/ml Zymolyase) added to give a final concentration of $8x10^9$ yeast cells/ ml. The cells were carefully resuspended.

8. An equal volume of agarose solution (1M sorbitol, 20mM EDTA pH 8.0, 2% SeaPlaque GTG LMP agarose, 14mM β-mercaptoethanol) was added to give a 50:50 ratio.
9. The solution was poured into prechilled plug moulds and allowed to set on ice.
10. The plugs were transferred to wash solution (1M sorbitol, 20mM EDTA pH 8.0, 10 mM Tris-HCl, 14mM β-mercaptoethanol, 2 mg/ml Zymolyase and incubated at 37°C for 2-3 hours with gentle agitation.
11. The solution was carefully poured off and 50ml 1% dodecyl lithium sulphate, 100 mM EDTA pH 8.0, 10 mM Tris-HCl pH 8.0 added. The plugs were incubated at 37°C with gentle agitation for at least 1 hour.
12. The buffer was poured off and replaced with fresh buffer and incubated overnight at 37°C with gentle agitation.
13. The plugs were washed in 50 ml of NDS solution (100mM EDTA, 1.7mM Tris-Base, 68mM N-laurylsarcosine (Sigma), pH 8.0) for 2 hrs at room temperature with agitation.
14. This wash was repeated three times.
15. The plugs were stored at 4°C in NDS solution. Prior to use the plugs were washed in 1xTAE for several hours.

Part II: Purification of YAC DNA for microinjection

16. A 1% SeaPlaque GTG (FMC) LMP PFGE gel was poured with a long continuous slot for a well.

17. Six plugs were loaded end-to-end in the well. Any trapped air bubbles were released using a pipette tip.
18. The plugs were covered with 1% SeaPlaque GTG LMP agarose made in 1% TAE.
19. Once the agarose had solidified the PFG was run. The optimal settings were worked out by trial and error to separate the YAC from the endogenous chromosomes. For the 426 kb Y1123 or Y374, the running buffer was 1% TAE, 4°C, running at 200 V, with an initial pulse of 23 seconds and a final pulse of 40 seconds. The gel was run for 26 hours.
20. Once the gel had finished, a small amount of the two edges of the gel were removed and stained with 50µl of 10mg/ml Ethidium Bromide for 30 minutes with very gentle agitation at room temperature.
21. Under UV light the precise location of the YAC chromosomal band was marked with a blade.
22. The PFG was reassembled using the marks to identify the location of the YAC chromosome. The YAC containing agarose slice was excised using a clean glass cover slip as a blade.
23. The agarose slice was equilibrated in the following buffer for a minimum of 2 hours at 4°C: (10 m Bis-Tris-HCl pH 6.5, 0.1 mM EDTA, 100 mM NaCl 30µM Spermine, 70 µM Spermidine).
24. The buffer was removed and the gel slice weighed.
25. The slice was melted at 65°C for 10 minutes.
26. 1U agarase (NEB) per 100mg of agarose slice was added.

27. The gel slice was incubated at 40°C for 2 to 3 hours.
28. The tube was then centrifuged at 15,000g for 20 minutes to get rid of undigested agarose bits.
29. 400 µl of the digested agarose with YAC DNA was carefully pipetted into the upper reservoir of a Millipore ultrafiltration Unit (Millipore).
30. The column was centrifuged for two min at 3000g.
31. The centrifugation was repeated until 300-320 µl had passed through the membrane.
32. The tube was left to stand at 4°C overnight.
33. Some of the YAC DNA was possibly still attached to the surface of the membrane so it was removed by pipetting up and down with a cut-off yellow tip once or twice very carefully. Then the entire solution was removed.
34. A Petri dish with 40 ml of Microinjection Buffer (10 mM Tris-HCl pH 7.5, 0.1 mM EDTA pH 8.0, 100 mM NaCl, 30µM Spermine, 70µM Spermidine) was prepared.
35. A Millipore dialysis filter (Millipore) with a pore size of 0.05µm was floated on the surface of the buffer.
36. The YAC DNA solution was carefully pipetted into the centre of the filter by transferring with a yellow cut off tip.
37. The solution was dialyzed for two to three hours at 4°C.
38. The YAC DNA solution was removed with a cut off yellow tip and stored at 4°C.
39. The integrity of the YAC DNA was verified by running an aliquot of the DNA on a PFG alongside a yeast plug.

Protocol 6: Isolation of YAC DNA for Pronuclear Injection

(Protocol from Dr Clare Huxley, Imperial College School of Medicine, UK)

1. Agarose plugs were prepared as described previously, see Protocol 4: Preparation of High Density Plugs Protocol C.
2. Six agarose plugs were equilibrated in 1xTBE for several hours before use.
3. A 1% SeaPlaque GTG (FMC) LMP PFGE agarose gel made in 1xTBE was poured with a long continuous slot for a well.
4. The six equilibrated plugs were loaded end-to-end in the well. Any trapped air bubbles were released using a pipette tip.
5. The plugs were covered with 1% SeaPlaque GTG LMP agarose made in 1% TBE.
6. Once the agarose had solidified the PFG was run. The optimal settings were worked out by trial and error to separate the YAC from the endogenous chromosomes. For the 426 kb Y1123, the running buffer was 1% TBE, kept at 4°C, running at 200 V, with an initial pulse of 23 seconds and a final pulse of 40 seconds. The gel was run for 48 hours.
7. Once the gel had finished, a small amount of the two edges of the gel were removed and stained with 50µl of 10mg/ml Ethidium Bromide for 30 minutes with very gentle agitation at room temperature.
8. Under UV light the precise location of the YAC chromosomal band was marked with a blade.

9. The PFG was reassembled using the marks to identify the location of the YAC chromosome. The YAC containing agarose slice was excised using a clean glass cover slip as a blade.
10. The agarose slice was equilibrated in the following buffer overnight at 4°C: 10 mM Bis-Tris-HCl pH 6.5, 0.2 mM EDTA, 100 mM NaCl made up in embryo quality water (Sigma).
11. The buffer was removed and the gel slice weighed.
12. The slice was melted at 68°C for 10 minutes.
13. Then the gel slice was placed at 40°C for 5 minutes.
14. 1U agarase (NEB) per 100mg of agarose slice was added.
15. The gel slice was incubated at 40°C for 2 hours.
16. The tube was then centrifuged at 6225g for 20 minutes to get rid of undigested agarose bits.
17. 400 µl of embryo quality water was pipetted into the upper reservoir of a Millipore Ultrafree-MC 30,000 NMWL Filter Unit (Millipore).
18. The column was centrifuged for five minutes at 3000g and the water discarded. This was to prepare the column.
19. 400 µl of the digested agarose with YAC DNA was carefully pipetted into the upper reservoir of the column and centrifuged for five minutes at 3000g.
20. The centrifugation was repeated until approximately 300 µl had passed through the membrane.
21. The tube was left to stand at 4°C overnight.

22. Some of the YAC DNA was possibly still attached to the surface of the membrane so it was removed by pipetting up and down with a cut-off yellow tip once or twice very carefully. Then the entire solution was removed.
23. A Petri dish with 40 ml of Microinjection Buffer (10 mM Tris-HCl pH 7.5, 0.2 mM EDTA pH 8.0, 100 mM NaCl) was prepared.
24. A Millipore dialysis filter (Millipore) with a pore size of 0.05µm was floated on the surface of the buffer and left to equilibrate for several hours at 4°C.
25. The filters were carefully transferred to fresh microinjection buffer.
26. The YAC DNA solution was carefully pipetted into the centre of the filter by transferring with a yellow cut off tip.
27. The solution was dialyzed overnight at 4°C.
28. The YAC DNA solution was removed with a cut off yellow tip and stored at 4°C.

The integrity of the YAC DNA was verified by running an aliquot of the DNA on a PFG alongside a yeast plug.

Appendix C

Modified Lithium Acetate Yeast Transformation

(Modified from Elble R (1992) *Biotechniques* 13(1):18-20)

1. The culture is grown in yeast selective media at 30°C overnight.

2. The overnight culture was spun down, using 1ml of cells for each transformation.

3. The supernatant was poured away, leaving cells and 40-100µl of liquid.

4. 2µl of 10mg/ml carrier DNA (Salmon sperm) was added. The cells were then resuspended with the pipette tip.

5. 1µg of the plasmid was added (pDT1).

6. The solution was vortexd briefly.

7. 0.5 ml of PLATE mixture was added

8. The solution was then vortexed again briefly

9. 20µl of 1.0M DTT was added.

10. The solution was then vortexed briefly.

11. The solution was then incubated at room temperature overnight. (The number of transformants increases linearly over time; where 24 hours gives 4-fold more than 6 hours. In practice 2 hours is sufficient.)

12. The cells were then heat shocked for 10 min at 42°C.

13. 50-100µl of the cells in PLATE mixture were removed.

14. The cells were then plated (50µl and 5µl aliquots, using a drop of sterile ddH_20 if necessary) on selective media and incubated at 30°C overnight.

Appendix D

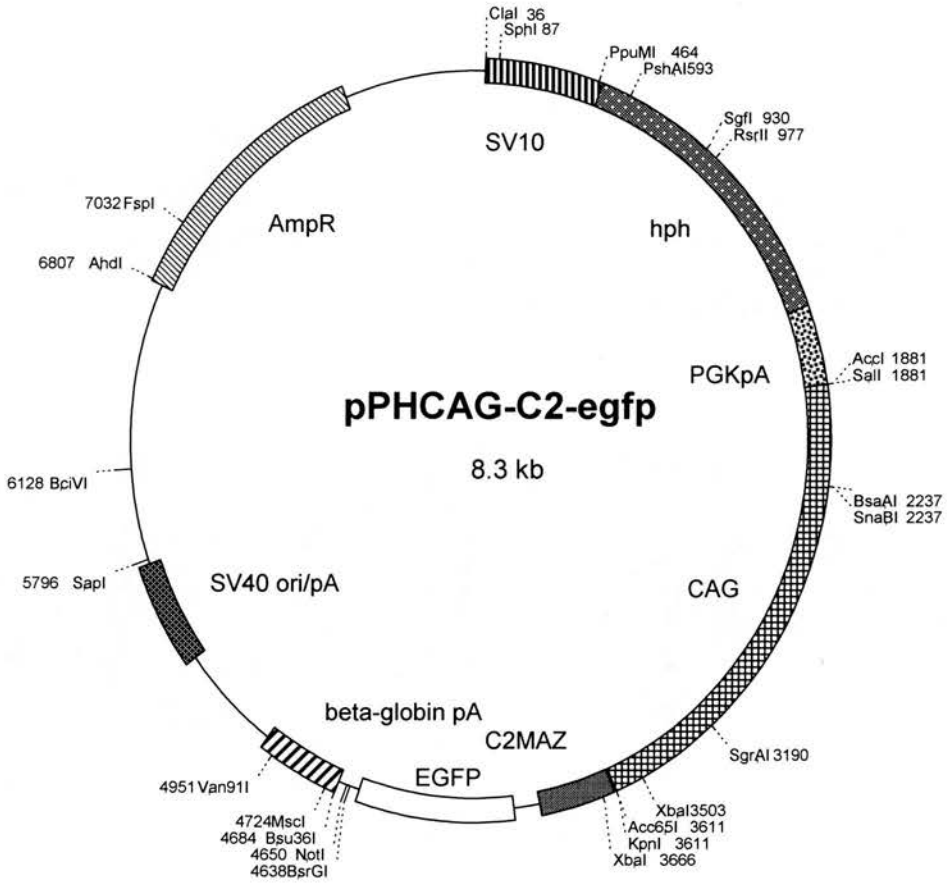
ClaI 36
SphI 87
PpuMI 464
PshAI593
SgfI 930
RsrII 977
SV10
hph
PGKpA
AccI 1881
SalI 1881
BsaAI 2237
SnaBI 2237
CAG
SgrAI 3190
XbaI3503
Acc65I 3611
KpnI 3611
XbaI 3666
C2MAZ
EGFP
beta-globin pA
4724MscI
4684 Bsu36I
4650 NotI
4638BsrGI
4951 Van91I
SV40 ori/pA
5796 SapI
6128 BciVI
AmpR
6807 AhdI
7032 FspI
pPHCAG-C2-egfp
8.3 kb

Appendix E

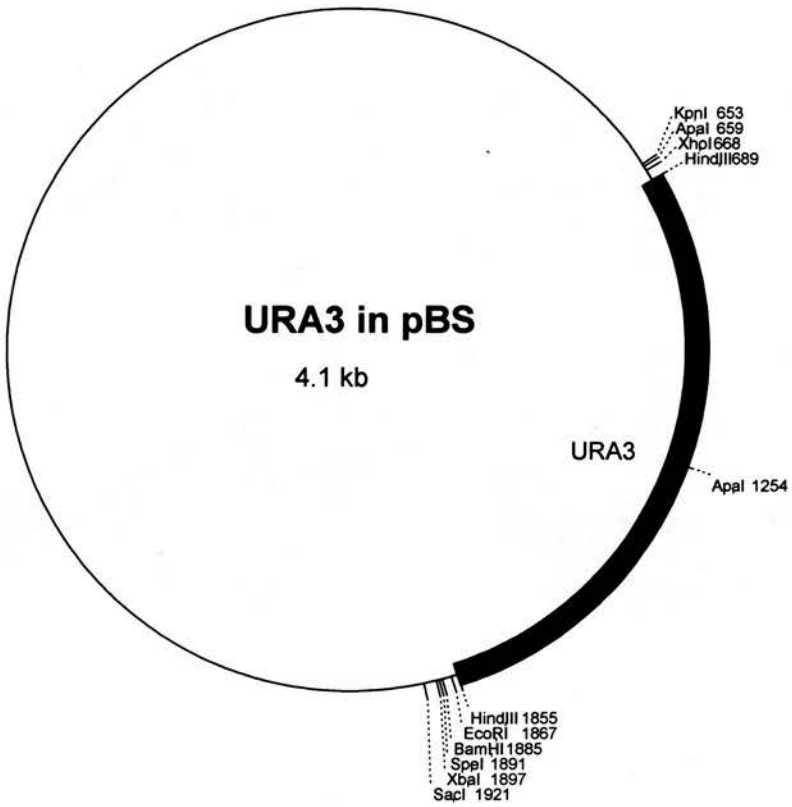
URA3 in pBS
4.1 kb
URA3
KpnI 653
ApaI 659
XhoI668
HindIII689
ApaI 1254
HindIII 1855
EcoRI 1867
BamHI 1885
SpeI 1891
XbaI 1897
SacI 1921

Appendix F

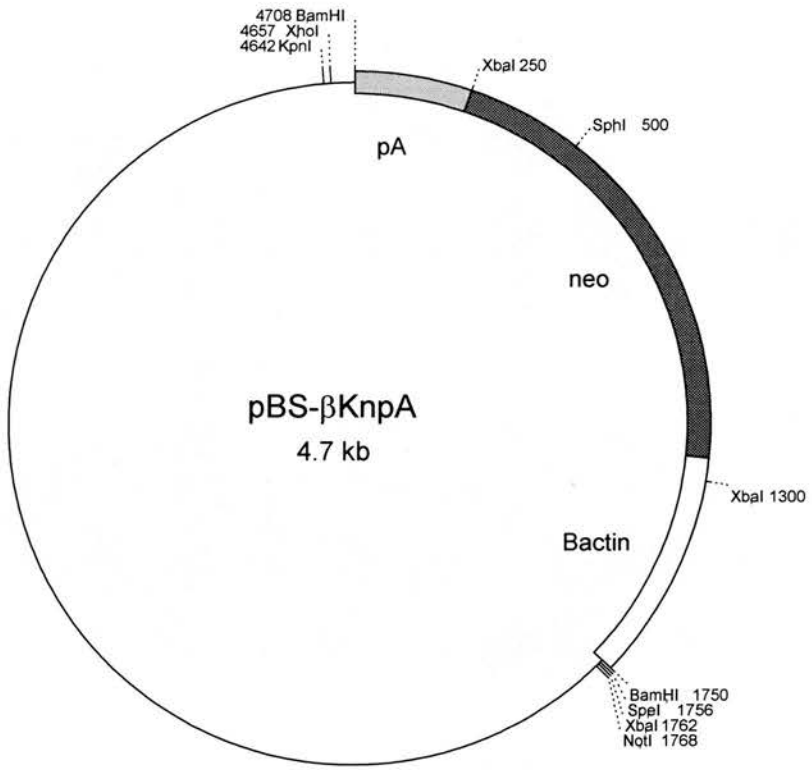
4708 BamHI
4657 XhoI
4642 KpnI
XbaI 250
SphI 500
pA
neo
pBS-βKnpA
4.7 kb
XbaI 1300
Bactin
BamHI 1750
SpeI 1756
XbaI 1762
NotI 1768

Appendix G

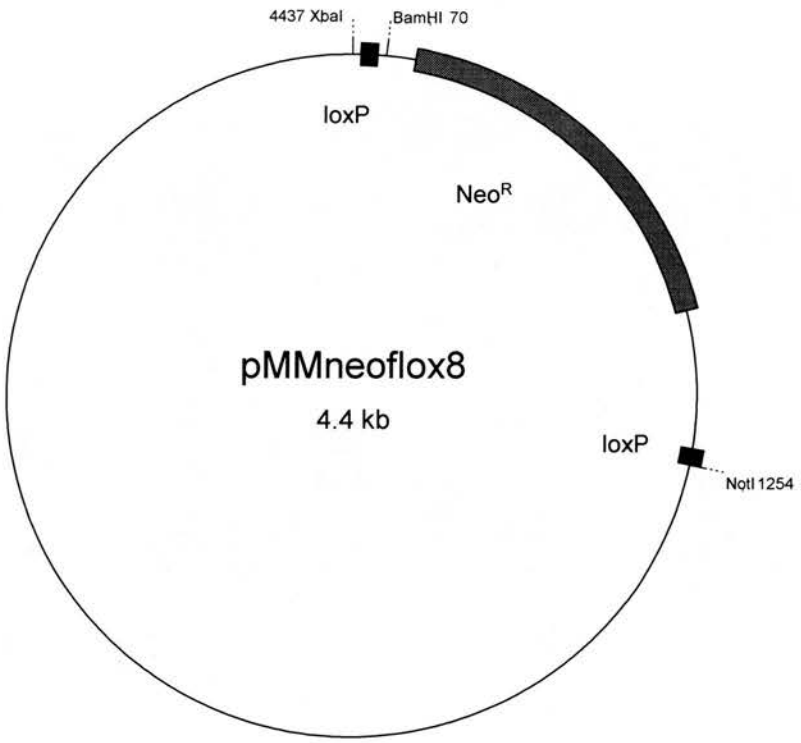
4437 XbaI
BamHI 70
loxP
Neo^R
pMMneoflox8
4.4 kb
loxP
NotI 1254

Appendix H

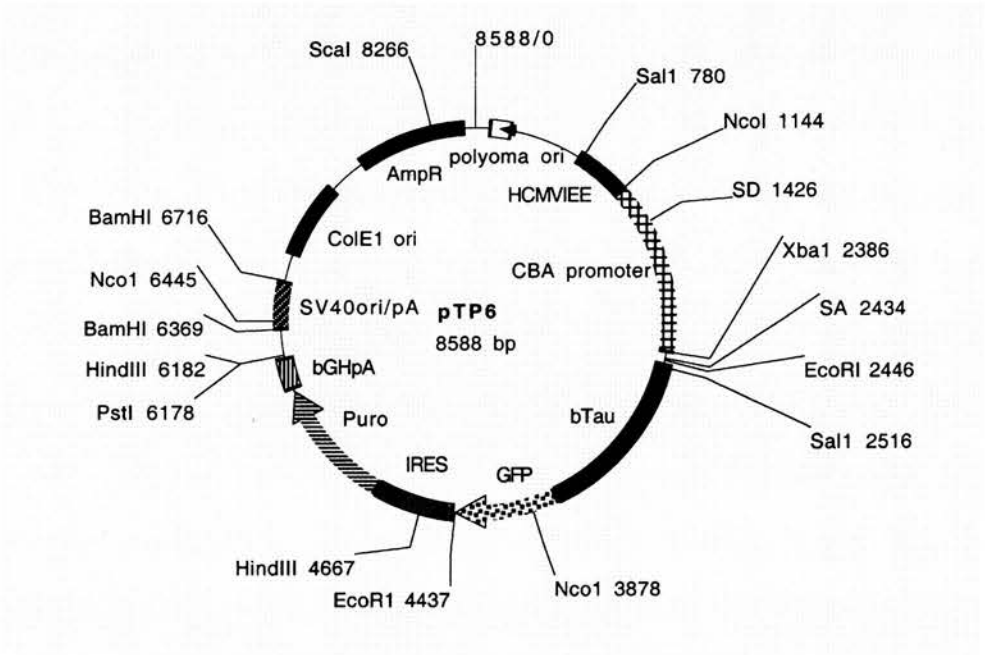
ScaI 8266
8588/0
SalI 780
NcoI 1144
polyoma ori
AmpR
HCMVIEE
SD 1426
BamHI 6716
ColE1 ori
Xba1 2386
CBA promoter
Nco1 6445
SV40ori/pA
pTP6
8588 bp
SA 2434
BamHI 6369
HindIII 6182
bGHpA
EcoRI 2446
PstI 6178
Puro
bTau
SalI 2516
IRES
GFP
HindIII 4667
EcoR1 4437
Nco1 3878

Identifying GFP-Transgenic Animals by Flashlight

BioTechniques 34:474-476 (March 2003)

In recent years, GFP has proven to be a valuable tool in many biological systems. Wild-type GFP has a major absorption in the UV region at 398 nm and a minor absorption in the blue region at 475 nm (3). Recently, several groups have independently carried out amino acid modifications of the GFP protein and have optimized these optical characteristics (6). For a comprehensive review on the photophysical behavior of GFP and GFP mutants, see Reference 7. Two widely used mutant forms of GFP, eGFP (BD Biosciences Clontech, Palo Alto, CA, USA) and mmGFP6 (6), have greatly enhanced absorbance at 475 nm, thus allowing excitation with blue light alone.

Many lines of transgenic mice expressing GFP and GFP fusion proteins have been described. Commonly, such mice are maintained by intercrossing of heterozygotes, a breeding strategy that necessitates the identification of transgenic and non-transgenic progeny. In animals that express GFP widely, this can be done by examining tissue under a suitable fluorescence microscope. Small pieces of tissue removed from animals during ear-notching (for identification purposes) are suitable. However, this approach has several drawbacks. Ear-notching is an invasive procedure that must be performed under appropriate animal husbandry practise, is open to errors of misidentifying from which mice biopsies have come, and is a relatively time-consuming way of screening large numbers of litters. In addition, ears are not sufficiently developed to allow ear-notching before around three weeks of age.

Previously, a genotyping protocol has been described that uses a UV light source and filters to visualize GFP in exposed tissue (1). Using this as a starting point, we investigated the possibility of using blue light excitation of GFP as a means to genotype GFP organisms. As a model, we used the tauGFP expressing transgenic line TgTP6.3 developed in our laboratory (4). These animals express a fusion protein in which GFP is joined to the microtubule-binding protein tau. The transgene is expressed at high levels and in most tissues. We decided not to use UV light, since we wanted to identify the GFP fluorescence in living animals and UV light is a hazard to both the operator and the animals. In addition, there were a number of other criteria for our GFP visualization equipment. We wanted it to be (i) noninvasive, (ii) easily brought in to the animal care facility, (iii) amenable to disinfection, (iv) quick to use (without significant warm-up time), (v) to be readily available, and (vi) inexpensive.

A survey of commercially available macroscopic GFP visualization equipment found that the cheapest was more than $1100 for a system that satisfies points i, ii, iii, and iv, and v. However, these systems are designed to high specifications that far exceed our requirements.

Blue light GFP visualization works by illuminating the tissue with light with a peak intensity at 475 nm and a steep decline in intensity at other wavelengths. Thus, the greatest possible amount of light from extraneous wavelengths is excluded. This is usually achieved by using an appropriate filter. The tissue is then visualized through a second barrier filter that excludes the blue light and passes only the emitted green fluorescent light. This is typically achieved using a filter that cuts out light from wavelengths less than 500 nm. These filters should also help to reduce the background autofluorescence.

A "homemade" system for GFP detection has been previously described (5). This system used a single blue light emitting diode (LED) to visualize GFP in E. coli transformed with a GFP containing plasmid. However, we considered that a single blue LED would be unlikely to generate enough light to excite GFP to detectable levels in the transgenic animals in vivo. In addition, this system used a photomultiplier tube (PMT) to convert photons to an electrical signal for computer analysis. PMTs are sensitive detectors for low-intensity applications such as fluorescence and typically can create millions of electrons for each photoelectron detected. This suggests that without the PMT amplification the GFP signal would not be strong enough from a single blue LED.

We have identified a commercially available blue LED flashlight (Inova X5 ; Emissive Energy, Warwick, RI, USA) with an emission wavelength of 470 nm. However, there are many available, and any blue LED flashlight with a wavelength of 470 nm would be suitable. The flashlight used here has five blue LEDs. Blue LEDs are also available from many semiconductor suppliers and a homemade flashlight could be produced. Several different types of blue LED are available. The compounds used in the LED manufacture govern the wavelength of the light. The majority of gallium nitride and indium gallium nitride on Al_2O_3 LEDs have a peak wavelength of around 470 nm; the exact wavelength is given in the

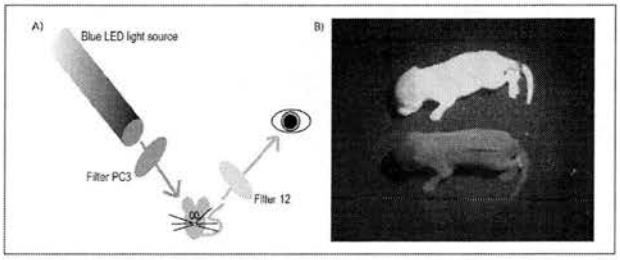

Figur e 1. Using a flashlight to visualize GFP in GFP-transgenic animals. (A) Schematic diagram of the GFP visualization system. (B) Photograph of a non-transgenic and transgenic newborn pup (top) taken using our system described here. The photograph was taken using a digital camera (Ricoh, Tokyo, Japan) with type 12 filter (Eastman Kodak) placed in front of the camera. The room in which this was done had no overhead illumination.

manufacturer's specifications.

Onto the front of the flashlight we have attached a Kodak® Polymax Filter PC3 (Eastman Kodak, Rochester, NY, USA), and we observe mice through a Kodak Wratten Gelatin Filter 12 (Sigma, Poole, UK). Details of the exact specifications for the filters are available from Eastman Kodak (2). Filter PC3 is no longer available on its own, but an equivalent is available as part of either the Kodak Polymax filter set or the ILFORD Multigrade filter set IV (ILFORD, Cheshire, UK). Any of the higher-contrast filters in the sets will work. Figure 1A illustrates the GFP visualization setup. Filter PC3 restricts the emitted light to around 475 nm, and filter 12 cuts out light below about 500 nm. These filters are not of a high enough quality for high-magnification photomicrographic work; however, for the purpose of identifying GFP expressing animals, they are acceptable. Figure 1B demonstrates the readily visible difference between transgenic and non-transgenic littermates. Using this system, we can identify transgenic animals immediately after birth. Indeed, the optimum time for identification of many transgenic mice is in the first week before hair grows. After the hair has grown, GFP-expressing tissue is still visible (e.g., parts of the nose and feet), but the effect in these areas is not as pronounced.

The system that we have described here fulfills all of our criteria for a GFP visualization system. It is noninvasive. The system is portable and so can be transported and used in an animal care facility with little logistical difficulties. The flashlight identified here is also waterproof and so is easily disinfected. The system requires no warm-up or cool-down period. The components are readily available, and it is relatively inexpensive. The setup described here costs less than $160.

From ethical, time-saving, and financial points of view, it is important to optimize the efficiency of breeding transgenic animals. As more and more laboratories make use of existing GFP transgenic animals, and more GFP transgenics are made, the importance of more effective screening will increase. We feel that the system described here will not be limited to genotyping widely or ubiquitously expressing GFP-transgenic mice but could probably be used for any GFP transgenic organism where the GFP protein is visible. The protein could be expressed either somewhere on the organism's surface or in superficial internal organs visible through the skin.

REFERENCES

1. Hadjantonakis, A.K., M. Gertsenstein, M. Ikawa, M. Okabe, and A. Nagy . 1998. Generating green fluorescent mice by germline transmission of green fluorescent ES cells. Mech. Dev. 76:79-90.
2. Kodak. 1999. Kodak publication b-3: Kodak photographic filters handbook. Silver Pixel Press, New York.
3. Morise, H., O. Shimomura, F .H. Johnson, and J. W inant. 1974. Intermolecular energy transfer in the bioluminescent system of Aequorea. Biochemistry 13:2656-2662.
4. Pratt, T ., L. Sharp, J. Nichols, D.J. Price, and J.O. Mason. 2000. Embryonic stem cells and transgenic mice ubiquitously expressing a tau-tagged green fluorescent protein. Dev. Biol. 228:19-28.
5. Randers-Eichhorn, L., C.R. Albano, J. Sipior, W.E. Bentley , and G. Rao. 1997. On-line green fluorescent protein sensor with LED excitation. Biotechnol. Bioeng. 55:921-926.
6. Siemering, K.R., R. Golbik, R. Sever , and J. Haseloff. 1996. Mutations that suppress the thermosensitivity of green fluorescent protein. Curr. Biol. 6:1653-1663.
7. Zimmer, M. 2002. Green fluorescent protein (GFP): applications, structure, and related photophysical behavior. Chem. Rev. 102:759-781.

Address correspondence to Mr David Tyas, Genes and Development Group, Biomedical Sciences, University of Edinburgh, Hugh Robson Building, George Square, Edinburgh EH8 9XD, UK. e-mail: david.tyas@ed.ac.uk

Received 23 October 2002; accepted 21 November 2002.

D.A. Tyas, T.Pratt,
T.I. Simpson, J.O. Mason,
and D.J. Price
University of Edinburgh
Edinburgh, UK

Pax6 Regulates Cell Adhesion during Cortical Development

David A. Tyas, Helen Pearson[1], Penny Rashbass[2] and David J. Price

Genes and Development Group, Biomedical Sciences, University of Edinburgh, Hugh Robson Building, George Square, Edinburgh EH8 9XD, [1]Nature Publishing Group, The Macmillan Building, 4 Crinan Street, London N1 9XW and [2]Centre for Developmental Genetics, Department of Biomedical Science, University of Sheffield, Western Bank, Sheffield S10 2TN, UK

Pax6 is a member of an evolutionarily conserved family of transcription factors. It is developmentally regulated and is required for the normal embryonic development of the central nervous system, eye and pancreas. *Pax6* mutations in the mouse result in the Small eye (*Sey*) phenotype. Heterozygous mice have eye defects and homozygotes die immediately after birth lacking eyes, nasal cavities and with severe brain abnormalities, including a malformed cerebral cortex. Recent work has established that there are changes in expression of cell adhesion molecules and these may underlie at least a part of the $Pax6^{Sey/Sey}$ phenotype. Here we used cell transplants and explant cultures to investigate the role of Pax6 in cell adhesion. $Pax6^{Sey/Sey}$ embryonic cortical cells transplanted into wild-type embryonic cortex were observed to segregate from wild-type cells and form dense clusters. Cells migrating from explants of $Pax6^{Sey/Sey}$ embryonic cortex clustered to a greater extent than cells migrating from wild-type controls. These new data support the hypothesis that *Pax6* exerts a cell-autonomous effect on the adhesiveness of cortical cells.

Introduction

Pax6 is a member of a family of transcription factors characterized by the presence of an N-terminal 128 amino acid DNA binding domain, the paired box. This domain is divided into two helical sub-domains called PAI and RED that can each bind DNA independently (Jun and Desplan, 1996). At least nine murine and human paired box genes have been identified to date (Callaerts *et al.*, 1997). Separated from the paired box by a 78 amino acid glycine-rich linker sequence is a second 60 amino acid DNA binding domain, the homeobox. These two domains can interact independently and cooperatively with DNA. At the C-terminal of Pax6 is a 153 amino acid proline-serine-threonine rich domain that is thought to be the transcriptional regulatory element.

Pax6 is expressed in the retina, lens and cornea of the developing vertebrate eye (Walther and Gruss, 1991; Grindley *et al.*, 1995). It is also expressed at a range of developmental stages in regions of the forebrain, hindbrain, cerebellum, the ventral neural tube and the pancreatic islet cells (Walther and Gruss, 1991; Stoykova and Gruss, 1994; Grindley *et al.*, 1995; St-Onge *et al.*, 1997; Warren and Price, 1997; Kioussi *et al.*, 1999). Humans heterozygous for mutations in *PAX6* suffer from aniridia (iris hypoplasia), which is associated with cataracts, lens dislocation, foveal dysplasia, optic nerve hypoplasia and nystagmus (Jordan *et al.*, 1992; Glaser *et al.*, 1994). The vast majority (92%) of known *PAX6* mutations in humans are nonsense mutations (Hanson *et al.*, 1999). Interestingly, there are a few cases where the mutation has been found several hundred kilobases away from the *PAX6* transcriptional start site (Fantes *et al.*, 1995; Lauderdale *et al.*, 2000), demonstrating the presence of distant regulatory domains. A rare case of an infant with a compound heterozygous mutation in *PAX6* suffered severe craniofacial and central nervous system defects, had no eyes, no adrenal glands, and died neonatally, a phenotype similar to the homozygous null mutation in mice (Glaser *et al.*, 1994).

Pax6 mutation in the mouse results in the Small eye (*Sey*) phenotype. At least eight alleles of *Pax6* have been identified in the mouse so far and all are similar loss-of-function mutants (Glaser *et al.*, 1990; Hill *et al.*, 1991; St-Onge *et al.*, 1997; Lyon *et al.*, 2000). It is unclear whether these alleles are complete nulls but they will be referred to here as $Pax6^{-/-}$. A premature stop codon in the linker domain generates the $Pax6^{SeyEd}$ allele (Hill *et al.*, 1991). Heterozygous mice have a reduced eye size, iris hypoplasia, corneal opacification, and cataracts. Homozygotes die immediately after birth with no eyes, no nasal structures and severe brain abnormalities, including malformed cerebral cortex (Hogan *et al.*, 1986; Hill *et al.*, 1991; Schmahl *et al.*, 1993; Caric *et al.*, 1997). The diencephalic equivalent is reduced in size, is not differentiated to a normal extent (Stoykova *et al.*, 1996; Warren and Price, 1997), and fails to innervate the cortex (Pratt *et al.*, 2000). As in the human, distant regulatory modules have been shown to be essential for the correct expression pattern of *Pax6* (Kleinjan *et al.*, 2001).

A Role for Pax6 in Cortical Development

In normal development of the mouse, neurogenesis occurs from embryonic day 12 (E12) to E18 (Gillies and Price, 1993; Levers *et al.*, 2001). At these ages, the lateral ventricle is lined by a population of cells in a region called the ventricular zone, which gives rise to most neurones and glial cells of the mammalian cortex. These cortical precursor cells are not a homogeneous population and there is mounting evidence that different precursor cells generate different differentiated cell types (Grove *et al.*, 1993; Luskin *et al.*, 1993; Reid *et al.*, 1995; Tan *et al.*, 1998; Heins *et al.*, 2002). The mechanisms controlling the fates of these precursor cells are not yet elucidated.

Nuclei of ventricular progenitor cells undergo dynamic intracellular migration during the cell cycle. Nuclei move away from the apical surface during G1, occupy the outer half of the ventricular zone during S phase and return apically in G2 so that mitosis occurs at the ventricular surface (Sidman *et al.*, 1959; Fujita, 1964). Neurons exit the cell cycle in contact with radial glial fibres to migrate into more superficial positions. When neurons reach the top of the cortical plate they detach and associate into layers with cohorts of a similar birth date. This results in the cortex being formed in an 'inside-out' laminar fashion. After neural production has finished, astrocytes and oligodendrocytes are produced in large numbers from precursors in the subventricular zone (Gleeson and Walsh, 2000; Morrison, 2000).

In $Pax6^{-/-}$ mice both the cortical ventricular zone and the subventricular zone are enlarged (Schmahl *et al.*, 1993; Stoykova *et al.*, 1996; Caric *et al.*, 1997). In addition, the cortical plate is thinner and within the intermediate zone (i.e. between the

subventricular zone and cortical plate) there are large collections of cells characteristic of those in the subventricular zone. Cumulative labelling with bromodeoxyuridine (BrdU) has revealed that proliferative rates in the early *Pax6*$^{-/-}$ embryonic cortex increase (Estivill-Torrus *et al.*, 2002). In addition, proliferating cells in S phase are found scattered throughout the ventricular zone, suggesting either a failure in interkinetic nuclear migration or asynchronous cycling of precursor cells in the mutant cortex (Götz *et al.*, 1998; Estivill-Torrus *et al.*, 2002). Birthdating studies with BrdU *in vivo* show that many later-born neurons fail to migrate to the cortical plate and accumulate in the subventricular zone (Caric *et al.*, 1997). Immunohistochemical analysis of neuron-specific class III β-tubulin isotype (TuJ1), an early marker for postmitotic neurons (Lee *et al.*, 1990), has shown that cells in *Pax6*$^{-/-}$ mutant cortices that fail to migrate do begin neuronal differentiation (Caric *et al.*, 1997). There is a similar defect in Small eye rats (*rSey*): the E20 cortices have an abnormal clustering of cells in the ventricular and intermediate zones of the cortex (Fukuda *et al.*, 2000).

Not all cells in the ventricular zone express Pax6; rather, expression appears to be localized to a subset of radial glial cells (Götz *et al.*, 1998). In *Pax6*$^{-/-}$ embryos, the morphology of radial glial cells is altered. At E15.5, wild-type radial glia have straight processes running towards the pial surface whereas mutant radial glial processes appear wavy and have frequent small extrusions and branches (Götz *et al.*, 1998). Co-culture experiments mixing E13.5 *Pax6*$^{-/-}$ cortical cells and wild-type cells failed to rescue the phenotype of mutant radial glial cells, suggesting that the defect may be cell-autonomous (Götz *et al.*, 1998). Work over the past few years has shown that radial glial cells are able to generate not only glial cells but also neurons (Campbell and Götz, 2002). In cultures of *Pax6*$^{-/-}$ radial glial cells, less neural clones and more non-neural clones were produced than in cultures of wild-type radial glial cells (Heins *et al.*, 2002). Furthermore, *in vivo* quantification showed a 50% reduction of radial glial-derived neurons in the *Pax6*$^{-/-}$ cortex at E14 and E16 (Heins *et al.*, 2002). Infecting cells from E14 *Pax6*$^{-/-}$ cortex with a retroviral vector containing full length *Pax6* cDNA increased the number of differentiated neurons and appeared to reduce proliferation (Heins *et al.*, 2002). These findings suggest that Pax6 may play a cell-autonomous role driving radial glial cells to produce cells of a neuronal fate.

Some defects in the developing central nervous system of *Pax6*$^{-/-}$ embryos are not due to a direct cell-autonomous requirement for Pax6 in the affected process. Transplantation of *Pax6*$^{-/-}$ cortical precursors into a wild-type cortical environment can rescue their migrational defect, suggesting that it may be secondary to defects of other cells such as radial glia which normally guide migration (Caric *et al.*, 1997). Abnormally high levels of cell death among late-embryonic *Pax6*$^{-/-}$ dorsal thalamic cells are most likely secondary to the inability of these cells to obtain trophic support from the cerebral cortex, to which they do not connect (Lotto *et al.*, 2001).

Here, we present new data on experiments to test whether *Pax6* has a cell-autonomous role regulating cell adhesion in the developing cortex. We examined the behaviour of *Pax6*$^{-/-}$ cortical cells when they were either transplanted into wild-type cortex or cultured as explants. The rationale behind the first approach was that embedding the mutant cells in a wild-type environment would reveal their cell-autonomous defects and ameliorate any defects that might arise in mutant embryos as a secondary consequence of abnormalities in other cells. The explant approach provided a means of testing the adhesive properties of mutant cortical cells in isolation from other cell types or from wild-type cells.

Materials and Methods

Animals

All mouse embryos were derived from *Pax6*$^{Sey/Sey}$ heterozygote crosses and were genotyped as previously described (Hogan *et al.*, 1986; Hill *et al.*, 1991; Caric *et al.*, 1997). Wild-type Long–Evans hooded rats were obtained from external suppliers. The day of the vaginal plug following mating was designated E0.5.

Transplants

Pax6$^{-/-}$ and wild-type embryos were obtained from pregnant mice that had been injected on E15.5 with BrdU (70 μg/g in sterile saline i.p.) 1 h prior to death by cervical dislocation. The embryonic cerebral neocortices were isolated and dissociated as described by Caric *et al.* (Caric *et al.*, 1997). Viabilities of dissociated cells were assessed by trypan blue exclusion and were ~95%. E15.5 pregnant rats were anaesthetized with ketamine (60 mg/kg i.m.) and xylazine (6 mg/kg i.m.), and dissociated mouse cells were injected into the telencephalic vesicles using methods described before (Caric *et al.*, 1997). The rats recovered and gave birth as normal. Their young were deeply anaesthetized with sodium pentobarbitone (1 mg i.p.) on postnatal day 7 (P7) and perfused transcardially with 4% paraformaldehyde. Wax sections were cut and reacted to reveal BrdU labelling, as described previously (Gillies and Price, 1993).

Explant Cultures

E13.5 or E15.5 wild-type and *Pax6*$^{-/-}$ neocortex was obtained as described above, sectioned parasagittally and divided into anterior, middle and posterior thirds. Anterior (A) and posterior (P) thirds were cut into pieces and placed in 9 × 9 mm wells on chambered coverglass slides coated with poly(L)-lysine and laminin in serum-free medium (Lotto and Price, 1999). Wild-type and *Pax6*$^{-/-}$ diencephalon from brains of the same age were dissected and added to the wells such that tissue was co-cultured in the following combinations. (i) Both wild-type A and P cortex were cultured with either wild-type or mutant diencephalon (four combinations); (ii) both mutant A and P cortex were cultured with either wild-type or mutant diencephalon (four combinations). Diencephalic explants were included since it is known that factors from this tissue, which interacts with the cortex *in vivo*, are required to ensure the survival, growth and migration of cortical cells (Lotto and Price, 1996; Price and Lotto, 1996; Lotto *et al.*, 1999; Edgar and Price, 2001). Cortical explants in contact with diencephalic tissue, or which became innervated by processes that grew from the diencephalon, were excluded from the analyses. For each age, the explant cultures were set up using three separate wild-type and *Pax6*$^{-/-}$ brains (in three independent experiments). After 24 h in culture, digital images of five randomly selected explants in each culture well were recorded. Explants were fixed in 4% paraformaldehyde and immunostained with antibodies using standard techniques.

Analysis of Clumping In Vivo *and* In Vitro

We observed differences in the degree of clumping of mutant and wild-type cells that had integrated into the wild-type cortex or migrated out of cultured explants. These differences were analysed quantitatively.

For analysis of the distributions of transplanted cells *in vivo*, a series of 1-in-10 sections through the cortex were examined and every BrdU labelled cell was scored for whether it had another BrdU labelled cell within 1, 2, 3, 4 or >4 nuclear diameters of it. The percentages of cells within each of the five categories were calculated from six transplants of mutant or eight transplants of wild-type cells.

To quantify clumping of cells migrating from cortical explants in culture, explant images were analysed using an IPLab script (Scanalytics Inc., Fairfax, VA). Measurements were made by defining a series of concentric rings of equal width surrounding the explant, calculating their area and counting the numbers of touching and non-touching cells in each ring. A measure of the degree to which cells clump together, I_C, independent of cell density, was obtained. I_C is calculated based on the expected proportion of isolated cells (cells not touching another cell) under the null hypothesis that cells are distributed randomly around an

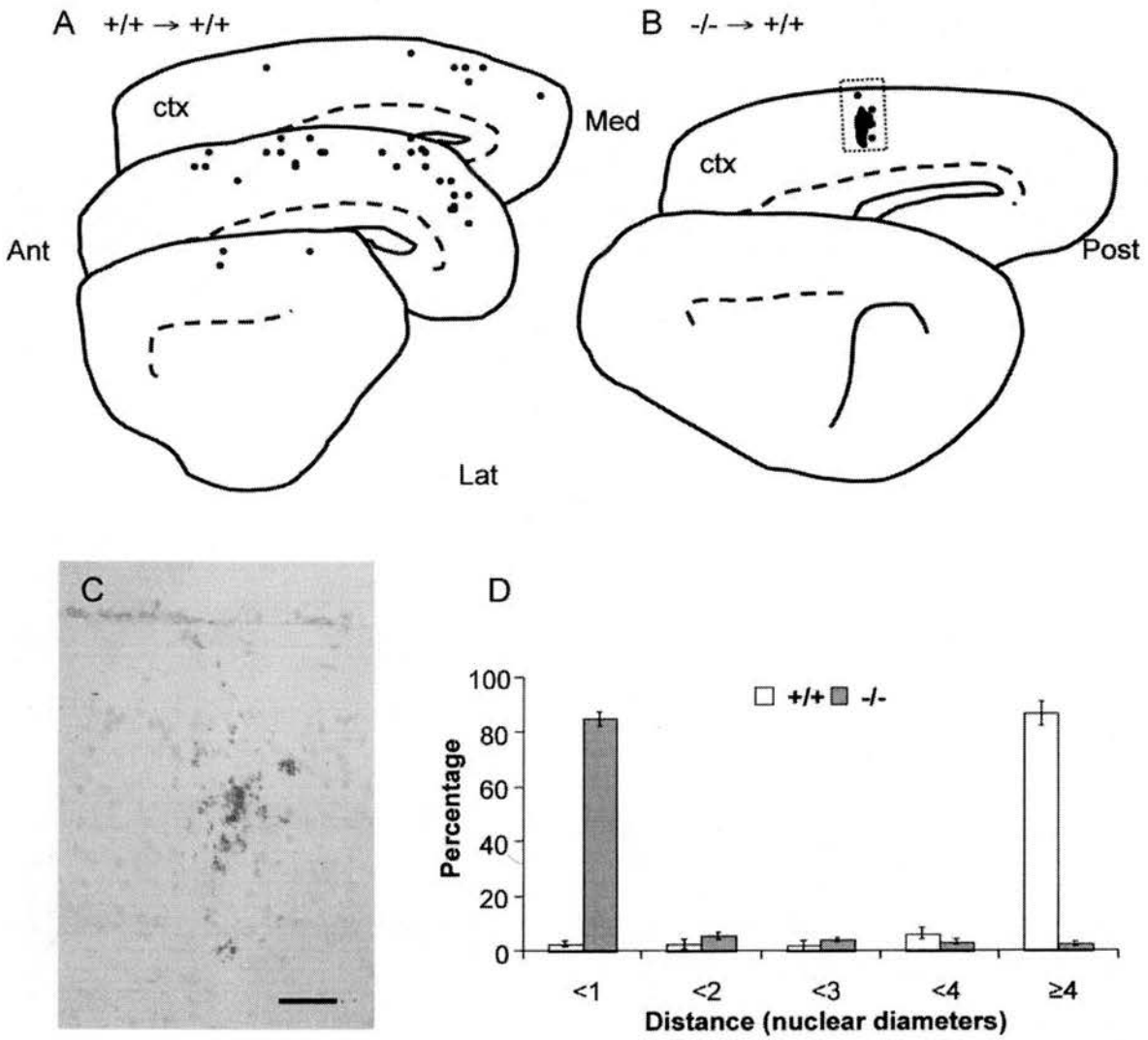

Figure 1. Results of transplants of E15.5 BrdU labelled wild-type or *Pax6*$^{-/-}$ cortical cells into E15.5 rat brains, examined at P7. (*A*) Camera lucida drawings of three parasagittal sections from brains that had received wild-type cells. The position of each labelled cell is marked with a small dot; broken lines mark the deep edge of layer 6. (*B*) Camera lucida drawings of two parasagittal sections from brains that had received mutant cells. Labelled cells were found in a small number of dense clusters, such as that outlined with a box. (*C*) Photomicrograph of the boxed area in *B*; scale bar, 50μm. (*D*) Histogram showing the proportions of labelled cells lying <1, <2, <3, <4 or ≥4 nuclear diameters from another labelled cell in sections through the P7 rat cortex. Labelled cells were either wild-type or mutant and values are means ± SEMs. Around 500 cells per brain from eight wild-type and six mutant transplants were counted. Abbreviations: Ant, anterior; Lat, lateral; Med, medial; Post, posterior; ctx, cortex.

explant. A scale of clumping is produced where $I_C = 0$ if all cells are isolated (not touching another cell), $I_C = \infty$ if all cells are touching one or more other cells, and $I_C = 1$ if the proportion of isolated cells is equal to that expected under the null hypothesis that cells are randomly distributed. The model was subjected to tests for validity and shown to produce a measure of clumping that fulfilled the criteria for analysis of variance [ANOVA; A. Carothers, described by Pearson (Pearson, 1999)].

Results

Transplants

Figure 1*A–C* shows examples of the distributions of wild-type and *Pax6*$^{-/-}$ BrdU labelled (on E15.5) cortical cells in P7 wild-type cortex following transplants at E15.5. As shown before, both mutant and wild-type cells migrated preferentially to the superficial layers of the cortex, a location that was appropriate for their birthdate (Caric *et al.*, 1997). Genotype had a clear effect on their tangential distribution. Wild-type cells were scattered throughout the cortex (Fig. 1*A*) whereas mutant cells were found in a small number of very dense clusters (Fig. 1*B,C*). These clusters were found throughout the rostrocaudal extent of the cortex. Combining quantitative data from eight wild-type and six mutant transplants showed that the vast majority of mutant cells were found within a single nuclear diameter of another mutant cell, whereas most transplanted wild-type cells were separated by much greater distances from other transplanted wild-type cells (Fig. 1*D*). The total numbers of transplanted mutant and wild-type cells identified in the analysis were comparable and represented tiny proportions of the overall numbers of cells in the recipient cortices. Analysis of transplanted wild-type and *Pax6*$^{-/-}$ cells labelled with fluorescent dyes revealed that they adopted neuronal morphologies and appeared viable (Caric *et al.*, 1997).

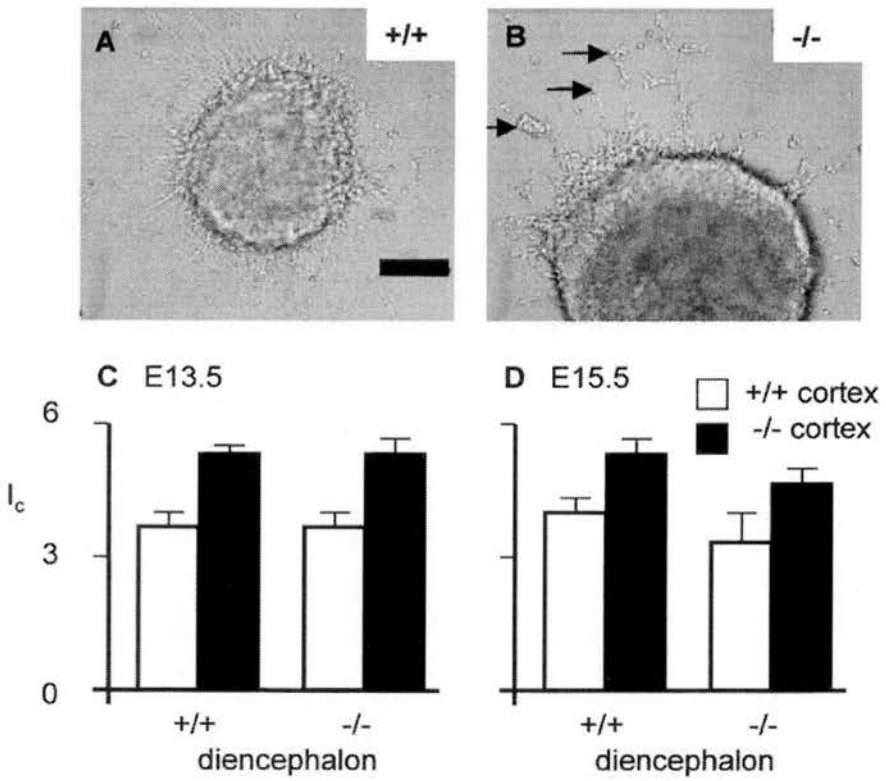

Figure 2. Results of explant cultures of E13.5 and E15.5 cerebral cortex. (*A*, *B*) Explants of wild-type and mutant explants at E13.5. Arrows in *B* point to clusters of cells that had migrated away from the explant. Scale bar, 50μm. (*C*, *D*) Average I_C values (±SEMs) from wild-type and mutant explants at E13.5 and E15.5, co-cultured with either wild-type or mutant diencephalon.

Explant Cultures

After 24 h in culture, both wild-type and *Pax6*$^{-/-}$ cortical explants had extended numerous processes and cells had migrated out from the explant body (Fig. 2*A*,*B*). A striking difference in behaviour between cells from the wild-type and mutant tissue was observed. Whereas wild-type cells migrated individually or in association with one or two other cells (Fig. 2*A*), many mutant cells migrated together in streams and formed distinct clusters away from the body of the explant (Fig. 2*B*). ANOVA on values of I_C revealed that, at both E13.5 and E15.5, clumping was significantly greater in cells migrating from mutant than from wild-type cortical explants ($P < 0.001$) (Fig. 2*C*,*D*). The analysis revealed no significant difference between co-culturing E13.5 or E15.5 explants (whether wild-type or mutant) with wild-type or mutant diencephalic tissue (Fig. 2*C*,*D*). This indicates that the clumping phenotype of *Pax6*$^{-/-}$ cortical cells is regulated independently of thalamic factors. Cellular clumping was not significantly different between anterior and posterior cortical explants at either age examined (data were combined for Fig. 2*C*,*D*). There were no differences in rates of cell death in explants of different genotypes (counts of dead cells were made on the basis of nuclear morphology after staining with fluorescent nuclear stains).

Immunostaining of cells migrating from the explants was performed to evaluate the cell types involved. Antibody TuJ1 stains the earliest born postmitotic neurons. Its use revealed that many cells migrating from both wild-type and mutant explants were neuronal and that some, but not all, cellular clumps contained neurons (Fig. 3*A*,*B*). Staining with an antibody against phosphorylated histone H3 marks metaphase cells (Estivill-Torrus *et al.*, 2002). This antibody revealed that most cell division occurred in the body of both wild-type and *Pax6*$^{-/-}$ explants and very rarely within clumped cells, indicating that the clumps were not due to cell division after migration (Fig. 3*C*,*D*). Finally, RC2 antibody revealed radial glial cells extending from both wild-type and mutant explants and, in both strains, some cells appeared to be migrating along them (Fig. 3*E*,*F*).

Discussion

The new data presented here indicate that Pax6 regulates the adhesive properties of cortical neurons. The transplant experiments show that cortical cells lacking Pax6 segregate from wild-type cells and form dense clusters, pointing to a difference in the cell surface properties of mutant and wild-type cells. The *in vitro* experiments indicate that *Pax6*$^{-/-}$ cortical cells have an increased tendency to aggregate with each other even in the absence of wild-type cells. This suggests that the cell-surface molecules whose expression is affected by Pax6 include cell adhesion molecules that regulate the absolute adhesiveness of cortical cells. The role of Pax6 in controlling these cellular properties appears to be cell-autonomous. Given the fundamental importance of cell adhesion in developmental processes, a defect of cell adhesion in *Pax6*$^{-/-}$ cells is likely to underlie many of the defective processes in mutant embryos.

Regulation of Cell Adhesion by Pax6

Other studies have indicated abnormalities in the adhesive properties of *Pax6*$^{-/-}$ cortical cells. Cortical cells express Pax6

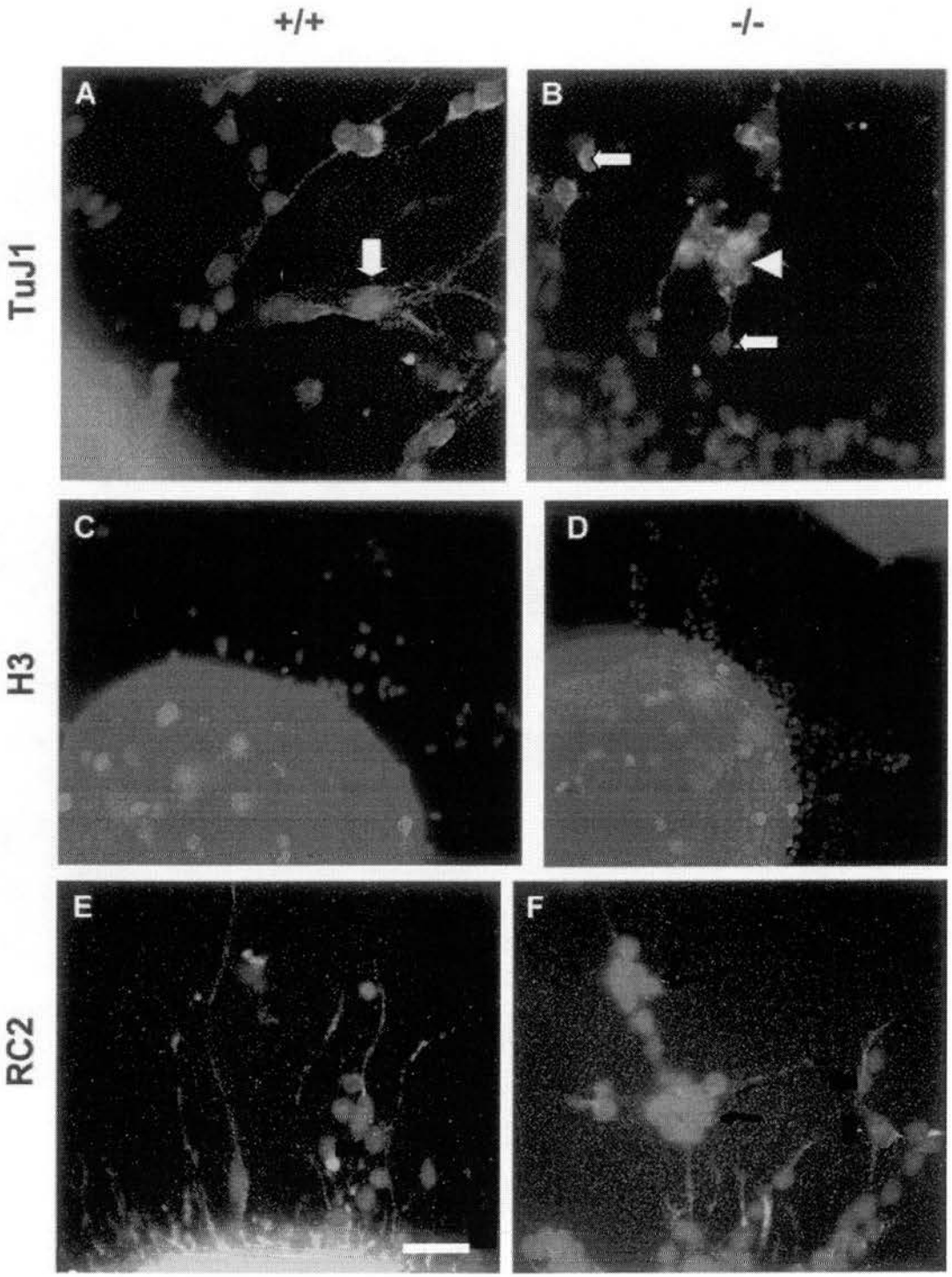

Figure 3. Cultures of E13.5 wild-type and mutant cortex stained with TuJ1 (*A, B*), phosphorylated histone H3 (*C, D*) and RC2 (*E, F*). Arrows in *A* and *B* indicate individual TuJ1-labelled cells; arrowhead indicates a cluster of such cells. Scale bar: *A* and *B*, 15 μm; *C–F*, 30 μm.

whereas striatal cells do not and when cells from E12.5 to E14.5 wild-type cortex and striatum are co-cultured in a short-term assay they segregate strongly from each other (Stoykova *et al.*, 1997; Götz *et al.*, 1996). *Pax6*$^{-/-}$ cortical and striatal cells, however, segregate only weakly from each other (Stoykova *et al.*, 1997). *Pax6*$^{-/-}$ cortical cells segregate from wild-type cortical cells but *Pax6*$^{-/-}$ striatal cells mix with wild-type striatal cells (Stoykova *et al.*, 1997). These results suggest that Pax6 regulates the adhesive properties of cells in the telencephalic region where it is expressed, i.e. the cerebral cortex.

The expression patterns of some adhesion molecules are altered in *Pax6*$^{-/-}$ forebrains. Expression of the extracellular matrix molecule tenascin-C (TN-C) at the cortico-striatal boundary is abolished and the expression of calcium dependent adhesion molecules, cadherins, is altered in the cortex (Stoykova *et al.*, 1997; Bishop *et al.*, 2000). The expression domain of the homophilic adhesion molecule R-cadherin and that of Pax6 have some overlap (Ganzler and Redies, 1995; Matsunami and Takeichi, 1995) and, in the absence of functional Pax6, expression of R-cadherin mRNA is reduced considerably in areas that normally show co-expression (Stoykova *et al.*, 1997).

Loss of Pax6 also seems to have an effect on the cell surface in E12.5–E13.5 mouse hindbrain. The migration of post-mitotic cells from the rhombic lip seems to be controlled in part by Pax6, whose actions may be mediated by regulation of the netrin receptor Unc5h3 (Engelkamp *et al.*, 1999), although alterations in the polarity of cytoskeletal components may also be involved (Yamasaki *et al.*, 2001). In small eye rats there is impaired migration of midbrain neural crest cells (Matsuo *et al.*, 1993; Nagase *et al.*, 2001). These cells use the frontonasal epithelium as a scaffold for their migration and frontonasal epithelial cells are known to express Pax6 (Matsuo *et al.*, 1993). Within this region the cell surface molecule HNK-1 carbohydrate epitope and the gene encoding an enzyme for the synthesis of the HNK-1 epitope are expressed ectopically in small eye rats (Nagase *et al.*, 2001). This suggests that the impairment of migration may be due in part to the inhibitory effect of the ectopically expressed HNK-1 epitope.

Changes in the adhesive properties of other cell types that express Pax6 have also been observed. Transgenic mice with an altered ratio of expression of different splice variants of Pax6 in the lens show a change in the expression of cell adhesion molecules (Duncan *et al.*, 2000). Expression of P120 catenin ($p120^{ctn}$), a member of the armadillo family of proteins implicated in cell–cell adhesion and signal transduction, and Paxillin, a focal adhesion adapter protein implicated in integrin mediated signalling pathways, are highly elevated. Expression of N cadherin and α-catenin are both slightly elevated, α5-integrin and β1-integrin accumulate in lens although E cadherin and α6-integrin expression appears normal (Duncan *et al.*, 2000).

Studies using microarrays of eye mRNA from various Pax6 over-expressing and null mutant cells have shown changes in the expression of ~400 genes (Chauhan *et al.*, 2002). These included Paralemmin and Tangerin A (Chauhan *et al.*, 2002), which are two putative cell surface molecules thought to be important in plasma membrane dynamics and cell process formation (Kutzleb *et al.*, 1998; Agassandian *et al.*, 2000; Chauhan *et al.*, 2002). Changes in these cell surface molecules could also contribute to the altered adhesion seen in Pax6 mutant cells.

Some experiments have suggested that Pax6 protein may directly interact with the regulatory elements of genes encoding adhesion molecules. The gene for neural cell adhesion molecule (N-CAM) has a Pax6 paired-domain binding region within its promoter (Holst *et al.*, 1997). In addition, Pax6 activates the expression of L1-luciferase reporter constructs in neuroblastoma cells (Meech *et al.*, 1999). Although this and other studies suggests an interaction between Pax6 and the cell adhesion molecule L1, which regulates axonal guidance and fasciculation during development (Chalepakis *et al.*, 1994; Meech *et al.*, 1999; Honig *et al.*, 2002), the interaction is likely to be complex. For example, the expression domains of Pax6 and L1 only partially overlap and it has been shown that there is no change in L1 expression in the intermediate, ventricular and subventricular zones of E19 *Pax6*$^{-/-}$ mice (Caric *et al.*, 1997).

The expression pattern of Pax6 in the developing mouse eye closely parallels that of the retinoic acid-responsive transcription factor (AP-2α) (Koroma *et al.*, 1997). Genes involved in cell–cell and cell-matrix adhesion have been shown to be regulated by AP-2α *in vitro* (Chalepakis *et al.*, 1994; Fini *et al.*, 1994; Chen *et al.*, 1997; Holst *et al.*, 1997). For example, AP-2α is required for activation of the E-cadherin promoter in epithelial cell cultures (Behrens *et al.*, 1991; Hennig *et al.*, 1996). Loss of AP-2α leads to a change in Pax6 expression in the developing eye (West-Mays *et al.*, 1999). The discovery of a number of possible binding sites for AP-2α in the *Pax6* promoter has generated the suggestion that Pax6 may be a required intermediary step for AP-2α controlled cell adhesion (Plaza *et al.*, 1995).

Overall, our results and those of others provide compelling evidence that a central role of Pax6 is to regulate cell–cell interactions and adhesion at many sites in the developing embryo, including the cerebral cortex. Further work is required to elucidate the molecular pathways by which its influence on the cell surface is mediated.

Notes

We thank Paul Perry for the IPlab script and Andrew Carothers for help with statistical analyses. D.T. is supported by the MRC. P.R. is a Lister Research Fellow.

Address correspondence to Dr David Price, Genes and Development Group, Biomedical Sciences, University of Edinburgh, Hugh Robson Building, George Square, Edinburgh EH8 9XD, UK. Email: dprice@ed.ac.uk.

References

Agassandian C, Plantier M, Fattoum A, Represa A, der Terrossian E (2000) Subcellular distribution of calponin and caldesmon in rat hippocampus. Brain Res 887:444–449.

Behrens J, Lowrick O, Klein-Hitpass L, Birchmeier W (1991) The E-cadherin promoter: functional analysis of a G.C-rich region and an epithelial cell-specific palindromic regulatory element. Proc Natl Acad Sci USA 88:11495–11499.

Bishop KM, Goudreau G, O'Leary DD (2000) Regulation of area identity in the mammalian neocortex by Emx2 and Pax6. Science 288:344–349.

Callaerts P, Halder G, Gehring WJ (1997) PAX-6 in development and evolution. Annu Rev Neurosci 20:483–532.

Campbell K, Götz M (2002) Radial glia: multi-purpose cells for vertebrate brain development. Trends Neurosci 25:235–238.

Caric D, Gooday D, Hill RE, McConnell SK, Price DJ (1997) Determination of the migratory capacity of embryonic cortical cells lacking the transcription factor Pax-6. Development 124:5087–5096.

Chalepakis G, Jones FS, Edelman GM, Gruss P (1994) Pax-3 contains domains for transcription activation and transcription inhibition. Proc Natl Acad Sci USA 91:12745–12749.

Chauhan BK, Reed NA, Zhang W, Duncan MK, Kilimann M, Cvekl A (2002) Identification of genes downstream of Pax6 in the mouse lens using cDNA microarrays. J Biol Chem 277:11539–11548.

Chen R, Amoui M, Zhang Z, Mardon G (1997) Dachshund and eyes absent proteins form a complex and function synergistically to induce ectopic eye development in *Drosophila*. Cell 91:893–903.

Duncan MK, Kozmik Z, Cveklova K, Piatigorsky J, Cvekl A (2000) Overexpression of PAX6(5a) in lens fiber cells results in cataract and upregulation of (alpha)5(beta)1 integrin expression. J Cell Sci 113:3173–3185.

Edgar JM, Price DJ (2001) Radial migration in the cerebral cortex is enhanced by signals from thalamus. Eur J Neurosci 13:1745–1754.

Engelkamp D, Rashbass P, Seawright A, van Heyningen V (1999) Role of Pax6 in development of the cerebellar system. Development 126:3585–3596.

Estivill-Torrus G, Pearson H, van Heyningen V, Price DJ, Rashbass P (2002) Pax6 is required to regulate the cell cycle and the rate of progression from symmetrical to asymmetrical division in mammalian cortical progenitors. Development 129:455–466.

Fantes J, Redeker B, Breen M, Boyle S, Brown J, Fletcher J, Jones S, Bickmore W, Fukushima Y, Mannens M *et al.* (1995) Aniridia-

Stoykova A, Fritsch R, Walther C, Gruss P (1996) Forebrain patterning defects in Small eye mutant mice. Development 122:3453–3465.

Stoykova A, Götz M, Gruss P, Price J (1997) Pax6-dependent regulation of adhesive patterning, R-cadherin expression and boundary formation in developing forebrain. Development 124:3765–3777.

Tan SS, Kalloniatis M, Sturm K, Tam PP, Reese BE, Faulkner-Jones B (1998) Separate progenitors for radial and tangential cell dispersion during development of the cerebral neocortex. Neuron 21:295–304.

Walther C, Gruss P (1991) Pax-6, a murine paired box gene, is expressed in the developing CNS. Development 113:1435–1449.

Warren N, Price D (1997) Roles of Pax-6 in murine diencephalic development. Development 124:1573–1582.

West-Mays JA, Zhang J, Nottoli T, Hagopian-Donaldson S, Libby D, Strissel KJ, Williams T (1999) AP-2alpha transcription factor is required for early morphogenesis of the lens vesicle. Dev Biol 206:46–62.

Yamasaki T, Kawaji K, Ono K, Bito HB, Hirano T, Osumi N and Mineko Kengaku N (2001) Pax6 regulates granule cell polarization during parallel fiber formation in the developing cerebellum. Development 128:3133–3144.